

Prepared in cooperation with the National Cave and Karst Research Institute and Hoffman Environmental Research Center and Center for Cave and Karst Studies at Western Kentucky University

U.S. Geological Survey Karst Interest Group Proceedings, Bowling Green, Kentucky, May 27–29, 2008



Scientific Investigations Report 2008–5023



Prepared in cooperation with the National Cave and Karst Research Institute and Hoffman Environmental Research Center and Center for Cave and Karst Studies at Western Kentucky University

U.S. Geological Survey Karst Interest Group Proceedings, Bowling Green, Kentucky, May 27–29, 2008

Edited by Eve L. Kuniansky

Scientific Investigations Report 2008–5023

**U.S. Department of the Interior
U.S. Geological Survey**

U.S. Department of the Interior
DIRK KEMPTHORNE, Secretary

U.S. Geological Survey
Mark D. Myers, Director

U.S. Geological Survey, Reston, Virginia 2008

For product and ordering information:
World Wide Web: <http://www.usgs.gov/pubprod>
Telephone: 1-888-ASK-USGS

For more information on the USGS—the Federal source for science about the Earth,
its natural and living resources, natural hazards, and the environment:
World Wide Web: <http://www.usgs.gov>
Telephone: 1-888-ASK-USGS

Suggested citation:
Kuniansky, E.L., 2008, U.S. Geological Survey Karst Interest Group Proceedings, Bowling Green, Kentucky,
May 27–29, 2008: U.S. Geological Survey Scientific Investigations Report 2008–5023, 142 p.
Online copies of the proceedings are available at:
<http://water.usgs.gov/ogw/karst/>

Any use of trade, product, or firm names is for descriptive purposes only and does not imply
endorsement by the U.S. Government.

Although this report is in the public domain, permission must be secured from the individual
copyright owners to reproduce any copyrighted material contained within this report.

Contents

| | |
|---|----|
| Introduction and Acknowledgments..... | 1 |
| Agenda, U.S. Geological Survey Karst Interest Group Workshop, May 27-29, 2008..... | 3 |
| National Programs 8 | |
| Overview of National Park Service policies for cave and karst management by Dale Pate | 8 |
| National Cave and Karst Research Institute: Partner for the USGS by Penelope J. Boston and George Veni..... | 12 |
| National Cave and Karst Research Institute's Karst Information Portal by E. Spencer Fleury..... | 14 |
| Mammoth Cave International Center for Science and Learning by Rickard S. Toomey, III, Shannon Trimboli, Blaine Ferrell, Bob Ward, and Mike Adams | 15 |
| Updating the USGS Karst Interest Group website by converting it into a dynamic web application by Bradley D. Garner and Barbara J. Mahler | 16 |
| Karst Mapping 17 | |
| Karst regions of the world (KROW): Global karst datasets and maps to advance the protection of karst species and habitats worldwide by Emily Hollingsworth, Van Brahana, Ethan Inlander, and Michael Slay | 17 |
| Characterizing regional karst types under the framework of the new National Karst Map by David J. Weary, Daniel H. Doctor, Jack B. Epstein, and Randall C. Orndorff..... | 25 |
| A karst aquifer map for the United States—Is it possible? by Daniel H. Doctor, David J. Weary, Jack B. Epstein, and Randall C. Orndorff..... | 34 |
| Karst Aquifer Systems 37 | |
| Tectonic control of hypogene speleogenesis in the southern Ozarks--Implications for NAWQA and beyond by Rodney Tennyson, Jim Terry, Van Brahana, Phil Hays, and Erik Pollock | 37 |
| Hydrologic characterization of a karst spring in north-central Arkansas by Rheannon M. Scheiderer and Joel M. Galloway..... | 47 |
| Analysis of methods for estimating continuous flows from Upper Floridan Aquifer springs by Nicasio Sepúlveda..... | 49 |

Estimating recharge to heterogeneous fractured-rock and karst aquifer systems in the Shenandoah Valley of Virginia and West Virginia by George E. Harlow, Jr., David L. Nelms, Richard M. Yager, Mark D. Kozar, Ward E. Sanford, and Roger M. Moberg.....50

Impact of 1998-2002 drought on the karst aquifers of Clarke County in the Shenandoah Valley of Virginia by David L. Nelms and Roger M. Moberg51

Ground-water/surface-water relations and water quality within the Mammoth Spring watershed, Dixie National Forest, Garfield and Iron Counties, Utah, by Lawrence E. Spangler.....52

Natural Resources and Karst Ecosystems 55

The effects of land-use change on an Ozark cave system : A paired study of Civil War and Copperhead Caves by Jonathan A. Gillip, Phillip D. Hays, and Joel M. Galloway55

Karst water resources in southwest China: Case study from the east plateau, Mengzi and Kaiyuan Counties, Yunnan, China, by Chris Groves, Jiang Yongjun, Pat Kambesis, Yuan Daoxian, and Amelia Chung57

Thermal infrared mapping of coastal-aquifer seeps and associations between seeps and coastal habitats by E.A. Raabe and E. Bialkowska-Jelinska.....58

Effects of Lock and Dam Number Six on aquatic ecosystems in Mammoth Cave National Park by Rick Olson.....61

Geochemistry / Contaminant Transport 63

Storm period fine sediment transport in Logsdon River, Turnhole Spring Basin, Mammoth Cave, Kentucky, by Stephen T. Kenworthy.....63

Water quality in selected carbonate aquifers of the United States, 1993-2005, by Bruce D. Lindsey, Marian P. Berndt, Brian G. Katz, Ann F. Ardis, and Kenneth A. Skach64

Effect of focused recharge on the geochemistry of Barton Springs, Edwards Aquifer, central Texas during base-flow conditions by Barbara J. Mahler and MaryLynn Musgrove66

An overview of the geochemistry of Edwards aquifer ground water in south-central Texas by MaryLynn Musgrove, Lynne S. Fahlquist, and Natalie A. Houston67

The role of free-living and attached bacteria in processing contamination in karst aquifers by Tom Byl, Kelly Ray, Chad Walden, Valetta Watson, and Roger Painter68

Characterization of bacteria and geochemistry of springs in Nashville, Tennessee, by Patrice Armstrong, Carlton Cobb, Brandon Cobb, Jennifer Stewart-Wright, and Tom Byl.....69

| | |
|---|----|
| Conduit-matrix interaction and the rate limiting step of contaminant transport in karst by K. J. McCoy, A. M. Shapiro, and M. D. Kozar | 70 |
| Assessing age distribution and contaminant movement in ground water in the contributing recharge area to a public supply well in the karstic Upper Floridan Aquifer by Brian G. Katz, Christy A. Crandall, W. Scott McBride, Patty A. Metz, Marion P. Berndt, and Sandra M. Eberts..... | 71 |
| Ammonia oxidation by bacteria collected from a karst-bedrock well by Kelly Ray, Roger Painter, and Tom Byl | 72 |
| Wetland removal of nutrients and pollution from a mixed sewer and karst spring system in Nashville, Tennessee, by Carlton Cobb, Jameka Johnson, Brandon Cobb, Patrice Armstrong, Lonnie Sharpe, and Tom Byl | 73 |
| Are karst bedrock aquifers at greater risk from alternative alcohol-fuel mixes compared to regular gasoline? by Baibai Kamara, Loreal Spear, Carlton Cobb, Keyshon Bachus, Roger Painter, Lonnie Sharpe, and Tom Byl | 74 |
| Residence time distribution derived from independent gamma distributions of tracer travel distance and linear velocity by Roger Painter, Tom Byl, and Valetta Watson..... | 75 |
| Episodic elevated coliform in vadose-zone water within Mammoth Cave National Park, Kentucky, by Rickard S. Toomey, III, Rick Olson, and Bob Ward..... | 76 |
| Numerical Modeling 77 | |
| Modeling ground-water flow and solute transport in karst with Lattice Boltzmann Methods by Michael C. Sukop, Shadab Anwar, Jeff S. Lee, Kevin J. Cunningham, and Christian D. Langevin | 77 |
| Simulation of turbulent ground-water flow with MODFLOW-2005—Overview by Eve L. Kuniansky, Keith J. Halford, and W. Barclay Shoemaker | 87 |
| Effects of turbulence on hydraulic heads and parameter sensitivities in preferential ground-water flow layers by W. Barclay Shoemaker and Eve L. Kuniansky..... | 89 |
| Simulation of ground-water flow in a fractured-rock karst aquifer, Shenandoah Valley, Leetown, West Virginia, by Mark D. Kozar and Kurt J. McCoy..... | 91 |
| Simulations of ground-water flow and particle pathline analysis in the contributing recharge area of a public-supply well in Temple Terrace, Tampa Bay region, Florida, by Christy A. Crandall, Leon J. Kauffman, and Brian G. Katz | 92 |
| Performance evaluation of the MODFLOW-2005 conduit flow process applied to a karst aquifer underlying west-central Florida by Melissa E. Hill, Angel Martin, and Marc T. Stewart | 93 |

Miscellaneous Topics in Modeling and Geophysics 99

| | |
|--|-----|
| The value of single-well tracer studies for characterizing karst sites by Tarra M. Beach, Michael W. Bradley, Roger Painter, and Thomas D. Byl | 99 |
| GIS and spatial statistical methods for determining sinkhole potential in Frederick Valley, Maryland, by Katarina Z. Doctor | 100 |
| Geophysical analysis of the Salmon Peak Formation near Amistad Reservoir Dam, Val Verde County, Texas, and Coahuila, Mexico, March 2006, to aid in piezometer placement by Gregory P. Stanton, Wade H. Kress, Andrew P. Teeple, Michael L. Greenslate, and Allan K. Clark..... | 103 |
| Construction and use of a fractured-rock simulator to test horizontal borehole flow-measuring technologies by E. Randall Bayless | 105 |
| Collection of bathymetric data along two reaches of the Lost River within Bluespring Cavern near Bedford, Lawrence County, Indiana, July 2007 by David C. Lampe and Scott E. Morlock..... | 106 |
| A multi-tool geophysical and hydrogeological investigation of a karst aquifer system, Cibolo Canyon development area, Bexar County, Texas, by Sachin D. Shah, Bruce D. Smith, Allan K. Clark, and Wade H. Kress | 107 |

Field Trip Guides 117

| | |
|--|-----|
| Mammoth Cave National Park Tour, Tuesday evening May 27, 2008, led by Rickard S. Toomey, III, and Rick Olson | 117 |
| Karst underground drainage in and around Mammoth Cave National Park by Cave Research Foundation and Mammoth Cave National Park | 118 |
| Geology of the Mammoth Cave area by Arthur N. Palmer | 119 |
| Guide to the historic route of Mammoth Cave by Arthur N. Palmer | 128 |
| Biospeleology of Mammoth Cave: A briefing paper by Rick Olson | 133 |
| Field trip road log: Karst features of the Mammoth Cave Kentucky Area, Thursday, May 29, 2008, led by Chris Groves and Rick Toomey | 139 |

INTRODUCTION AND ACKNOWLEDGMENTS

Karst aquifer systems are present throughout parts of the United States and some of its territories. The complex depositional environments that form carbonate rocks combined with post-depositional tectonic events and the diverse climatic regimes under which these rocks were formed result in unique hydrologic systems. The dissolution of calcium carbonate and the subsequent development of distinct and beautiful landscapes, caverns, and springs have resulted in some karst areas of the United States being designated as national or state parks and commercial caverns. Karst aquifers and landscapes that form in tropical areas, such as the north coast of Puerto Rico, differ greatly from karst areas in more arid climates, such as central Texas or western South Dakota. Many of these public and private lands contain unique flora and fauna associated with the hydrologic systems in these karst areas. As a result, multiple Federal, State, and local agencies have an interest in the study of karst terrains.

Carbonate sediments and rocks (limestone and dolomite) are composed of greater than 50 percent carbonate minerals and the predominant carbonate mineral is calcium carbonate or limestone (CaCO₃). Unlike terrigenous clastic sedimentation, the depositional processes that produce carbonate rocks are complex, involving both biological and physical processes. These depositional processes impact greatly the development of permeability of the sediments. Carbonate minerals readily dissolve or precipitate depending on the chemistry of the water flowing through the rock, thus the study of both marine and meteoric diagenesis of carbonate sediments is multidisciplinary. Even with a better understanding of the depositional environment and subsequent diagenesis, the dual porosity nature of karst aquifers presents challenges to scientists attempting to study ground-water flow and contaminant transport.

Many of the major springs and aquifers in the United States are developed in carbonate rocks and karst areas. These aquifers and the springs that discharge from them, serve as major water-supply sources and as unique biological habitats. Commonly, there is competition for the water resources of karst aquifers, and urban development in karst areas can impact the ecosystem and water quality of these aquifers.

The concept for developing a Karst Interest Group evolved from the November 1999 National Ground-Water Meeting of the U.S. Geological Survey (USGS), Water Resources Division. As a result, the Karst Interest Group was formed in 2000. The Karst Interest Group is a loose-knit grass-roots organization of USGS employees devoted to fostering better communication among scientists working on, or interested in, karst hydrology studies.

The mission of the Karst Interest Group is to encourage and support interdisciplinary collaboration and technology transfer among USGS scientists working in karst areas. Additionally, the Karst Interest Group encourages cooperative studies between the different disciplines of the USGS and other Department of Interior agencies and university researchers or research institutes.

The first Karst Interest Group workshop was held in St. Petersburg, Florida, February 13-16, 2001, in the vicinity of karst features of the Floridan aquifer system. The proceedings of that first meeting, Water-Resources Investigations Report 01-4011 are available online at:

<http://water.usgs.gov/ogw/karst/>

The second Karst Interest Group workshop was held August 20-22, 2002, in Shepherdstown, West Virginia, in close proximity to the carbonate aquifers of the northern Shenandoah Valley. The proceedings of the second workshop were published in Water-Resources Investigations Report 02-4174, which is available online at the previously mentioned website.

The third workshop of the Karst Interest Group was held September, 12-15, 2005, in Rapid City, South Dakota, which is in close proximity to karst features in the Madison Limestone in the semi-arid Black Hills of South Dakota and Wyoming, including Wind Cave National Park and Jewell Cave National Monument. The proceedings of the third workshop were published in Scientific Investigations Report 2005-5160, which is available online at the previously mentioned website. The USGS, Office of Ground Water, provides support for the Karst Interest Group website and public availability of the proceedings from these workshops.

This fourth workshop is sponsored by the USGS; the Hoffman Environmental Research Center and Center for Cave and Karst Studies at Western Kentucky University in Bowling Green, Kentucky; the National Cave and Karst Research Institute; and Mammoth Cave National Park. The majority of funding for the proceedings preparation and workshop was provided by the USGS Ground-Water Resources Program and the USGS Eastern Region. Western Kentucky University provided the rooms and facilities for the technical and poster presentations of the workshop. The National Cave and Karst Research Institute provided funds for the printed copies of these proceedings distributed at the meeting. The superintendent of Mammoth Cave National Park graciously agreed to allow the Karst Interest Group access to Mammoth Cave for a private evening tour of the cave system.

The session planning committee for this fourth workshop included Randall Bayless, Thomas D. Byl, Kevin F. Dennehy, Daniel H. Doctor, Brian G. Katz, Barbara J. Mahler, Randall C. Orndorff, Rodney A. Sheets, W. Barclay Shoemaker, Bruce D. Smith, Lawrence E. Spangler, Charles J. Taylor, and J. Judson Wynne of the USGS. The field trip committee included Joe Meiman, National Park Service; Chris Groves, Director of the Hoffman Environmental Research Institute, Western Kentucky University; and Rickard Toomey, Director, Mammoth Cave International Center for Science and Learning and Department of Geography and Geology, Western Kentucky University. Local logistics for the meeting were coordinated by Eve Kuniansky, USGS, along with Pat Kambesis and Amber Williams, Western Kentucky University. We sincerely hope that this workshop promotes future collaboration among scientists of varied backgrounds and improves our understanding of karst systems in the United States and its territories.

The extended abstracts of USGS authors were reviewed and approved for publication by the U.S. Geological Survey. Articles submitted by university researchers and other Department of Interior agencies did not go through the USGS review process and, therefore, may not adhere to USGS editorial standards or stratigraphic nomenclature. All articles were edited for consistency of appearance in the published proceedings. The use of trade names in any article does not constitute endorsement by the U.S. Government.

The cover illustration was designed by Ann Tihansky, USGS, St. Petersburg, Florida, for the first Karst Interest Group workshop.

Eve L. Kuniansky

USGS Karst Interest Group Coordinator

AGENDA
U.S. GEOLOGICAL SURVEY
KARST INTEREST GROUP WORKSHOP
May 27-29, 2008
Bowling Green, Kentucky
Western Kentucky University Campus

Tuesday, May 27

Registration

Start at 8:00 am-- All day – pick up name tags and proceedings

Welcome and Introductions

8:45 – 9:20 Eve Kuniansky, U.S. Geological Survey, Karst Interest Group Coordinator; Dr. Gary Ransdell, President of Western Kentucky University; and Mr. Pat Reed, Superintendent of Mammoth Cave National Park

National Programs

9:20 – 9:40 Overview of National Park Service policy for cave and karst management - by Dale Pate, National Park Service

9:40 – 10:00 National Cave and Karst Research Institute's Karst Information Portal - by Spencer Fleury, National Cave and Karst Research Institute

10:00 – 10:40 **BREAK**

Karst Mapping

10:40 – 11:00 Karst regions of the world (KROW): Global karst datasets and maps to advance the protection of karst species and habitats worldwide - by Emily Hollingsworth and Van Brahana, Geology Department, University of Arkansas; and Ethan Inlander and Michael Slay, The Nature Conservancy, Arkansas

11:00 – 11:20 Characterizing regional karst types under the framework of the new National Karst Map - by David J. Weary, Daniel H. Doctor, Jack B. Epstein, and Randall C. Orndorff, U.S. Geological Survey

11:20 – 11:40 A karst aquifer map for the United States—Is it possible? - by Daniel H. Doctor, David J. Weary, Jack B. Epstein, Randall C. Orndorff, U.S. Geological Survey

11:40 – 1:00 **LUNCH ON YOUR OWN**

Karst Aquifer Systems

1:00 – 1:20 Tectonic control of hypogene speleogenesis in the southern Ozarks--Implications for NAWQA and beyond - by Rodney Tennyson, Jim Terry, Van Brahana, Phil Hays, and Erik Pollock - presented by Van Brahana, Geology Department, University of Arkansas

1:20– 1:40 Hydrologic characterization of a karst spring in north-central Arkansas - by Rheannon M. Scheiderer and Joel M. Galloway, U.S. Geological Survey

1:40 – 2:00 Analyses of methods for estimating continuous flow from Upper Floridan Aquifer springs - by Nicasio Sepúlveda, U.S. Geological Survey

2:00 – 2:40 BREAK

Natural Resources and Karst Ecosystems

2:40 – 3:00 The effects of land use change on an Ozark cave system : A paired study of Civil War and Copperhead Caves - by Jonathan A. Gillip, Phillip D. Hays, and Joel M. Galloway, U.S. Geological Survey

3:00 – 3:20 Karst water resources in southwest China: Case study from the east plateau, Mengzi and Kaiyuan Counties, Yunnan, China - by Chris Groves¹, Jiang Yongjun^{2,1}, Pat Kambesis¹, Yuan Daoxian^{2,1} Amelia Chung^{3,1}
¹China Environmental Health Project, Hoffman Environmental Research Institute, Department of Geography and Geology, Western Kentucky University;
²Institute of Karst and Rehabilitation of Rock Deserts, Department of Geographical Sciences, Southwest University of China, Chongqing, China;
³International Institute of Rural Reconstruction, Kunming, Yunnan, China

3:20 – 3:40 Thermal infrared mapping of coastal aquifer seeps and associations between seeps and coastal habitats - by Ellen Raabe, U.S. Geological Survey and Ela Bialkowska-Jelinska, Jacobs Technology

3:40 – 4:00 Effects of lock and dam Number Six on aquatic ecosystems in Mammoth Cave National Park - by Rick Olson, Mammoth Cave National Park

4:20 – 7:00 **Go to dinner and get carpools together for driving to MAMMOTH CAVE -(provide maps for meeting at 7 pm at Park)**

7:00 – 10:00 **OPTIONAL TOUR OF MAMMOTH CAVE - lead by Rickard Toomey**

Wednesday, May 28

Geochemistry /Contaminant Transport

8:00 – 8:20 Storm period fine sediment transport in Logsdon River, Turnhole Spring Basin, Mammoth Cave, Kentucky - by Stephen T. Kenworthy, Dept. of Geography and Geology, Western Kentucky University

8:20 – 8:40 Water quality in selected carbonate aquifers of the United States 1993-2005 - by Bruce D. Lindsey, Marian P. Berndt, Brian G. Katz, Ann F. Ardis, and Kenneth A. Skach, U.S. Geological Survey

8:40 – 9:00 Effect of focused recharge on the geochemistry of Barton Springs, Edwards Aquifer, central Texas during base-flow conditions - by Barbara Mahler and MaryLynn Musgrove, U.S. Geological Survey

9:00 – 9:20 An overview of the geochemistry of Edwards aquifer ground water in south-central Texas - by MaryLynn Musgrove, Lynne Fahlquist, and Natalie Houston, U.S. Geological Survey

9:20 – 10:00 BREAK

- 10:00 – 10:20 The role of free-living and attached bacteria in processing contamination in karst aquifers - by Tom Byl, U.S. Geological Survey and Tennessee State University; Kelly Ray, Chad Walden, Valetta Watson, and Roger Painter, Tennessee State University
- 10:20 – 10:40 Characterization of bacteria and geochemistry of springs in Nashville, Tennessee - by Patrice Armstrong, Carlton Cobb, Brandon Cobb, student interns, U.S. Geological Survey and Tennessee State University; Jennifer Stewart-Wright, Tennessee State University; and Tom Byl, U.S. Geological Survey and Tennessee State University
- 10:40 – 11:00 Conduit matrix interaction and the rate limiting step of contaminant transport in karst - by Kurt J. McCoy, Allen M. Shapiro, and Mark D. Kozar, U.S. Geological Survey Presented by Mark Kozar
- 11:00 – 11:20 Assessing age distribution and contaminant movement in ground water in the contributing recharge area to a public supply well in the karstic Upper Floridan Aquifer - by Brian G. Katz, Christy A. Crandall, W. Scott McBride, Patty A. Metz, and Sandra M. Eberts, U.S. Geological Survey
- 11:20 – 1:00 **LUNCH ON YOUR OWN**
- Numerical Modeling***
- 1:00 – 1:20 Modeling ground-water flow and solute transport in karst with lattice Boltzmann methods - by Michael C. Sukop, Shadab Anwar, and Jeff S. Lee, Dept. of Earth Sciences, Florida International University; and Kevin J. Cunningham and Christian D. Langevin, U.S. Geological Survey
- 1:20 – 1:40 Simulation of turbulent ground-water flow with MODFLOW-2005—Overview by Eve L. Kuniansky, Keith J. Halford, and W. Barclay Shoemaker, U.S. Geological Survey
- 1:40 – 2:00 Effects of turbulence on hydraulic heads and parameter sensitivities in preferential ground-water flow layers - by W. Barclay Shoemaker and Eve L. Kuniansky, U.S. Geological Survey
- 2:00 – 2:20 Simulation of ground-water flow in a fractured rock karst aquifer, Shenandoah Valley, Leetown, West Virginia - by Mark D. Kozar and Kurt J. McCoy, U.S. Geological Survey
- 2:20 – 3:00 **BREAK**
- Miscellaneous Topics in Modeling, Geophysics, and National Programs***
- 3:00 – 3:20 The value of single-well tracer studies for characterizing karst sites - by Tarra M. Beach, Vanderbilt University; Michael Bradley, U.S. Geological Survey; Roger Painter, Tennessee State University; and Tom Byl, U.S. Geological Survey and Tennessee State University
- 3:20 – 3:40 GIS and spatial statistical methods for determining sinkhole potential in Frederick Valley, Maryland - by Katarina Z. Doctor, George Mason University
- 3:40 – 4:00 Geophysical analysis of the Salmon Peak Formation near Amistad Reservoir Dam, Val Verde County, Texas, and Coahuila, Mexico, March 2006, to aid in piezometer placement - by Gregory P. Stanton, Wade H. Kress, Andrew P. Teeple, Michael L. Greenslate, and Allan K. Clark, U.S. Geological Survey

4:00 – 4:20 National Cave and Karst Research Institute: Partner for the USGS by Penny Boston, New Mexico National Institute of Mining and Technology and George Veni, National Cave and Karst Research Institute

4:20 – 6:20 **POSTER SESSION**

Thursday, May 29

8:00 – 5:00 Field Trip to Karst Features of the Mammoth Cave Area, Kentucky NOTE: BUS LEAVES FROM THE HAMPTON INN PARKING LOT.

Poster Session Titles

Mammoth Cave International Center for Science and Learning - by Rickard S. Toomey III and Shannon Trimboli, Western Kentucky University and Mammoth Cave National Park; Blaine Ferrell, Western Kentucky University; Bob Ward and Mike Adams, Mammoth Cave National Park

Estimating recharge to heterogeneous fractured-rock and karst aquifer systems in the Shenandoah Valley of Virginia and West Virginia - by George E. Harlow, Jr., David L. Nelms, Richard M. Yager, Mark D. Kozar, Ward E. Sanford, and Roger M. Moberg, U.S. Geological Survey

Impact of 1998-2002 drought on the karst aquifers of Clarke County in the Shenandoah Valley of Virginia - by David L. Nelms and Roger M. Moberg, U.S. Geological Survey

Ground-water/surface-water relations and water quality within the Mammoth Spring watershed, Dixie National Forest, Garfield County, Utah - by Lawrence E. Spangler, U.S. Geological Survey

Updating the USGS Karst Interest Group website by converting it into a dynamic web application - by Bradley D. Garner and Barbara J. Mahler, U.S. Geological Survey

Simulations of ground-water flow and particle pathline analysis in the contributing recharge area of a public-supply well in Temple Terrace, Tampa Bay region, Florida - by Christy A. Crandall, Leon J. Kauffman, and Brian G. Katz, U.S. Geological Survey

Performance evaluation of the MODFLOW-2005 conduit flow process applied to a karst aquifer underlying west-central Florida - by Melissa E. Hill and Angel Martin, Southwest Florida Water Management District

Ammonia oxidation by bacteria collected from a karst-bedrock well - by Kelly Ray and Roger Painter, Tennessee State University and Tom Byl, U.S. Geological Survey and Tennessee State University

Wetland removal of nutrients and pollution from a mixed sewer and karst spring system in Nashville, Tennessee - by Carlton Cobb, Jameka Johnson, Brandon Cobb, and Patrice Armstrong, Tennessee State University and U.S. Geological Survey; Lonnie Sharpe, Tennessee State University and Tom Byl, U.S. Geological Survey and Tennessee State University

Are karst bedrock aquifers at greater risk from alternative alcohol-fuel mixes compared to regular gasoline? - by Baibai Kamara, Carlton Cobb, Keyshon Bachus, Roger Painter, and Lonnie Sharpe, Tennessee State University; Tom Byl, U.S. Geological Survey and Tennessee State University

Residence time distribution for karst derived from independent gamma distributions of tracer travel distance and linear velocity - by Roger Painter and Valetta Watson, Tennessee State University

Episodic elevated coliform in vadose-zone water within Mammoth Cave National Park, Kentucky - by Rickard S. Toomey III, Western Kentucky University and Mammoth Cave National Park; Rick Olson, Mammoth Cave National Park ; and Bob Ward, Mammoth Cave National Park

Construction and use of a fractured-rock simulator to test horizontal borehole flow-measuring technologies - by Randall Bayless, U.S. Geological Survey

Collection of bathymetric data along two reaches of the Lost River within Bluespring Cavern near Bedford, Lawrence County, Indiana, July 2007 - by David C. Lampe, Scott E. Morlock, U.S. Geological Survey

A Multi-Tool Geophysical and Hydrogeological Investigation of a Karst Aquifer System, Cibolo Canyon Development Area, Bexar County, Texas by Sachin D. Shah, Bruce D. Smith, Allan K. Clark, and Wade H. Kress, U.S. Geological Survey

NATIONAL PROGRAMS

Overview of National Park Service Policies for Cave and Karst Management

By Dale Pate

National Park Service, 3225 National Parks Highway, Carlsbad, NM 88220

Abstract

The National Park Service (NPS) is the premier conservation agency of the United States Government and, as such, is bound by laws and policies to protect all resources including cave and karst resources. This paper will include a brief history of cave and karst management within the NPS and highlight important laws and policies that have shaped management policies and that currently govern the management of cave and karst resources at units of the NPS. Additionally, there will be a brief general discussion on scientific studies and research policies and their ties back to the credible “management” of cave and karst resources within the NPS.

INTRODUCTION

Management of cave and karst areas within National Park Service (NPS) units began in most places before the term “management” was put into play. Management for significant caves meant development and visitor access while the concept of karst landforms was not in the vocabulary or experience of managers. The world was a different place then and people had much different perspectives. Resources were items to be used. Early efforts to bring visitors into the parks, including cave parks, meant development. In many cases, this development proceeded without real knowledge of its effect on the resources. Mammoth Cave, Carlsbad Cavern, and Wind Cave are classic examples where buildings, sewer lines, and other infrastructure were built directly on top of the caves for convenience without a working knowledge of the relationship between the surface and the cave passages and rooms below. This happened in many parks, not just cave parks. As an example, buildings, parking lots, and other infrastructure were built directly on the roots of some of the big trees in Sequoia National Park. These structures were not placed to purposely harm the resources, but rather were placed to enhance the visitor’s experience.

As the environmental movement of the 1950s and 60s brought change to the American population, it also brought change to the NPS and, ultimately, to cave and karst management. While visitation and support for our National Parks will always be important, recent years have seen more emphasis on using science-

based data to support protection and conservation programs. These changes have made their way into laws, regulations, policies, and the general consciousness of managers, employees, and the public at large. This paper will explore a brief history of cave and karst management within the NPS, some of the laws and policies that have shaped this management, and end with a brief general discussion on scientific studies and research policies and their ties back to the credible “management” of cave and karst resources within the NPS.

EARLY HISTORY

Early cave and karst management efforts in National Park Service (NPS) units consisted mostly of making areas more convenient for visitors to see the great natural wonders the parks were created for. This included buildings, parking lots, sewer lines, and other infrastructure placed directly on top of important caves, elevators installed to quickly whisk visitors to and from the underground, and other amenities such as lunchrooms where visitors could eat in the cave. At the time, little was known about the surface and its direct relationship with the cave underneath. Trails and lighting were usually installed for maximum enjoyment of the cave scenery, many times along routes already established before an area was added to the NPS system. Cave management was not all bad during these times, but park units usually addressed visitor accommodation first while protecting resources as much as possible. As might be expected, more obvious and

spectacular resources received the most active protection.

Cave management in the National Park Service began to change during the early 1970's when Carlsbad Caverns National Park in New Mexico hired Charlie Petersen as a "cave specialist." Duties for the position were mostly to travel into the park's backcountry to look for new caves. This position was deemed a success and so a few years later when the position became vacant, Ronal Kerbo was hired as the new "cave specialist". During the next 15 years, Mr. Kerbo moved the position from a basic field technician into the management realm, taking on more and more complex issues and providing input into major park decisions involving caves, especially Carlsbad Cavern. Also during this time, Mr. Kerbo's knowledge and expertise on cave management issues became well-known throughout the NPS and many other entities such as various state parks. Much of his time in his later years at Carlsbad Caverns NP was actually spent traveling to other NPS units, state parks, and other areas to provide recommendations to solve perceived problems.

Karst systems and their management have not been at the forefront of park resource management despite the fact they are a major landform. The fact that they are often complex and hidden contributed to the lack of notice. Even today, some key managers do not really understand how karst systems work. This is not the case at Mammoth Cave National Park where the entire region consists of hundreds of thousands of acres of a karst landscape that is interconnected by hundreds of miles of cave passages. This is an area where hundreds of small farms dot a sinkhole plain with poor or no septic systems and where many sinkholes were used for trash dumps for decades. Threats to cave ecosystems and public health, inside and outside of the park, brought about significant changes in sewage disposal and a better understanding of the human-caused problems created in this amazing karst area. A regional sewage system now incorporates most local entities and does a much better job of keeping raw sewage out of the karst systems. While this region still faces daunting challenges, significant improvements have been made in understanding the regional karst systems and implementing

mitigation measures to better protect those systems.

Due to the needs of various cave and karst parks and the success of the program at Carlsbad Caverns National Park, a position was created at the national level in October 1995 within the Geologic Resources Division (GRD) to provide technical assistance for park units and to address problems and needs from a national perspective. Because of his expertise and knowledge, Ronal Kerbo filled this first national level Cave and Karst Program Coordinator position within the GRD. Before and during this time, cave parks were beginning to hire specialist positions within resource management divisions to help actively manage specialized cave and karst resources. There are now approximately 15 permanent and a number of seasonal positions in cave parks across NPS park units. These specialized positions have made significant contributions to the long-term understanding and protection of these important resources including oversight of high-quality surveys and inventories, the completion of a number of cave and karst management plans, airlock systems on elevator shafts to return airflow patterns to original conditions, double-walled sewer lines where these run directly over sensitive cave and karst resources, and a host of other projects too numerous to mention here.

The establishment of this position at the national level of the NPS also helped spur the establishment of national level positions of a similar nature within the U.S. Forest Service and the Bureau of Land Management. Both of these agencies manage numerous cave and karst areas within their properties.

IMPORTANT LAWS AND POLICIES

Every park unit has been created by a legislative act and signed by the President. The legislation that created each park has its own set of directives that determine what can happen in that park. Some are very vague while some are very specific. As an example, it is usually the directives within this initial enabling legislation for specific parks that has allowed fishing within many of the older established parks. An even more extreme example is that of Padre Island National Seashore. Its enabling legislation

recognizes existing private or state ownership of the mineral estate for much of the property and allows oil and gas drilling to occur within the National Seashore.

Another document important for park units is 36CFR – Code of Federal Regulations – Parks, Forests, and Public Property. This document spells out specific regulations for specific parks. In addition, the National Park Service Management Policies 2006 provides over-arching policies for all NPS units.

Numerous other laws enacted by Congress and signed by the President and the subsequent regulations for these laws have guided the NPS in the conservation and protection of cave and karst resources and other natural and cultural resources as well. A list of some of these more important laws is as follows:

- The Organic Act of 1916
- Wilderness Act of 1964
- National Environmental Policy Act of 1969 (NEPA)
- Endangered Species Act of 1973
- Clean Water Act of 1977
- Archeological Resources Protection Act of 1979 (ARPA)
- National Park Omnibus Management Act of 1988
- The Redwood National Park Act of 1988
- Clean Air Act of 1990
- Omnibus National Park Management Act of 1998

Two laws, in particular, have been enacted specifically for caves. The first and most important for the Department of Interior and the Department of Agriculture is the Federal Cave Resources Protection Act of 1988 with the subsequent regulations released in 1993. This act specifies that affected agencies will consider caves and the effects on them when allowing

and proceeding with other projects. This is especially important on U.S. Forest Service and Bureau of Land Management lands where conservation and preservation of resources is only one of numerous other competing land uses along with grazing, lumber production, and oil and gas extraction. For the NPS, whose mission to conserve and protect resources, one of the more valuable aspects of this law was to exempt cave locations and other pertinent information from the Freedom of Information Act. Combined with portions of the other laws mentioned above, caves and much of their contents within NPS units are well protected. The second law, The Lechuguilla Cave Protection Act of 1993, was specifically created to protect one cave located within Carlsbad Caverns National Park from extractive oil and gas activities on adjacent federal properties. This law created a Cave Protection Zone outside the park boundary based on the recommendations of a geology panel convened to provide a scientific rationale for the long-term protection of the cave.

The Superintendents of individual park units have the ultimate responsibility to care for the lands that have been set aside as America's treasures. This ultimate responsibility requires consistent policies from the national level while allowing flexibility at the park level. There are numerous policies, regulations, and planning documents that each park unit depends on. Planning documents within each park unit are important tools that define policies and future directions for park units. General Management Plans (GMP) are the primary planning document for each park with numerous other planning documents tied to these GMPs. To provide guidance and to dictate policy, many cave parks have prepared Cave and Karst Management Plans. One final document within a Superintendent's toolbox is the Superintendent's Compendium. Usually updated annually, this document spells out specific rules and policies for individual parks that are not found in other documents, but are considered necessary to operate parks.

One other key law that has less effect on how park's manage cave and karst areas, but is important to mention is the National Cave and Karst Research Institute Act of 1998. The efforts

of numerous individuals and organizations including the NPS culminated in the establishment of this important Institute in Carlsbad, New Mexico.

RESEARCH AND RESOURCE MANAGEMENT

The NPS encourages research within park units and as stated on pages 40-41 of the NPS Management Policies 2006, “*studies must abide by applicable laws, policies, and guidelines ...and be conducted by qualified personnel and conform to current standards of scholarship.*” The types of studies that can be allowed vary greatly, from inventory and monitoring activities to applied research. There is a NPS website where all research applications for work in any park must be filed. This website is: <http://science.nature.nps.gov/research/ac/ResearchIndex>

It is important to know that while a researcher uses a national-level website to apply for doing research in a specific park, personnel from that park will be deciding whether to allow the research or not and what limitations will be placed on the research. There are a number of factors that go into making a decision to allow research particularly if it involves collection of non-renewable resources such as speleothems. Potential researchers are encouraged to discuss the proposed research with appropriate personnel at the park where the research needs to be done. Each park has different needs and different ways of handling research requests so communication with the park as early as possible is an important means to accomplishing potential research.

Additionally, each park is a separate unit and for most, the research permit received for one park does not apply to other parks. Separate research applications have to be submitted for each park, even if it is the same research project.

In recent years, one factor has contributed to better protection and conservation of resources within NPS units. This has been the recognition by the NPS that a better staffed science and resource management division within parks will (1) provide better facilitation for scientific

studies and, (2) allow better access to the information derived from these studies when important decisions need to be made. An informed staff that can work with researchers as well as represent the park’s management helps bridge the gap between scientific research and the need to manage park resources for the future.

SUMMARY

Various laws, regulations, policies, and rules have been enacted over the years to refine how natural and cultural resources are cared for within NPS units. With cave and karst areas being recognized as complex, important resources, a number of cave parks have hired “cave specialist” positions to improve understanding and to provide and to provide accurate information to park management during the decision-making process. The Federal Cave Resources Protection Act of 1988 was the first law enacted to specifically recognize the value of cave resources and instruct the Departments of Interior and Agriculture to document “significant” caves and to consider potential adverse impacts to them during the decision-making process. NPS units have an array of documents that they use to provide protection and conservation to cave and karst areas. In recent years, there has been a move to use more accurate scientific data during the decision-making process on projects that may affect cave and karst areas.

REFERENCES

- Burger, P., and Pate, D., 2001, Using science to change management perspectives at Carlsbad Caverns National Park; *in* Kuniansky, E., ed., U.S. Geological Survey Water-Resources Investigations Report 01-4011, p. 47-51.
- Management Policies 2006, Department of the Interior, National Park Service, p. 1–168.
- Pate, D., 2003, A comprehensive cave management program at Carlsbad Caverns National Park; *in* Rea, G. T., ed., Proceedings of the 2003 National Cave and Karst Management Symposium, p. 38-42.
- Sellers, R., 1997, Preserving Nature in the National Parks: A History, p. 1-380.

National Cave and Karst Research Institute: Partner for the USGS

By Penelope J. Boston^{1,2}, and George Veni¹

¹ National Cave and Karst Research Institute, Carlsbad, NM 88220

² New Mexico Institute of Mining and Technology, Socorro, NM 87801

Abstract

The National Cave and Karst Research Institute (NCKRI), created by Congress in January 1998 and headquartered in Carlsbad, New Mexico, aims to provide the cave and karst community with an unprecedented opportunity to further research, education, information transfer, and resource management revolving around these critical, fragile, globally significant, yet poorly understood terrains. The Institute's legislation offers the opportunity to develop a unique style of national effort with a broad base of both federal and non-federal support including 1) collaborative projects, 2) shared administrative responsibilities, 3) matching funds, 4) joint publications, 5) potential as a go-to organization for other agencies, other organizations, and individuals, and 6) other partnership arrangements of a nature possibly not yet even conceived.

NCKRI is an unusual, possibly unique, amalgam of a federal agency (National Park Service [NPS]), a state-supported academic institution (New Mexico Institute of Mining and Technology, aka NMT), and a highly karst-aware municipality (Carlsbad, New Mexico). These three entities joined together to implement the enabling legislation and to create a unified institute from very disparate components. The initial organizational structure, with direct control through NPS and a civil service NPS director, proved cumbersome and difficult in light of unprecedented budget constraints on NCKRI. Unlike other federally mandated organizations, NCKRI has been charged with finding *at least* half of its funding from non-federal sources. The impossibility of a federal entity engaging in active non-federal fundraising became clear and in 2006, NCKRI transitioned to a new arrangement as a non-profit corporation under the aegis of NMT. All employees of NCKRI are thus NMT employees and have full ability to engage in fund raising, grant writing, and solicitation of donations from the business and private sectors. The new permanent director, Dr. George Veni, was brought on board in early 2007 under this new arrangement. Current staff includes Director Veni, Dr. Penelope Boston (Associate Director for the NCKRI Academic Program and Professor at NMT), Dr. Lewis Land (NCKRI karst hydrologist through the New Mexico Bureau of Geology and Mineral Resources), Ms. Deborah Herr (Administrative Services Coordinator), and Ms. Lisa Majkowski (Program Manager for NCKRI and Cave and Karst Studies at NMT). The staffing plan is in hand and new staff members will be added as the financial situation allows and needs dictate. An education coordinator position is planned for later in 2008.

Growing pains have also occurred in other areas. The construction of NCKRI Headquarters in Carlsbad suffered setbacks not unusual for public buildings. It is now back on track with construction to begin soon. The building will be located along the Pecos River near downtown Carlsbad. Its roughly 1,600 m² (17,000 ft²) will include a bookstore, a laboratory, classrooms, and interactive educational and museum space on the first floor. A library and administrative space will occupy most of the second floor. Given the high vulnerability of karst terrains to adverse environmental impacts, the building will be a model for sustainable building and management practices, which will be highlighted throughout the facility. Some features will include recycled materials, water and energy efficient fixtures and equipment, creative building design to minimize energy consumption, and a rainwater harvesting system. The structure will be solar-ready; panels will be installed at a later date. In collaboration with Bat Conservation International, NCKRI Headquarters will be the first building constructed with an artificial bat roost as part of its design. Cameras, microphones, and various probes in the roost will provide live images and data into the museum and the NCKRI website for research and public education.

In spite of the infant nature of the organization, NCKRI has already achieved some significant accomplishments. These include:

- Participation in the development of the U.S. Geological Survey's (USGS) National Karst Map (2001-present);
- Facilitation and support for several karst conferences: Karst Interest Group workshops (2002, 2005, 2008), National Cave and Karst Management Symposia (2005, 2007), Karst Waters Institute symposia (2007, 2008), 15th International Congress of Speleology (2009);

- Coordination, co-authorship, and funding for *Recommendations and Guidelines for Managing Caves on Protected Lands* (2003) published by the Karst Waters Institute;
- Sponsorship for *Ice Age Cave Fauna of North America* (2003) published by the Denver Museum of Nature and Science;
- Organization of symposia and instruction for workshops at the Geological Society of America Convention (2004, 2008);
- Support and education for NCKRI scholars in the Cave and Karst Program at NMT: Setsuko Shindo (MS, 2005), Erin Kay (MS 2008), Kevin Stafford (Ph.D., 2008), Megan Curry (MS, 2008 anticipated), Laura Rosales-Lagarde (Ph.D., 2008 anticipated), four senior thesis students;
- Establish a Visiting Scientist Program, which has included Dr. Thomas Strong, Dr. Scott Rice-Snow, and Dr. Alexander Klimchouk, who as a result of his work with NCKRI produced NCKRI Special Paper No. 1, *Hypogene Speleogenesis: Hydrological and Morphological Perspective*.
- Development of the landmark Karst Information Portal (posted to the Internet in 2007 and discussed separately at this meeting by Spencer Fleury) with the University of South Florida, University of New Mexico, and the International Union of Speleology.

In late 2007, representatives of NCKRI and USGS met in Reston, Virginia, to discuss potential partnerships, especially in lieu of NCKRI's change in status from being part of NPS to a non-profit. They found ample possibilities to work together in the future, but also two significant impediments: limited NCKRI staff and restrictions on federal support for NCKRI without matching non-federal funds. At least one impediment will be removed in the near future. Construction of NCKRI Headquarters is expected by the end of 2009, allowing NCKRI to hire additional staff to more effectively work with USGS and other potential partners. Meanwhile, efforts to rewrite NCKRI's enabling legislation are in progress to allow NCKRI and federal agencies to cooperatively work on the many karst issues that need study, and without the present encumbrances.

National Cave and Karst Research Institute's Karst Information Portal

By E. Spencer Fleury

Karst Information Portal, University of South Florida, LIB 122, 4202 E. Fowler Ave, Tampa, FL 33620

Abstract

Founded in 2005 and rolled out in 2007, the Karst Information Portal (KIP) (<http://www.karstportal.org>) represents an effort to resolve certain recurring challenges inherent to locating and accessing existing karst literature. First, the publication of karst-related research in academic journals has historically crossed disciplinary lines; researchers working in one discipline may be unaware of relevant literature from another discipline, or may even be unable to identify the “flagship” journals of other fields. Second, much of the existing karst literature is in the form of grey literature, which can be notoriously difficult to track down and acquire. This fragmentation of karst-related resources makes it difficult to address questions of karst science without significant duplication of effort. Third, many difficult-to-find resources are available in hard copy only, often stored in private libraries or collections where they could be lost forever in the case of a fire or flood.

The KIP is intended to remedy these difficulties by providing an online, centralized repository of karst literature, accessible to anyone with an Internet connection. KIP combines aspects of traditional web portals (in that it provides up-to-date links to karst information stored elsewhere on the web) and databases (in that some of the resources provided by KIP are stored locally on its own server). As of January 2008, the KIP catalog contained more than 4,000 content records. While KIP shall attempt to acquire the widest possible variety of karst resources, the project’s emphasis is on grey literature and raw data that have historically been most difficult to locate. KIP is also intended to facilitate collaboration among karst professionals and enthusiasts across the globe. Registered users are able to upload descriptions of recent research projects, as well as communicate directly with one another in the portal’s forums.

This presentation will demonstrate the basic functionality of the KIP and describe the contents of the catalog, as well as discuss some of the portal’s ongoing projects and long-term goals. These include acquiring and scanning hard copy resources, developing a library of oral histories of leading figures in karst science, and participating in effort to develop a world karst map.

Mammoth Cave International Center for Science and Learning

By Rickard S. Toomey, III¹, Shannon Trimboli¹, Blaine Ferrell², Bob Ward³ and Mike Adams³

¹Mammoth Cave International Center for Science and Learning, 1906 College Heights Blvd #31066, Bowling Green, KY 42101-1066

²Western Kentucky University, 1906 College Heights Blvd #31066, Bowling Green, KY 42101-1066

³Mammoth Cave National Park, PO Box 7, Mammoth Cave, KY 42259

Abstract

The Mammoth Cave International Center for Science and Learning (MCICSL) is a cooperative venture of Mammoth Cave National Park and Western Kentucky University. Funding, logistical support, and governance of MCICSL are shared equally by both entities. It is a part of a network of 17 research learning centers within the National Park Service. The goals of MCICSL and the other centers are to

- I. Facilitate the use of parks for scientific inquiry
- II. Support science-informed decision making
- III. Communicate the relevance and provide access to knowledge gained through scientific research
- IV. Promote science literacy, and resource stewardship.

MCICSL has been operational since the middle of 2005, so we are still building programs. Current staffing of the MCICSL consists of a Research Director (Toomey) and a part-time Education Program Specialist (Trimboli). In spite of the limited staff, the center is leading both research and education based programs.

MCICSL coordinates scientific research and research permitting at Mammoth Cave National Park and consults with the park on scientific issues. MCICSL staff also assists researchers in arranging the logistics of research in the park. Toomey is co-lead on several research projects involving NPS caves including a multi-park lighting research project, research to address on-going E. coli issues in cave waters, and a study to improve monitoring of visitation to backcountry caves. Toomey has also participated in several projects to implement changes in cave infrastructure and management by providing technical expertise and links to outside researchers. These include projects to modify cave lighting and paleontological compliance for a cave trails project. The center also helps recruit researchers and volunteers.

MCICSL staff lead or participate in numerous educational activities that highlight research at the park. Our educational efforts serve a variety of internal and external audiences. The methods employed to reach such diverse audiences are also widely varied. They include such things as workshops, internships, research-focused field opportunities, internal educational presentations, and internal and external research summaries. Some examples of education projects include teacher training workshops, WKU's Karst Field Studies Program, the Geoscience-Teachers-in-the-Parks pilot project and a demonstration project with Caverna High School.

Updating the USGS Karst Interest Group Website by Converting it into a Dynamic Web Application

By Bradley D. Garner¹ and Barbara J. Mahler²

¹U.S. Geological Survey, 5522 Research Park Drive, Baltimore, MD 21228

²U.S. Geological Survey, 8027 Exchange Dr., Austin, TX 78727

Abstract

The Karst Interest Group (KIG) maintains a website that is a valuable resource for USGS scientists and also is a gateway for bringing USGS science to the broader scientific community and the general public (<http://water.usgs.gov/usgs/ogw/karst>). Historically, the website has been maintained on a volunteer basis and its content has been relatively limited. Recognizing the importance of karst-water resources and the expertise of the USGS in this field, the authors are expanding and updating the website by developing new content and presenting it using dynamic web technologies. New content includes a national-scale map of karst regions, a list of major USGS karst investigations and monitoring stations (past and present), and a list of key karst publications by USGS scientists both in journals and USGS publications. The new content is stored in relational database tables and linked together using common keys. Content is being presented using dynamic web technologies, which create web pages on-demand using information from a database (as an example, NWISWeb uses dynamic web technologies). The dynamic nature of the website allows the map to be interactive, presents the latest content in a flexible and maintainable way, and provides the ability for internal USGS users to submit suggestions for content updates and corrections.

KARST MAPPING

Karst Regions of the World (KROW): Global Karst Datasets and Maps to Advance the Protection of Karst Species and Habitats Worldwide

By Emily Hollingsworth¹, Van Brahana¹, Ethan Inlander², and Michael Slay²

¹University of Arkansas, Ozark Hall 113, Fayetteville, AR 72701

²The Nature Conservancy of Arkansas, 675 Lollar Lane, Fayetteville, AR 72701

Abstract

Owing to the lack of a single accessible and comprehensive source of information on the global distribution of karst habitats and species, The Nature Conservancy and the University of Arkansas are collaborating on compiling a comprehensive database of karst distribution and biodiversity. This compilation will serve as the preliminary foundation for a digital global karst dataset which will be used to delineate (1) a worldwide map of karst regions, and (2) a geologic and biogeographic framework for initiating karst conservation and planning on a global scale.

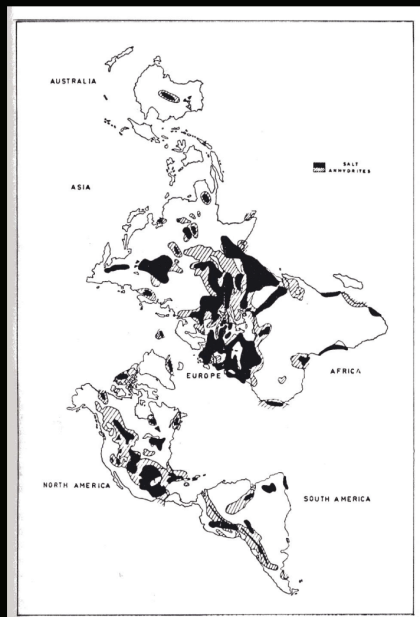
Rapid advancements and expanding technologies in both karst science and Geographic Information Systems (GIS) make the timing of this effort optimum. Multiple groups in multiple disciplines are actively working on developing regional and global karst maps, reflecting the growing perception that land use in karst settings is becoming a critical problem. Thus far, the efforts have not generated major redundancy, but the expanding activity suggests that duplication of effort is drawing near, and integration of data-set population and map generation requires communication and coordination to optimize the needs of all karst stakeholders. The importance of characterizing, conserving, and protecting the karst regions of the world cannot be emphasized strongly enough, given the increasing population density of humans that reside in these settings, and the ecosystems that rely on karst environments and karst water to sustain life. This paper summarizes a brief history of the problem, the rationale behind our specific effort, initial progress we have made thus far, and our perceived needs to draw the entire karst community into this long-term, ongoing effort.

INTRODUCTION

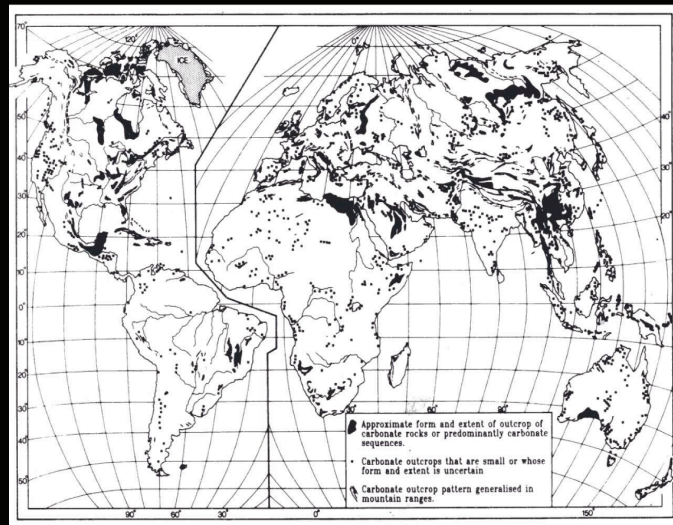
Owing to the lack of a single accessible and comprehensive source of information on the global distribution of karst habitats and species, The Nature Conservancy (TNC) and the University of Arkansas (UofA) are collaborating on delineating the worldwide distribution of karst regions of the world (KROW) using current and past karst maps and research. This compilation will serve as the preliminary foundation for a digital global karst dataset which will be used to delineate (1) a worldwide map of karst regions, and (2) a geologic and biogeographic framework for initiating karst conservation and planning on a global scale.

Mapping of karst features has long been an important tool for conservation scientists, but typically mapping has been undertaken at local or regional scale (Johnson and Quinlan, 1994; Weary, 2005; Jianhua et al., 2007). At a continent scale (Culver, 1999; Veni et al., 2001; Epstein et

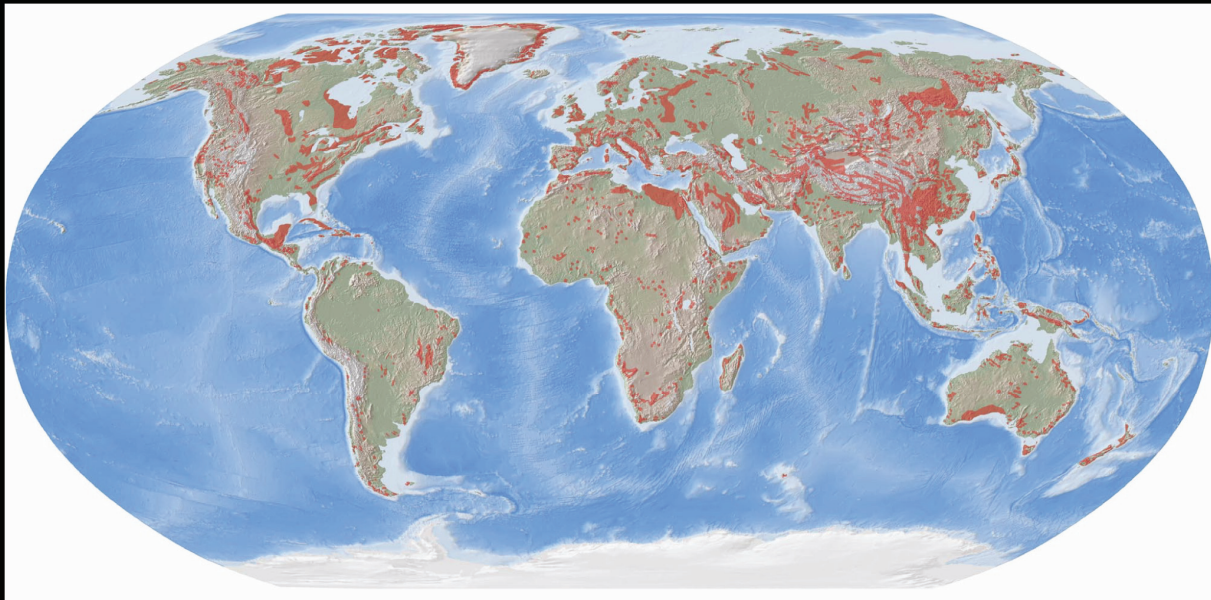
al., 2001; Epstein et al., 2002) or global scale (Kozary et al., 1968; Ford and Williams, 1989; Ford and Williams, 2007), several efforts to integrate all known data into a meaningful map of karst of the world have been undertaken (figure 1). Unfortunately, the variability of existing data and maps, and the disparity of project goals which have led to construction of component maps have made integration of these world maps truly difficult. Highly variable project objectives, funding, map scales, karst understanding, discipline focus, resource needs, data formats, accuracy, precision, completeness, and willingness to share available data have limited efforts to compile such a product.



a) Kozary et al. 1968



b) Ford and Williams, 1989



c) Ford and Williams, 2007

Figure 1.-Global occurrence of evaporite and carbonate rock. Figure 1a shows evaporite rocks, most of which (90% of gypsum/anhydrite, 99% of halite) are covered (after Kozary et al., 1968). Figure 1b shows major outcrops of carbonate rocks of the world (after Ford and Williams, 1989). Figure 1c shows the latest revision to major outcrops of carbonate rocks of the world (after Ford and Williams, 2007).

Brief History of TNC Involvement in Karst

TNC has established the goal to protect 10% of each of the world's major habitat types by 2015. Despite its importance to humans and species, the 2015 goal does not address karst conservation directly. Inasmuch as karst landscapes occur in at least 26 of 29 countries where TNC works, it is their intent to address and protect karst settings through ecoregional planning efforts. Prior to this project, no mapping or analyses were available to steer global karst conservation efforts. This project represents the preliminary effort to delineate these areas, and to establish an interactive ongoing data base that will facilitate the needs of TNC and the karst community for the upcoming decade.

Developing a more complete and accurate set of global karst tools is a necessity. Karst areas are underrepresented in globally protected areas, adding urgency to the need for tools to support conservation. Not only will the creation of a digital karst map and archive allow for ranking and delineation of areas of environmental and ecological sensitivity by blending detailed data based on hydrology, land use, biodiversity, and distribution of endangered and threatened species, it also will serve as the framework for developing a GIS karst toolbox. It is believed that this classification will be of critical importance in directing future efforts in karst management and conservation.

Objectives and Scope of This Report

The objectives of this report are twofold: (1) to introduce the rationale and planned methodology of the project, in hopes of eliciting meaningful suggestions for improvement before the project is fully underway; and (2) to share a case study from Australia as an example to illustrate problems, approaches, and work products that have been encountered thus far. The report is preliminary, and reflects an early stage of what is hoped to be a long-term project.

Terminology/Definitions

Understanding data base construction and mapping needs of KROW requires a precise definition of the following terms. The first three represent distinct types of subterranean environments, and the last provides limits to the meaning of regions.

Carbonate Karst. Carbonate karst is a terrain with distinctive hydrology and landforms arising from the combination of high rock solubility and well-developed secondary porosity. Ground-water flow velocities typically are much faster here than they are in porous media, contaminant attenuation mechanisms typically are much less effective, and flow tends to be anisotropic and heterogeneous. In most cases, carbonate karst is produced by chemical dissolution by slightly acidic water on a soluble layer of bedrock, notably limestone or dolomite.

Evaporite Karst. Evaporite karst is similar to carbonate karst in that dissolution is the dominant process, but unlike carbonate karst, the very high solubility of evaporite minerals produces highly-mineralized ground water. Environments and ecosystems in evaporite karst would be expected to organisms that are more tolerant of dissolved solutes. The most common of these lithologies include gypsum, anhydrite, and halite

Pseudokarst. Pseudokarst is an environment or setting that resembles karst, but where solution is not a critical formative process to produce cavities, isolated voids or connected passages or tubes. The subsurface environment in these areas is similar in many ways to other types of karst, but because they were formed by processes other than dissolution, ground-water flow, water quality, and environmental factors typically are distinct.

Regions. Regions are areas of land or water that contain a geographically distinct assemblage of ecosystems and natural communities; each may be differentiated by climate, subsurface geology, physiography, hydrology, soil, and vegetation.

METHODOLOGY

Following the approach of Veni et al. (2001), this study has divided KROW into 3 broad categories, carbonate, evaporite, and pseudokarst. Carbonate and evaporite karst were distinguished from one another because of the major differences in water quality created by rock-water interaction in these settings, and pseudokarst was distinguished from the other two because its process of formation is so completely different than normal karst. All methods contribute to similar subsurface ecosystems, but each has the potential to harbor a distinct group of organisms based on unique physical and chemical attributes of lithology and mode of formation.

The distinction between buried and surface karst was determined to be outside the scope of the overarching needs of TNC. Although buried versus surface distinction was included in the map of U.S. karstlands (Veni et al., 2001), and is obviously important to hydrogeologists and others in the karst community, with respect to environments suitable for cave-adapted organisms, it was considered and rejected. The reason for rejection was the fact that almost all subsurface karst environments have the potential to and likely do host microbes, yet fewer than 1% have been studied or sampled. Based on this dearth of data, and the widespread distribution potential, any delineation of deeply buried karst regions would include most of the continental land masses. Such a gross overestimation of karst regions would detract from those surface areas that are truly home to fragile ecosystems.

Data-set architecture and maps are initially being created at the continent scale. Geologic maps of countries exist for most of the world, and where these are accessible in digital format, shape categories for carbonate karst, evaporite karst, and pseudokarst will be captured to generate preliminary continent-scale work maps. Obviously, if karst maps exist for countries, these will be incorporated directly. Where no digital data sets are available, paper maps will be scanned and incorporated into ArcMap 9.2, where they will be transformed into the projection of the referenced base map.

Data-base population will be a continuing and an ongoing process. Within continents, further subdivision by country, state, region, and local area will be undertaken as necessary to adequately delineate the preliminary karst boundaries based on the geology maps. The data base will be keyed by a location number to identify attributes, accuracy, and relations between karst features. Specific documentation regarding map scale, display attributes, analysis properties, map use, data source, and relevant annotations will be input as available into the data base, and made accessible through the GIS by pointing at locations on the map.

ArcMap 9.2 and ArcInfo GIS and mapping software have been chosen as the spatial analysis, visualization, and spatial data-management tool for KROW. Digital-processing techniques will be applied for data visualization, enhancement, and interpretation of multiple geodata sets.

Data mining is being undertaken from search engines and internet resources, as well as obvious publications and maps in the public domain. Major data sources include geological surveys, journal articles, speleological and caving societies, unpublished theses, university and karst institutes, conference proceedings, textbooks, engineering reports, water-tracing studies, and caving-club newsletters. These sources are further supplemented with personal contacts across the wide range of science, engineering, and caving—in fact, contact with any groups that focus on some aspect of karst. Selected examples of these groups and their information dissemination outlets include the Karst Interest Group (KIG) of the U.S. Geological Survey (USGS), the Karst Commission of the International Association of Hydrogeologists, the International Union of Speleology, the Karst Information Portal, the National Speleological Society, the Karst Waters Institute, Cave Research Foundation, British Cave Research Association, National Cave and Karst Research Institute, Australasian Cave and Karst Management Association, Canadian Karst Resources and Issues, Slovenian Karst Research Institute, Karstica European Network, UIS Commission on Karst Hydrogeology and Speleogenesis, South American Landscape,

DISCUSSION—CASE STUDY OF DELINEATING KARST REGIONS OF AUSTRALIA

To show problems, approaches, and work products thus far encountered, we have chosen the case study of distribution of karst in Australia for an example of the methods followed (figure 2). Australia served as a suitable example because extensive work had been done for the continent, yet the complexity was not so great as to overwhelm the data base.

The first step was capture of the referenced base map of Australia, with geographic coordinate system GCS_WGS_1984, added to an active ArcMap window, (figure 2a). The map “Karst of Australia” (Ken G. Grimes, written commun., 2007) was selected to be incorporated into this GIS representation (figure 2b). This map was individually incorporated into an active map where the projection of the specific raster dataset was identified. The raster image was overlain on the base map and the two maps showed comparably different projections. It was necessary to align the two maps where they most closely “fit” together. Using the Georeferencing toolbar, (figure 2c), the raster image was georeferenced to the referenced data by adding control points of known locations on the two maps, (figure 2d). A suitable number of links were required to be added to keep the residual error to a minimum, thereby optimizing accuracy. At this stage, the raster image was able to be transformed into the projection of the base map, and align with the vector dataset, (figure 2e).

Karst features represented on raster images require transformation into individual geographic and georeferenced entities. When applicable, different features, such as surface, subsurface, pseudokarst, and cave locations will be spatially referenced. This will yield data layers of specific karst extents for individual areas.

As additional karst distribution maps are added to the GIS representation, it will be a

necessity to determine which of the different karst boundaries to follow when there are discrepancies from map to map. When an inconsistency occurs, each area will be researched to determine the most representative delineation. If possible, local experts will be addressed for site specific input.

A main challenge at a continent scale was integrating and distilling large amounts of different data types, obtained from different sources, compiled from different formats emphasizing different purposes, and developed on different scales. In order to use these data for mapping and interpretation, sources had to be evaluated for fitness of use before point data could be spatially linked to a map. Individual map scales, spatial representations, accuracy, and format required assessment prior to incorporation into a GIS database.

Examples of difficulties to representing continent-scale karst are represented by sites on figure 2e that are shown by small circles and isolated + symbols. Also, the smooth and straight boundaries of the Nullarbor Plain in the south-central part of the continent are typical of generalized boundaries that we feel require revision based on the geologic map. Although these problems are philosophically based, relating to the potential for karst development based on the known lithology, they are likely justified when it comes to characterizing intervening areas that have yet to be studied. The overall objective of protecting karst ecosystems seems to warrant a conservative approach on this first preliminary mapping, and that is the approach we followed.

Yet another problem dealt with the need to identify ecosystems within various areas of karst occurrence. The emphasis thus far has been on distribution mapping, but the database system required flexibility of expansion on the front end of the project to minimize adding fields later, essentially modifying the data base after the project was underway. Intensive planning was critical, and involvement of TNC and karst ecologists was essential to the preliminary phase of the project.

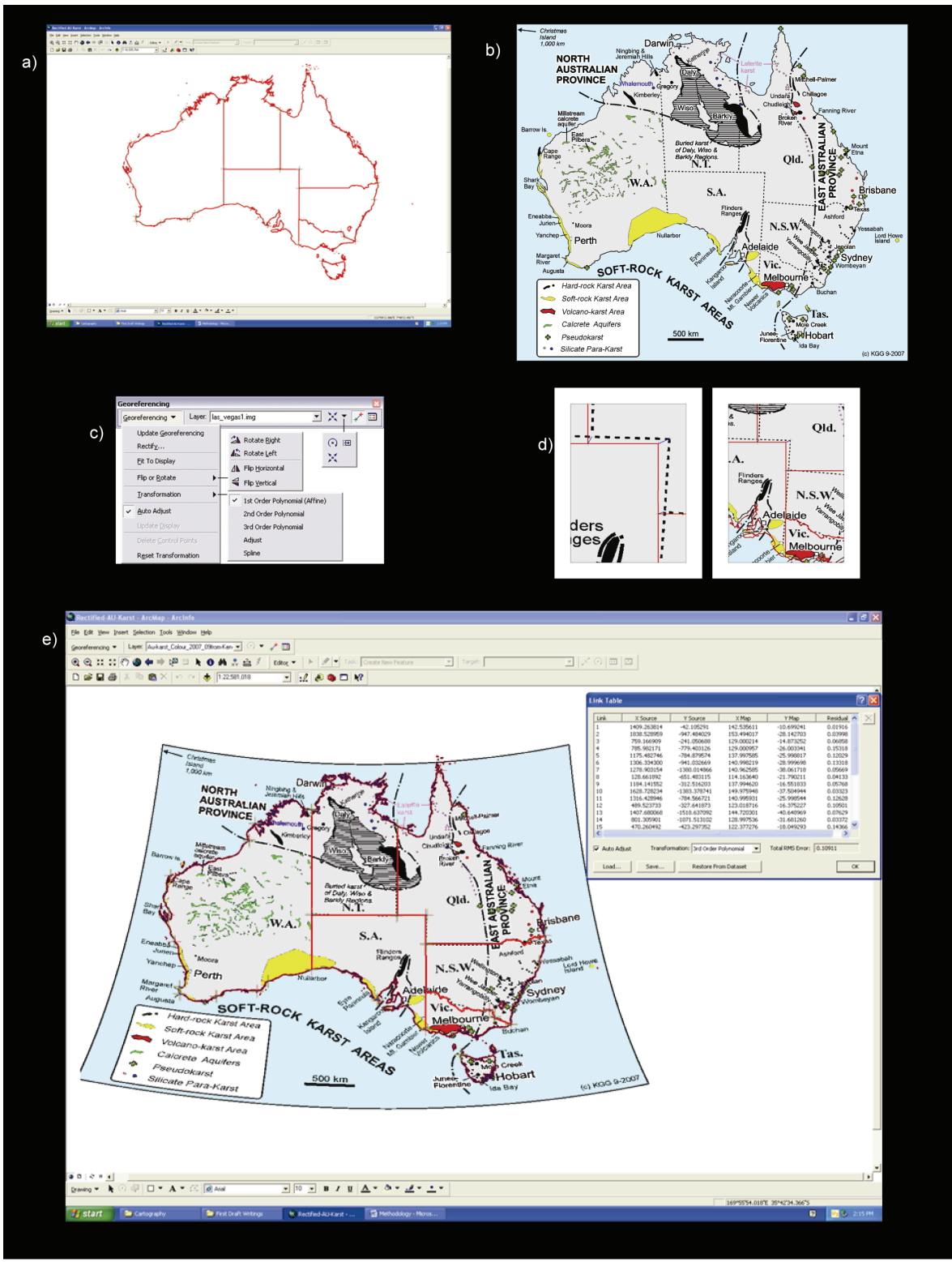


Figure 2a (top left). Image of the referenced base map that depicts the geographical boundaries of Australia. Figure 2b (top right) Raster image of Karst Distribution of Australia by Grimes et al 2007. Figure 2c (middle left) Standard Georeferencing tool bar associated with ArcMap 9.2. Figure 2d (middle right) is a representation of control points before transformation takes place. Figure 2e (bottom) A view in ArcMap 9.2 of the raster image of karst of Australia aligned with the vector dataset of the geographical boundaries of Australia and the two are projected in the GCS_WGS_1984, and the associated data points needed for the transformation.

SUMMARY

The creation of the global karst dataset and map described herein should facilitate worldwide communication on karst distribution, and provide the framework for ongoing input and construction of a meaningful GIS. The final products will be the first step toward organizing sources of karst research and references that hopefully will foster collaboration and understanding among karst scientists and conservationists.

The current status regarding the KROW map and archive is promising. The progress of data compilation is progressing rapidly, and although far from complete, it represents a strong first step. The rationale of the methodology allows the database to be built modularly, expanding in a logical progression to accommodate refinements in karst understanding, and new data.

Finally, Karst Regions of the World will help focus conservation where it is most needed, by making useful information accessible to decision makers and conservation practitioners around the world. The map of KROW will be a useful tool for conservation planning across a range of scales, and will help assess conservation efforts and data gaps worldwide.

If you think you have information that could be a valuable component to this effort, please don't hesitate to contact Emily Hollingsworth at ehollin@uark.edu

SELECTED REFERENCES

- Carbonates and Evaporites, 1997, (Special issue containing papers presented at a Symposium on Evaporite Karst: Processes, Landforms, Examples, and Impacts), v. 12, no. 1.
- Culver, D.C., 1982, *Cave life: Evolution and ecology*: Cambridge, Mass., Harvard University Press, 223 p.
- Culver, D.C., 1999, Terrestrial ecoregions of North America. A Conservation Assessment: in Ricketts, T.H., ed., *Ecosystem and Species Diversity Beneath Our Feet*: Washington, DC, Island Press, p. 56-60.

- Culver, D.C., and White, W.B., 2005, *Encyclopedia of Caves*: Burlington, MA, Elsevier Academic Press, 654 p.
- Davies, W.E., Simpson, J.H., Ohlmacher, G.C., and Kirk, W.S., and Newton, E.G., 1984, *Engineering aspects of karst*: U.S. Geological Survey, National Atlas, scale 1:7,500,000.
- Epstein, J.B., and Orndorff, R.C. and Weary, D.J., 2001, U.S. Geological Survey National Karst map [abs.]: National Speleological Society Convention Program Guide, p. 87.
- Epstein, J.B., Weary, D.J., Orndorff, R.C., Bailey, Z.C., and Kerbo, R.C., 2002, U.S. Geological Survey Karst Interest Group Proceedings, Shepherdstown, West Virginia:
- National Karst Map Project, an Update: U.S. Geological Survey, Report Water-Resources Investigations Report 02-4174, p. 43-44
- Finalyson, B., and Hamilton-Smith, E., 2003, *Beneath the surface: A natural history of Australian caves*: Sydney, Australia, University of New South Wales Press, 199 p..
- Florea, L.J., Fratesi, B., and Chaves, T., 2005, The reflection of karst in the online mirror: A survey within scientific databases, 1960-2005. *Journal of Cave Karst Studies*, v. 69, no.1, p. 229-236.
- Ford, D.C., and Williams, P.W., 2007, *Karst Hydrology and Geomorphology*: London, Wiley Chichester, 2nd ed., 576 p..
- Ford, D.C., and Williams, P.W., 1989, *Karst Geomorphology and Hydrology*: London, Unwin Hyman, 601 p.
- Gao, Y., Alexander, E.C., and Tipping, R.G., 2002, The development of a karst feature database for southeastern Minnesota: *Journal of Cave and Karst Studies*, v. 64 (1), p. 51-57.
- Gunn, J., 2004, *Encyclopedia of Caves and Karst Science*. New York, Fitzroy Dearborn, 902 p.
- Hamilton-Smith, E., 1997, *The IUCN Guidelines for Cave and Karst Protection: Report Proceedings of the 1997 Karst and Cave Management Symposium*, 82 p.

- Harmon, R.S., and Wicks, C.M., 2006, Perspectives on karst geomorphology, hydrology, and geochemistry - a tribute volume to Derek C Ford and William B. White: Geological Society of America, Special Paper 404, 366 p.
- Jianhua, C., Daoxian, Z., Cheng, Z., and Zhongcheng, J., 2007, Karst ecosystem of Guangxi zauang Autonomous Region Constrained by Geological Setting: Relationship between carbonate rock exposure and vegetation coverage, in International Confrence on Karst Hydrogeology and Ecosystems, Bowling Green, USA: Bowling Green, KY, Hoffman Environmental Research Institute, p. 15-16.
- Johnson, K.S., and Quinlan, J.F., 1994, Regional mapping of karst terranes in order to identify potential environmental problems; Changing karst environments; hydrogeology, geomorphology and conservation; abstracts of papers: Cave and Karst Science, v. 21, p. 15.
- Klimchouk, A., Ford, D.C., Palmer, A.N., and Dreybrodt, W., January 2000, Speleogenesis. Evolution of karst aquifers: Huntsville, Alabama, National Speleological Society, 527 p.
- Klimchouk, A., 2007, Hypogene Speleogenesis: Hydrogeological and morphogenetic perspective: National Cave and Karst Research Institute Special Paper no.1, v. 1, 106 p.
- Kozary, M.T., Dunlap, J.C., and Humphrey, W.E., 1968, Incidence of saline deposits in geologic time. Geological Society of America, Special Paper 88, p. 43-57.
- Kranjc, A., Gabrovsek, F., Culver, D.C., and Sasowsky, I.D., 2007, Time in karst: Charles Town, West Virginia, Karst Waters Institute Special Publication 12, p. 246.
- Palmer, A.N., 1991, Origin and morphology of limestone caves: Geological Society of America Bulletin, v. 103, no. 1, p. 1-21.
- Spalding, M.D., Fox, H.E., Allen, G.R., Davidson, N., Ferdana, M.F., Halper, B.S., Jorge, M.A., Lomban, A., Lourie, S.A., Martin, K.D., McManus, D., Molnar, J., Recchia, D.A., and Robertson, J., 2007, Marine Ecoregions of the World: A bioregionalization of coastal and shelf areas: *BioScience*, v. 57, no.7, p. 573-583.
- Taylor, C.J., Nelson, Jr., H.S., Hileman, Gregg, Kaiser, W.P., 2005, Hydrogeologic framework mapping of shallow, conduit-dominated karst—Components of a regional GIS-based approach: in Kuniansky, E.L., ed., U.S. Geological Survey Karst Interest Group Proceedings, Rapid City, South Dakota, September 12-15, 2005: U.S. Geological Survey Scientific Investigations Report 2005-5160, p. 103-113.
- Veni, G., April 2002, Revising the karst map of the United States: *Journal of Cave and Karst Studies*, v. 64 (1), p. 45-50.
- Veni, G., DuChene, H., Crawford, N.C., Groves, C.G., Huppert, G.N., Kastning, E.H., Olson, R., and Wheeler, B.J., 2001, Living with Karst- A Fragile Foundation: American Geological Institute Environmental Awareness Series 4, Alexandria, Virginia, 64 p.
- Weary, D.J., 2005, An Appalachian regional karst map and progress towards a new National karst map: in Kuniansky, E.L., ed., U.S. Geological Survey Karst Interest Group Proceedings, Rapid City, South Dakota, September 12-15, 2005: U.S. Geological Survey Scientific Investigations Report 2005-5160, p. 93-102.
- White, W.B., 1988, Geomorphology and hydrology of karst terrains: New York, Oxford University Press, 464 p.

Characterizing Regional Karst Types Under the Framework of the New National Karst Map

By David J. Weary¹, Daniel H. Doctor¹, Jack B. Epstein¹, and Randall C. Orndorff²

¹U.S. Geological Survey, 12201 Sunrise valley Drive, MS 926A, Reston, VA 20192

²U.S. Geological Survey, 12201 Sunrise valley Drive, MS 908, Reston, VA 20192

Abstract

Compilation of a new national karst map based on lithologic descriptions chiefly derived from state geologic maps is complete. This is a first approximation of areas with potential for karst development in carbonate, evaporate, and volcanic (features analogous to karst) rocks. Classification schemes are being developed to further subdivide these areas into useful karst type divisions. Since karst landscapes exhibit variable development in different areas of the United States, we need to first develop a geographic classification hierarchy. Implementation of a system similar to the ecologic classification scheme of Bailey and others (1994) would enable organization of karst areas within naturally defined regions of the United States and provide a framework under which multidisciplinary karst research can be organized at all scales.

INTRODUCTION

As the initial phase of compilation of a new national karst map is nearing completion, the next logical steps are to refine the delineation of potentially karstic areas and also to segregate karst areas within a geographic framework, preferably along natural boundaries. We propose to organize karst in the United States into a nested hierarchy of geographic areas similar to the ecological classification scheme of Bailey and others (1994).

Status of the national karst map

A preliminary map of potentially karstic areas of the conterminous United States, based primarily on state-scale (1:24,000 up to 1:1,000,000) geologic maps, has been constructed (fig. 1). This map reflects the presence of soluble bedrock lithologies, carbonate and evaporite rocks, or low-viscosity lava extrusive volcanic rocks. These are the most important factors in developing karst or volcanic pseudokarst. Lava tube caves are predominantly found in rocks younger than about 40 million years old, so areas of older volcanic rock have been deleted (Palmer, 2007; Kolev and Shopov, 1992). This is a first approximation of potentially karstic, or volcanic pseudokarstic areas based on compilations from state geologic maps and is a work in progress.

The National Atlas Engineering Aspects of Karst map (Davies and others, 1984) categorized carbonate karst areas by (1) generalized length and depth of fissures, tubes, and caves; (2) general lithologic type; and (3) structural setting (steeply dipping versus flat-lying rocks).

As part of the national karst map project, a regional map of Appalachian karst has been constructed (Weary, 2008, unpublished data). This map covering the states of New York, Pennsylvania, New Jersey, Delaware, Ohio, West Virginia, Maryland, Virginia, Kentucky, Tennessee, North Carolina, South Carolina, Georgia, Alabama, and Mississippi, is in the final stages of technical review for publication as an online Open-file Report and should be available by the time of the May, 2008 USGS karst Interest Group (KIG) meeting.

The potentially karstic units on the Appalachian karst map are classified in similar fashion to the map of Davies and others (1984), although for the time being, cave length and depth are being ignored. The units from the Appalachian map are incorporated into figure 1 with extension of its classification scheme into the states of Florida, Indiana, Michigan, Wisconsin, as well as the New England states. The map units are: (1) CPCR, Coastal Plain carbonate rocks; (2) CPCRC, Coastal Plain carbonate rocks with a siliciclastic overburden up to 200 ft thick (chiefly in Florida); (3) CPU, Coastal Plain

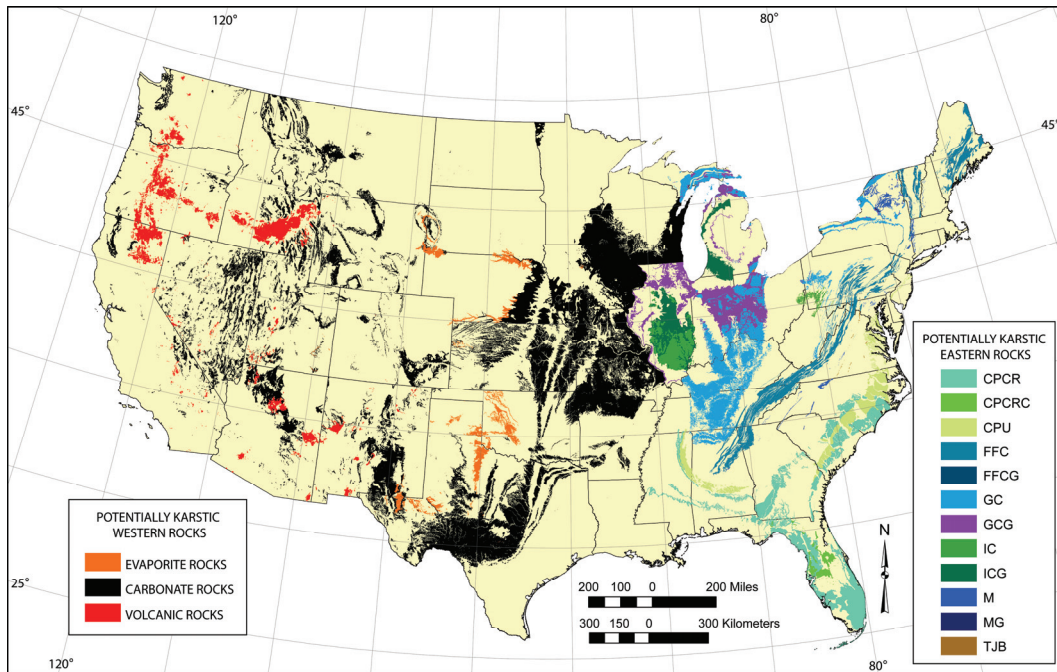


Figure 1. Potentially karstic areas of the conterminous United States delineated from mapping of surficial expression of carbonate, evaporate, and relatively young (Post Oligocene) volcanic rocks. See text for a description of map units.

unconsolidated carbonate rich sediments; (4) FFC, folded and faulted carbonate rocks, chiefly limestone and dolostone in the Valley and Ridge physiographic Province (Fenneman and Johnson, 1946); (5) FFCG, folded and faulted carbonate rocks, with a glacially derived overburden of at least 50 ft (15.2 m); (6) GC, gently folded to flat-lying carbonate rocks, chiefly found in the Appalachian Plateaus, Central Lowlands, and Interior Low Plateaus; (7) GCG, gently folded to flat-lying carbonate rocks, with a glacially derived overburden of at least 50 ft (15.2 m); (8) IC, carbonates interbedded with relatively insoluble rocks, chiefly in the cyclothemic rocks of the Appalachian, Michigan, and Illinois basins; (9) ICG, carbonates interbedded with relatively insoluble rocks, with a glacially derived overburden of at least 50 ft (15.2 m); (10) M, marble, found chiefly in the Piedmont, Blue Ridge, and Adirondack physiographic provinces; (11) MG, marble with a glacially derived overburden of at least 50 ft (15.2 m); (12) TJB,

carbonate rocks in Triassic and Jurassic aged basins of the Piedmont.

In states west of the Mississippi, potentially karstic areas are currently shown as simply carbonate, evaporate, or, volcanic rocks. Portrayal of karst areas in the states of California, Oregon, Washington, Arizona, and Utah has been refined in more detail based on interaction with local experts, from the state geological surveys and members of the National Speleological Society (NSS). Work is ongoing to devise an appropriate classification scheme for western karst areas.

TOWARDS A GEOGRAPHIC HIERARCHICAL KARST CLASSIFICATION

The longer we work towards a new national karst map, and the more requests and inquiries we field for various derivative maps and data,

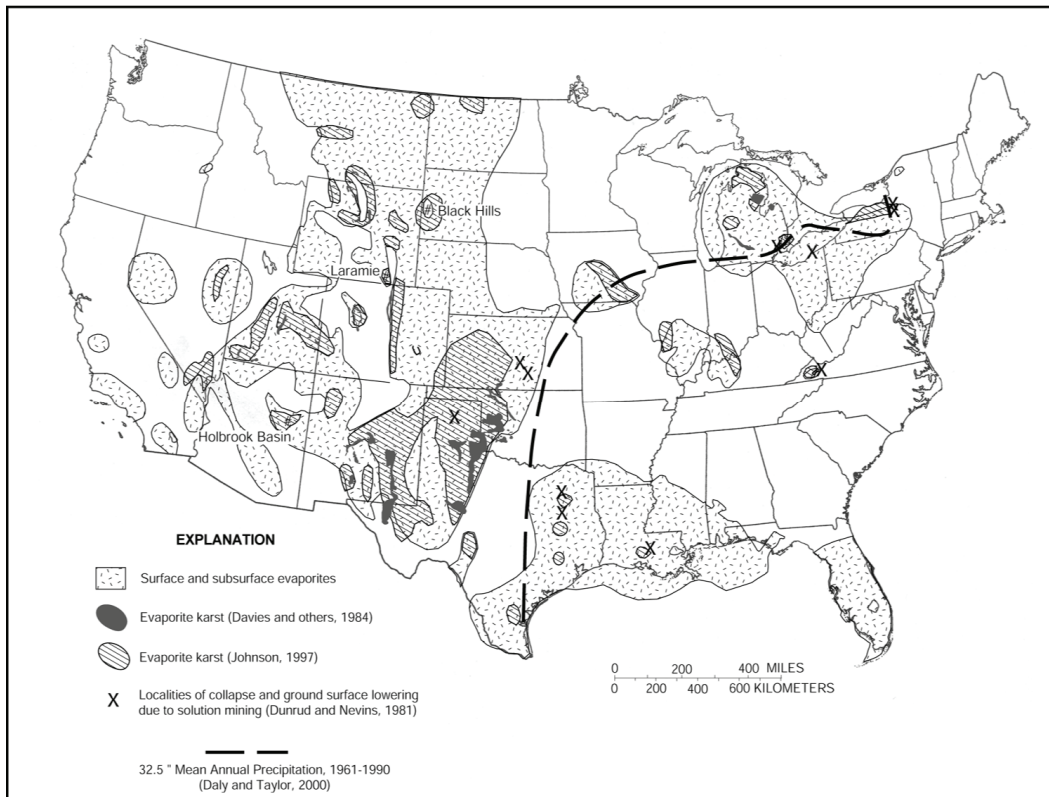


Figure 2. Map showing distribution of outcropping and subsurface evaporite rocks in the conterminous United States and areas of reported evaporite karst. The 32.5-in. (mean-annual-precipitation line approximates the boundary between eastern and western karst (from Epstein and Johnson, 2003, fig. 5.).

the more apparent it becomes that there is a need for an organizational framework for classifying karst areas in the United States. One advantage to establishing a national framework is the ability to integrate data and research within it from national scale surveys down to site-specific studies.

On a national scale, the two most important factors in development and expression of karst landforms are amount of precipitation and the solubility of the bedrock. It has been observed that karst terrains in the eastern part of the U.S. are dominantly areas underlain by carbonate rocks with large numbers of sinkholes developed on them. In the western part of the country, sinkholes in carbonates are far fewer and surface expression of sinkholes and other karst features in areas underlain by evaporate rocks become common (Epstein and Johnson, 2003). The

dividing line between these areas lies approximately along the 32.5 in. (826 mm) mean annual precipitation line (figure 2). A relatively detailed precipitation map overlain with areas of carbonate and evaporate rocks from our new national map (figure 3) shows this same pattern. Note that there are smaller areas of relatively high precipitation in the western part of the country in the Pacific Northwest, Sierra Nevada and Rocky Mountains.

A Physiographic Hierarchy

The karst classification scheme of Davies and others (1984) and the scheme used on the new Appalachian regional map (Weary, 2008, unpublished data) are based primarily on geologic factors: rock type, tectonic setting, and thickness of insoluble overburden. These data alone are not sufficient for parsing karst areas

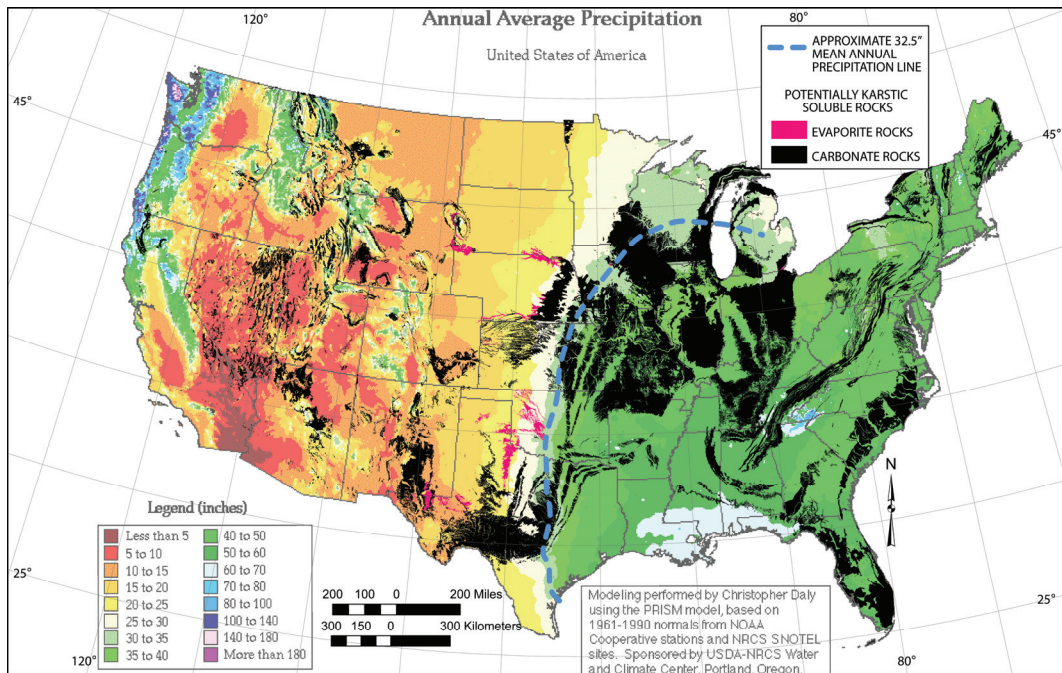


Figure 3. Map showing the surface distribution of carbonate and evaporate rocks of the conterminous United States and detailed mean-annual-precipitation. Precipitation map from the Oregon Climate Center, online link: http://www.wrcc.dri.edu/pcpn/us_precip.gif.

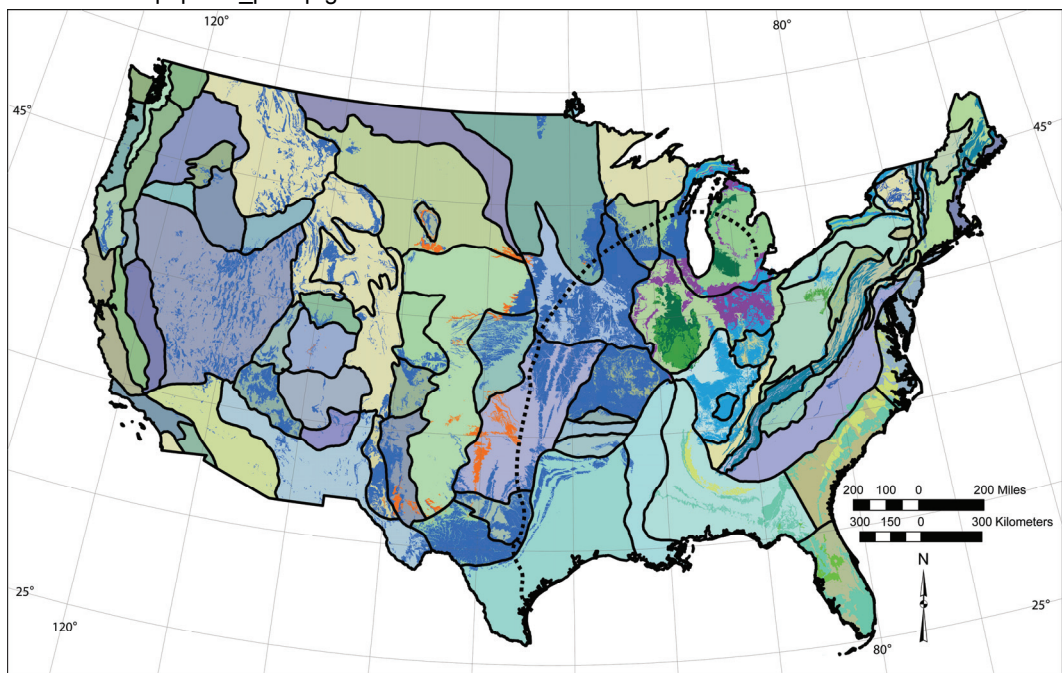


Figure 4. Map of the conterminous United States showing physiographic sections (outlined in black, not labeled for clarity), areas of soluble bedrock (superimposed unbounded areas, see figure 1), and the approximate location of the 32.5 in. (826 mm) mean annual precipitation line (dashed).

into smaller units, and the areas, as depicted, do not always coincide with natural physiographic and ecologic boundaries. In the quest for further subdivision of the karst map, and in lieu of availability of extensive karst feature data sets, our approach was to follow physiographic mapping, for which the US is organized into a 3-tiered, nested hierarchy of topographically defined divisions, provinces, and sections (Fenneman and Johnson, 1946) (figure 4) The physical characteristics of each of these physiographic regions are the result of the geologic and climate/erosional history of each

area over long geologic time scales. Many of the section boundaries coincide with boundaries of known karst terrains (e.g. the Ozark Plateaus, the Adirondacks, etc). The boundaries of the physiographic sections in some areas of the country do not correspond well to present precipitation patterns as their characteristics are the result of time-averaging of the climatic effect over the age of each landscape rather than present weather patterns. This long-term climate/erosion history is also related to the epigenetic karstification history of each landscape.

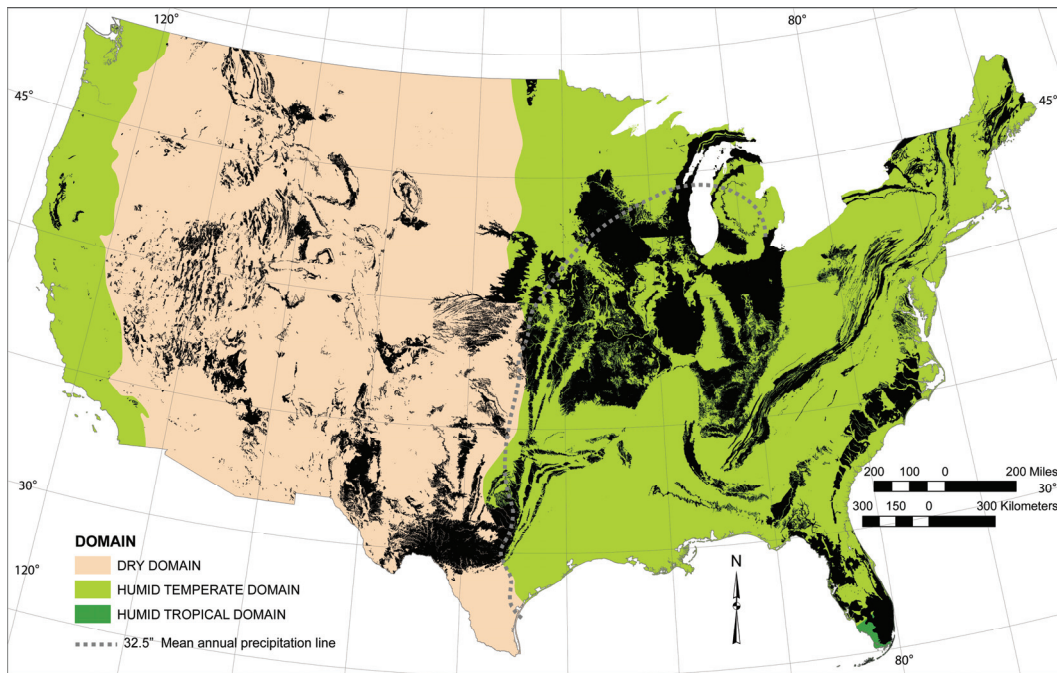


Figure 5. Map of the conterminous United States showing ecologic Domains with areas of soluble rock overlain (see figure 1). The 32.5 in. (826 mm) mean annual precipitation line from figure 3 included for reference.

A Ecologic Classification Scheme

A better choice for organizing karst terrains in the U.S. is the use of a scheme similar to ecologic landtype classification. Many states and other agencies follow the ecoregion classifications scheme of Bailey and others (1994) or similar hierarchical classifications that incorporate climate, geology, and physical and biological features that are significant for natural resource management. Because the ecoregion scheme considers factors related to climate, it tends to fit the precipitation patterns better than the physiographic hierarchy. Another advantage

of using this scheme is that it incorporates factors that have biologic importance and thus makes a suitable framework for biologic studies at various scales.

The largest unit in the ecologic classification scheme is the Domain. These are continental-scale areas defined by climate, primarily precipitation (figure 5, table 1). Notice that there are non-contiguous Humid Temperate Domains in the east and the west. The boundary between the Dry Domain and the eastern Humid Temperate Domain follows the 32.5 in (826 mm) mean annual precipitation line fairly closely in the southern half of the midwest.

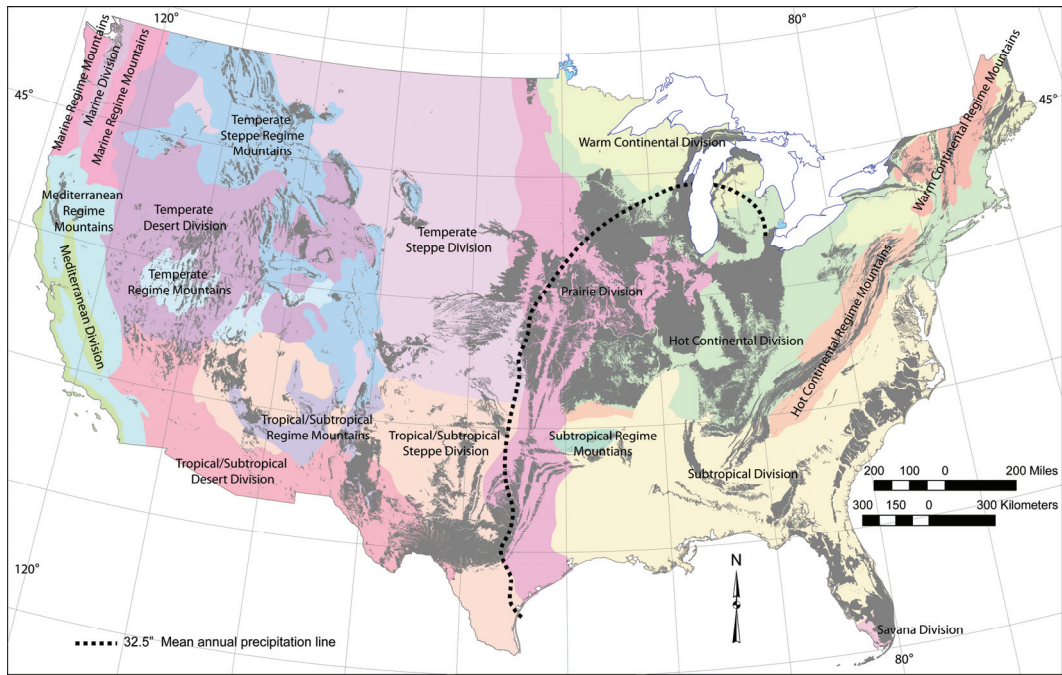


Figure 6. Map of the conterminous United States showing ecologic Divisions. 32.5 in. (826 mm) mean annual precipitation line from figure 3 included for reference.

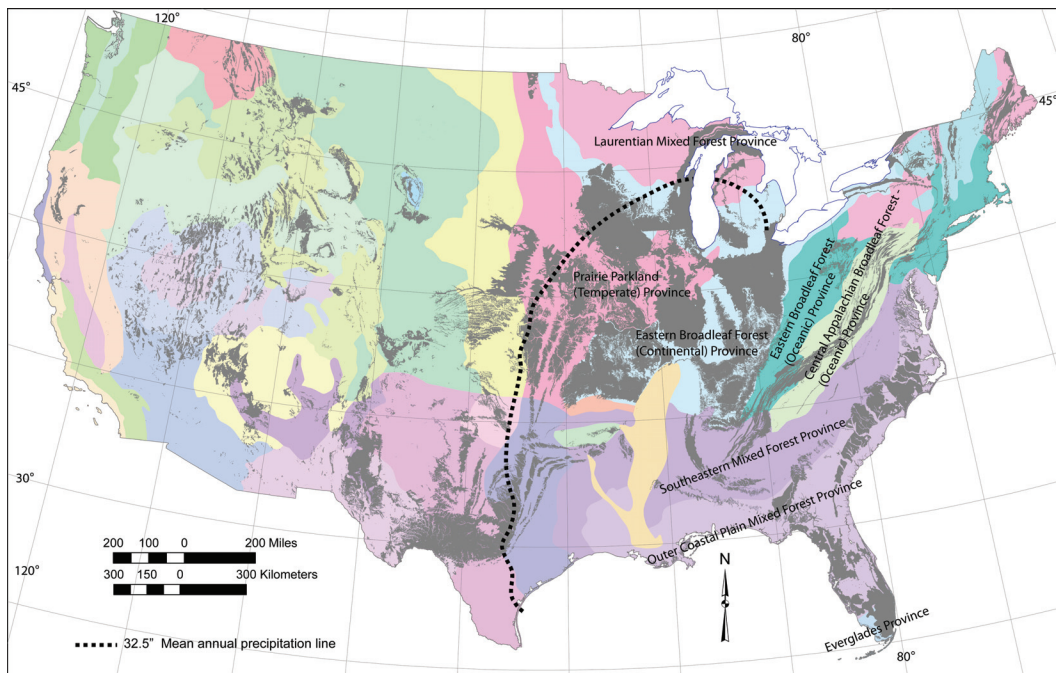


Figure 7. Map of the conterminous United States showing ecologic Provinces (only some labeled). 32.5 in. (826 mm) mean annual precipitation line from figure 3 included for reference.

The next level down in the classification scheme is the Division. These are regional-scale areas defined primarily by climate and relief (figure 6, table 1). Divisions are then subdivided into Provinces (figure 7, table 1). Provinces are regional-scale areas combining predominant vegetation and climate patterns.

Provinces are, in turn, divided into Sections and Subsections (figure 8, table 1). The Sections often coincide with large karst terranes like the Ozark Highlands and the Subsections are at the level of specific karst areas like the Springfield

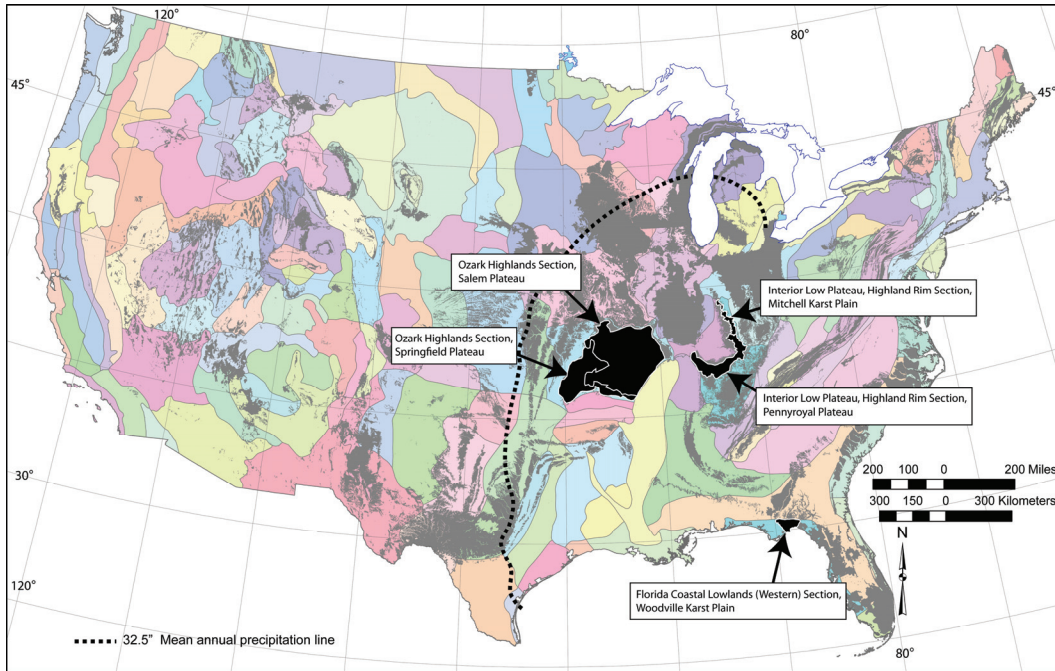


Figure 8. Map of the conterminous United States showing ecologic Sections and subsections (only some labeled). 32.5 in. (826 mm) mean annual precipitation line from figure 3 included for reference.

Plateau, Woodville Karst Plain, Mitchell Karst Plain, and Pennyroyal Plateau (figure 8). It is at about the Section level that various karst constants (Curl, 1966), or karst development and karst vulnerability scoring or indexing studies such as EPIK (Doerflinger and Zwahlen, 2000) and a new Karst Potential Index (KPI) being developed for Kentucky (Currens and others, 2004, unpublished manuscript) may be applied. At this scale the weights of various factors affecting karstification should be relatively uniform within each Section.

Below the level of Subsection in the ecologic hierarchy are Landtype Associations and Landtype Phases (table 1). In karst terranes these may be equivalent in scale to karst basins and then discrete karst features such as sinkholes or areas underlain by caves respectively. Most karst research studies occur within these levels.

Nomenclature

A GIS copy of ecologic landtype polygons at each level in the hierarchy can easily be overlain on the distribution of carbonate, evaporate and volcanic rocks on the national map to facilitate assignment of the various karst areas within the classification scheme. Since this is a karst classification, names of the various units could be altered to make more sense in a karst/physiographic frame of reference (table 1).

For example, at the Province level it makes more sense for karst scientists to use “Midcontinent Karst Province” than “Eastern Broadleaf Forest (Continental) Province”. At lower levels in the classification, previously named karst terrains would have precedence and retain their historic names (e.g. Woodville Karst Plain).

Table 1. Example of an ecologic landtype-based classification (Bailey and others, 1994) and a suggested parallel karst classification using an Ozark karst area.

| General size range | Ecological Units | Ecological Unit Examples | Karst Terrane Units | Suggested Karst example |
|---|-------------------------|--|----------------------------|---|
| Millions to tens of thousands of square miles | Domain | Humid Temperate Domain | Karst Domain | Humid Temperate karst of eastern North America |
| | Division | Hot Continental Division | Karst division | Allegheny/Cumberland Plateau and Midcontinent karst |
| | Province | Eastern Broadleaf Forest (Continental) Province | Karst Province | Midcontinent Karst Province |
| Hundreds of square miles | Section | Ozark Highlands Section | Karst Section | Ozark Highlands Karst Section |
| | Subsection | Current-Eleven Point Hills Subsection | Karst Subsection | Salem Plateau Karst Subsection |
| Thousands to hundreds of acres | Landtype Association | Ozark Limestone/Dolomite Glade/Woodland Hills, Knobs, and Basins | Karst Basin | Big Spring Karst Basin |
| Hundreds to less than ten acres | Landtype Phase | North-facing dolomite cliffs | Karst Feature | Jam Up Cave |

CONCLUSIONS

There is a need for organizing the karst lands of the United States, and by extension, North America, into a hierarchical geographic classification scheme. We suggest a system paralleling the ecologic classification scheme of Bailey and others (1994) which is widely used by natural resource agencies across the country. This would link the karst classification to both physiographic and biological factors and establish a framework for organizing karst data at all scales.

REFERENCES

- Bailey, R.G.; Avers, P.E.; King, T.; McNab, W. H., eds. 1994. Ecoregions and subregions of the United States: U.S. Geological Survey, Accompanied by a supplementary table of map unit descriptions compiled and edited by McNab, W.H., and Bailey, R.G., Prepared for the U.S. Department of Agriculture, Forest Service, Scale 1: 7,500,000.
- Curl, R.L., 1966, Caves as a measure of karst: *Journal of Geology*, v. 74, no. 5, pt. 2, p. 798-830.

- Currens, J.C., Paylor, M., and Crawford, M., 2004, Karst potential and development indices; tools for mapping and comparing karst development at the local or regional scale: Kentucky Geological Survey, unpublished manuscript, 45 p.
- Davies, W.E., Simpson, J.H., Ohlmacher, G.C., Kirk, W.S., and Newton, E.G., 1984, Engineering aspects of karst: U.S. Geological Survey, National Atlas, scale 1:7,5000.
- Doerflinger, N. and Zwahlen, F., 2000, Groundwater vulnerability mapping in karstic regions (EPIK): Swiss Agency for the Environment, Forests, and Landscapes, Berne, VU-2504-E, 56 P.
- Epstein, J.B., and Johnson, K.S., 2003, The need for a national evaporate karst map, in Johnson, K.S. and Neal, J.T., eds., Evaporite karst and engineering/environmental problems in the United States: Norman, Oklahoma Geological Survey, Circular 109, p. 21-30
- Fenneman, N.M., and Johnson, D.W., 1946, Physiographic divisions of the conterminous U. S.: U.S. Geological Survey special map series, scale 1:7,000,000.
- Kolev, B., and Shopov, Y., 1992, Volcanic caves in Bulgaria: Huntsville, AL, National Speleological Society, Proceedings of 6th International symposium on volcanospeleology, p. 171-175.
- Palmer, A.N., 2007, Cave Geology: Dayton, OH, Cave Books, 454 p.

A Karst Aquifer Map for the United States—Is it possible?

By Daniel H. Doctor¹, David J. Weary¹, Jack B. Epstein¹, and Randall C. Orndorff²

¹U.S. Geological Survey, 12201 Sunrise valley Drive, MS 926A, Reston, VA 20192

²U.S. Geological Survey, 12201 Sunrise valley Drive, MS 908, Reston, VA 20192

Abstract

Is it possible to classify karst aquifers? This question is central to any attempt to construct a map of karst aquifers for the United States. To make such a map, one must assign spatial boundaries to karst aquifers that are defined by an encompassing set of classifying criteria. The classification paradigm used to make such a map should permit comparison of studies conducted in different regions of the nation and world, and facilitate knowledge transfer between karst regions. However, even attempting to classify different types of karst terrain presents obstacles (Veni, 2002; Weary, 2005). Criteria for establishing boundaries of karst aquifers may call for compromise in “transitional” areas (Taylor, 2001). For example, does a karst aquifer end at a lithologic contact with less soluble rock? How does the definition of a karst aquifer differ from that of a fractured carbonate aquifer? What role does hypogenic speleogenesis play in regulating flow regimes and storage within a karst aquifer (Klimchouk, 2007)? What techniques does one employ when dye-tracing is not practicable for defining basin boundaries and establishing ground water transit time distribution in karst?

An encompassing classification of karst aquifers is one based upon measurable parameters derived from discharge and chemistry at springs and wells within the context of known geologic controls on aquifer extent and speleogenetic development (White, 2003). Such a paradigm presents two main challenges: (1) establishing a conceptual model of karst aquifer development through construction of the geologic framework and speleogenetic history, and (2) determining quantitative indices of the hydrologic response of an aquifer to recharge events from records of flow and water chemistry, supplemented by targeted water tracing experiments and local well tests. The geologic framework provides the basic information on the physical constraints on water storage and movement in the aquifer, including its boundaries and internal structures that guide permeability development through solution. The geologic framework is built through detailed geologic mapping (1:24,000 scale or larger), supplemented by geophysical investigations (e.g., Orndorff and others, 2001; Kozar and others, 2008). The speleogenetic history provides the information on how the permeability structure has been integrated into a highly conductive flow network. The speleogenetic history is reconstructed through the study of caves throughout the geographic extent of the aquifer, their relations to the geologic framework, and what they reveal of former hydrogeologic regimes experienced by the aquifer (Palmer, 2007). Caves represent the greatest degree of integration of the high-transmissivity conduits within the aquifer flow system, thus the processes which lead to their development help to classify the aquifer. Together, the geologic framework and the speleogenetic history provide the conceptual model for the development of the karst. The broadest categories for karst aquifer classification are therefore determined by the conceptual model of karst development. Examples of such broad categories include epigenic (unconfined) versus hypogenic (confined) karst aquifer formation (Klimchouk, 2007; Ford and Williams, 2007), and eogenetic (diagenetically immature) versus telogenetic (diagenetically mature) rocks which host karst aquifers (Florea and Vacher, 2006).

Spring flow records provide the most vital information for karst aquifer resource assessment. Working backwards from discharge may yield more fruitful and realistic aquifer assessment than attempting to work forward from site-specific porosity/permeability characterization and scaling up to the regional aquifer (Bredehoeft, 2007; Fleury and others, 2007). This is best achieved by determining diagnostic parameters of aquifer response to recharge from hydrograph and chemograph analysis. For example, multiple aquifer flow regimes can be identified through hydrograph recession analysis, and aquifer storage volumes drained by springs can be estimated by integrating across recession curves (Doctor and Alexander, 2005). Hydrograph recession analysis thus provides useful quantitative indices

for karst aquifer classification, such as the base flow recession coefficient, α (day^{-1}), and the ratio of dynamic phreatic storage volume to total annual volume discharged, or the “regulating power” of the aquifer system, k (dimensionless) (El-Hakim and Bakalowicz, 2007).

While important for karst aquifer classification, quantitative indices derived from hydrograph recession analysis are insufficient for aquifer mapping. A necessary component is the water balance. The exercise of constructing a balanced water budget may reveal the presence of additional water sources or sinks across previously hypothesized aquifer boundaries, and provides a check on the storage capacity of the aquifer estimated from spring flow recession analysis for a particular basin of interest. A balanced water budget will require that the spatial extent for recharge of a particular ground water basin has been properly delineated, thus enabling a mapped representation of the karst aquifer on the land surface. Boundary refinement is best achieved through well-designed tracing experiments. For example, dye-tracing provides information on groundwater flowpaths and subsurface basin divides. In addition, dye-tracing provides quantitative information on the distribution of travel times within an aquifer. Where dye-tracing is impractical, tracing with natural environmental isotopes and chemistry may provide needed information, particularly in aquifers with a significant artesian component (e.g., Doctor, 2007).

In summary, we suggest a classification paradigm for karst aquifers with two primary components: (1) an initial broad categorization based upon a conceptual model for karst development grounded in geologic and speleogenetic data, and (2) refinement within the initial category based upon quantitative indices of aquifer response to recharge from discharge records obtained at springs. Thus, long-term, high frequency hydrologic data are necessary for determining quantitative parameters for karst aquifer classification. However, karst aquifer classification ought not to be based solely upon the prevailing climatic factors of the broader aquifer region. Although climate is often the driving force for karst development, climate is dynamic and variable over time. Rather, the long-term aquifer response (centennial to millennial) to climatic forcing needs to be assessed independently of the short-term aquifer response (annual to decadal) to hydrologic factors that may be used for aquifer classification. In this way, comparisons among a single aquifer type existing under different climatic regimes may facilitate predictions of aquifer response to future climate change.

REFERENCES

- Bredehoeft, J., 2007, It is the discharge: *Ground Water*, v. 45, no. 5, p. 523.
- Doctor, D.H., in press, Hydrologic connections and dynamics of water movement in the trans-boundary Classical Karst aquifer: evidence from frequent chemical and stable isotope sampling. *Acta Carsologica*.
- Doctor, D.H., and Alexander, E.C., Jr., 2005, Interpretation of water chemistry and stable isotope data from a karst aquifer according to flow regimes identified through hydrograph recession analysis, in Kuniandy E.L. (ed.) U.S. Geological Survey Karst Interest Group Proceedings, Rapid City, South Dakota, 12–15 September, 2005, U.S. Geological Survey Water-Resources Investigations Report 2005-5160, p. 82-92.
- El-Hakim, M., and Bakalowicz, M., 2007, Significance and origin of very large regulating power of some karst aquifers in the Middle East: Implication on karst aquifer classification: *Journal of Hydrology*, vol. 333, p. 329-339.
- Fleury, P., Plagnes, V., and Bakalowicz, M., 2007, Modelling of the functioning of karst aquifers with a reservoir model: application to Fontaine de Vaucluse (south of France): *Journal of Hydrology*, vol. 345, p. 38-49.
- Florea, L.J., and Vacher, H.L., 2006, Springflow hydrographs: eogenetic vs. telogenetic karst: *Ground Water*, vol. 44, no. 3, p. 352-361.
- Ford, D., and Williams, P., 2007, *Karst Hydrogeology and Geomorphology* (revised edition): Chichester, West Sussex, John Wiley and Sons Ltd., 562 p.

- Klimchouk, A., 2007, Hypogene Speleogenesis: Hydrogeological and Morphogenetic Perspective: National Cave and Karst Research Institute, Carlsbad, NM, Special Paper No. 1, 106 p.
- Kozar, M., Weary, D.J., Paybins, K.S., and Pierce, H.A., 2007, Hydrogeologic setting and ground-water flow in the Leetown area, West Virginia, U.S. Geological Survey Scientific Investigations Report 2007-5066, 70 p.
- Orndorff, R.C., Weary, D.J., and Šebela, S., 2001 Geologic Framework of the Ozarks of South-Central Missouri- Contributions to a Conceptual Model of Karst, *in* Kuniansky E.L. (ed.) U.S. Geological Survey Karst Interest Group Proceedings, Shepherdstown, West Virginia, August 20-22, 2002, U.S. Geological Survey, Water-Resources Investigations Report 01-4011, p. 18-24.
- Palmer, A.N., 2007, Cave Geology, Dayton, Ohio, Cave Books, 454 p.
- Taylor, C.J., 2001. Hydrogeologic characterization of a “transitional” karst aquifer, south-central Louisville, Kentucky, *in* Kuniansky E.L. (ed.) U.S. Geological Survey Karst Interest Group Proceedings, Shepherdstown, West Virginia, August 20-22, 2002, U.S. Geological Survey, Water-Resources Investigations Report 01-4011, p. 45.
- Veni, G., 2002, Revising the karst map of the United States: Journal of Cave and Karst Studies, vol. 64, no. 1, p. 45-50.
- Weary, D.J., 2005, An Appalachian regional karst map and progress towards a new national karst map, *in* Kuniansky E.L. (ed.) U.S. Geological Survey Karst Interest Group Proceedings, Rapid City, South Dakota, 12–15 September, 2005, U.S. Geological Survey, Water-Resources Investigations Report 2005-5160, p. 93–102.
- White, W.B., 2003, Conceptual models for karstic aquifers, *in* A.N. Palmer, M.V. Palmer, and I.D. Sasowsky (eds.), Karst Modeling: Charles Town, West Virginia, The Karst Waters Institute Special Publication 5, p. 11-16.

KARST AQUIFER SYSTEMS

Tectonic Control of Hypogene Speleogenesis in the Southern Ozarks—Implications for NAWQA and Beyond

By Rodney Tennyson¹, Jim Terry², Van Brahana³, Phil Hays⁴, and Erik Pollock⁵

¹MOLES, 1303 CR 919, Alpena, AR 72611

²MOLES, 1103 W. Olive, Rogers, AR 72756

³Department of Geosciences, 113 Ozark, University of Arkansas, Fayetteville, AR 72701 and Research Hydrologist Emeritus, U.S. Geological Survey

⁴Department of Geosciences and U.S. Geological Survey, 113 Ozark, University of Arkansas, Fayetteville, AR 72701

⁵Stable Isotope Lab, Department of Biological Sciences, University of Arkansas, Fayetteville, AR 72701

Abstract

The Ozark Plateaus are an ancient, variably karstified region of the mid-continent that have more than 8000 reported caves, tens of thousands of springs, and a wide and diverse suite of accompanying karst landforms and hydrogeologic features. The importance of aquifers of the Ozark Plateaus led to their inclusion as one of the initial National Water-Quality Assessment study units in 1991, and the resulting studies have enhanced significantly our understanding of the processes and controls affecting water quality throughout the region.

This report describes the integration of recent data from diverse types of research to develop a conceptual model of hypogene speleogenesis for one selected data set of cave and karst locations within the Ozark Plateaus that overlie or are contiguous to deep basement faults. Data encompass geologic mapping, cave mapping, structural geology, gravity mapping, hydrogeology, ground-water tracing, endangered species distribution mapping, cave mineralogy, stable-isotope geochemistry, and fluid inclusion studies. This conceptual model draws on reactivation of preexisting basement faults during tectonic pulses, with the formation of caves and selected cave minerals created by geothermally heated water that recharged from below along integrated systematic joints and faults, driven by hydrostatic pressure. Structurally, flow pathways and cave passages range from slightly-tilted blocks (dips generally less than several degrees), to numerous fault features, only a few of which are of a magnitude to be shown on published geological quadrangle maps. Although most of these faults and fractures are not regional in scale, they appear to be very important at controlling ground-water flow that formed cavern passages. Cave erosional features and deposits have been found that indicate past episodes of thermal ground-water circulation. These include upper-level paleo-cave passages and chambers, now reactivated by present-day stream drainage, dolomite breccia linings, and remarkable dog-tooth spar (calcite) crystals, some of which are as long as 1.9 meters. The stable isotopic signature of these crystals is anomalous, and inconsistent with a meteoric fluid origin. Although the source of the thermal water is not known with certainty at this time, the proximity of these features and deposits to basement faults is consistent with upwelling of deep basin brines, and may likely be related to economic mineral deposits found nearby. Soft-sediment deformation, in the form of olistoliths, is documented from one recently excavated road cut within 50 meters of the northeast-trending Bella Vista fault, indicating that movement on basement faults was active as early as Osagean time. Gravity data and deep drilling records reflect the displacement of basement rocks across major faults, and distribution of several endangered species suggest that brittle overlying carbonate rocks were fractured and that the faults served as pathways for dispersal of these species, as well as flow conduits. Although these tectonically controlled karst features likely impact a small component of NAWQA sites in the Ozark Plateaus, the depth of faulting and the vertical interconnectivity warrants additional scrutiny, especially near areas of these northeast-trending basement faults.

INTRODUCTION

The Ozark Plateaus (figure 1) are an ancient, variably karstified region of the mid-continent that have more than 8000 reported caves, tens of thousands of springs, and a wide and diverse suite of accompanying karst landforms and hydrogeologic features (Imes and Emmett, 1994; Brahana et al., 2005). The importance of aquifers of the Ozark Plateaus led to their inclusion as one of the initial National Water-Quality Assessment (NAWQA) study units in 1991 (Leahy et al., 1990), and the resulting studies have enhanced significantly our understanding of the processes and controls affecting water quality throughout the region.

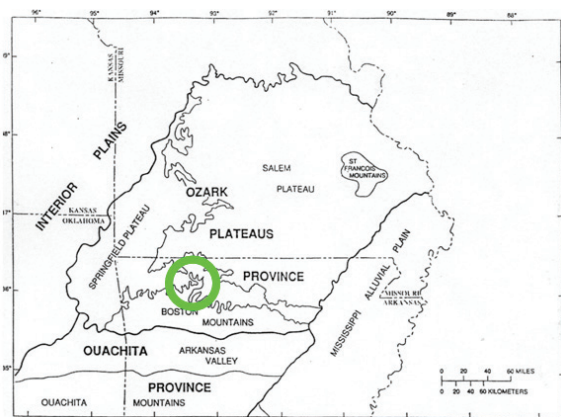


Figure 1. The Ozark Plateaus, showing the approximate location of northeast-trending basement faults in northern Arkansas. The Upper Flatrock Creek fault study area is shown by the circle in figure 2 (modified from Imes and Emmett, 1994).

Whereas the Ozark Plateaus NAWQA studies focused on karst formed by epigenetic processes, hypogenic karst also is present within the Ozarks, although it has seldom been recognized or been the object of major research. Epigenetic karst is formed by aggressive recharge descending from the land surface; hypogenic karst is formed by aggressive recharge ascending from ground water under artesian conditions. The distinction between these types of karst and the dominant factors that control them has been rapidly evolving over the past several decades, and only recently has been clearly elucidated (Hill, 2000; Klimchouk, 2007). The full understanding of these

differences requires different management practices for water quality and land use for each, and has implications for future regional studies the Survey may undertake.

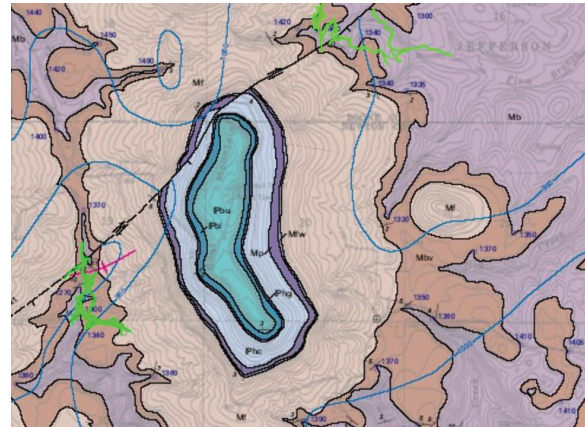


Figure 2. Relation of the northeast-trending Flatrock Creek fault to the surface geology and cave locations (shown in green). Chilly Bowl Cave is furthest west, Endless Cave is furthest east, and Big Hole Cave is in between (modified from Hudson and Murray, 2004). North is at the top of the figure. The width of the map is approximately 5 kilometers.

This report focuses on a subset of hypogenic features that overlie deep northeast-trending faults that extend from land surface to the basement in northern Arkansas, and specifically, the area of the Upper Flatrock Creek fault in Newton County. We herein describe the integration of data from diverse research incorporating geologic mapping (Hudson, 1998; Hudson et al., 2001; Braden and Ausbrooks, 2003; and Hudson and Murray, 2004), cave mapping (David Taylor, 2008, written commun., Clarksville, Arkansas), structural geology (Granath, 1989; Hudson, 2001), gravity mapping (Hendricks et al., 1981), hydrogeology (Brahana, 1997), ground-water tracing (Dawn Cannon, 2001, written commun., Fayetteville, Arkansas; Chuck Bitting, 2008, written commun., Harrison, Arkansas), endangered species distribution mapping (Brown and Graening, 2003), cave mineralogy, stable-isotope geochemistry (P.D. Hays, 2008, written commun., Fayetteville, Arkansas), economic mineral occurrence (McKnight, 1935), and fluid inclusion studies (Leach, 1979; Leach and Rowan, 1986) to constrain our understanding of the factors that control

hydrogeology and karst development in the region, both hypogenic and epigenetic.

Purpose and Scope

The purpose of this study is to develop a preliminary conceptual model of hypogene speleogenesis for areas of the Ozark Plateaus that overlie reactivated Precambrian faults. The term hypogene speleogenesis used herein follows the definition of Ford (2006), in which "the formation of caves is by water that recharges the soluble formation from below, driven by hydrostatic pressure or other sources of energy, independent of recharge from the overlying or immediately adjacent surface." The lack of discernible genetic relation with recharge from the overlying surface is the main characteristic of this process (Klimchouk, 2007).

This report is limited in scope to the six-county area of northwest Arkansas, where major faults are well defined by mapping and remote sensing (Haley et al., 1993; Hudson, 1998; Hudson et al., 2001; Braden and Ausbrooks, 2003; and Hudson and Murray, 2004). Emphasis and most examples are drawn from Newton County, and specifically the Flatrock Creek fault (figure 2).

This report is limited in scope to the six-county area of northwest Arkansas, where major faults are well defined by mapping and remote sensing (Haley et al., 1993; Hudson, 1998; Hudson et al., 2001; Braden and Ausbrooks, 2003; and Hudson and Murray, 2004). Emphasis and most examples are drawn from Newton County, and specifically the Flatrock Creek fault (figure 2).

DISCUSSION

A recent program to refine geologic mapping at a 1:24,000 scale within and near the study area has been undertaken by several agencies and universities, most notably the U.S. Geological Survey, the National Park Service, the Arkansas Geological Commission, and the University of Arkansas (Hudson, 1998; Hudson et al., 2001; Braden and Ausbrooks, 2003; and Hudson and Murray, 2004). Surface geology in the six-county study area ranges in age from Ordovician to Pennsylvanian. Lithologies

include a thick sequence of carbonate rocks in the deeper part of the section, with dolomite dominant up to the Ordovician, and limestone dominant from the Ordovician through the middle Mississippian (figure 3). The Boone Formation, a major karst former in the region, has significant (as much as 70%) chert throughout much of the area. The chert and other insoluble materials mantle surface-karst features, and provide a distinct nonkarst appearance to the untrained eye, especially in that portion of the northwest Arkansas Ozarks classified as the Springfield Plateau (figure 1). Terrigenous sediments characterize Mississippian though Pennsylvanian rocks, with shales dominant, and interlayered sandstones and limestones forming local aquifers. The shales shed most of their recharge laterally to surface streams, and recharge and karst development below shale outcrops is limited, although locally it may be well developed if fracturing prevails.

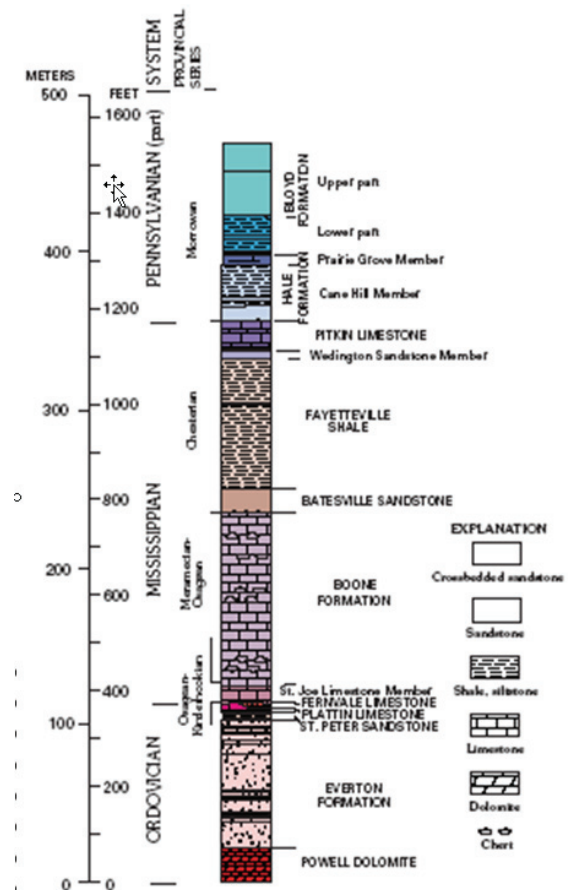


Figure 3. Partial stratigraphic column in the area of interest (modified from Hudson and Murray, 2004).



Figure 4. Entrance into Chilly Bowl Cave requires a double-pitched rappel of about 25 meters. The vertical relief in caves in this part of the Ozarks reflects uplift that is thought to be related to Ouachita tectonics.

Structurally, the rocks in this area are nearly flat-lying. Dips typically are less than 3° , except for locations where faulting has occurred. Uplift is observed to increase from west to east across the study area, and near Flatrock Creek fault, in Newton County, and the nearby Buffalo National River, river bluffs and vertical cave entrances (figures 4 and 5) are consistent with uplift of from tens to hundreds of meters compared with the same formations in nearby counties (Fanning, 1994). Fracturing dominates the structural geology (Hudson, 2001) suggesting that the sedimentary cover overlying these formations was thin.

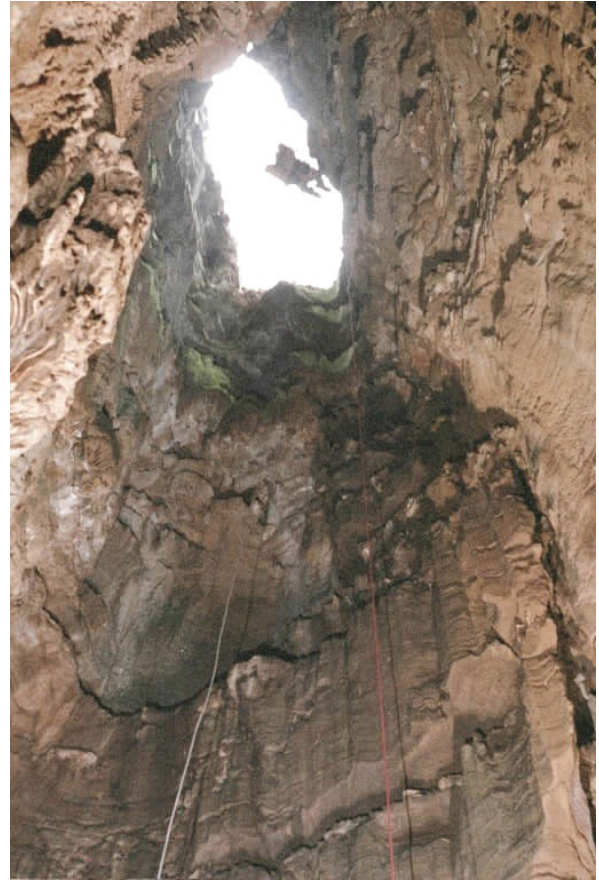


Figure 5. View from inside Big Hole Cave looking up at the entrance about 38 meters above.

Within Chilly Bowl Cave, faults are common (figure 6) and clearly visible (figure 7). Only a few of these faults are of a magnitude to be shown on published geological quadrangle maps at a scale of 1:24,000, however (Hudson, 1998; Hudson et al., 2001; Braden and Ausbrooks, 2003; and Hudson and Murray, 2004). Most of these individual faults appear to be very important at controlling ground-water flow that formed cavern passages.

Bouguer gravity anomalies suggest that reactivation of basement faults has been a major control on fracturing in this part of the Ozarks (Hendricks et al., 1981). Deep drilling records are yet additional data sources that reflect the displacement of basement rocks across major faults (Hendricks et al., 1981). The occurrence,

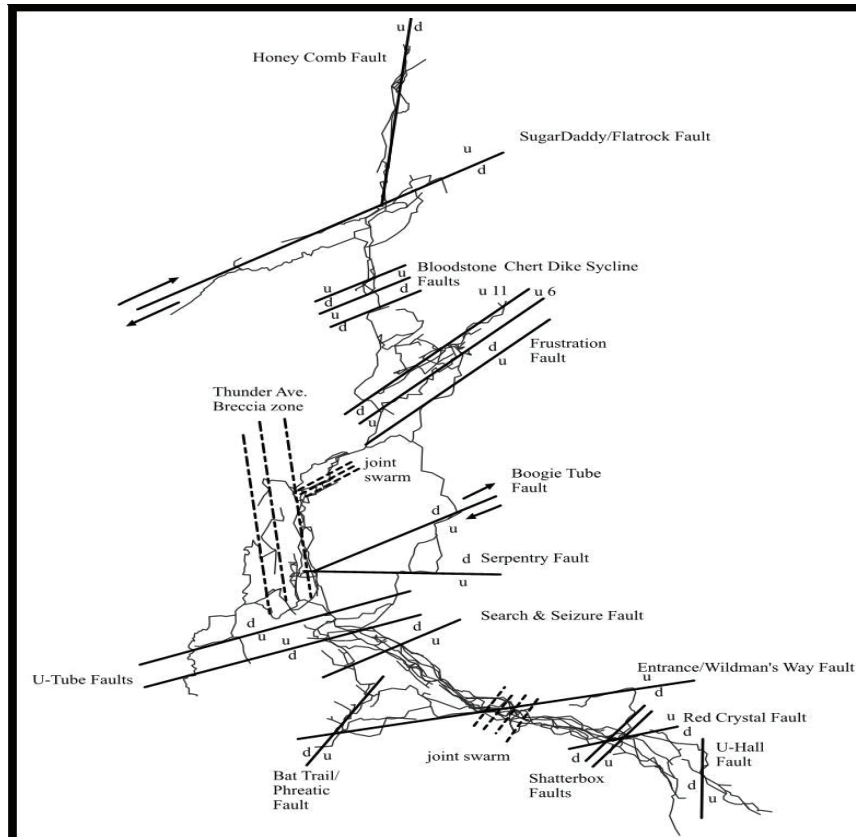


Figure 6. Plan view of Chilly Bowl Cave illustrating the tectonic control and faulting that are present and mapped within the cave.



Figure 7. Tube and canyon development on Boogie Tube Fault in Chilly Bowl Cave.

symmetry, and magnitude of the anomalies is such that basement rocks are required to be involved; rocks of the sedimentary cover alone cannot explain the observed data. Brahana (1997) has used orthogonal fracturing to successfully delineate spring basins boundaries in shallow karst aquifers elsewhere in the region, and the mechanism proposed appears to be applicable to Newton County, as well.

Hydrogeologically, flow pathways and cave passages tend to be aligned and to lie on near-horizontal bedding planes of slightly-tilted blocks (Brahana, 1997), or along near-vertical shafts that follow joints and fractures. In a cave such as Chilly Bowl, dozens of faults and fracture features are common (figure 6).

Hydraulic gradients of the present groundwater flow system, which generally appear to follow the tilt (structural dip) of the rock formations, act independently (are decoupled) from surface-water bodies where confinement by chert layers in the Boone Formation is effective. This decoupling is also lithologically

controlled, but in areas of faults and major joints, exhibits strong structural control. Stream piracy is one manifestation of combined lithologic and structural control that is obvious.

Dye tracing studies within (Dawn Cannon, 2000, written commun., Fayetteville, Arkansas) and near the study area (Tom Aley, 2004, written commun., Protom, Missouri) indicate that flow beneath surface drainage basins is common, that passages formed by hypogene processes likely have been pirated by later epigenetic processes, with a reversal of flow, and that faults in the system also may act as ground-water dams (figure 11).

The distribution of endangered species of cave crayfish and cavefish [*Cambarus setosus*, *Cambarus aculabrum*, and *Ambyopsis rosea*] (Brown and Graening, 2003; David Kampwerth, 2008, written commun., Conway, Arkansas) suggest that brittle overlying carbonate rocks were fractured from basement to land surface. These dominant faults underwent dissolution and later served as pathways for dispersal of subterranean species, as well as flow conduits for ground-water. These species are found in caves that lie at the distal end of the flow system and are large enough for human entry. Hydrocarbon spills in the southern Missouri part of the Ozarks indicate that endangered species live within carbonate aquifers, and are not restricted just to caves. In several reported instances, dead cavefish were observed where spills occurred yet no caves were present (Carol Wicks, 2001, written commun., Columbia, Missouri).

Soft-sediment deformation, in the form of olistoliths (figure 10), is documented from one recently excavated road cut within 50 meters of a major northeast-trending basement fault (Bella Vista fault). This outcrop lies near the highway 412 bridge that crosses the Illinois River near Robinson, in Benton County (~123 km east of the Flatrock Creek fault), indicative that movement on this basement fault was active as early as Osagean time, when St. Joe sediments had yet to be indurated (Chandler, 2001). Energy released from the surface waves associated with this faulting had to be significant enough to initiate sliding on basal bedding plane with a dip of about 3°.

Cave mapping (figure 6) indicates that passages in Chilly Bowl Cave appear to have been formed by recharge from below along integrated systematic joints and faults (figures 6 and 10), driven by hydrostatic pressure. Erosional features and deposits have been found that indicate past episodes of thermal ground-water circulation, with scallops in conduits and flow tubes showing upward flow (figure 7). Additional documentation of thermal hypogene flow includes upper-level paleo-cave passages and chambers, now reactivated by present-day stream drainage, dolomite breccia linings on cave walls, and remarkable, beautifully preserved large crystals of dog-tooth spar (figures 8 and 9). These crystals occur in the highest level of the cave, and are protected from erosion above by a sandstone caprock. Piracy of surface streams and surface drainage has been diverted to lower levels in the cave (figure 11) by older hypogene features, bypassing those few remaining passages where the crystals have been spared. Uranium series dating of these crystals is currently in progress.

Stable-isotopic analyses of samples taken from a transect of one of these broken dog-tooth spar crystals *in situ* from Chilly Bowl Cave reveal an anomalous $\delta^{13}\text{C}$ signature. The $\delta^{13}\text{C}$ has a strong organic carbon signature (~ -20 per mil), unlike other calcite samples from the region (P.D. Hays, 2008, written commun., Fayetteville, Arkansas). Although speculative at this time, one hypothesized source is the organic-rich, Arkoma hydrocarbon basin that overlies on the flowpath from the Ouachita Mountains in the south to our study area in northern Arkansas.

Economic minerals (sphalerite, galena, and chalcocopyrite) are present in the Rush mining district (McKnight, 1935), north and east of the study area, and are disseminated throughout much of the area in noncommercial quantities. Although these are not directly related to the karst focus of this report, the source of the metals and the details of the hydrogeology associated with mineral emplacement is hypothesized to be the same as with the hypogene fluids responsible for early karst initiation along Flatrock Creek Fault.



Figure 8. An upper-level passage in Chilly Bowl Cave, uniquely preserved with large dogtooth spar crystals that are thought to have been precipitated by thermal brines from hypogene sources. The caver's head serves as scale.

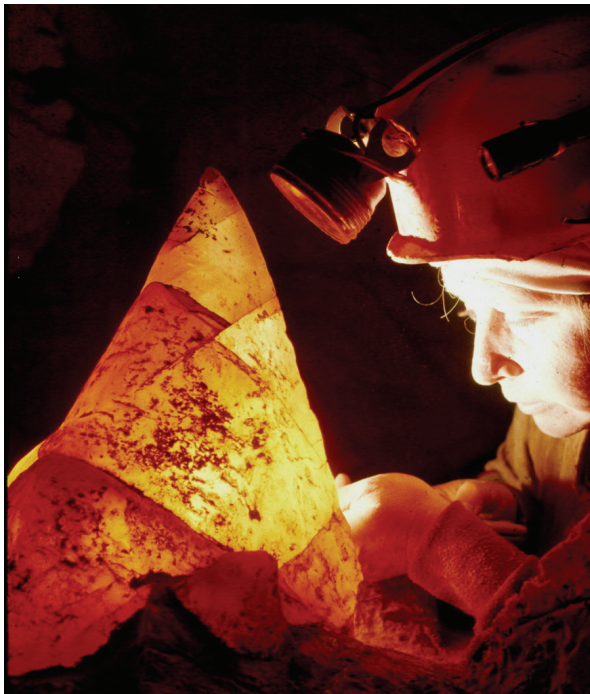


Figure 9. Backlit dogtooth spar crystal from Chilly Bowl Cave showing incipient cleavage planes. A broken sample from an *in situ* crystal was used for stable isotope analysis.

Fluid-inclusion research (Leach, 1979; Leach and Rowan, 1986) provide insight into the hot temperatures of mineralizing fluids that were hypothesized to have been expelled northward from the Arkoma Basin through permeable Paleozoic carbonate rocks toward the Ozark uplift. Using homogenization temperatures of fluid inclusions in sphalerite, these authors

showed a northward cooling of deep basinal brines that deposited sphalerite; temperatures ranged from ~120° C at ~100 kilometers north of the Ouachita Mountains to ~80° C in deposits ~400 kilometers north of the Ouachitas. The hydrogeology associated with these deposits appears to be quite similar to the study area.



Figure 10. Soft-sediment deformation (olistoliths) caused by intense shaking of slightly dipping sediments thought to be caused by an earthquake on the nearby Bella Vista fault, which underlies a valley approximately 50 meters from the right edge of the photo. Olistoliths indicate that faulting on these major northeast-trending basement faults was active at least as early as St. Joe time. The Northview Shale, with a dip toward the fault of about 3°, served as the glide plane along which the loose sediments slid (after Chandler, 2001).

SUMMARY

The compilation briefly discussed herein yields a preliminary conceptual model of hypogene speleogenesis (figures 11 and 12) that is consistent with all available data from a wide range of disciplines. Simply, the Ouachita orogeny was the driving force for fluid migration, basinal sediments of the Arkoma Basin were the source of organics, metals, and aggressive solutions, faulting, primarily along reactivated basement faults supplied the preexisting faults, created preferred flow paths for fluid flow, faulting on reactivated basement faults provided the major pathways of upward vertical migration into near-surface carbonates, the geothermal gradient supplied the heat, and the shale and sandstone cover of terrigenous sedimentary rocks supplied the insulation and pressure confinement such that the heated water

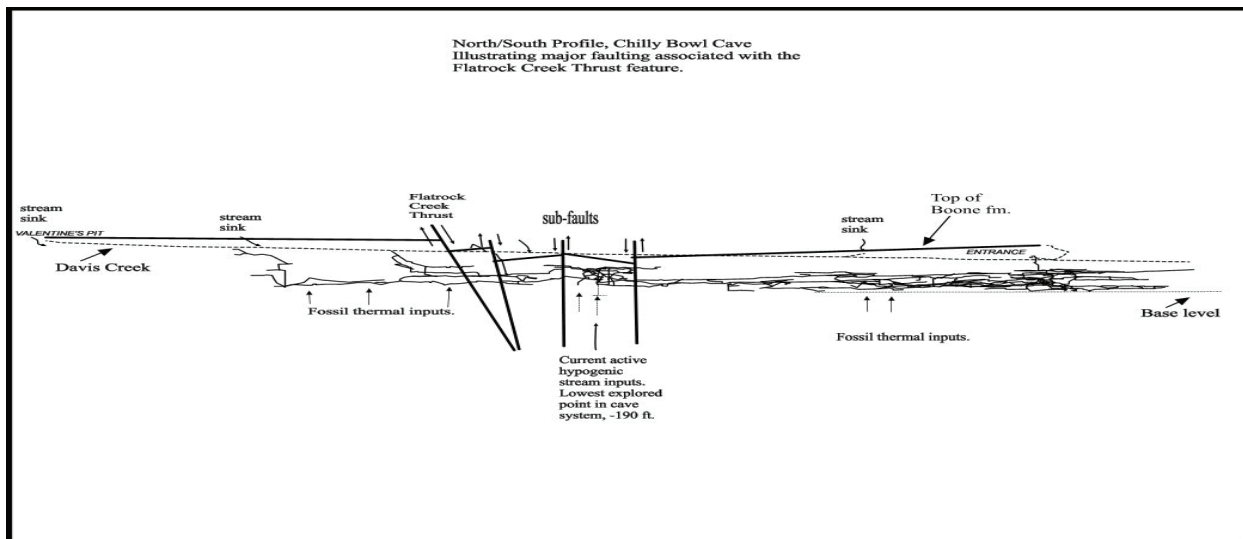


Figure 11. Conceptual profile of Chilly Bowl Cave illustrating the vertical speleogenetic development, major faulting associated with the Flatrock Creek fault, current level of Davis Creek, current base level, the top of the Boone Formation, and sources of thermal input that are preserved within the cave.

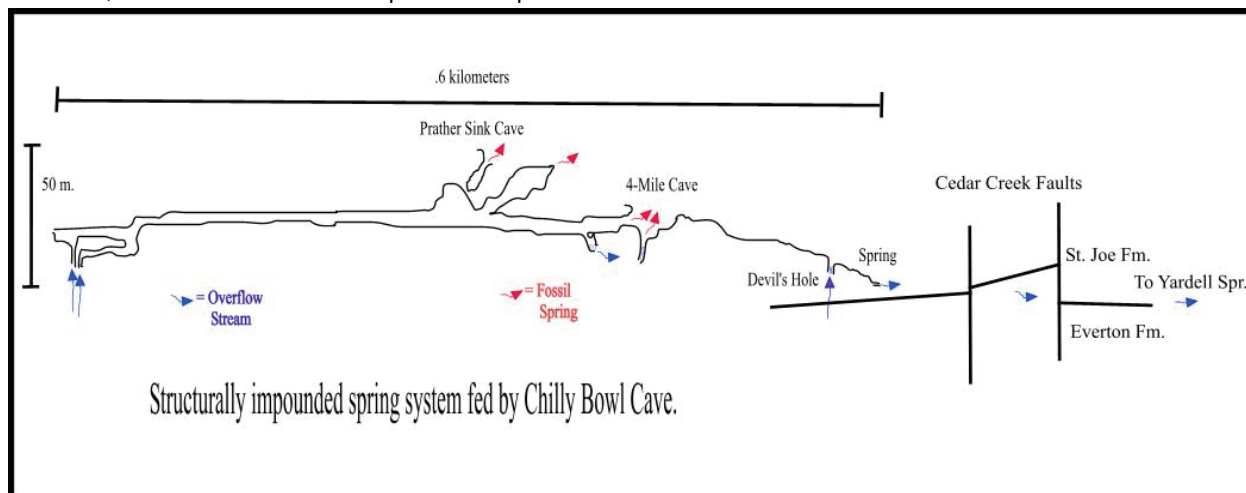


Figure 12. Conceptual flow system currently active in Chilly Bowl Cave showing the damming nature of multiple faults at the distal end of the integrated drainage way.

was advectively transported and cooled slowly. The strength of the crystalline basement rocks allowed much of the energy transmission, acting as a broad, thick lever to facilitate uplift. Uplift was responsible for fracturing the relatively thin overlying sedimentary cover in a systematic stress field of orthogonal jointed and faulted rocks. This overlying cover was karstified with multiple pulses of deep hot water, especially in areas overlying the deep faults. Epigenetic karstification was overprinted based on local factors, primarily hydrologic (Brahana et al.,

1988). Insofar as NAWQA focused on epigenetic karst aquifers, it seems justified to reassess sampling sites along deep-seated faults.

SELECTED REFERENCES

Braden, A.K., and Ausbrooks, S.M., 2003, Geologic map of the Mt. Judea quadrangle, Newton County, Arkansas: Arkansas Geological Commission Digital Geologic Quadrangle Map DGM-AR-00590, scale 1:24,000.

- Brahana, J.V., 1997, Rationale and methodology for approximating spring-basin boundaries in the mantled karst terrain of the Springfield Plateau, northwestern Arkansas: *in* Beck, B.F. and Stephenson, J. Brad, eds., Sixth Multidisciplinary Conference on Engineering Geology and Hydrogeology of Karst Terranes, A.A. Balkema, Rotterdam, p. 77-82.
- Brahana, J.V., Thrailkill, John, Freeman, Tom, and Ward, W.C., 1988, Carbonate rocks: *in* Back, W. Rosenshein, J.S., and Seaber, P.R., eds., Hydrogeology, Boulder, CO, Geological Society of America, The Geology of North America, v. O-2, p. 333-352.
- Brahana, J.V., Hays, P.D., Al-Qinna, Mohammed, Murdoch, John F., Davis, Ralph K., Killingbeck, Jonathan J., Szilvagy, Eva, Doheny-Skubic, Margaret, Chaubey, Indrajeet, Ting, Tiong Ee, and Thoma, G., 2005, Quantification of hydrologic budget parameters for the vadose zone and epikarst in mantled karst: *in* Kuniansky, E.L., 2005, U.S. Geological Survey Karst Interest Group proceedings, Rapid City, South Dakota, September 12-15, 2005: U.S. Geological Survey Scientific Investigations Report 2005-5160, p. 144-152.
- Chandler, Sandra L., 2001, Carbonate olistoliths, St. Joe and Boone Limestones (Lower Mississippian), northwestern Arkansas: unpublished M.S. thesis, University of Arkansas, Fayetteville, 49 p.
- Fanning, B.J., 1994, Geospeleologic analysis of cave and karst development within the Boone and St. Joe Formations of Benton and Madison counties, Northwest Arkansas: unpublished M.S. thesis, University of Arkansas, Fayetteville, 144 p.
- Fischer, M.P., and Christensen, R.D., 2004, Insights into the growth of basement uplifts deduced from a study of fracture systems in the San Rafael monocline, east central Utah: *Tectonics*, v. 23, p. TC1018, doi: 10.1029/2002TC001470.
- Fischer, M.P., and Jackson, P.B., 1999, Stratigraphic controls on deformation patterns in fault-related folds: A detachment fold example from the Sierra Madre Oriental, northeast Mexico: *Journal of Structural Geology*, v. 21, p. 613-633, doi: 10.1016/S0191-8141(99)00044-9.
- Ford, D.C., 2006, Karst geomorphology, caves and cave deposits: A review of North American contributions during the past half century: *in* Harmon, R.S., and Wicks, C.W., eds., Perspectives on Karst Geomorphology, Hydrology, and Geochemistry, Geological Society of America Special Paper 404, Boulder, Colorado, p. 1-14.
- Granath, J.W., 1989, Structural evolution of the Ardmore Basin, Oklahoma: Progressive deformation in the foreland of the Ouachita collision: *Tectonics*, v. 8, p. 1015-1036.
- Hale-Erlich, W.S., and Coleman, J.L., Jr., 1993, Ouachita-Appalachian juncture: A Paleozoic transpressional zone in the southeastern U.S.A.: *American Association of Petroleum Geologists (AAPG) Bulletin*, v. 77, p. 553-568.
- Haley, B.R., Glick, E.E., Bush, W.V., Clardy, B.F., Stone, C.G., Woodward, M.B., and Zachry, D.L., 1993, Geologic map of Arkansas: Arkansas Geological Commission and U.S. Geological Survey, scale 1:500,000.
- Hendricks, J.D., Keller, G.R., and Hildenbrand, T.G., 1981, Bouguer gravity map of Arkansas: U.S. Geological Survey Geophysical Investigations Map GP-944, scale 1:500,000.
- Hill, C.A., 2000, Sulfuric acid hypogene karst in the Guadalupe Mountains of New Mexico and West Texas: *in* Klimchouk, Alexander, Ford, D.C., Palmer, A.N., Dreybrodt, Wolfgang, 2000, Speleogenesis—Evolution of karst aquifers: National Speleological Society, Huntsville, Alabama, p. 309-316.
- Houseknecht, D.W., and Matthews, S.M., 1985, Thermal maturity of Carboniferous strata, Ouachita Mountains: *American Association of Petroleum Geologists (AAPG) Bulletin*, v. 69, p. 335-345.
- Hudson, M.R., 1998, Geologic map of parts of the Jasper, Hasty, Ponca, Gaither, and Harrison quadrangles in and adjacent to the Buffalo National River, northwestern Arkansas: U.S. Geological Survey Open-File Report 98-116, scale 1:24,000.
- Hudson, M.R., 2001, Coordinated strike-slip and normal faulting in the southern Ozark dome of northern Arkansas—Deformation in a late Paleozoic foreland: *Geology*, v. 28, p. 511-514.

- Hudson, M.R. and Murray, K.E., 2004, Geologic map of the Hasty Quadrangle, Boone and Newton Counties, Arkansas: U.S. Geological Survey Scientific Investigations Map 2847, Version 1.0, scale 1:24,000.
- Hudson, M.R., Murray, K.E., and Pezzutti, D., 2001, Geologic map of the Jasper quadrangle, Newton and Boone Counties, Arkansas: U.S. Geological Survey Miscellaneous Field Studies Map MF-2356, scale 1:24,000.
- Imes, J.L. and Emmett, L.F., 1994, Geohydrology of the Ozark Plateaus aquifer system in parts of Missouri, Arkansas, Oklahoma, and Kansas: U.S. Geological Survey Professional Paper 1414-D, 127 p.
- Ingebritsen, S.E., Sanford, W.E., and Neuzil, C.E., 2007, *Groundwater in geologic processes*: Cambridge University Press, 2nd ed., 334 p.
- Klimchouk, Alexander, 2007, Hypogene Speleogenesis: Hydrogeological and morphogenetic perspective: National Cave and Karst Research Institute Special Paper No. 1, 106 p.
- Klimchouk, Alexander, Ford, D.C., Palmer, A.N., Dreybrodt, Wolfgang, 2000, *Speleogenesis—Evolution of karst aquifers*: National Speleological Society, Huntsville, Alabama, 527
- Kranjc, Andrej, Gabrovsek, Franci, Culver, David C., and Sasowsky, Ira D., 2007, *Time in karst*: Karst Waters Institute Special Publication 12, Charles Town, West Virginia, 246 p.
- Leach, D. L., 1979, Temperature and salinity of the fluids responsible for minor occurrences of sphalerite in the Ozark region of Missouri: *Economic Geology*, v. 74, p. 931-937.
- Leach, D.L. and Rowan, E.L., 1986, Genetic link between Ouachita foldbelt tectonism and the Mississippi Valley-type lead-zinc deposits of the Ozarks, *Geology*, v. 14, p. 931-935.
- Leahy, P.P., Rosenshein, J.S., and Knopman, D.S., 1990, Implementation plan for the National Water-Quality Assessment Program: U.S. Geological Survey Open-File Report 90-174, 10 p.
- McKnight, E.T., 1935, Zinc and lead deposits of northern Arkansas: U.S. Geological Survey Bulletin 853, 311 p.
- Meckel, L.D., Smith, D.G., and Wells, L.A., 1992, Ouachita foredeep basins: Regional paleogeography and habitat of hydrocarbons, *in* Macqueen, R.W., and Leckie, D.A., eds., *Foreland basins and fold belts: Tulsa, Oklahoma*, American Association of Petroleum Geologists Memoir 55, p. 427-444.
- Palmer, A.N., 2007, *Cave Geology*: Cave Books, Dayton, Ohio, 454 p.
- Viele, G.W., and Thomas, W.A., 1989, Tectonic synthesis of the Ouachita orogenic belt, *in* Hatcher, R.D., Jr., Thomas, W.A., and Viele, G.W., eds., *The Appalachian-Ouachita orogen in the United States*: Boulder, Colorado, Geological Society of America, *The Geology of North America*, v. F-2, p. 695-728.
- Withjack, M.O. and Jamison, W.R., 1986, Deformation produced by oblique rifting: *Tectonophysics*, v. 126, p. 99-124.

Hydrologic Characterization of a Karst Spring in North-Central Arkansas

By Rheannon M. Scheiderer and Joel M. Galloway

U.S. Geological Survey, 401 Hardin Road, Little Rock, AR 72211, Tele: 501-228-3600 Fax: 501-228-3601, Email: rmscheid@usgs.gov, jgallowa@usgs.gov

Abstract

Nesbitt Spring, located in north-central Arkansas, lies within the Springfield Plateau section of the Ozark Plateaus physiographic province (Fenneman and Johnson, 1946) and is known to be an important habitat for the Hell Creek Cave crayfish (*Cambarus zophonastes*), a federally listed endangered species. Nesbitt Spring, a privately owned spring, is one of two known locations where the rare crayfish is found (Graening and others, 2006). The source, occurrence, local recharge, and age of the waters discharging from Nesbitt Spring were characterized to better understand threats to the endangered species' habitat. The hydrogeologic framework of the area includes karst terrain; hence, the cave is susceptible to contamination from surface sources within its local-recharge area. The predominant land use within the local recharge area of Nesbitt Spring is agricultural (poultry and cattle) and mixed forest.

Nesbitt Spring discharges from the Ordovician-age Platin Limestone but it receives recharge through the overlying Mississippian-age Boone Formation of the Springfield Plateau aquifer (<http://waterdata.usgs.gov/nwis/qw>) (fig. 1). Two water samples were collected from Nesbitt Spring (above base flow and base flow conditions; February 2006 and July 2006, respectively) and analyzed for major ions, radioactive isotopes, and stable isotopes. The water-quality characteristics were similar to water from wells and springs sampled within the Boone Formation where the flow is mainly conduit controlled and concentrated along joints and bedding planes. The age and recharge characteristics of Nesbitt Spring's discharge were determined using radioactive and stable isotopes of carbon, hydrogen, and oxygen. Oxygen and hydrogen stable isotope data indicate precipitation is infiltrating quickly with little time for evaporation, and tritium data indicate the water discharging from Nesbitt Spring is a mixture of modern and submodern water.

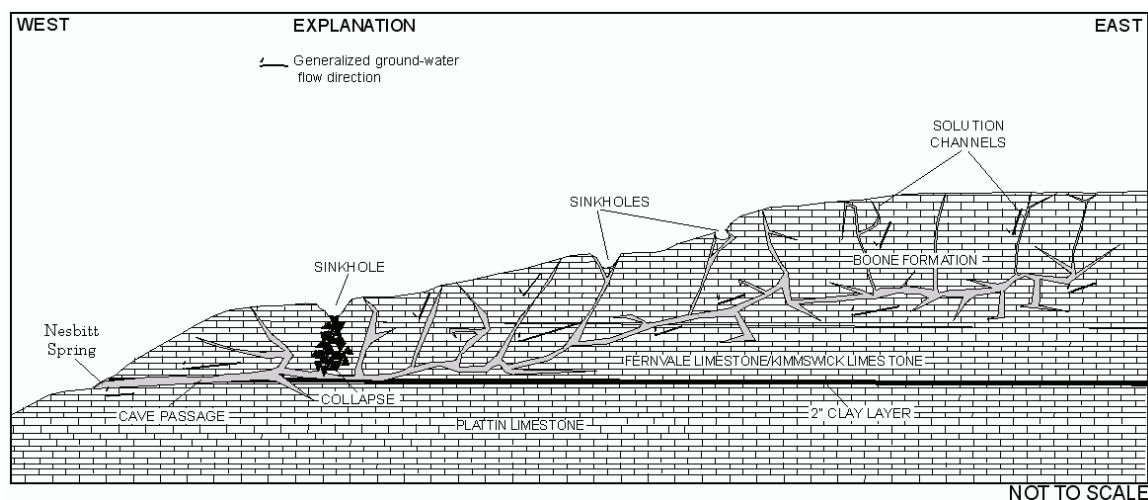


Figure 1. Conceptual model of Nesbitt Spring with geology and generalized flowpaths.

Dye tracer tests were performed and stage, water temperature, and precipitation were monitored to aid in the estimation of the local-recharge area and to help define flow characteristics. Three separate fluorescent dyes were used for simultaneous injection into open sinkholes or swallow holes and two of the dyes were recovered. The dyes were collected on passive charcoal detectors and positive detections were used to establish flow paths, but not to quantify the tracer concentrations.

Hydrograph-separation techniques (Base Flow Index computer program (Wahl and Wahl, 1995)) were applied to the spring hydrograph to determine relative proportions of local flow and regional flow. The contribution of regional flow to the spring was obtained by determining base flow; based on stormflow and dye tracer data, infiltration is occurring at a close proximity to the spring and accounts for the contribution of local flow. The spring responded rapidly to storm events with a range in recession time of 2 to 3 days, depending on the size of the event. The average daily discharge for the period of record (2006) was 4.51 cubic feet per second with a large component being base flow (47 percent), probably from the regional ground-water system. Water-temperature variations (ranging from 13.3 to 14.9 degrees Celsius) were observed seasonally and during storm events. The local-recharge area for Nesbitt Spring was estimated at approximately 2.5 square miles based on geologic characteristics, a water balance equation using spring discharge (Galloway, 2004), and dye tracer tests.

REFERENCES

- Fenneman, N.M., and Johnson, D.W., 1946, Physical divisions of the United States (Map): Washington, D.C., U.S. Geological Survey.
- Galloway, J.M., 2004, Hydrogeologic characteristics of four public drinking-water supply springs in northern Arkansas: U.S. Geological Survey Water-Resources Investigations Report 03-4307, 68 p.
- Graening, G.O., Koppelman, J.B., Wagner, B.K., Slay, M.E., and Brickey, C.L., 2006, Range extension and status update of the endangered Hell Creek Cave crayfish, *Cambarus zophonastes* (Decapoda: Cambaridae): The Southwestern Naturalist, vol. 51, no. 3, p. 392-396.
- Wahl, K.L. and Wahl, T.L., 1995, Determining the flow of Comal Springs at New Braunsfel, Texas: Proceedings of Texas Water '95, A Component Conference of the First International Conference of Water Resources Engineering, American Society of Civil Engineers, August 16-17, 1995, San Antonio, Texas, p. 77-86.

Analysis of Methods for Estimating Continuous Flows from Upper Floridan Aquifer Springs

By Nicasio Sepúlveda

U.S. Geological Survey, 12703 Research Parkway, Orlando, FL 32826

Abstract

Measured continuous flows from Upper Floridan aquifer springs were examined to determine the nature of their flows and to identify the most accurate method to predict the flows. A comparative analysis was conducted to identify the most accurate method to simulate continuous spring flows at Blue Spring, Rainbow Springs, Rock Springs, Silver Glen Springs, Silver Springs, and Wekiwa Springs in central Florida. Data used as independent variables were water levels at observation wells, spring-pool altitudes, and distance between observation wells and spring pools. The measured spring flows were used as dependent variable. Methods used to predict spring flows were the Darcy-Weisbach (DW) equation for conduit flow, multiple linear regressions (MLR), and artificial neural networks (ANNs). The DW equation for conduit flow with no source terms also was used to determine whether flows at each spring were turbulent or laminar. Flows at all springs were estimated to be turbulent. The ANNs had considerably lower residuals between measured and predicted spring flows than the DW or MLR methods (Table), and proved to be the best tool for water-resource managers to establish conditions on the hydraulic gradient between the spring and the observation well to maintain safe specified spring flows.

Table 1- Root-mean square errors, in cubic meters per second, between measured and predicted spring flows for the DW, MLR, and ANN methods. Root-mean-square percentage errors from measured spring flows are shown between parentheses.

[*M*, number of measurements of spring flow, spring-pool altitude, and water level at observation well made on the same day]

| Spring | Well | DW | MLR | ANN | <i>M</i> |
|---------------------|---------|-------------|-------------|------------|----------|
| Blue Spring | V-0083 | 0.26 (6.0) | 0.29 (6.9) | 0.13 (3.1) | 1,739 |
| Blue Spring | V-1091 | 0.36 (6.5) | 0.29 (6.7) | 0.13 (3.1) | 1,707 |
| Blue Spring | V-0867 | 0.23 (5.2) | 0.56 (12.9) | 0.12 (2.7) | 1,457 |
| Rainbow Springs | RS Well | 1.00 (5.4) | 0.86 (5.6) | 0.26 (1.6) | 2,505 |
| Rock Springs | OR-0662 | 0.24 (14.6) | 0.12 (13.7) | 0.04 (2.5) | 1,184 |
| Silver Glen Springs | M-0021 | 0.36 (13.0) | 0.36 (13.0) | 0.14 (5.3) | 1,478 |
| Silver Springs | M-0026 | 1.65 (9.1) | 1.74 (9.7) | 0.78 (4.6) | 5,349 |
| Silver Springs | CE-76 | 1.16 (6.4) | 1.25 (6.8) | 0.60 (3.6) | 1,913 |
| Wekiwa Springs | OR-0548 | 0.11 (6.1) | 0.10 (6.1) | 0.08 (4.4) | 1,102 |

Estimating Recharge to Heterogeneous Fractured-Rock and Karst Aquifer Systems in the Shenandoah Valley of Virginia and West Virginia

By George E. Harlow, Jr.¹, David L. Nelms¹, Richard M. Yager², Mark D. Kozar³, Ward E. Sanford⁴, and Roger M. Moberg¹

¹U.S. Geological Survey, 1730 East Parham Road, Richmond, Virginia 23228

²U.S. Geological Survey, 30 Brown Road, Ithaca, New York, 14850

³U.S. Geological Survey, 11 Dunbar Street, Charleston, West Virginia, 25301

⁴U.S. Geological Survey, 12201 Sunrise Valley Drive, Reston, Virginia 20192

Abstract

In recent years, the Northern Shenandoah Valley of Virginia and West Virginia has been experiencing rapid growth along the I-81 corridor and the eastern margin of the Valley. Increased development in rural areas is expected to continue as new residents commute to the Washington, D.C. metropolitan area. This growth has the potential to profoundly influence the region's land, water, and biological resources. Regional and local resource managers have major concerns over the region's ability to sustain future growth. Of particular concern is the sustainability and vulnerability of the region's water resources and the ability to provide a reliable long-term water supply. As of 2000, consumptive water use in the Shenandoah River Basin was estimated to be 33.4 million gallons per day, and is forecast to increase to over 40 million gallons per day by the year 2030. Water use is expected to increase by 30-percent in the main stem of the Shenandoah, while water use in the South Fork and North Fork are expected to increase by 16- and 25-percent, respectively. To address these concerns, the U.S. Geological Survey (USGS) Virginia, West Virginia and Leetown Science Centers are conducting cooperative investigations in the counties of Clarke, Frederick, and Warren in Virginia and the counties of Berkeley and Jefferson in West Virginia. These investigations focus on characterizing the carbonate and fractured-rock aquifer systems in these counties and providing relevant hydrogeologic information that can be used to guide the development and management of the ground-water resources. Since 2003, the Virginia and West Virginia Science Centers have also participated in a multidisciplinary regional assessment of the water resources of the Shenandoah Valley utilizing USGS Integrated Science Funding to develop and investigate methods to provide insight into the complex ground-water systems in the Valley.

A specific goal of our current studies is to improve our understanding of the recharge of ground water in the complexly folded and faulted fractured-rock and karst aquifer systems. Estimates of recharge to these fractured-rock and karst aquifer systems have been derived historically using graphical hydrograph separation techniques and, more recently, from linear regression techniques. These estimates are presented for the Valley as a whole, for different rock classes across the Valley, for individual watersheds within the Valley and, finally, for individual watersheds during both "average" and "drought" conditions. In spite of the fact that estimates of base flow and recharge from graphical separation techniques have been used for decades, substantial uncertainty is still associated with these estimates. While older, graphical methods for separating runoff from base flow are based on visual intuition, a newer chemical hydrograph-separation method is based on a physical process that can be measured in the field. An ongoing investigation using a chloride mass balance approach to calculate the components of the hydrologic budget for individual watersheds will verify and/or constrain recharge estimates obtained by graphical hydrograph-separation methods. The Shenandoah Valley was selected for more intense data collection where all current streamflow gaging stations are instrumented in addition to selected wells and springs. The objectives of this study are to (1) develop hydrologic budgets for the watersheds and counties of central and western Virginia, and (2) display this information as maps of Virginia by watershed and by county. The hydrologic budget components that will be shown in map view include rainfall, total evapotranspiration, riparian evapotranspiration, infiltration, recharge, runoff, and base flow.

Impact of 1998-2002 Drought on the Karst Aquifers of Clarke County in the Shenandoah Valley of Virginia

By David L. Nelms, and Roger M. Moberg¹

¹ U.S. Geological Survey, 1730 East Parham Road, Richmond, Virginia 23228

Abstract

The prolonged drought between 1998 and 2002 focused attention on the quantity and sustainability of the ground-water resources of Clarke County, Virginia. The County is underlain by complexly folded and faulted Paleozoic and Precambrian rocks with a majority of the area characterized by karst aquifers. During this drought, over 20 wells and numerous springs and stream segments went dry. Above normal precipitation in the fall of 2002 and winter of 2003 brought an end to this drought. The magnitude of the recovery varied between the Opequon Creek and Shenandoah River watersheds. Ground-water levels in the Opequon Creek watershed recovered between 30 and 50 feet within a 6-month period; whereas levels in the Shenandoah River watershed generally recovered less than 10 feet. During this same period, flow in streams and springs returned after several dry years. In one case, spring 46XS 8 that had been dry for several years began to flow at a rate of 1,000 gallons per minute. Results from hydrograph separation indicate that the ground-water component accounts for more than 80 percent of the streamflow during both dry and wet periods. Generally, the majority of this ground-water component is derived from the discrete discharge of springs.

Ground-Water/Surface-Water Relations and Water Quality Within the Mammoth Spring Watershed, Dixie National Forest, Garfield and Iron Counties, Utah

By Lawrence E. Spangler

U.S. Geological Survey, 2329 Orton Circle, Salt Lake City, Utah 84119

Abstract

In October 2006, the U.S. Geological Survey in cooperation with the U.S. Forest Service began a 3-year study to investigate the hydrology and water quality of the Mammoth Spring watershed in southwestern Utah. The principal objective of this study is to delineate the recharge area and ground-water flow system for Mammoth Spring and determine its relation to the surface-water drainage basin. The scope of the study includes (1) identifying potential point sources such as losing streams and sinkholes where surface water can rapidly recharge and impact the aquifer directly, (2) determining ground-water travel times through the aquifer, and (3) determining variations in water quality of Mammoth Spring during base and peak flow conditions.

Mammoth Spring is one of the largest springs in Utah, with a discharge that ranges from less than 5 to over 300 cubic feet per second (cfs) (Mundorff, 1971). The spring discharges at an altitude of 8200 feet on the Markagunt Plateau in Dixie National Forest, about 6 miles east of Cedar Breaks National Monument (NM) (fig. 1). Flow from Mammoth Spring immediately merges with Mammoth Creek, the principal outlet for surface flow within the watershed. Seepage from lower reaches of the creek and from tributaries to the creek may be possible sources of water to the spring. Discharge from Mammoth Spring is probably from Quaternary-age volcanic rock (basalt) that caps large parts of the Markagunt Plateau and overlies the Tertiary-age Claron Formation, a marly limestone that is locally cavernous (Moore and others, 2004). Dissolution within the Claron and subsequent collapse of the basalt have resulted in an extensive volcanokarstic terrain at an altitude of about 9500 feet, which is characterized by ephemeral sinking streams and sinkholes (dolines) as much as 100 feet deep. Recharge to the aquifer that supplies Mammoth Spring likely takes place by both focused and diffuse infiltration through the highly-permeable basalt and into the underlying limestone. Previous tracer studies in the Navajo Lake watershed immediately south of the Mammoth Spring watershed, have shown ground-water travel times through the basalt and underlying limestone ranging from 348 to 750 feet per hour, and bifurcations of ground-water flow paths that ultimately discharge into different surface-water drainage basins (Wilson and Thomas, 1964). Ground-water movement in the Navajo Lake watershed and likely in the Mammoth Spring watershed is along fractures or lineaments, rubble zones between successive basalt flows, and in lava tubes (basalt) or caves (limestone).

Water samples for major ions, selected trace metals, nutrients (nitrate plus nitrite, ammonia, and orthophosphate), gross alpha/beta, coliform bacteria, selected isotopes (oxygen/deuterium, sulfur-35, tritium) and chlorofluorocarbons (CFCs) were collected from Mammoth Spring during base flow conditions (less than 10 cfs) in the fall and winter of 2006-2007. Results of chemical analyses indicate a calcium-bicarbonate type water containing very low dissolved-solids concentrations (about 100 milligrams per liter (mg/L)) that are more characteristic of ground water that has been in contact with basalt than with the underlying limestone. Water samples collected from Arch Cave Spring, which discharges from the Claron Formation within Cedar Breaks NM, are characterized by considerably higher dissolved-solids concentrations (170 mg/L), more representative of flow within carbonate rock. Analyses of water samples collected from several other springs near Mammoth Spring may represent a mixture of water from both the basalt and limestone. Results of analyses for sulfur-35, tritium, and CFCs indicate that residence time within the aquifer that supplies Mammoth Spring probably is a mixture of short (months or less) and long-term (years) components. Samples collected during base flow when most water is presumed to be from storage within the fractured matrix, contained CFC-11, 12, and 113 concentrations that indicate an apparent age of about 6 years or younger since recharge and tritium concentrations of 28.4

picocuries/Liter (8.8 tritium units). In addition, results of analysis for sulfur-35, an age-dating tool for waters less than about 2 years old (87-day half-life), showed concentrations of 0 millibecquerels/Liter (mBq/L) during base flow conditions to about 4.0 mBq/L at the onset of snowmelt runoff, indicating ground-water residence times that are greater than 2 years to less than 6 months, respectively.

Continuous monitoring of springflow (stage), specific conductance, and water temperature from November 2006 to November 2007 also shows a response to snowmelt runoff and rainfall events that is indicative of potentially rapid ground-water residence times (fig. 2). During this period, which represents one snowmelt runoff cycle, water temperature ranged from 3.8 to 5.4 degrees Celsius, and specific conductance ranged from 127 to 170 microSiemens per centimeter at 25 degrees Celsius, while discharge ranged from about 6 to at least 50 cfs. Increases in discharge of the spring resulted in decreases in specific conductance and dissolved-solids concentrations (fig. 2). The pH of water from the spring also fluctuated from 7.7 to 8.3 over this same time period. Although not monitored, turbidity also was observed in water from the spring during the snowmelt runoff period and after precipitation events. This, combined with the detection of total and fecal coliform bacteria in the spring water indicates the potential for fractures or other highly permeable pathways to transmit particulate material from surface sources through the aquifer to the spring in a relatively short timeframe.

The second and third years of the study will include (1) continued field reconnaissance to locate focused recharge sources to the aquifer that have the potential to directly impact the water quality of Mammoth Spring, (2) the collection of water-quality samples during high springflow, (3) continuous measurement of field parameters to further characterize water from the volcanic rocks and the underlying Claron Formation to evaluate hydrologic relations between these units, and (4) conducting dye-tracing studies to delineate generalized flow paths and ground-water basin boundaries for the spring and to determine short-term travel times through the aquifer.

REFERENCES

- Moore, D.W., Nealey, L.D., Rowley, P.D., Hatfield, S.C., Maxwell, D.J., and Mitchell, E., 2004, Geologic map of the Navajo Lake 7.5' quadrangle, Kane and Iron Counties, Utah: Utah Geological Survey Map 199, 2 pl.
- Mundorff, J.C., 1971, Nonthermal springs of Utah: Utah Geological and Mineralogical Survey Water-Resources Bulletin 16, 70 p.
- Wilson, M.T., and Thomas, H.E., 1964, Hydrology and hydrogeology of Navajo Lake, Kane County, Utah: U.S. Geological Survey Professional Paper 417-C, 26 p., 3 pl.

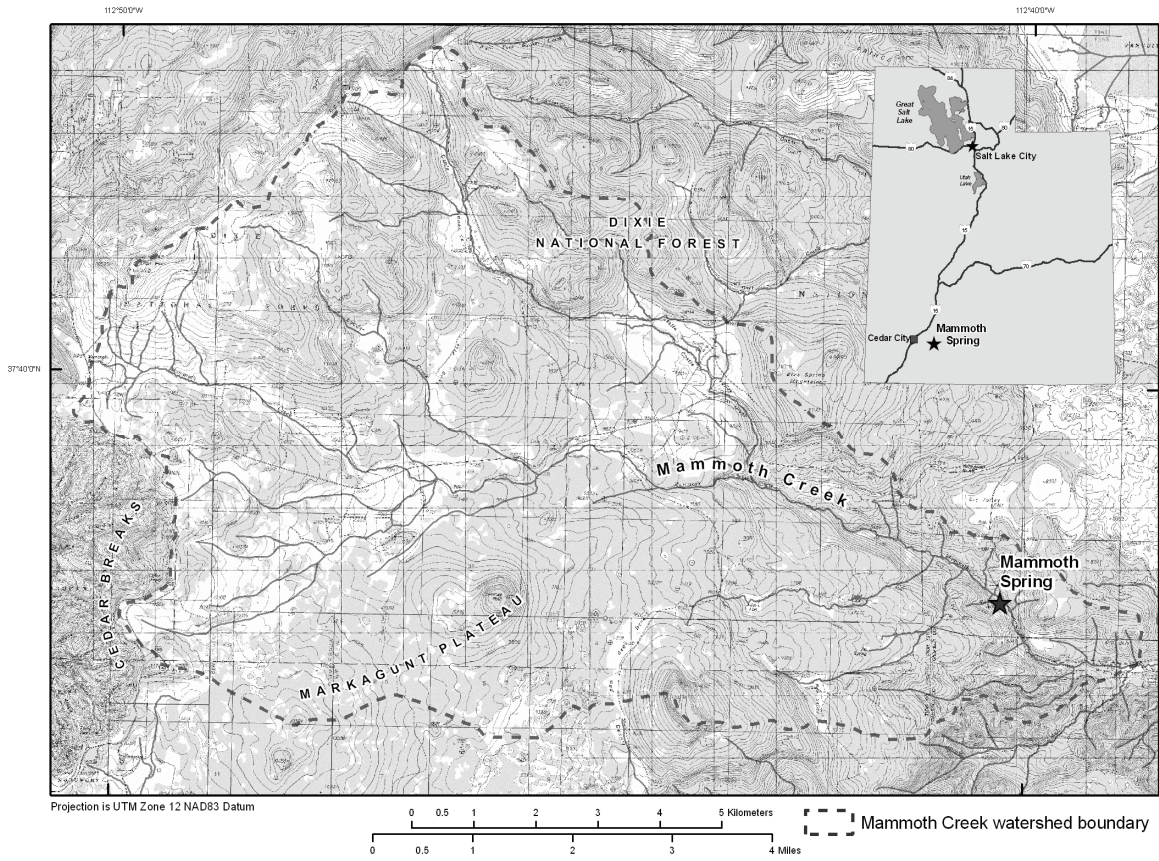


Figure 1. Location of Mammoth Spring on the Markagunt Plateau, southwestern Utah.

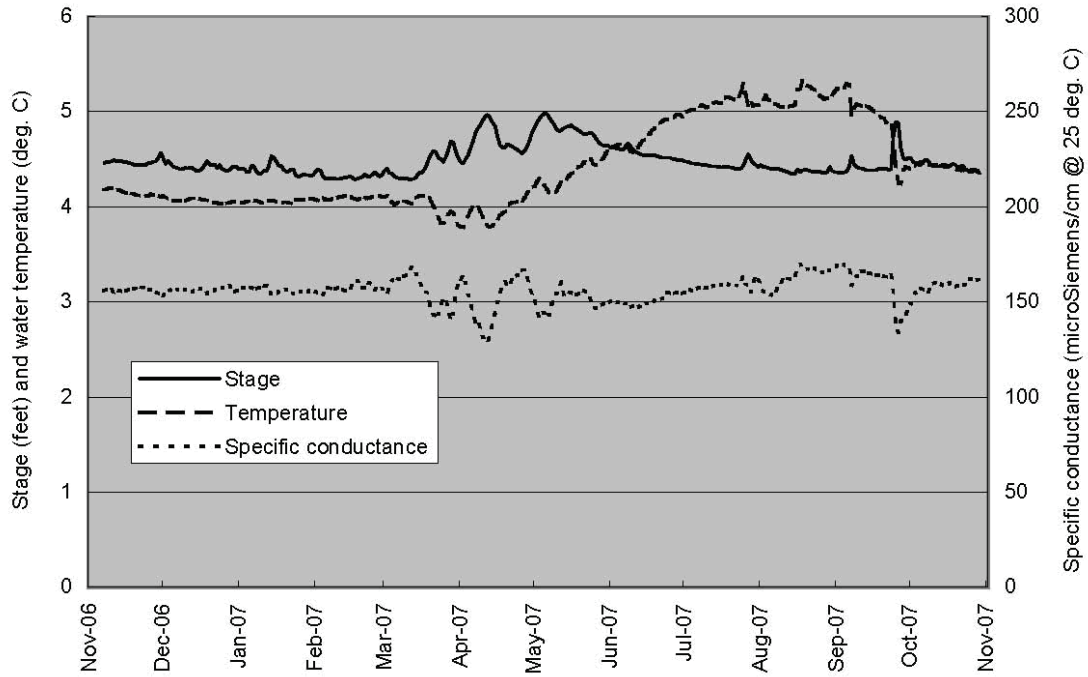


Figure 2. Relation between stage (discharge), water temperature, and specific conductance of Mammoth Spring.

NATURAL RESOURCES AND KARST ECOSYSTEMS

The Effects of Land-Use Change on an Ozark Cave System: A Paired Study of Civil War and Copperhead Caves

By Jonathan A. Gillip¹, Phillip D. Hays², and Joel M. Galloway¹

¹U.S. Geological Survey, 401 Hardin Road, Little Rock, AR 72211

²U.S. Geological Survey, 115 Ozark Hall, Fayetteville, AR 72701

Abstract

Much of the Ozark Plateaus is characterized by shallow mantled karst. In this setting, caves typically are hydraulically well-connected to the land surface and show a rapid response to the quantity and quality of water infiltrating through their recharge area. In a natural setting, this connection simply means the amount of water in the cave increases rapidly with rain events. However, in a developed setting, this connection may dramatically change the quantity and quality of recharge to the cave. Civil War Cave, located in northwestern Arkansas, is located in an area that is experiencing change from agricultural land use (mainly pasture) to urban land use. With no record of pre-development water quality, the effects of land use change on water quality could not be evaluated quantitatively. To better understand the impact of land-use change on cave water quality, a comparison was made between Civil War Cave and Copperhead Cave, a cave in the same region with similar geology and hydrology, but with no urban development and little human activity. Copperhead Cave is located within the boundaries of the Buffalo National River and is surrounded by undeveloped forest.

The geology of Civil War and Copperhead Caves is similar, with Civil War Cave being entirely in the Mississippian-age Boone Formation, and the part of Copperhead Cave considered in this study also being contained in the Boone Formation. The Boone Formation crops out across the entire recharge area of Civil War Cave (Glick, 1974). In the area of Copperhead Cave, the Boone Formation crops out (Hudson and Murray, 2003). The general hydrology is similar, with both caves recharged through the Boone Formation of the Springfield Plateau aquifer. In both caves, the ground-water recharge area is larger than the topographic recharge area. The topographic recharge areas are 0.18 square kilometers for Civil War Cave and 0.35 square kilometers for Copperhead Cave. Using a normalized base-flow method (Brahana, 1997), the ground-water recharge area was determined to be approximately 7.5 square kilometers for Civil War Cave and approximately 1.75 square kilometers for Copperhead Cave. In both cases, the regional flow is enhanced by fractures and karst features.

During recent (2005-2006) urban development in the vicinity of Civil War Cave, increased sedimentation was observed in Civil War Cave. The sedimentation is likely a result of surface excavation in the immediate recharge area and has decreased since the completion of excavation activities. Streamflow and dye-tracing data suggest the complex flow system recharging Civil War Cave may have been altered by recent development.

Water-quality data also suggest that Civil War Cave is affected by land use within the recharge area. Examination of water-quality data indicates both caves are recharged through the Springfield Plateau Aquifer. Because nitrate has low background concentrations and is enriched by human activity, it serves as an indicator of human impact (Adamski, 1997; Davis and Bell, 1998; Hem, 1985). Ground water from the Springfield Plateau aquifer in northwestern Arkansas commonly has nitrate concentrations exceeding 2 milligrams per liter as nitrogen in areas where the recharge is affected by human activity (Adamski, 1997), and generally has a nitrate concentration of 0.2 milligrams per liter as nitrogen or less (Steele, 1983) in unimpacted areas. Ground water nitrate concentrations indicate that Civil War Cave is impacted by human activity; with nitrate concentrations averaging 6.3 milligrams per liter as nitrogen in the upper level of Civil War Cave and 6.5 milligrams per liter as nitrogen in the lower level of Civil War Cave. Copperhead Cave is not impacted by human activity, with nitrate concentrations averaging less than 0.2 milligrams per liter nitrate as nitrogen.

The main threats to cave and karst communities include hydrologic threats, land development, nutrient stress, exotic or pest species, chemical pollution, human interaction, and isolation (Elliot, 2000). At Civil War Cave, human activity and urban development in the ground-water recharge area appears to have altered the hydrology, increased nutrient concentrations, and temporarily increased sedimentation within the cave system. The only impact observed in Copperhead Cave was the result of human interference within the cave.

REFERENCES

- Adamski, J.C., 1997, Nutrients and pesticides in ground water of the Ozark Plateaus in Arkansas, Kansas, Missouri, and Oklahoma: U.S. Geological Survey Water-Resources Investigation Report 96-4313, 28 p.
- Brahana, J.V., 1997, Rational and methodology for approximating spring-basin boundaries in the mantled karst terrane of the Springfield Plateau, northwestern Arkansas, In: B.F. Beck, B.F. and Stephenson, J.B. (Eds.), The engineering geology and hydrogeology of karst terranes, 453 p.
- Davis, J.V., and Bell, R.W., 1998, Water-quality assessment of the Ozark Plateaus study unit, Arkansas, Kansas, Missouri, and Oklahoma – Nutrients, bacteria, organic carbon, and suspended sediment in surface water, 1993-1995: U.S. Geological Survey Water-Resources Investigations Report 98-4164, 56 p.
- Elliot, W.R., 2000, Conservation of the North American cave and karst biota. Chap. 34, pp. 665-689. In: H. Wilkens, D.C. Culver, and W.F. Humphreys (Eds.), Subterranean Ecosystems. Ecosystems of the World, 30. Elsevier, Amsterdam. 791 p.
- Glick, E.E., 1974, Geologic worksheet of the Hiwasse Quadrangle: U.S. Geological Survey, unpublished report, 1 sheet.
- Hem, J.D., 1985, Study and interpretation of the chemical characteristics of natural water, 3rd Edition: U.S. Geological Survey Water Supply Paper 2254, 264 p.
- Hudson, M.R. and Murray, K.E., 2003, Geologic map of the Ponca quadrangle, Newton, Boone, and Carroll Counties, Arkansas: U.S. Geological Survey Miscellaneous Field Studies Map, 1 sheet.
- Steele, K.F., 1983, Chemistry of the springs of the Ozark Mountains, northwestern Arkansas: Arkansas Water Resources Center, University of Arkansas, no. 98, 48 p.

Karst Water Resources in Southwest China: Case Study from the East Plateau, Mengzi and Kaiyuan Counties, Yunnan, China

By Chris Groves¹, Jiang Yongjun^{2,1}, Pat Kambesis¹, Yuan Daoxian^{2,1} Amelia Chung^{3,1}

¹China Environmental Health Project, Hoffman Environmental Research Institute, Department of Geography and Geology, Western Kentucky University, Bowling Green, KY 42101 USA

²Institute of Karst and Rehabilitation of Rock Deserts, Department of Geographical Sciences, Southwest University of China, Chongqing, China

³International Institute of Rural Reconstruction, Kunming, Yunnan, China

Abstract

The East Plateau is a fault-bounded plateau with an altitude of about 2000 meters in far southern Yunnan, near China's border with Vietnam. It lies almost on the boundary of the Indian and Eurasian plates to the east of the Himalayan chain, and has a surface underlain in part by pure carbonate rocks of the middle Triassic Gejiu Group that form variations of peak cluster-depression karst morphology over some 250 square kilometers.

Serious water resource challenges occur on the plateau because of the well-developed karst, with little surface water available during the monsoon-climate's dry season. Only about 15 percent of the year's rainfall typically falls between November and May. Extensive deforestation and associated soil loss starting in the late 1950's has also severely diminished epikarstic storage, so that many villages established years ago with epikarstic springs are now without continuously reliable water supply. The water table is as much as 400 meter below the surface of the plateau. The 30,000 or so residents on the plateau are largely of Hani and Yi minority nationality, and typically very poor, in most cases subsistence farmers with incomes below China's poverty level of 680 yuan (\$91) per year.

With major support from the US Agency for International Development and the ENVIRON Foundation, Western Kentucky University's China Environmental Health Project is working to increase the technical infrastructure for karst water resource development in southwest China through partnerships with Southwest University in Chongqing Municipality as well as government scientists in the karst-rich provinces of the southwest. Yunnan's East Plateau is serving as demonstration site, both in an effort to increase local environmental health and awareness, as well to serve as a training vehicle for our Chinese partners in state-of-the-art methods of karst hydrogeology, including associated skills and infrastructure in cave survey, fluorescent dye tracing, and geographic information systems (GIS), and expedition management in remote rural areas. New laboratories were implemented and training workshops held at the university, followed by expeditions to the Plateau in early spring 2007 and 2008, late in the winter dry season each year.

This applied work has a challenging human element, and we are working closely with the International Institute of Rural Reconstruction and a local, non-government organization (NGO), the Honghe Prefecture Minority Nationality Research Institute, to develop local stakeholder networks with the team members, rural residents, and local governments to effectively engage community participation.

Thermal Infrared Mapping of Coastal-Aquifer Seeps and Associations Between Seeps and Coastal Habitats

By E. A. Raabe¹ and E. Bialkowska-Jelinska²

¹U.S. Geological Survey, 600 Fourth Street South, St. Petersburg, FL 33701

²Jacobs Technology, Inc., contractor for USGS, 600 Fourth Street South, St. Petersburg, FL 33701

Abstract

Aquifer seeps along Florida's Gulf Coast were detected as temperature anomalies in airborne thermal infrared imagery. The coastal lowland is characterized by relatively flat terrain, near-surface and water-bearing limestone, sinkholes, and other surficial karst features (Crane, 1986; Rupert, 1988; Rupert, 1991). Several 1st and 2nd order springs are documented in the region (Suwannee River Water Management District, 2007). Anecdotes about aquifer seeps along the coast are common, but confirmation of their location and distribution has been lacking. This oral presentation describes the results of an analysis of temperature anomalies in the lower Suwannee River and nearby tidal creeks as derived from thermal infrared imagery acquired in late winter 2005 (VeriMap, 2005). Field reconnaissance and comparisons to other data sources confirmed the distribution of numerous seeps along the coast near Cedar Key, Florida (Fig. 1).

A key component to the analysis is the consistent temperature of the Floridan aquifer at approximately 22o Celsius year-round (Suwannee River Water Management District, 2007). During extended cold-winter or hot-summer weather, water temperature from the aquifer can contrast sharply with that of surrounding surface waters (Siegel et al., 1996; Spechler, 1996). Airborne acquisition of thermal imagery during a winter-cold spell made it possible to generate maps of multiple aquifer-discharge locations and their associated thermal plumes. Nighttime thermal infrared-image acquisition eliminated the possibility of false positives such as solar-heated sand. Water features exceeding ambient temperatures by 4o Celsius or more were mapped as "hot spots." Thermal plumes from these features were mapped when they exceeded ambient water temperature by 1o Celsius or more. Field reconnaissance confirmed temperature anomalies, small boils, and a variety of discharge-location characteristics. Full methodology and results were published by Raabe and Bialkowska-Jelinska (2007).

Identified "hot spots" included linear sections of tidal creeks, "tadpole-shaped" features leading into tidal creeks, sinkholes within the coastal forest, and thermal plumes associated with temperature anomalies (Fig. 1). Mobile species, such as manatee and sturgeon, use seep locations as thermal refugia during cold winter weather (Carr et al., 1996; Packard and Wetterquist, 1986). Local plant communities can indicate distinct water quality and discharge characteristics. Additionally, the discharge associated with these submarine features can play an important role in estuarine water quality (Katz et al., 1999; Katz and Raabe, 2005). Comparison of these features with existing data sources such as habitat maps, historic change analysis, satellite thermal imagery, and biomass fluctuation reveal unique habitat characteristics at coastal-aquifer exit points in the coastal ecosystem. The application of thermal infrared imagery in mapping the distribution of coastal-aquifer seeps shows promise in visualizing underlying karst, fracture zones, and underground conduits.

REFERENCES

- Carr, S.H., Tatman, F., and Chapman, F.A., 1996, Observation on the natural history of the Gulf of Mexico sturgeon (*Acipenser oxyrinchus de sotoi* Vladykov 1955) in the Suwannee River, southeastern United States: Ecology of Freshwater Fish, v. 5, no. 4, 169p.
- Crane, J.J., 1986, An investigation of the geology, hydrogeology, and hydrochemistry of the Lower Suwannee River basin: Florida Geological Survey Investigation Report 96: 110.

- Katz, B.G., Hornsby, H.D. Bohlke, J.F., and Mokray, M.F., 1999, Sources and Chronology of Nitrate Contamination in Spring Waters, Suwannee River Basin, Florida: U.S. Geological Survey Water-Resources Investigations Report 99-4252: 54.
- Katz, B.G., and Raabe, E.A., 2005, Suwannee River Basin and Estuary: Integrated Watershed Science Program: U.S. Geological Survey Open-File Report; 2005-1210: 20. <http://gulfsci.usgs.gov/suwannee/reports/index.html>
- Packard, J.M. and Wetterquist, O.F., 1986, Evaluation of Manatee Habitat Systems on the Northwestern Florida Coast: Coastal Zone Management Journal, v. 14, no. 4, p. 279-310.
- Raabe, E.A. and Bialkowska-Jelinska, E., 2007, Temperature Anomalies in the Lower Suwannee River and Tidal Creeks, Florida, 2005: U.S. Geological Survey Open-File Report 2007-1311. <http://pubs.usgs.gov/of/2007/1311/>
- Rupert, F.R., 1988, Geology and geomorphology of Levy County, Florida: U.S. Geological Survey Open-File Report, no. 19, 18p.
- Rupert, F.R., 1991, Geology and geomorphology of Dixie County, Florida: U.S Geological Survey Open-File Report, no. 45, 6p.
- Siegel, E.M., Weisberg, R.H., Donovan, J.C., and Cole, R.D., 1996, Physical factors affecting intrusions in wetlands: the Suwannee River Estuary: University of South Florida, St. Petersburg, FL, Department of Marine Science, 127p.
- Spechler, R.M., 1996, Detection and quality of previously undetermined Floridian aquifer system discharge to the St. Johns River, Jacksonville to Green Cove Springs, northeastern Florida: U.S. Geological Survey Water-Resources Investigations Report, 95-4257, 29p.
- Suwannee River Water Management District, 2007, Technical Information about Springs. <http://www.srwmd.state.fl.us/water+data/springs/technical+info.htm>
- Verimap, 2005, Fresh Water Seeps Project Overview: VeriMap PLUS Inc., 30p. www.verimap.com

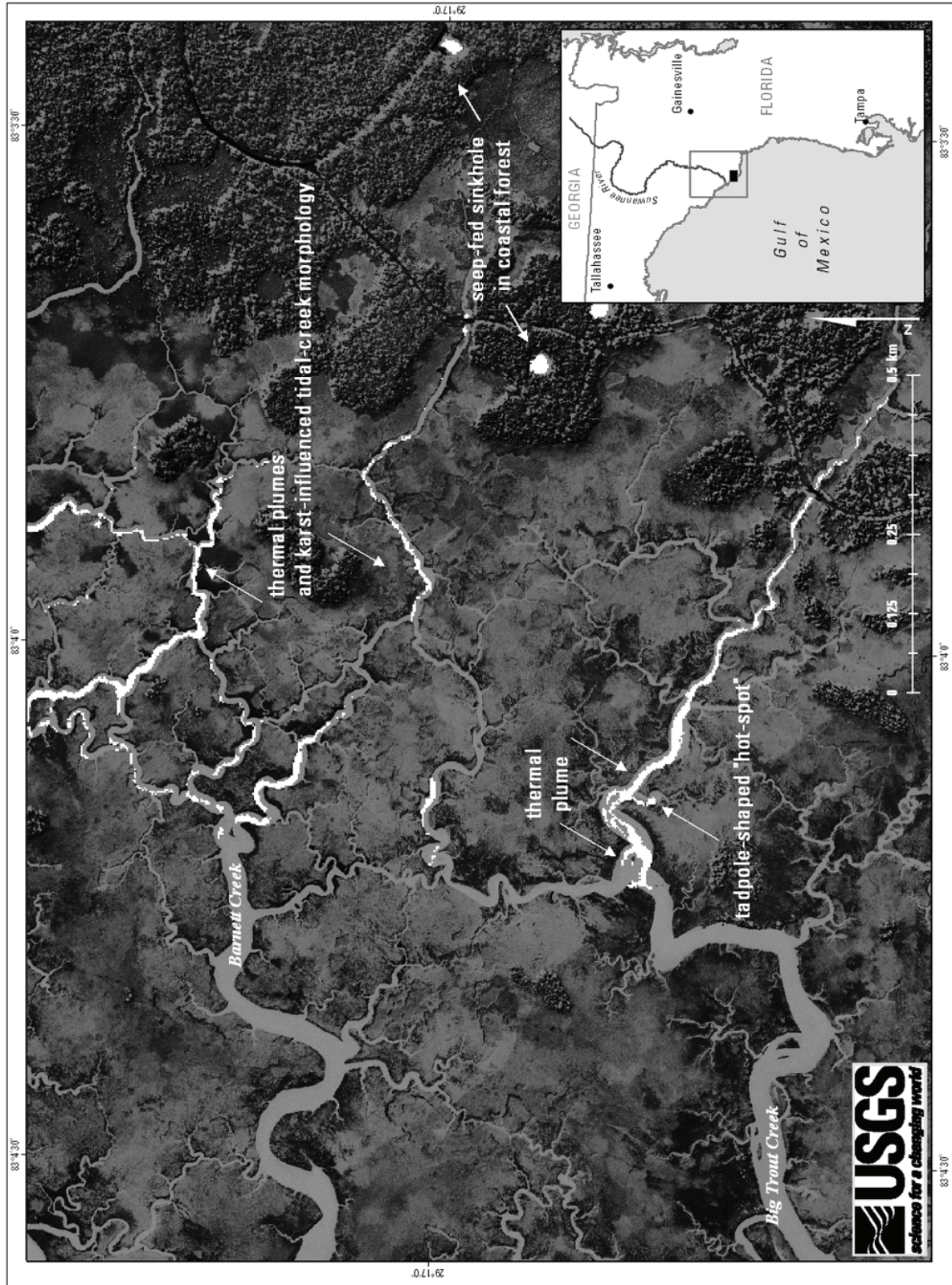


Figure 1. Tidal-creek temperature anomalies in nighttime thermal infrared imagery near Cedar Key, FL. Thermal plume direction reflects an incoming tide.

Effects of Lock and Dam Number Six on Aquatic Ecosystems in Mammoth Cave National Park

By Rick Olson

Mammoth Cave National Park, P.O. Box 7, Mammoth Cave, KY 42259

Abstract

Lock and Dam No. 6 was built in 1905-06 for barges carrying natural asphalt from mines at Kyrock on the Nolin River. Petroleum based asphalt replaced this natural tar sand for paving, and the decline of the mines resulted in the Lock being decommissioned in 1951. Normal flow of 16 miles of the Green River and 7 miles of the Nolin River in the park is retarded by the dam. Habitat for the endangered Kentucky cave shrimp has been degraded through loss of cave stream sediment variation due to siltation. Habitat for six species of freshwater mussels listed as endangered are seriously degraded through reduction of natural flow velocity and inundation of riffle habitat. Because of this, Lock and Dam No. 6 is the most severe ecosystem management issue in Mammoth Cave National Park. Green and Nolin Rivers possess one of the most diverse fish (82 species) and invertebrate faunas (51 species of mussels alone) in North America, and these populations would benefit from restoration of free flow.



Figure 1. The Kentucky Cave Shrimp (*Palaemonias ganteri*) is found only in the Mammoth Cave vicinity and is listed as endangered. Habitat degradation due to the Lock and Dam No. 6 impoundment is considered a prime causative factor in the decline of this species. (Photo courtesy of Chip Clark)

There are many reasons to remove the dam and preserve the lock at Brownsville. U. S. Fish and Wildlife Service has concluded that habitat for seven aquatic endangered species, six mussels and the Kentucky Cave Shrimp, will be restored. As well, conditions for many species in decline can be improved, and future listings prevented. The U. S. Army Corps of Engineers has agreed that such restoration is the best option for the needs of both wildlife and people, and that removal of the dam is the best way to save the lock from being undermined and destabilized.

Both ferries on Green River in the park will continue operations if the dam is removed, and a dredged channel will enable ferries to cross the river during periods of low water that currently prevent people from crossing the river. With restoration of free flow, the ability of river biota to clean water will be enhanced, and therefore water quality at the intake for the City of Brownsville will improve. Marginal sedimentation in the currently impounded portions of the Green and Nolin rivers will cease, smallmouth bass fishing will improve, and populations of rough fish such as carp and gar will decrease. Recreational opportunities, particularly canoeing, will increase with significant economic benefits for Edmonson County. With the dam removed and the lock stabilized, the history of navigation on Green and Nolin rivers could be shared with public through interpretive waysides.

GEOCHEMISTRY / CONTAMINANT TRANSPORT

Storm Period Fine Sediment Transport in Logsdon River, Turnhole Spring Basin, Mammoth Cave, Kentucky

By Stephen T. Kenworthy

Western Kentucky University, 1906 College Heights Blvd. #31066, Bowling Green, Kentucky 42101-1066

Abstract

Flow rate, water quality, and suspended sediment concentrations were measured in Logsdon River, a karst conduit within the Turnhole Spring Basin. Logsdon River drains approximately 25 square kilometers. Turnhole Spring drains approximately 240 square kilometers and discharges into the Green River within Mammoth Cave National Park. River stage and flow velocity were monitored continuously with an upward-looking acoustic doppler current profiler. Turbidity, water temperature, pH, and specific conductivity were recorded continuously with a multi-parameter water quality sonde. A laser-diffraction suspended sediment sensor (LISST 25x, Sequoia Scientific, Inc.) provided measurements of suspended solids concentration and grain size. Storm period water samples were collected with an automatic water sampler triggered on a turbidity threshold. Suspended solids concentrations were estimated based on LISST concentration estimates and on empirical correlations between turbidity and laboratory analysis of measured sediment concentrations.

Analyses of several flow events reveal that peaks in turbidity and suspended solids concentration display a complex relationship to variations in flow hydraulics. There is often a peak in turbidity and suspended sediment concentration that corresponds to peak stage and flow rate, followed by a secondary turbidity peak on the falling limb. Decreases in specific conductivity correlate with increases in turbidity and suspended solids concentration, supporting the interpretation that the peaks in suspended solids concentration correspond to the arrival of surface water at the monitoring site. The magnitude of the initial peak in sediment concentration scales with peak flow rate, whereas the magnitude of the secondary turbidity peak is weakly correlated with flow rate. The concentration of sand sizes (greater than 63 micron), tends to track flow rates closely, suggesting that the transport of these coarser fractions is dependent on local hydraulics and local supplies of sand in the conduit system. These patterns suggest that the initial sediment peak represents hydraulically controlled mobilization of sediment stored within the conduit system in response to proximal inputs from surface water sink points and rapid transmission of increases in hydraulic head through phreatic portions of the karst aquifer. The secondary suspended solids peak appears to represent inputs of finer suspended solids from distal surface inputs to the karst aquifer. This pattern of suspended solids concentration relative to discharge variation contrasts with typical surface water catchment responses in which suspended solids concentration peaks precede peak flow rates. These differences are likely important for understanding spatial and temporal patterns of contaminant transport in karst conduit systems.

Water Quality in Selected Carbonate Aquifers of the United States, 1993-2005

By Bruce D. Lindsey¹, Marion P. Berndt², Brian G. Katz², Ann F. Ardis³, and Kenneth A. Skach⁴

¹ U.S. Geological Survey, 215 Limekiln Road, New Cumberland, PA 17070

² U.S. Geological Survey, 2010 Levy Avenue, Tallahassee, FL 32310

³ U.S. Geological Survey, 8027 Exchange Drive, Austin, TX 78754

⁴ U.S. Geological Survey, 2130 SW 5th Avenue, Portland, OR 97201

Abstract

The U.S. Geological Survey (USGS) National Water-Quality Assessment Program collected 1,048 samples from wells and springs in 12 carbonate aquifers across the United States during 1993-2005; results for all samples were available to assess the factors affecting ground-water quality. The carbonate aquifers sampled are the Basin and Range carbonate-rock aquifers, Biscayne aquifer, Castle Hayne aquifer, Edwards-Trinity aquifer system, Floridan aquifer system, Mississippian aquifers, Ordovician aquifers, Ozark Plateaus aquifer system, Piedmont and Blue Ridge carbonate-rock aquifers, Prairie du Chien of the Cambrian-Ordovician aquifer system, Silurian-Devonian aquifers/Upper Carbonate aquifer, and Valley and Ridge carbonate-rock aquifers. Samples were analyzed for major ions, radon, nutrients, 47 pesticides, and 54 volatile organic compounds (VOCs). Water quality in the 12 carbonate aquifers was highly variable. The occurrences of anthropogenic contaminants (those derived from human activities) were related to potential sources inferred by land-use characteristics but were also affected by extent of aquifer confinement, ground-water age, and oxidation-reduction state. Unconfined aquifers overlain by agricultural or urban land were the most likely to have elevated concentrations of nitrate or detections of pesticides. Unconfined aquifers overlain by urban land were the most likely to have detections of VOCs.

Differences in concentrations of dissolved oxygen and dissolved organic carbon and in ground-water age were directly related to the occurrence of anthropogenic contaminants. Other geochemical indicators, such as mineral saturation indices, were used to infer relative residence time within an aquifer, an indirect indicator of potential for anthropogenic contamination. In general, land use, oxidation-reduction status, residence time, and aquifer confinement were the most important factors affecting occurrence of anthropogenic contaminants. Although none of these factors individually accounts for all the variation in water quality among the aquifers, a combination of these factors explains most of the variation.

Concentrations of nitrate were related to contaminant sources and aquifer characteristics. Concentrations of nitrate were significantly higher in unconfined aquifers than in water from confined aquifers and aquifers with mixed confinement. Water recharged in 1953 or later had significantly higher concentrations of nitrate than water recharged prior to that date. Oxidation-reduction state was also a key factor affecting nitrate concentrations; in recently recharged waters, samples of oxic waters had significantly higher concentrations of nitrate than anoxic waters, regardless of land use in the area near the well. This implies that denitrification had occurred in the older, anoxic waters. Samples from 54 wells (5 percent) exceeded the U.S. Environmental Protection Agency (USEPA) Maximum Contaminant Level (MCL) of 10 mg/L for nitrate in drinking water. The vast majority of these samples were in the Piedmont and Valley and Ridge aquifers. The median concentrations of nitrate ranged from 9 mg/L in the Piedmont to near the detection limit of 0.06 mg/L in three other aquifers. None of the water recharged prior to 1953 and only a single sample from a confined aquifer had nitrate concentrations that exceeded 10 mg/L as nitrogen.

At least 1 of the 47 pesticides analyzed was reported as present in about half samples from the 1,033 sites where pesticide data were collected. The criteria for determining pesticide detections included those values greater than or equal to the laboratory reporting level for each specific pesticide (ranging from 0.018 µg/L to as low as 0.001 µg/L) and also included values that were below the laboratory reporting

level but positively identified in the sample (estimated values). The most frequently occurring pesticide compounds were four herbicides—atrazine, simazine, metolachlor, and prometon—and deethylatrazine, a degradate of atrazine. Multiple pesticides frequently were present in a single sample of water; 34 percent of the samples had two to five pesticides in the same sample, and 4 percent of the samples had six or more pesticides. Water recharged in 1953 or later had a significantly higher number of pesticides detected than water recharged before 1953, and water from unconfined aquifers had a significantly higher number of pesticides detected than water from confined or mixed confinement aquifers. Water from sites in unconfined aquifers where land use was agricultural or urban accounted for the majority (81 percent) of detections of pesticides. Three of the aquifers had at least one pesticide detected in greater than 80 percent of the wells, and three other aquifers had at least one pesticide detected in less than 15 percent of the wells.

Concentrations of organic compounds are compared to MCLs for regulated compounds and to USGS Health-Based Screening Level (HBSL) concentrations for unregulated compounds. HBSLs are benchmark concentrations used to evaluate water-quality data in a human-health context but are not enforceable standards. No sample had a pesticide concentration that was greater than a USEPA MCL; however, two pesticides had concentrations that were greater than the HBSLs in one or more samples. Dieldrin concentrations were greater than the HBSL of 0.002 $\mu\text{g/L}$ in 20 samples, 9 of which were from either domestic or public supply wells. A single sample from a domestic supply well had a diazinon concentration greater than the HBSL (1 $\mu\text{g/L}$).

One or more VOCs were detected at a concentration greater than 0.2 $\mu\text{g/L}$ (the highest common laboratory reporting level) in 157 of the 799 samples in which VOCs were analyzed (20 percent). The most frequently occurring VOCs were chloroform, carbon disulfide, toluene, tetrachloroethene (PCE), and chloromethane. Detections of VOCs were more frequent in urban and mixed land-use settings than in agricultural and undeveloped settings. Three VOCs, PCE, trichloroethene (TCE) and 1,2-dichloropropane, had one sample each with a concentration greater than the USEPA MCL—the MCL is 5 $\mu\text{g/L}$ for each of these VOCs.

This study has shown that water quality in carbonate aquifers has a substantial amount of variation across the aquifers studied. Common factors, such as extent of confinement or ground-water age, help explain why some carbonate aquifers have higher levels of contamination than others. A land-use practice that contributes a source of a contaminant is necessary for the presence of that contaminant in ground water; however, in some cases, transformation processes mitigate the effects of land use. These findings can be used by water-resource managers to help manage water quality in these aquifers.

Effect of Focused Recharge on the Geochemistry of Barton Springs, Edwards Aquifer, Central Texas during Base-Flow Conditions

By Barbara J. Mahler, and MaryLynn Musgrove

U.S. Geological Survey, 8027 Exchange Drive, Austin, TX 78754

Abstract

Geochemical variability of karst spring flow has been shown to be closely linked to storm events (for example, Andrews and others, 1984; Ryan and Meiman, 1996; Personné and others, 1998; Vesper and White, 2004; Mahler and Massei, 2007). Less attention, however, has been paid to the relation between focused recharge and spring geochemistry under base-flow conditions. The Barton Springs segment of the Edwards aquifer, Austin, Texas, is well situated for studying this relation: An estimated 85 percent of aquifer recharge occurs as focused recharge through the beds of six ephemeral creeks, and an estimated 90 percent of aquifer discharge occurs at Barton Springs (Slade and others, 1986). Concentrations of major ions, nutrients, soluble pesticides, and volatile organic compounds were measured at Main Barton Spring at two or three week intervals from 2003 through 2005 (Mahler and others, 2006). The relations between estimated recharge rate through creek beds and concentrations of major ions, nutrients, the pesticide atrazine, and the volatile organic compound tetrachloroethene in spring flow were investigated. Recharge rate was inversely correlated with concentrations of some constituents and contaminants, including sodium, chloride, and nitrate. This indicates that concentrations of these compounds are higher in water stored in the aquifer than in focused recharge, which dilutes them as it mixes with water already in the aquifer. Recharge rate was positively correlated with other constituents and contaminants, including tetrachloroethene, indicating that focused recharge are transporting these compounds into the aquifer. Additionally, some relations indicated that geochemical processes were ongoing within the aquifer, including water-rock interaction and degradation of organic matter. The results highlight the quantifiable influence of surface-water quality on karst ground-water quality under a range of flow conditions.

REFERENCES

- Andrews, F.L., Schertz, T.L., Slade, R.M., Jr., and Rawson, Jack, 1984, Effects of storm-water runoff on water quality of the Edwards aquifer near Austin, Texas: U.S. Geological Survey Water-Resources Investigations Report 84-4124, 50 p.
- Mahler, B.J., Garner, B.D., Musgrove, M., Guilfoyle, A., and Rao, M., 2006, Recent (2003-05) water quality of Barton Springs, Austin, Texas, with emphasis on factors affecting variability: U.S. Geological Survey Scientific Investigations Report 2006-5299, 83 p., 5 appendixes.
- Mahler, B.J., and Massei, N., 2007, Anthropogenic contaminants as tracers in an urbanizing karst aquifer: *Journal of Contaminant Hydrology*, v. 91, p. 81-106.
- Personné, J.-C., Poty, F., Vaute, L., and Drogue, C., 1998, Survival, transport, and dissemination of *Escherichia coli* and enterococci in a fissured environment. Study of a flood in karstic aquifer: *Journal of Applied Microbiology*, v. 84, p. 431-438.
- Ryan, M., and Mieman, J., 1996, An examination of short-term variations in water quality at a karst spring in Kentucky: *Ground Water*, v. 34, p. 23-30.
- Slade, R.M., Jr., Dorsey, M.E., and Stewart, S.L., 1986, Hydrology and water quality of the Edwards aquifer associated with Barton Springs in the Austin area, Texas: U.S. Geological Survey Water-Resources Investigations Report 86-4036, 117 p.
- Vesper, D.J., and White, W.B., 2004, Storm pulse chemographs of saturation index and carbon dioxide pressure: implications for shifting recharge sources during storm events in the karst aquifer at Fort Campbell, Kentucky/Tennessee, USA: *Hydrogeology Journal*, v. 12, p. 135-143.

An Overview of the Geochemistry of Edwards Aquifer Ground Water in South-Central Texas

By MaryLynn Musgrove, Lynne S. Fahlquist, and Natalie A. Houston
U.S. Geological Survey, 8027 Exchange Drive, Austin, TX 78754

Abstract

The U.S. Geological Survey collected 249 ground-water samples from 136 sites in the San Antonio segment of the Edwards aquifer during June 1996 through December 2006 as part of the National Water-Quality Assessment Program. The Edwards aquifer is a highly-productive, fractured, karst aquifer developed in Cretaceous-age carbonate rocks and is well-suited for examination of ground-water evolution processes as well as urban influences on ground-water quality. Samples were analyzed for a broad range of geochemical and isotopic constituents, including some anthropogenic contaminants. The resulting geochemical dataset was evaluated to assess regional-scale geochemistry, processes controlling ground-water evolution, natural and anthropogenic factors affecting water quality, spatial and temporal trends in ground-water geochemistry, and the interaction between hydrologic conditions and ground-water geochemistry.

Edwards aquifer ground water is dominantly fresh, Ca-Mg-HNO₃, oxygenated water (median specific conductance is 550 microsiemens per centimeter). Carbonate mineral-solution reactions and ground-water residence time can account for most of the observed range of regional-scale geochemical and isotopic variability. A few samples are influenced by downdip saline water or water from the underlying Trinity aquifer. Variations in Mg/Ca ratios, which are indicators of residence time and water-rock interaction in carbonate aquifers, and Sr isotope compositions, provide insight into sources of dissolved constituents in ground water, water-rock interaction pathways, and ground-water residence time. Hydrologic conditions exert strong control on both regional- and local-scale geochemistry. Data for a small number of sites sampled relatively frequently indicate close links between surface water and ground water in this aquifer, particularly with respect to ground-water quality.

Some organic contaminants were frequently detected in Edwards aquifer samples at very low (less than 1 microgram per liter) concentrations: atrazine, deethylatrazine (a degradate of atrazine), and chloroform (a byproduct of drinking-water treatment) were detected in more than 50 percent of the samples and were more frequently detected (in more than 75% of the samples) from shallow, unconfined, recharge-zone wells in the urban San Antonio area. The variation in concentration of frequently detected organic compounds, such as atrazine, and nitrate with respect to hydrologic conditions provides insight into their sources and transport into the aquifer. Nitrate concentrations range from less than 0.05 to 8.2 milligrams per liter with a median concentration of 1.7 milligrams per liter; nitrate concentrations greater than 3 were restricted to a few samples and might indicate anthropogenic influences. Mg/Ca ratios vary inversely with concentrations of some of the frequently detected organic contaminants, which indicate that these compounds likely are entering the aquifer with recharging surface water.

The Role of Free-Living and Attached Bacteria in Processing Contamination in Karst Aquifers

By Tom Byl^{1,2}, Kelly Ray², Chad Walden², Valetta Watson², and Roger Painter²

¹U.S. Geological Survey, 640 Grassmere Park, Suite 100, Nashville, TN 37211

²College of Engineering, Technology and Computer Science, Tennessee State University, 3500 John A. Merritt Blvd., Nashville, TN 37209

Abstract

In karst aquifers, biodegradation can be accomplished both by surface-attached and free-living bacteria. Biodegradation by attached bacteria is dependent upon and limited by the relatively low surface area to volume ratio (SA/V) of karst aquifers. Biodegradation due to free-living bacteria, however, is not limited by SA/V, but by residence time. The objective of this research was to determine if free-living karst bacteria contributed as much to the removal of ammonia (NH₃) as attached, indigenous karst bacteria. These results were compared with the results of a toluene biodegradation study conducted using the same set up (Painter and others, 2005 KIG). The experimental setup included flow-through karst microcosms with high and low SA/V ratios. The low SA/V ratio system consisted of three 1-L cylinders connected together with non-stick tubing. The high SA/V ratio karst system was similar except the cylinders were packed with glass beads to increase the SA/V ratio by approximately 500%. Microscopic examination confirmed that bacteria colonized the interior surfaces of the lab karst systems. Fresh spring water containing between 10,000 and 20,000 indigenous karst bacteria was continuously pumped through each system. A known quantity of NH₃ was added as a food source and measured at the exit port. Flow rates were similar and residence time differences were compensated for with the residence-time distribution (RTD) formula described by King and others (2005). First-order NH₃-biotransformation rate constants were 0.17 day⁻¹ for the low SA/V system and 0.27 day⁻¹ for the high SA/V system. In the previous toluene study, the first-order rate constants were 0.014 hour⁻¹ for the low SA/V system and 0.016 hour⁻¹ for the high SA/V ratio system leading Painter (2005) to conclude that free-living bacteria contribute as much to toluene biodegradation processes as attached bacteria in karst aquifers. This study suggests that this is not the case with respect to NH₃ biotransformation in karst systems.

Characterization of Bacteria and Geochemistry of Springs in Nashville, Tennessee

By Patrice Armstrong^{1,2}, Carlton Cobb^{2,3}, Brandon Cobb^{2,3}, Jennifer Stewart-Wright⁴, Tom Byl^{2,1}

¹Biological Science, Tennessee State University, 3500 John A Merritt Blvd, Nashville, TN 37209

²U.S. Geological Survey, 640 Grassmere Park, Suite 100, Nashville, TN 37211

³Civil and Environ. Engineering Dept., Tennessee State University, 3500 John A. Merritt Blvd., Nashville, TN 37209 .

⁴Office of Research and Sponsored Programs, Tennessee State University, 3500 John A Merritt Blvd., Nashville, TN, 37209

Abstract

The objective of the project was to evaluate the water quality of four limestone bedrock springs in an urban environment during a severe drought in the summer of 2007. Three of the springs were discovered on the Tennessee State University (TSU) campus in Nashville, TN in May, 2007. Two are located near a poultry research facility and a third near the TSU athletic center. An additional spring flowing from a cave in the Charlotte Park neighborhood of west Nashville (Carlos Cave) was also included in the study. The two TSU springs behind the poultry barns were sampled approximately every week from June through September, 2007. The cave and TSU athletic center springs were sampled less frequently. Water quality parameters included temperature, specific conductance, and dissolved oxygen, pH, sulfate, nitrogen, *E. coli*, and bacteria Biological Activity Reaction Tests (BART). Continuous water-quality monitoring devices were installed at two of the springs to measure changes associated with different weather patterns. Water temperatures were very stable, ranging from 16°C in June to 19°C in September. Sulfate concentrations were consistently higher in the spring water than the receiving surface waters, suggesting that surface vegetation may have removed the sulfate. Conversely, nitrogen levels were lower in the spring water (< 10 mg/L) than the surface waters, suggesting denitrification by bacteria in the subsurface. Fecal bacteria levels fluctuated randomly with no discernable correlation to weather pattern. BART tests confirmed the presence of denitrifying, iron-reducing, sulfur-reducing, and slime-producing bacteria at each of the springs. Spring discharges decreased at all sites as the drought continued but never decreased below 10 gallons per minute. The data showed that each spring had unique water quality characteristics reflective of the different hydrologic recharge areas that replenish them.

Conduit-Matrix Interaction and the Rate Limiting Step of Contaminant Transport in Karst

By K.J. McCoy¹, A.M. Shapiro², and M.D. Kozar³

¹U.S. Geological Survey, 4338 Montgomery NE, Suite 400, Albuquerque, NM 87109

²U.S. Geological Survey, 12201 Sunrise Valley Drive, Reston, VA 20192

³U.S. Geological Survey, 11 Dunbar Street, Charleston, WV 25301

Abstract

Conceptualizations of karst aquifers are often rooted in early research and exploration of solutionally enlarged conduits. As a result, models of the karst continuum fail to fully characterize telogenetic systems that show evidence of significant contribution from non-conduit processes. In a unique setting in the northern Great Valley of the eastern United States, extensive characterization of a Paleozoic karst aquifer provides the opportunity to explore non-conduit processes and the contributions of secondary porosity to overall fluid budgets in karst. At the U.S. Geological Survey Leetown Science Center, geophysical data and water-level hydrographs indicate that the extent of conduits in Paleozoic karst may be spatially limited and that secondary porosity may, in part, control the rates of downgradient chemical migration.

To improve our understanding of the influence of secondary porosity components on transport in telogenetic karst aquifers, two forced gradient tracer tests were conducted in wells intersecting solutionally modified zones. In each test, tracers were injected in shallow conduits (~15m depth) while vertical gradients were induced by pumping in packer-isolated deep conduits (~40m depth). Tracer concentrations were monitored in both injection and pumping wells. The results show that (1) contaminants may persist in zones of high permeability for much longer periods than previously expected, (2) the rates of mass transfer in individual karst conduits varies over distances less than tens of meters, and 3) fully saturated conduits may serve primarily as areas of storage at times of baseflow. These experiments offer additional information on flow across non-conduit zones under variable stresses, provide detail on the architecture of faulted conduit zones, and establish an understanding of transport properties along complex structural zones in telogenetic karst systems.

Assessing Age Distribution and Contaminant Movement in Ground Water in the Contributing Recharge Area to a Public Supply Well in the Karstic Upper Floridan Aquifer

By Brian G. Katz¹, Christy A. Crandall¹, W. Scott McBride², Patty A. Metz², Marion P. Berndt¹, and Sandra M. Eberts³

¹U.S. Geological Survey, 2010 Levy Ave., Tallahassee, FL 32310

²U.S. Geological Survey, 10500 University Center Dr., Ste.215, Tampa, Florida 33612

³U.S. Geological Survey, 6480 Doubletree Ave., Columbus, Ohio 43229

Abstract

Multiple isotopic and other chemical tracers were used to assess age distribution and contaminant movement in ground water within a contributing recharge area to a public supply well (PSW) near Tampa, Florida, as part of the U.S. Geological Survey National Water Quality Assessment Program. During 2003-2006, water samples were collected from the PSW [open interval 39-53 m below land surface (bls)] and 28 monitoring wells in the karstic Upper Floridan aquifer (UFA) and the overlying surficial aquifer system (SAS). Concentrations of the transient age tracers, SF₆ and ³H/³He, in water from the oxic SAS indicated recent recharge (<7 years), but tracer concentrations in water from monitoring wells and the PSW in the anoxic UFA were consistent with binary mixtures that contained varying amounts of recent recharge and tracer-free water (>50 years). Although ground-water age generally increased with depth in the UFA, monitoring wells that tapped a 43-49 m zone (bls) had higher fractions of young water than water from wells at shallower depths (23-31 m bls). Mixtures of water in the PSW also were consistent with delta ³⁴S of sulfate, ²²²Rn, nitrate-N, and VOC concentrations that fell between end-member values for waters from the SAS and various zones in the UFA. Ratios of ⁸⁷Sr/⁸⁶Sr in the PSW water were slightly less radiogenic (0.70779) than water from other UFA monitoring wells (0.70790-0.70804) indicating that the PSW also withdraws some water from deep parts of the aquifer. Geochemical mass-balance mixing models for the PSW indicate a 40-60% contribution of water from the SAS based on various isotopic and chemical indicators. Geophysical data from the PSW borehole indicated a highly transmissive zone at 43-49 m bls, which likely is related to a large solution feature that is hydraulically connected to the surface and SAS, thus yielding the younger age water mentioned above.

Ammonia Oxidation by Bacteria Collected from a Karst-Bedrock Well

By Kelly Ray¹, Roger Painter¹, and Tom Byl^{1,2}

¹College of Engineering, Technology and Computer Science, Tennessee State University, 3500 John A. Merritt Blvd., Nashville, TN 37209

²U.S. Geological Survey, 640 Grassmere Park, Suite 100, Nashville, TN 37211

Abstract

Elevated ammonia concentrations in groundwater pose health and environmental problems. In karst systems where water can enter directly through sinkholes or disappearing streams without any filtration, ammonia contamination can be exacerbated. The rate of ammonia oxidation by nitrifying bacteria in karst systems is not known. The objective of this study was to characterize the aerobic and anaerobic rate of NH_3 oxidation using bacteria indigenous to a karst aquifer in Middle Tennessee. Static batch reactors using indigenous karst bacteria collected from a spring established a first-order rate of NH_3 -oxidation (k) = 0.0209 per day. Because this rate appeared to be slow, in a follow-up experiment, the effect of supplements and surface area were investigated. It was found that, in a flow-through karst system, a 500% increase in surface area to volume (SA/V) ratio increased the k value 54%. Addition of 1 g of lactate/L further increased the k value almost 10-fold. Because NH_3 -oxidizing bacteria are autotrophs (CO_2 fixing), it is hypothesized the lactate stimulated the growth of symbiotic bacteria that significantly enhanced the activity of NH_3 -oxidizing bacteria. Anaerobic NH_3 oxidation was also investigated using data collected in 2002 from an anaerobic karst site in northern Tennessee with high levels of NH_3 . The tracer and ammonia data were entered into the RTDB model and yielded a calculated ammonia oxidation k of 0.0168/day. The observation of ammonia biotransformation at an anaerobic site is circumstantial evidence that the anaerobic ammonia oxidation pathway called anammox was active. Additional research, however, is needed to confirm if the anammox pathway was responsible for the observed anaerobic removal of NH_3 .

Wetland Removal of Nutrients and Pollution from a Mixed Sewer and Karst Spring System in Nashville, Tennessee

By Carlton Cobb^{1,3}, Jameka Johnson^{1,3}, Brandon Cobb^{1,3}, Patrice Armstrong^{2,3}, Lonnie Sharpe¹, and Tom Byl^{1,3}

¹College of Engineering, Technology and Computer Science, Tennessee State University, 3500 John A. Merritt Blvd., Nashville, TN 37209

²Biology Dept., Tennessee State University, 3500 John A. Merritt Blvd., Nashville, TN 37209 .

³U.S. Geological Survey, 640 Grassmere Park, Suite 100, Nashville, TN 37211

Abstract

Wetlands have been shown to attenuate suspended sediments and agricultural pollution in rural areas but little work has been conducted regarding the benefits of the wetlands in mitigating urban non-point source pollution (NPS). The objective of this project was to determine if an 80 acre natural wetland located down gradient of bedrock springs, parking lots, city streets and leaky sewer systems in Nashville, Tennessee helped to mitigate urban NPS runoff. Sampling points were selected by reconnaissance during rainfall events to determine general flow paths. Water samples were collected at these sampling points during base-flow and rain runoff events. Water-quality monitors were also placed in the springs and along the flow path during the 12 month period of study. Water samples were analyzed within 48 hours for turbidity, specific conductance, pH, and volatile organic compounds (VOC). Additional analyses were performed for sulfate (SO₄), nitrate (NO₃), ammonia (NH₃) and chemical oxygen demand (COD). It was found that runoff from parking lots and roads during winter storms had relatively high VOC levels (62 µg/L benzene, 132 µg/L toluene, 106 µg/L xylenes, and a number of unidentified compounds). Water samples collected downstream of the wetland, however, had VOC concentrations below detection levels. Water samples collected at the most downstream site also had significantly lower levels of turbidity (90 % lower), NH₃ (99% lower), COD (95% lower), NO₃, (90% lower), and SO₄ (63% lower) on average for the year. The results indicated that routing water through the urban wetland resulted in significant water-quality improvements during the study period.

Are Karst Bedrock Aquifers at Greater Risk from Alternative Alcohol-Fuel Mixes Compared to Regular Gasoline?

By Baibai Kamara¹, Loreal Spear¹, Carlton Cobb^{1,2}, Keyshon Bachus¹, Roger Painter¹, Lonnie Sharpe¹, and Tom Byl^{1,2}

¹College of Engineering, Technology and Computer Science, Tennessee State University, 3500 John A. Merritt Blvd., Nashville, TN 37209

²U.S. Geological Survey, 640 Grassmere Park, Suite 100, Nashville, TN 37211

Abstract

The United States government is promoting alternative fuels that reduce our dependency on foreign oil. Tennessee is promoting E-85, a fuel that consists of 85 percent ethanol and 15 percent gasoline. The environmental fate of gas-alcohol mixtures, however, has not been investigated. The consequences of an uncontrolled spill of E-85 or a related mixture would, therefore, be very difficult to predict. The objective of this research was to determine if a commercial grade E-85 mixture would dissolve more readily in water and move faster through water-saturated soil than regular gasoline. A better understanding of E-85 mobility in the subsurface is of practical importance if E-85 is to become widely used and stored in underground storage tanks like conventional fuels. Solubility-in-water studies comparing gasoline with E-85 found that the ethanol component in E-85 acted as a co-solvent and enabled aromatic compounds to dissolve five times more rapidly in water than regular gasoline. These enhanced solubility characteristics may allow the aromatic rings to move faster and further through water-saturated soils and karst conduits than regular gasoline. Additional experiments were conducted to determine if regolith soils would affect the dispersal rate of E-85 fuel compounds. Sterile soil-column studies using soils collected from karst regions of Middle Tennessee demonstrated that aromatic compounds, such as benzene, toluene or xylene (BTX), from the E-85 moved 3 to 4 times faster than BTX compounds in regular gasoline when transported by water through the soil. These results suggest that leakage of E-85 from underground storage tanks could result in wider contamination of aquifer materials in a shorter time than regular gasoline. Additional work compared the biodegradation of E-85 with regular gasoline. Using static reactors with karst bacteria, E-85 biodegradation rates were almost 5 times greater than regular gasoline. This is in agreement with previous reports finding that dissolved-phase fuels were more bioavailable and degraded faster. Additional studies are needed to more thoroughly address issues concerning E-85 solubility and biodegradation.

Residence Time Distribution Derived from Independent Gamma Distributions of Tracer Travel Distance and Linear Velocity

By Roger Painter¹, Tom Byl^{1,2}, and Valetta Watson¹

¹College of Engineering, Technology and Computer Science, Tennessee State University, 3500 John A. Merritt Blvd., Nashville, TN 37209

²U.S. Geological Survey, 640 Grassmere Park, Suite 100, Nashville, TN 37211

Abstract

The advection dispersion equation (ADE) is widely used as a predictor of residence time distributions (RTDs) for tracer breakthrough curves for karst systems. Solutions of the ADE for tracer breakthrough studies with near plug flow behavior are characteristically Gaussian in appearance. However, very few, if any, quantitative tracer studies result in tracer concentrations that are normally distributed about the mean residence time. While the symmetry of Gaussian breakthrough curves often correctly predicts finite tracer concentrations at zero time, it generally does not accurately predict actual tracer breakthrough curves, which invariably are characterized by relatively long tails. This suggests that a different conceptual approach may be appropriate for describing these systems in easily visualized terms. The objective of this project was to develop a more descriptive approach of tracer break-through data based on the gamma probability density function. The tracer travel distance and tracer linear velocity were assumed to be randomly distributed variables with gamma distributions. The RTD for tracer breakthrough curves was derived from the individual distributions of tracer travel distance and linear velocity. This approach was compared and contrasted with the traditional approach based on the ADE for modeling tracer break-through data at a karst site, as well as, modeling the rate of biodegradation of toluene in laboratory karst aquifers.

Episodic Elevated Coliform in Vadose-Zone Water within Mammoth Cave National Park, Kentucky

By Rickard S. Toomey III¹, Rick Olson², and Bob Ward²

¹Mammoth Cave International Center for Science and Learning, 1906 College Heights Blvd #31066, Bowling Green, KY 42101

²Mammoth Cave National Park, PO Box 7, Mammoth Cave, KY 42259

Abstract

In October 2006, microbiology researchers identified elevated levels of fecal coliforms (and in many cases *Escherichia coli*) in some vadose-zone waters in Mammoth Cave National Park (the Park). They were identified in several waterfalls and seeps that are fed by water from the area of the park containing the visitor center, parking lots, and campground. The fecal coliform levels vary from less than ten colony-forming units per 100 milliliter to several thousand colony-forming units per 100 milliliter. Often spikes in coliform level are linked to rain events. Spikes have not been identified from areas that are not associated with development.

The identification of the elevated coliform levels led to several responses. Rapid testing determined what areas were showing fecal coliform contamination. Initial testing and discussions with the Public Health Service determined that Kentucky secondary contact standards would apply to the situation. Synoptic testing of two areas (the waterfalls at the Historic Entrance and Mammoth Dome) is continuing to monitor for possible risks to human health; however, the health standard has not been exceeded to date. A more research oriented program involving dye tracing to better understand vadose-zone flow in the developed area, systematic synoptic and event-based sampling, and efforts to source-type the bacteria has started. In addition, inspections of the sewer lines in the park indicated locations of some breaks in sewer pipes. These breaks were repaired.

Elevated coliform within Mammoth Cave is an on-going issue of concern at the Park. The current status of both the research and the Park's response will be discussed.

NUMERICAL MODELING

Modeling Ground-water Flow and Solute Transport in Karst with Lattice Boltzmann Methods

By M.C. Sukop¹, S. Anwar¹, J.S. Lee¹, K.J. Cunningham², and C.D. Langevin²

¹ Department of Earth Sciences, Florida International University, Miami, FL 33199

² U.S. Geological Survey, 3110 SW 9th Avenue, Fort Lauderdale, FL 33315

Abstract

Lattice Boltzmann Methods (LBMs) are relatively new and have not yet been widely applied to ground-water systems. LBMs are particularly attractive for numerical modeling of flow and solute transport in karst aquifers because they are able to:

- Simulate inertial flows
- Incorporate complex wall and conduit geometries
- Solve adjacent Darcian and Navier-Stokes flow regimes
- Solve the appropriate advection-diffusion equation in conduit zones characterized by laminar or eddy flow and solve a linked anisotropic advection-dispersion equation in porous media zones with Darcian flow

Examples are provided for each of these capabilities.

INTRODUCTION

Simulation of flow and transport in karst aquifers is widely recognized to be a remaining frontier in ground-water research. There are two primary reasons why this is the case: (1) characterization of karst aquifers is more challenging than characterization of aquifers composed of porous media because conduits that convey the bulk of the flow can be present and (2) within the conduits, the fundamental equations familiar to ground-water hydrologists—Darcy's law-based ground-water flow equation and the Advection-Dispersion Equation (ADE)—are not applicable to inertial flows and resulting eddy mixing, which are commonly present.

The Lattice Boltzmann Method (LBM) is capable of simultaneously solving for inertial flows and advection-diffusion needed to simulate flow and transport in conduits. The LBM is based on the 'stream and collide' paradigm of Boltzmann's kinetic theory of gasses. It is the offspring of earlier lattice gas cellular automata, which were based on explicit particle collisions but often prove too cumbersome for practical flow calculation. To compute the inertial flows, LBM essentially solves the Navier-Stokes (N-S) equations. In

hydrology, the LBM has most often been applied to pore-scale flow, transport, and reaction modeling [Zhang and Kang, 2004; Pan et al., 2006; Kang et al., 2006] and its value in that realm can not be disputed. Substantial gains in understanding pore-scale processes have been achieved. For field-scale problems however, pore-scale simulation is currently limited by computational resources and may always be limited by the availability of detailed input data required.

Recent advances [Zhang et al., 2002a,b; Ginzburg, 2005] have demonstrated the viability of LBM for solving the traditional solute transport equations in simple ground-water flow systems. Earlier work [e.g., Dardis and McCloskey, 1998a,b; Kang, et al. 2002] demonstrated steady state adherence to Darcy's law using similar macroscale LBM. This upscaling of LBM to the macroscopic equations obviates the scale problem and allows the use of traditional aquifer and solute transport parameterizations. The solute transport and heterogeneous flow solvers have generally not been linked in previous literature. Moreover, integration of such models with more common LBM flow and transport codes would enable solution of the full Navier-Stokes and appropriate advective-diffusive equations in

conduits, allowing for inertial flows and resulting eddy mixing while addressing matrix diffusion in the porous medium [Anwar et al., 2008]. However, it remains for the components of such a model to be selected from among several variants, fully developed, tested, and integrated into a package that utilizes a conceptual and pragmatic framework accessible to the ground-water modeling community.

Efforts to simulate karst and fracture hydrology using the pipe and slit flow models of hydraulic engineers have led to some advances, though representing complex aquifers with simple pipe elements is oversimplified for certain purposes [White, 2002]. For example, in one state-of-the-art model [Birk et al., 2003] the Darcy-Weisbach equation gives the average velocity in a pipe in terms of pipe diameter, head gradient, gravity, and a friction factor. For Reynolds numbers (Re) less than 2000 (often taken as the transition to fully developed turbulence) the friction factor is approximated as inversely proportional to Re. At higher Re, the implicit Colebrook-White equation is used iteratively to determine the friction factor in terms of the “roughness height” and hydraulic radius. Flow between conduits and surrounding porous media is assumed to be governed by a proportionality constant that relates the flow to the head difference. The proportionality constant has a complex dependence on numerous factors [Birk et al., 2003].

LBM's can directly simulate flows in the complex geometry of karst and fractured rock aquifers and automatically transition between laminar, inertial, and turbulent flow over a complete spectrum of behavior as appropriate for the geometry and imposed conditions. LBM's are also highly effective at simulating the coupled movement of contaminants in these flows. No substantial previous applications of LBM's to karst hydrology are known, though the potential was recognized some years ago [Watson et. al., 2003].

LBM's can be used to address solute retention due to entrapment in eddies, in porous media directly adjacent to conduits (“matrix diffusion”), and in low permeability formations where flow and transport are governed by the

standard ground-water flow and solute transport equations.

This paper reviews the current status of some potential components of this new approach, and is organized as follows. First, traditional pore-scale simulation of flow and transport is reviewed and an example involving non-Darcian flow in a macroporous limestone is presented. Two different methods of solving ground-water flow with LBM's are then introduced and demonstrated. Next, approaches for incorporating solute transport are discussed and an example of the capabilities of the model for solute transport in a conduit within a heterogeneous porous medium is presented. Finally, examples of available data and their utilization in the proposed model are presented.

PORE-SCALE FLOW AND TRANSPORT SIMULATION USING LBM

Pore-scale modeling of single-phase flow and reactive transport has advanced rapidly in the last few years [Zhang and Kang, 2004; Pan et al., 2006; Kang et al., 2006]. In this paper, we discuss only advective and diffusive/dispersive solute transport, though advances in density-dependent flows are being made [Thorne and Sukop, 2004; Bardsley et al, 2006]. Inclusion of multiphase fluid capabilities [e.g., Pan et al., 2004; Sukop and Or, 2004; Li et al. 2005] and reaction models that account for precipitation and dissolution [e.g., Kang, et al., 2006] would represent the ultimate foreseeable evolution of the model.

The most common LBM for single-phase fluid flow is based on the gas collision model of Bhatnagar, et al. [1954] and is commonly referred to as the Bhatnagar-Gross-Krook (BGK) model. This model employs a single relaxation time, τ , for each component (fluid, solute, energy) that controls the viscosity of simulated fluids and the diffusion of solutes and heat.

The fundamental collide-and-stream BGK LBM equation is

$$f_a(\mathbf{x} + \mathbf{e}_a \Delta t, t + \Delta t) = f_a(\mathbf{x}, t) - \frac{\Delta t [f_a(\mathbf{x}, t) - f_a^{eq}(\mathbf{x}, t)]}{\tau}, \quad (1)$$

where the collision operator is the right-hand side of the equation. Here \mathbf{x} is a position vector, ‘ a ’ represents one of the principal directions on the particular lattice; $a = 0$ for zero-velocity rest particles. We use consistent LBM space and time units of ‘lu’ (lattice length units) and ‘ts’ (lattice time steps). The term \mathbf{e}_a represents lattice-bound velocity vectors, t represents time, Δt is the time step (taken as 1 ts here), τ is the relaxation time (which determines viscosity), f_a represents the density of particles in the a direction, and f_a^{eq} represents the components of the equilibrium distribution function. The f_a and f_a^{eq} can be thought of as a directional histogram of densities (Figure 1).

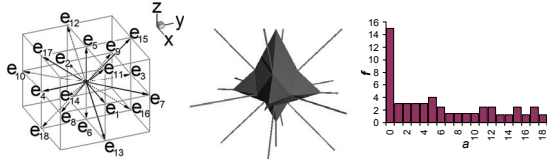


Figure 1. Unit velocity vectors, directional histogram of f_a values at a node, and unrolled histogram for D3Q19 (3 dimensions, 19 velocities) model.

The f_a^{eq} are given by

$$f_a^{eq}(\mathbf{x}) = w_a \rho(\mathbf{x}) \left[1 + \frac{\mathbf{e}_a \cdot \mathbf{u}}{c_s^2} + \frac{1}{2} \frac{(\mathbf{e}_a \cdot \mathbf{u})^2}{c_s^4} - \frac{1}{2} \frac{u^2}{c_s^2} \right], \quad (2)$$

for $a = 0, 1, 2, \dots, 18$ on the D3Q19 lattice. The w_a are direction-specific weights. The sound speed on the lattice is c_s ($1/\sqrt{3}$ lu ts $^{-1}$). The practical maximum macroscopic velocity is considerably smaller ($|\mathbf{u}| < \sim 0.1c_s$). The macroscopic fluid density, ρ , at \mathbf{x} is the sum of the individual directional densities, $\rho(\mathbf{x}) = \sum_a f_a(\mathbf{x})$, and the macroscopic velocity \mathbf{u} at \mathbf{x} is $\mathbf{u} = \sum_a \mathbf{e}_a f_a(\mathbf{x}) / \rho(\mathbf{x})$. Following collision in (1), streaming completes momentum transfer by moving the f_a to downstream nodes at $t + \Delta t$ (by simply reassigning spatial subscripts for f_a from \mathbf{x} to $\mathbf{x} + \mathbf{e}_a \Delta t$).

These equations form the basis of the single-fluid LBM. In general, one begins with some initial distribution, f_a , at all lattice nodes followed by incorporating the effects of boundaries and forcing. Equilibrium distributions are computed via (2), and densities and velocities—the moments of f_a —at the next time step are computed using the summations

above. Finally, streaming yields the f_a at the new time step and the process begins again.

“Bounce back” boundaries are easy to implement and account for much of the popularity of LBM among pore-scale modelers who must contend with highly irregular flow domain boundaries. Bounce back boundaries enforce no-slip conditions at the walls. The simplest forms have limitations, and new methods—for example, Multi-Reflection [Ginzburg and d’Humières, 2003; Pan et al., 2006]—offer improvements.

The detailed position of solid-fluid boundaries between model nodes is incorrectly computed as a function of viscosity in the BGK model, and Multi-Relaxation Time (MRT) models have been shown to provide more accurate solutions [Ginzburg and d’Humières, 2003; Pan et al., 2006]. The emphasis here is on demonstrating the linked N-S, Darcy, ADE, and advection-diffusion models, and differences due to incorporation of a full MRT model are not likely to be substantial—especially for conduits represented by more than several nodes.

This simple LBM yields transient solutions to complex flows including unstable flows at higher Reynolds numbers and has been shown to be capable of solving the N-S equations for fluid flow. Incorporating a second component allows simulation of coupled solute transport, and including an interaction force makes simulation of single component multiphase systems (such as water and its vapor) or multicomponent multiphase systems (such as oil and water) possible [Sukop and Thorne, 2006].

Solutes and heat in free-flowing fluid are transported by advection along with the fluid and by diffusion. Except in the case of density-driven effects, which are treated separately along with gravitational forcing, solutes and heat are not considered to carry or impart momentum, but move instead as passive scalars. Thus, a truncated equilibrium distribution function applies to their transport:

$$f_{\sigma,a}^{eq} = w_a \rho_\sigma (1 + 3\mathbf{e}_a \cdot \mathbf{u}), \quad (3)$$

where σ denotes the solute or heat component and the macroscopic velocity \mathbf{u} is obtained

directly from the fluid flow solution. This yields solutions of the advection-diffusion equation (which also applies to heat transport, but henceforth only solutes are mentioned for brevity)

$$\frac{dC}{dt} = -\mathbf{u}\nabla C + D\nabla^2 C, \quad (4)$$

where C is the concentration, t is time, and D is the diffusion coefficient.

The close coupling between the LBM N-S solver and the LBM approach to this advection-diffusion equation allows the solution of problems not accessible to traditional groundwater models. In particular, the entrapment of solutes in eddies, which can arise at quite low Reynolds numbers ($Re \sim 1$) in conduits and fractures, and mixing due to inertial eddies at moderate Re or full turbulence at high Re can not be simulated with traditional models. An example of inertial eddy mixing ($Re \sim 900$) in a conduit is presented below.

Inertial Effects on Apparent Hydraulic Conductivity in a Complex Domain

Despite the focus of LBM on pore-scale models in the past, there is no intrinsic limit to the size of conduits that can be simulated with LBM. Alvarez [2007] measured the hydraulic

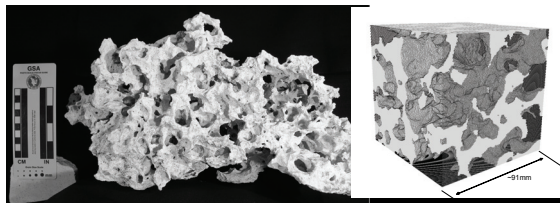


Figure 2. Left: Macroporous limestone digitized with high-resolution computed tomography. Scale bar on far left shows centimeters and inches. (Photo by Michael Wacker, USGS). Right: The ~ 0.1 -m cube extracted from the data set. (Data acquired at the High-Resolution X-ray Computed Tomography Facility of the University of Texas at Austin.)

conductivity of karstic rocks from a stratiform macroporous unit of the Miami Limestone in the Biscayne aquifer using LBM applied to high-resolution computed tomography data on samples up to almost 0.1 m on a side, with

common 2-cm pores (Figure 2). The study demonstrated the reduction in apparent hydraulic conductivity caused by inertial flow with increasing hydraulic gradient.

It is possible to directly probe the simulation results for the signatures of inertial flow—in particular, the presence of eddies. In Figure 3, stream-traces passing through 7 different points of a sample are plotted for cases of $Re=0.31$ and $Re=152$. For the very low Reynolds number the flow is a creeping flow: no vortices were observed in the flow field and the hydraulic conductivity is at a maximum. For $Re=152$, the hydraulic conductivity is reduced and rich patterns of vortices are evident.

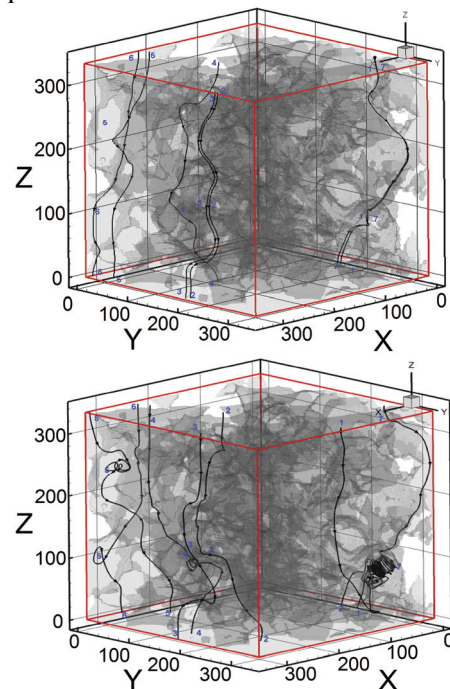


Figure 3. Streamlines for $Re=0.31$ with $K=34$ m/s (top) and for $Re=152$ with $K=20$ m/s (bottom) in 336 lu sub-sample ML-01.

There is a substantial reduction in the apparent hydraulic conductivity as the applied gradient increases to realistic field gradients (Figure 4). This suggests that under field conditions in the Biscayne aquifer, inertial flows and departures from the linear gradient-flow relation assumed in Darcy's law are likely to be common and important. Hydraulic conductivity and transmissivity measurements in such aquifers may commonly be reflective of inertial flow conditions and consequently are lower than

they would be if these properties corresponded to the intrinsic permeabilities.

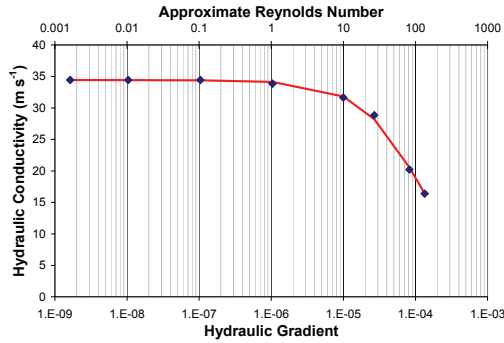


Figure 4. Effect of increasing gradient on apparent hydraulic conductivity for macroporous sample. Fitted Darcy-Forchheimer curve (solid line) and LBM simulation results (points).

SOLUTION OF TRANSIENT GROUND-WATER FLOW EQUATION WITH LBM

Although LBMs are effective pore-scale flow solvers, computation requirements make it unrealistic to consider solving aquifer-scale problems that involve matrix flow and transport through pore-scale simulation. Fortunately, there are two different approaches, briefly reviewed here, that can be adopted to simulate ground-water flow with LBM that are based on the macroscopic perspective inherent in Darcy's law and are not scale-dependent. One approach that utilizes a damping factor or force has been proposed in various forms and focuses on flow without considering solute transport. The literature describing these methods generally has not considered transient conditions nor internal source/sinks needed to simulate wells or recharge.

The second approach, which has rarely been considered previously in the literature (an exception might be Serván Camas [2007]), solves the transient ground-water flow equation using the well-established heat or diffusive mass transport analogy. We develop and demonstrate source/sink incorporation for that approach here.

The advantage of both of these methods for modeling flow and transport in karst comes from the linkage with the LBM's ability to solve the N-S and advection-diffusion equations in conduits within the porous matrix.

Damping Factor/Forcing Approach

Numerous papers have demonstrated the ability of LBM to characterize Darcian flow using an approach that damps out the inertial components of flow arising from the LBM's solution of the N-S equations with a damping factor or forcing related to the permeability of the domain [Dardis and McCloskey, 1998a,b; Freed, 1998; Martys, 2001; Kang et al, 2002; Guo and Zhao, 2002]. These approaches can solve a generalized N-S equation that includes the Brinkman-extended Darcy model (accounts for conduit/porous medium boundary conditions) and non-linear drag often represented by the Forchheimer equation. Following Freed [1998], Kang et al [2002] presented a similar model but also incorporated non-uniform grid spacing and used the model to draw conclusions about relative fracture/matrix permeabilities that justify the use of discrete fracture models that ignore matrix effects. The approach of Dardis and McCloskey [1998a,b] is described in more detail below; improved methods are in review.

In accordance with Darcy's law, the flow of fluid in a porous medium is proportional to the medium's permeability. Dardis and McCloskey [1998a,b] introduced a damping parameter $0 < n_s < 1$, along with a new step in the LBM procedure to damp momentum in proportion to n_s . The n_s term can be a function of \mathbf{x} , $n_s = n_s(\mathbf{x})$, which allows simulation of heterogeneous porous media. If $n_s = 0$, the porous media step has no effect, and the process reduces to the usual free-fluid LBM. If $n_s = 1$, however, then flow is completely eliminated. The porous media step is applied only to the fluid component, not solute or heat components.

Dardis and McCloskey [1998a,b] indicated that the permeability k of a medium with damping factor n_s could be computed as

$$k = \frac{\nu}{2n_s}, \quad (5)$$

where ν is the kinematic viscosity of the fluid phase. This has led to misunderstanding in the past because k is a medium property and should not depend on viscosity. In this particular

macroscopic porous media approach, the viscosity no longer retains its normal meaning but instead, along with n_s , determines k in lattice units according to (5). Conversion to k in real units is straightforward:

$$k^{physical} = k^{LBM} \left(\frac{L^{physical}}{L^{LBM}} \right)^2, \quad (6)$$

where the L terms are the lengths of any comparable feature in physical and LBM units. Subsequent conversion to hydraulic conductivity is accomplished by multiplying by the physical fluid density and gravitational acceleration and dividing by the physical viscosity.

Figure 5 shows a simple conduit traversing a porous medium. A pressure gradient is applied across the domain from left to right. The conduit exerts a strong influence on the pressure field inside the domain. Dardis and McCloskey [1998a,b] and Kang et al. [2002] present similar results.

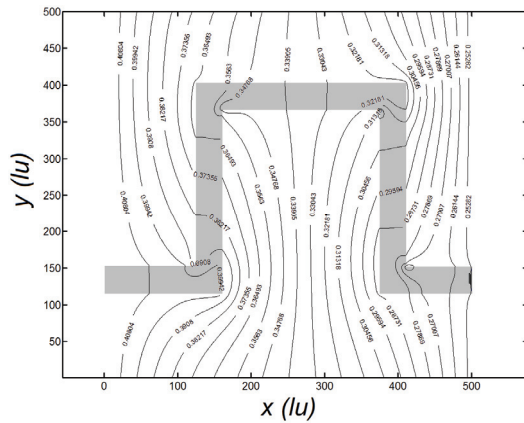


Figure 5. Pressure field in porous medium with conduit (gray).

Diffusion Equation Analogy Approach

There is a long tradition of simulating diffusion with LBM. It has recently been recognized that a less computationally intensive and more expedient approach to solving the transient ground-water flow equation

$$\frac{\partial h}{\partial t} = \frac{T}{S} \nabla^2 h + \frac{R}{S} \quad (7)$$

(where h , T , S and R represent the hydraulic head, transmissivity, storativity, and recharge respectively) in the LBM context is to solve it directly by exploiting its similarity to the diffusion or “heat” equation. One apparent advantage over standard explicit numerical methods is that the time step is not limited by the normal stability criterion [Wolf-Gladrow, 2000]. Also, unlike the damping methods, increasing T does not allow inertial effects, which can be considered a benefit in the context of a Darcy’s law solver.

Other than specialized treatment of boundary conditions and source/sink terms, the only modification to the LBM technique involves truncating the equilibrium distribution function computation (3) (although models involving only 4 or 6 directions rather than 8 or 18 in 2- and 3-D, respectively, are viable for this approach [Wolf-Gladrow, 2000] and lead to substantial computational savings).

Below, we present two example LBM solutions of (7) that involve classic problems that have analytical solutions. The first is based on a 1-D problem that appears in Wang and Anderson [1982] and considers a confined aquifer bounded by two constant-head reservoirs (Figure 6). The aquifer is $l=100$ -m long, has a T of $0.02 \text{ m}^2 \text{ min}^{-1}$, and a storativity of 0.002 . The head is initially uniform at 16 m (i.e., the initial condition is $h|_{x,0} = 16 \text{ m}$) and drops to 11 m at $x = 100$ at time 0 (i.e., the boundary conditions are $h_1 = h|_{0,t} = 16 \text{ m}$ and $h_2 = h|_{100,t} = 11 \text{ m}$).

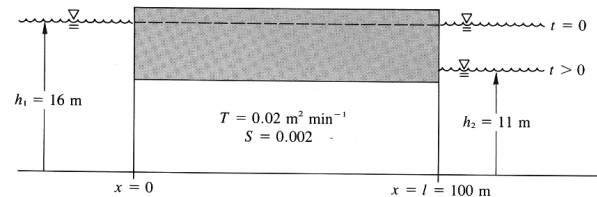


Figure 6. Transient ground-water flow problem with two reservoirs (from Wang and Anderson, 1982).

We solve the problem and present the results relative to the analytical solution in Figure 7 below. The LBM results are excellent.

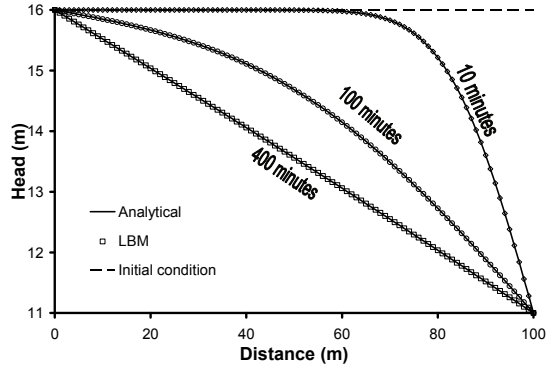


Figure 7. Comparison of LBM with analytical solution for transient reservoir problem.

The second test problem involves a pumping well in an infinite domain that is governed by the Theis well function. This test problem can be used to verify the LBM solution of the transient equipotential field (drawdown curve) in a 2-D aquifer with recharge/discharge. We use consistent LBM space and time units of “lu” (lattice length units) and “ts” (lattice time steps) in this case. Figure 8 shows drawdown as a function of time for a confined aquifer with $T=1.0 \text{ lu}^2/\text{ts}$ and relaxation parameter equal to 0.95 ts , which gives the hydraulic diffusivity equal to $0.15 \text{ lu}^2/\text{ts}$. The $50 \text{ lu} \times 50 \text{ lu}$ domain is initialized with uniform head of 1 lu . The pumping well is set in the center $(25, 25)$ and was pumped at a constant rate of $0.003 \text{ lu}^3/\text{ts}$. Drawdown is measured 7 lu from the pumping well.

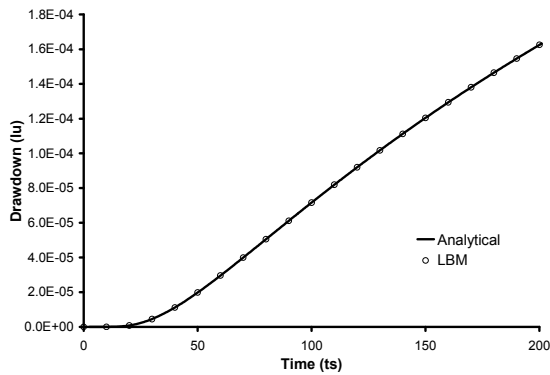


Figure 8. Well drawdown as a function of time; consistent LBM units.

There is a rich variety of possibilities for development of this method that need to be investigated. In particular, we have considered only quasi-3-D models and isotropic hydraulic conductivity so far.

The benefits of these macroscopic porous media approaches for karst ground-water flow simulation are substantial. First, they raise LBM from primarily a pore-scale N-S solver with computational limitations when field- and regional-scale simulations are required, to a standard ground-water flow solver applicable at any scale. Second, the spatial transition between the Darcy’s law simulation and the full N-S solution in conduits is more straightforward than it is in other conduit/matrix models because the same algorithm underlies all of the computational domain, and switching between the different solutions involves only switching between $n_s = 0$ or $n_s > 0$ or between the two forms ((2) and (3)) of the equilibrium distribution function.

SOLUTE TRANSPORT FOR MACROSCOPIC POROUS MEDIA USING LBMs

The combination of the solute transport and Darcy’s law capabilities of LBM discussed so far makes many types of simulations possible. One important characteristic of solute and heat transport in porous media is not addressed by simply combining these capabilities; unlike diffusion, dispersion under flow conditions in a porous medium is anisotropic. Zhang et al [2002a,b] and Ginzburg [2005] have introduced LBMs to simulate anisotropic dispersion. The approach of Zhang et al. [2002a,b] is described more fully and used in the examples below.

The dispersion tensor, $D_{\alpha\beta}$, is given by Zhang et al [2002a,b]

$$D_{\alpha\beta} = \Gamma_T \sqrt{u_x^2 + u_y^2} \delta_{\alpha\beta} + \frac{(\Gamma_L - \Gamma_T) u_\alpha u_\beta}{\sqrt{u_x^2 + u_y^2}}, \quad (8)$$

where $\delta_{\alpha\beta}$ is the Kronecker Delta, Γ_L and Γ_T are the longitudinal and transverse dispersivities, respectively, ($\delta_{\alpha\beta} = 1$ for $\alpha = \beta$), and u_α and u_β are the α and β components, respectively, of the velocities. This equation is solved at each node. The dispersion tensor components D_{xx} , D_{yy} , D_{xy} and D_{yx} in terms of directional relaxation parameters, τ_a , are expressed as [Zhang et al, 2002a,b]:

$$\begin{aligned}
D_{xx} &= \frac{\delta x^2}{18\delta t} [4\tau_1 + \tau_5 + \tau_6 - 3] \\
D_{yy} &= \frac{\delta y^2}{18\delta t} [4\tau_2 + \tau_5 + \tau_6 - 3] \\
D_{xy} &= D_{yx} = \frac{\delta x \delta y}{18\delta t} [\tau_5 - \tau_6]
\end{aligned} \tag{9}$$

Given the dispersion tensor, these equations are inverted to solve for relaxation times that are subsequently used at each node in the model. To ensure mass conservation, Zhang et al [2002a,b] used a weighted summation of the particle distribution function as shown below to compute the density (concentration), ρ_σ , of species subjected to the anisotropic dispersion:

$$\rho_\sigma = \sum_a \frac{f_a}{\tau_a} \left(\sum_i \frac{w_a}{\tau_a} \right)^{-1}, \tag{10}$$

where the weighting factors are represented by w_a and i represents a summation index.

Anisotropic dispersion of a solute plume moving at an angle to the main coordinate axes is shown in Figure 9. The longitudinal to transverse dispersivity ratio is 5:1 and the results compare well to the analytical solution.

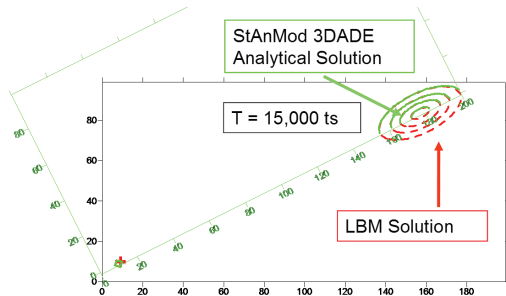


Figure 9. Anisotropic dispersion of 2-D solute plume (dashed contours) compared to the analytical solution (solid). $\Gamma_L = 0.5$, $\Gamma_T = 0.1$ lu. Flow unaligned with coordinate axes.

Incorporating this modification and combining it with the ground-water flow solvers discussed above yields an LBM ground-water flow simulator and a tightly coupled anisotropic dispersion ADE solver comparable to a number of available finite difference/finite element models. The new LBM ground-water/transport model inherits at least one exceptional capability from its foundation however—it can accurately simulate flow and transport in large conduits or

fractures that may involve higher Reynolds number flows and associated eddy mixing.

We present one example that illustrates the power of the combination of processes that can be simulated. In Figure 10, a heterogeneous porous medium is cut by a conduit. A solute pulse is applied at the left boundary that quickly fills the conduit and begins invading the porous medium, particularly in zones of higher hydraulic conductivity such as the light colored areas above and left of center and at the lower right. The domain is then flushed with solute-free water. Clear “mushroom cap” plumes of solute-free water develop in the conduit illustrating the eddy-mixing phenomenon. Flushing of the conduit will be complete long before the adjacent porous medium is flushed. We expect this type of behavior in karstic aquifers and existing models offer less appropriate approximations.

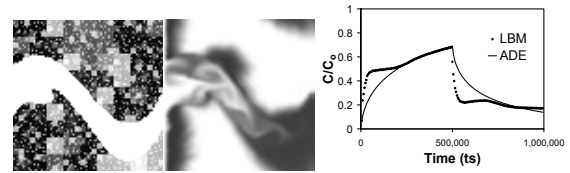


Figure 10. Model domain (left) showing conduit (white) in porous medium of variable permeability (proportional to whiteness), solute invasion into porous medium, and eddy mixing in conduit (center). Periodic top and bottom boundaries account for appearance of solute in upper right. Breakthrough curve for domain (right) is complex and cannot be well-fitted with standard advection-dispersion model.

FUTURE APPLICATIONS

One of the main challenges in karst hydrology is characterizing/modeling the complex geometry present at many scales within karst aquifers and their macropore and conduit systems. Data for use in models proposed here can be obtained at different scales through thin sectioning of rock, imaging of hand- to body-sized specimens via digital photography or tomography, borehole viewers or cross-hole tomography, ground penetrating radar, and traditional aquifer tests. Identification and characterization of macropore and conduit zones are logical next steps for enhancing understanding of karst aquifers and are active research areas [e.g., Cunningham et al., 2006].

We have completed preliminary work at the 1-m scale, based on borehole imagery from the Biscayne aquifer. In our approach, a borehole image is subject to thresholding to separate it into macropores and rock. Then the 3-D information available from the image is reconstituted by extracting the coordinates and presence or absence of rock at each pixel on the borehole wall. Variograms for the 3-D data are computed and simulation of 3-D rock is possible. Figure 11 shows a preliminary example of the potential of this method.

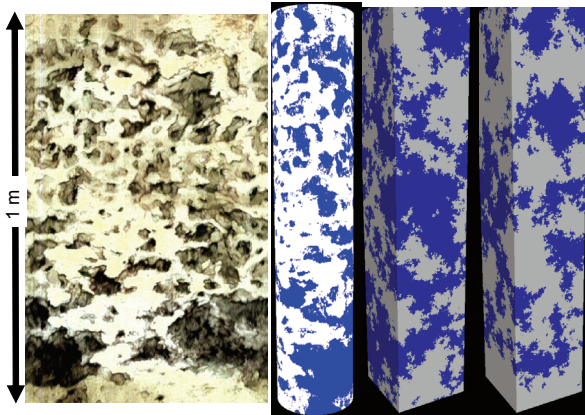


Figure 11. Left: Borehole televiewer image from 8-inch (~20 cm) diameter USGS borehole (G-3849) and thresholded 3-D data. (Photo by Michael Wacker, USGS). Right: Two simulations of 3-D rock based on borehole image variogram.

Suitable data from large caves are also available. Highly specialized dive teams have collected geometrical data from karst aquifers near Tallahassee, Florida. Figure 12 shows a portion of the cave system that discharges to Wakulla Spring based on these data. Such data would be combined with traditional data on the properties of the surrounding aquifer to provide input for the combined LBM aquifer-conduit model.

CONCLUSION

LBM offers solutions to challenges facing modelers of karst aquifer hydraulics and solute transport. Inertial flows expected when the Reynolds number is high enough and their effect on apparent hydraulic properties and solute transport can be simulated. Integration with LBM-based transient ground-water flow and

anisotropic dispersion solvers may offer better solutions for karst problems.

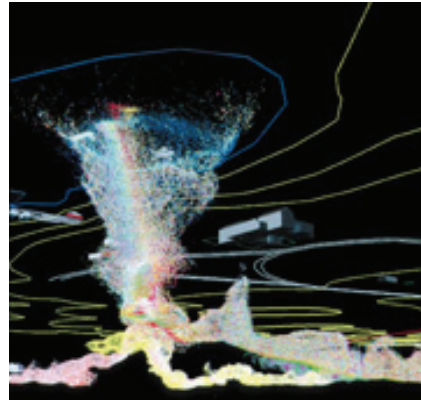


Figure 12. Geometry of Wakulla Spring viewed from below ground surface. Digital Wall Mapper data (courtesy Dr. Barbara Am Ende).

REFERENCES

- Alvarez, P.F., 2007, Lattice Boltzmann modeling of fluid flow to determine the permeability of a karst aquifer. M.S. thesis, Florida International University, 96 pp.
- Anwar, S., Cortis, A., and Sukop, M.C., 2008 (In press), Lattice Boltzmann simulation of solute transport in heterogeneous porous media with conduits to estimate macroscopic Continuous Time Random Walk model parameters. *Progress in Computational Fluid Dynamics*
- Bardsley, K.J., Anwar, S., and Sukop, M.C., 2006, Simultaneous heat and solute transport modeling of ground-water with lattice Boltzmann methods. *CMWR XVI – Computational Methods in Water Resources, XVI International Conference, Copenhagen, Denmark, June 19-22*
- Bhatnagar, P.L. Gross, E.P., and Krook, M., 1954, A model for collision processes in gases. I. Small amplitude processes in charged and neutral one-component systems. *Physics Review*, 94, 511-525
- Birk, S., Liedl, R., Sauter, M., and Teutsch, G., 2003, Hydraulic boundary conditions as a controlling factor in karst genesis: A numerical modeling study on artesian conduit development in gypsum. *Water Resources Research* 39 (1), 1004, doi:10.1029/2002WR001308.

- Cunningham, K.J., Wacker, M.A., Robinson, E. Dixon, J.F., and Wingard, G.L., 2006, A cyclostratigraphic and borehole-geophysical approach to development of a three-dimensional conceptual hydrogeologic model of the karstic Biscayne Aquifer, southeastern Florida. U.S. Geological Survey Scientific Investigations Report 2005-5235, 69 p., plus CD.
- Dardis, O., and McCloskey, J., 1998a, Permeability porosity relationships from numerical simulations of fluid flow. *Geophys. Res. Lett.*, 25, p. 1471-1474.
- Dardis, O., and McCloskey, J., 1998b, Lattice Boltzmann scheme with real numbered solid density for the simulation of flow in porous media. *Phys. Rev. E.*, 57, (4), p. 4834-4837.
- Freed, D.M., 1998, Lattice Boltzmann method for macroscopic porous media modeling, *Int. J. Modern Phys. C* 9, p. 1491-1503
- Ginzburg, I., 2005, Equilibrium-type and link-type lattice Boltzmann models for generic advection and anisotropic-dispersion equation. *Adv. Wat. Resour.*, 28(11), p. 1171-1195.
- Ginzburg, I., and d'Humières, D., 2003 Multireflection boundary conditions for lattice Boltzmann models *Phys. Rev. E* 68, 066614
- Guo, Z., and Zhao, T.S., 2002, Lattice Boltzmann model for incompressible flows through porous media, *Phys. Rev. E* 66, 036304
- Kang, Q., Lichtner, P.C., and Zhang, D., 2006, Lattice Boltzmann pore-scale model for multicomponent reactive transport in porous media. *J. Geophys. Res.* 111, B05203, doi:10.1029/2005JB003951
- Kang Q., Zhang, D., and Chen, S., 2002, Unified lattice Boltzmann method for flow in multiscale porous media *Phys. Rev. E* 66 (5): 056307
- Li, H., Pan, C., and Miller, C.T., 2005, Pore-scale investigation of viscous coupling effects for two-phase flow in porous media. *Phys. Rev. E* 72, 026705
- Martys, N.S., 2001, Improved approximation of the Brinkman equation using a lattice Boltzmann method. *Phys. Fluids*, 13(6), p. 1807-1810
- Pan, C., Hilpert, M., and Miller, C.T., 2004, Lattice-Boltzmann simulation of two-phase flow in porous media. *Water Resour. Res.*, 40, W01501, doi:10.1029/2003WR002120.
- Pan, C., Luo, L.-S., and Miller, C.T., 2006, An evaluation of lattice Boltzmann schemes for porous medium flow simulation, *Computers & Fluids* 35(8/9), p. 898-909
- Serván Camas, B., 2007, Saltwater intrusion simulation in heterogeneous aquifer using Lattice Boltzmann method, M.S. Thesis, Louisiana State University, 77 pp.
- Sukop, M. C., and Or, D., 2004, Lattice Boltzmann method for modeling liquid-vapor interface configurations in porous media, *Water Resour. Res.*, 40, W01509, doi:10.1029/2003WR002333.
- Sukop, M.C., and Thorne, D.T., 2006, *Lattice Boltzmann Modeling: An Introduction for Geoscientists and Engineers*, Springer, Heidelberg-Berlin-New York. 172 pp.
- Thorne, D.T., and Sukop, M.C., 2004, Lattice Boltzmann model for the Elder problem, In *Proceedings of the XVth International Conference on Computational Methods in Water Resources (CMWR XV)*, June 13-17, 2004, Chapel Hill, NC, USA. C.T. Miller, M.W. Farthing, W.G. Gray, and G. F. Pinder Eds. Elsevier, Amsterdam.
- Wang H.F., and Anderson, M.P., 1982, *Introduction to Ground-water Modeling*. W. H. Freeman and Company, San Francisco. 237 pp.
- Watson, V., Painter, R., and By, T., 2003, Numerical simulation of flow and contaminant transport in a complex karst conduit. *Society of Environmental Toxicology and Chemistry, 24th Annual Meeting in North America* 9 - 13 November, Austin, Texas
- White, W.B., 2002, Karst hydrology: Recent developments and open questions. *Engineering Geology* 65, p. 85-105
- Wolf-Gladrow, D.A., 2000, *Lattice-gas automata and lattice Boltzmann models: An introduction*. Springer, Berlin. 308 pp.
- Zhang, D.X., and Kang, Q. J., 2004, Pore scale simulation of solute transport in fractured porous media. *Geophys. Res. Lett.* 31 (12): L12504
- Zhang X., Bengough, A.G. Crawford, J.W., and Young, I.M., 2002a, A lattice BGK model for advection and anisotropic dispersion equation, *Adv Wat Resour* 25, p. 1-8.
- Zhang X., Crawford, J.W., Bengough, A.G., and Young, I.M., 2002b, On boundary conditions in the lattice Boltzmann model for advection and anisotropic dispersion equation. *Adv Wat Resour* 25, p. 601-609.

Simulation of Turbulent Ground-Water Flow with MODFLOW-2005— Overview

By Eve L. Kuniandy¹, Keith J. Halford², and W. Barclay Shoemaker³

¹U.S. Geological Survey, 3850 Holcomb Bridge Rd, Ste. 160, Norcross, GA 30092

²U.S. Geological Survey, 2730 N. Deer Run Road, Carcon City, NV 89701

³U.S. Geological Survey, 3110 SW 9th Avenue, Ft. Lauderdale, FL 33315

Abstract

The Conduit Flow Process (CFP) is a recently released module for MODFLOW-2005 that can simulate turbulent flow in aquifers with pipe-like (such as karst) features or preferential flow layers. The CFP simulates turbulent flow as a discrete pipe network connected to the MODFLOW cells via head-dependent flux terms using Mode 1 (CFPM1), or as continuous preferential flow layers where flow can transition between laminar and turbulent in the row and column direction using Mode 2 (CFPM2). Additionally, both a pipe network and preferential flow layers can be simulated in the same model, Mode 3 (CFPM3). Preferential flow layers in CFPM2 simulate flow through interconnected pores and vugs more than 0.01 m in diameter, such as those that are present in the carbonate rock making up the Biscayne aquifer in southern Florida. CFPM2 requires less data than CFPM1 or CFPM3 because discrete pipe networks are not simulated. However, CFPM1 is designed to simulate laminar and turbulent flow in large networks of submerged conduits (partially filled conduits can be simulated, but should have almost no slope). CFPM1 is an update of subroutines to MODFLOW-2005 (Harbaugh, 2005) from the Carbonate Aquifer Void Evolution (CAVE) code previously published (Teutsch, 1993; Sauter, 1993; Clemens and others, 1996; Clemens, 1998; Hückinghaus, 1998; Bauer and others, 2000; 2003; Liedl and others, 2003; and Birk, 2002). CFPM2 is a new simple empirical algorithm for simulation of turbulent flow in preferential flow layers modified from Halford (2000). This oral presentation focuses on the theory of the code and the validation of the new algorithm for CFPM2. The code and documentation is public domain and will be available through the U.S. Geological Survey website (Shoemaker and others, 2008):

http://water.usgs.gov/software/ground_water.html

REFERENCES

- Bauer, Sebastian, Liedl, Rudolf, and Sauter, Martin. 2000. Modelling of karst development considering conduit-matrix exchange flow, in Stauffer, F., Kinzelbach, W., Kovar, K., and Hoehn, E., eds., Calibration and reliability in groundwater modelling: Coping with uncertainty—Proceedings of the ModelCARE'99 Conference: International Association of Hydrological Sciences Publication 265, 10-15.
- Bauer, Sebastian, Liedl, Rudolf, and Sauter, Martin. 2003. Modeling of karst aquifer genesis: Influence of exchange flow: *Water Resources Research* v. 39, no. 10, 1285.
- Birk, Steffen, 2002. Characterization of karst systems by simulating aquifer genesis and spring responses: Model development and application to gypsum karst: Vol. 60 of *Tübinger Geowissenschaftliche Arbeiten: Tübingen*, Germany, Reihe C. Institut und Museum für Geologie und Paläontologie der Universität Tübingen. Also available at: <http://w210.ub.uni-tuebingen.de/dbt/volltexte/2002/558/>.
- Clemens, T., Hückinghaus, D., Sauter, M., Liedl, R., Teutsch, G. 1996: A combined continuum and discrete network reactive transport model for the simulation of karst development. In: Kovar, K., van der Heijde, P. (eds.), Calibration and reliability in groundwater modelling. IAHS Publication 237: 309-318.
- Clemens, Torsten, 1998. Simulation der Entwicklung von Karstaquiferen: Ph.D. dissertation submitted to Eberhard-Karls Universität Tübingen, Germany.

- Halford, K.J. 2000. Simulation and interpretation of borehole flowmeter results under laminar and turbulent flow conditions: Seventh International Symposium on Logging for Minerals and Geotechnical Applications, Golden, Colorado, October 24-26, 2000, 157-168.
- Harbaugh, A.W. 2005. MODFLOW-2005. the U.S. Geological Survey modular ground-water model -- the Ground-Water Flow Process: USGS Techniques and Methods 6-A16.
- Hückinghaus, Dirk, 1998. Simulation der Aquifergenese und des Wärmetransports in Karstaquiferen: Vol. 42 of Tübinger Geowissenschaftliche Arbeiten: Tübingen, Germany, Reihe C. Institut und Museum für Geologie und Paläontologie der Universität Tübingen. Also available at: <http://w210.ub.uni-tuebingen.de/dbt/volltexte/2005/2030/>.
- Liedl, R., Sauter, M., Hückinghaus D., Clemens T., Teutsch, G. 2003: Simulation of the development of karst aquifers using a coupled continuum pipe flow model. Water Resour. Res., 39 (1), 1057, doi:10.1029/2001WR001206.
- Sauter, Martin, 1993. Double porosity models in karstified limestone aquifers: Field validation and data provision, in Hydrogeological Process in Karst Terranes, International Association of Hydrological Sciences, v. 207, p. 261-279.
- Shoemaker, W.B., Kuniatsky, E.L., Birk, Steffen, Bauer, Sebastian, and Swain, E.D., 2008. Documentation of a Conduit Flow Process (CFP) for MODFLOW-2005: U.S. Geological Survey Techniques and Methods 6-A24.
- Teutsch, Georg, 1993. An extended double-porosity concept as a practical modeling approach for a karstified terrain, in Gultekin, Johnson, and Back, eds., Hydrogeological Processes in Karst Terranes, Proceedings of the Antalya Symposium and Field Seminar, October 1990: International Association of Hydrological Sciences, v. 207, 281-292.

Effects of Turbulence on Hydraulic Heads and Parameter Sensitivities in Preferential Ground-Water Flow Layers

By W. Barclay Shoemaker¹ and Eve L. Kuniansky²

¹U.S. Geological Survey, 3110 SW 9th Ave., Ft. Lauderdale, FL 33315

²U.S. Geological Survey, 3850 Holcomb Bridge Rd., Ste. 160, Norcross, GA 30092

Abstract

The U.S. Geological Survey created a Conduit Flow Process (CFP) (Shoemaker and others, 2008) for the Modular Finite-Difference Ground-Water Flow Model, MODFLOW-2005. An application of the CFP on the Biscayne aquifer in southern Florida is described that examines (1) the potential for turbulent groundwater flow, and (2) the effects of turbulent flow on hydraulic heads and parameter sensitivities. Turbulent flow was spatially extensive (Figure 1) in preferential groundwater flow layers with mean void diameters equal to about 3.5 centimeters, groundwater temperature equal to about 25 degrees Celsius, and critical Reynolds numbers less than about 400. Turbulence either increased or decreased simulated heads from laminar altitudes. Specifically, head differences from laminar altitudes ranged from about -18 to +27 centimeters, and were explained by the magnitude of net flow to the finite-difference model cell. Turbulence also influenced the sensitivities of model parameters. Specifically, the composite-scaled sensitivities of horizontal hydraulic conductivities decrease by as much as 70% when turbulence is removed. Resultant hydraulic head and sensitivity differences due to turbulent groundwater flow highlight potential errors in models which assume laminar flow in an equivalent porous-media having uniformly distributed void spaces.

http://water.usgs.gov/software/ground_water.html

REFERENCES

Shoemaker, W.B., Kuniansky, E.L., Birk, Steffen, Bauer, Sebastian, and Swain, E.D., 2007. Documentation of a Conduit Flow Process (CFP) for MODFLOW-2005: U.S. Geological Survey Techniques and Methods 6-A24.

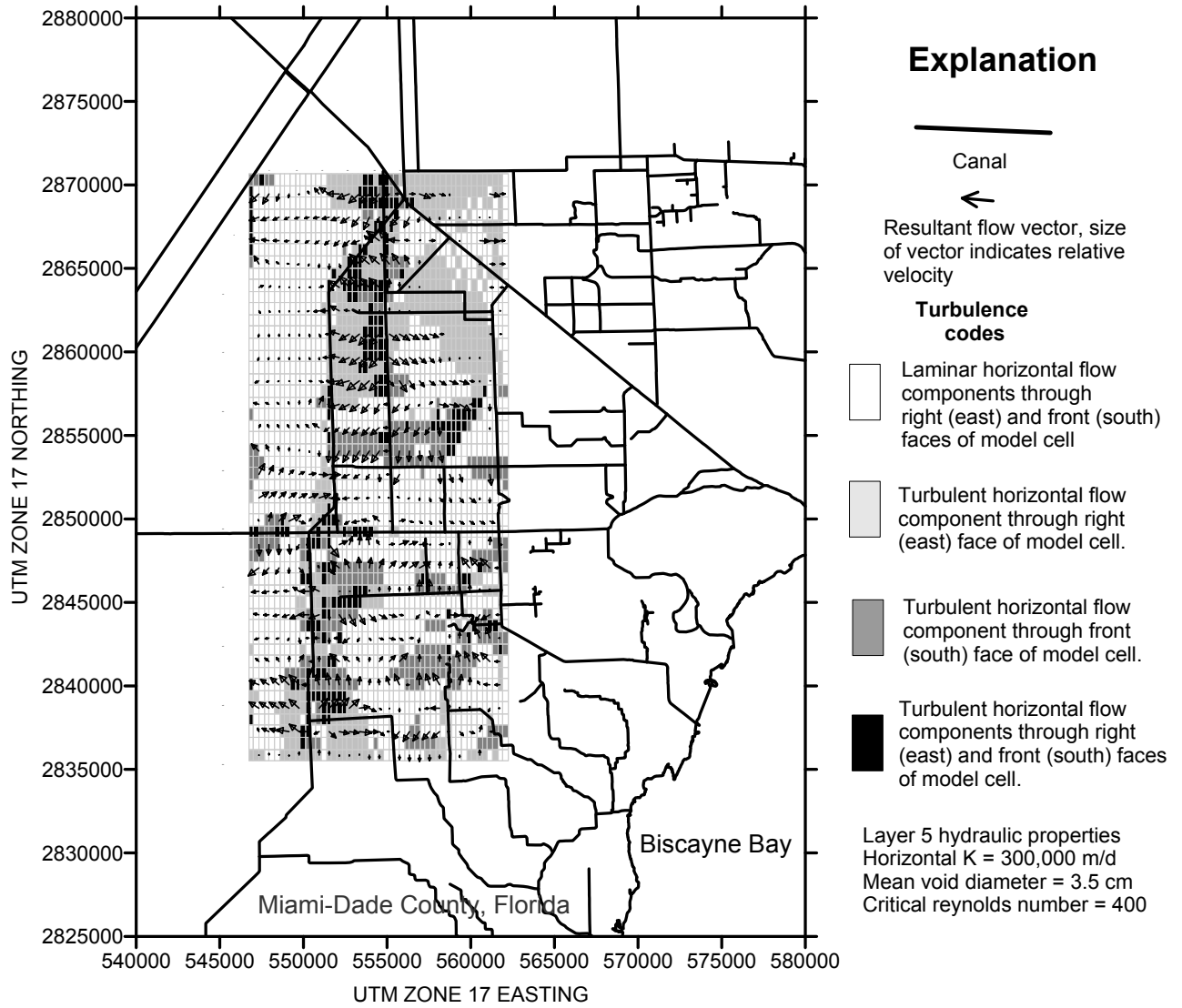


Figure 1. Extent of turbulence in preferential ground-water flow layer 5.

Simulation of Ground-Water Flow in a Fractured-Rock Karst Aquifer, Shenandoah Valley, Leetown, West Virginia

By Mark D. Kozar¹ and Kurt J. McCoy²

¹ U.S. Geological Survey, West Virginia Water Science Center, Charleston, WV, 25301

² U.S. Geological Survey, New Mexico Water Science Center, Albuquerque, NM, 87109-1311

Abstract

Karst scientists are sometimes reluctant to pursue ground-water modeling of karst terranes. This is largely because many of the assumptions of Darcian flow on which models are predicated are violated in the turbulent flow systems of karst aquifers, especially within large conduit drains and caverns. However, ground-water models have been effectively developed for numerous karst systems. This abstract presents the results of a ground-water flow model developed for a fractured rock dominated karst aquifer beneath the Leetown Science Center (LSC) in the Shenandoah Valley of West Virginia, Leetown, West Virginia. The aquifer is a karst system but with a significant diffuse-flow component. As a result, both classic dye tracing and fractured rock techniques were used to collect the data necessary to develop the ground-water flow model.

The LSC is a research facility operated by the U.S. Geological Survey that occupies approximately 455-acres near Kearneysville, Jefferson County, West Virginia. The recent construction of a second research facility (National Center for Cool and Cold Water Aquaculture) operated by the U.S. Department of Agriculture and co-located on Center property has placed additional demands on available water resources in the area. To address the concerns of future water availability, a three-dimensional steady-state finite-difference ground-water flow model was developed to simulate ground-water flow in the Leetown area under normal and drought conditions.

Results of geologic mapping, LiDAR derived DEMs, and surface-geophysical surveys verified the presence of several prominent thrust faults and identified additional faults and other complex geologic structures (including overturned anticlines and synclines) in the area. These geologic structures are known to control ground-water flow in the region. Results of this study indicate that cross-strike faults and fracture zones are major avenues of ground-water flow. Prior to this investigation, the conceptual model of ground-water flow for the region focused primarily on bedding planes and strike-parallel faults and joints as controls on ground-water flow but did not recognize the importance of cross-strike faults and fracture zones that allow ground water to flow down gradient across or through less permeable geologic formations.

Results of the ground-water flow simulation indicate that current operations at the Center do not substantially affect either streamflow (less than a 5-percent reduction in annual streamflow) or ground-water levels under normal climatic conditions but potentially could have greater effects on streamflow during long-term drought (reduction in streamflow of approximately 14 percent). On the basis of simulation results, ground-water withdrawals based on the anticipated need for an additional 150 to 200 gal/min (gallons per minute) of water at the Center also would not seriously affect streamflow (less than 8 to 9 percent reduction in streamflow) or ground-water levels during normal climatic conditions. During drought conditions, however, the effects of current ground-water withdrawals and anticipated additional withdrawals of 150 to 200 gal/min to augment existing supplies result in moderate to substantial declines in water levels of 0.5-1.2 feet (ft) in the vicinity of the Center's springs and production wells. Streamflow was predicted to be reduced locally by approximately 21 percent. Such withdrawals during a drought or prolonged period of below normal ground-water levels would result in substantial declines in the flow of the Center's springs and likely would not be sustainable for more than a few months. The potential reduction in streamflow is a result of capture of ground water that would otherwise have been discharged to Hopewell Run or its tributaries as base-flow discharge. The net effect on streamflow downstream of the facility is minimal, as the majority of water withdrawn is returned to the stream after treatment.

Simulations of Ground-Water Flow and Particle Pathline Analysis in the Contributing Recharge Area of a Public-Supply Well in Temple Terrace, Tampa Bay Region, Florida

By A. Christy A. Crandall¹, Leon J. Kauffman², and Brian G. Katz¹

¹U.S. Geological Survey, 2010 Levy Ave., Bldg B, Ste. 100, Tallahassee, FL 32310

²U.S. Geological Survey, 810 Bear Tavern Rd. Ste. 206, West Trenton, NJ 8628

Abstract

Shallow ground water in the north-central Tampa Bay region is affected by nitrate concentrations above background concentrations (the detection level (<0.06 milligrams per liter as Nitrogen (mg/L-N)) and detectable concentrations of volatile organic compounds and pesticides as a result of ground-water development and intensive urban land use. The region relies primarily on ground water for drinking water supplies. Sustainability of ground-water quality for public supply requires monitoring and understanding of the mechanisms controlling the vulnerability of public-supply wells to contamination. One representative public-supply well was selected based on the detection of a variety of chemical constituents for intensive study to evaluate the dominant processes affecting the vulnerability of public-supply wells in the Upper Floridan aquifer in the City of Temple Terrace near Tampa, Florida. A ground-water flow model was calibrated and used to determine the area contributing recharge to the selected public-supply well. A network of 28 monitoring wells was installed, and water and sediment samples were collected within the area contributing recharge to support a detailed analysis of physical and chemical conditions and processes affecting the water chemistry. Samples from the monitoring-well network indicated that nitrate concentrations, derived primarily from residential/commercial fertilizer use and atmospheric deposition, were highest (median 2.4 mg/L as N and maximum 6.11 mg/L as N) in shallow ground water from the surficial aquifer system and lowest (less than the detection level) in water from the Upper Floridan aquifer. Dissolved gas analysis indicated that denitrification had occurred near the interface of the surficial aquifer system and the intermediate confining unit, within the intermediate confining unit, and in the Upper Floridan aquifer because of reducing conditions. Simulations also indicated that the rapid movement of water from the surficial aquifer system to the selected public-supply well with high pumping rates, allows nitrate to reach the selected public-supply well in concentrations that resemble those of the overlying surficial aquifer system. Recharge water is most likely traveling through karst features such as sinkholes and conduits that bypass the denitrifying zones. Estimated advective travel times resulting from particle tracking from the time of recharge until discharge at the public supply well ranged from a few hours to 127 years, with a median of 13 years; nearly 45 percent of the particle ages reached the well within 10 years or less. Water from the surficial aquifer system with higher concentrations of nitrate and detectable volatile organic compounds and pesticides, is expected to continue moving to the selected public-supply well. Land-use and the proportion of young affected water contributing to the well is likely to remain relatively constant over time. The calculated nitrate concentration in the selected well indicates a lag of 1 to 10 years between peak concentrations of non-point source contaminants in recharge water and arrival at the well.

Performance Evaluation of the MODFLOW-2005 Conduit Flow Process Applied to a Karst Aquifer Underlying West-Central Florida

By Melissa E. Hill¹, Angel Martin¹, and Marc T. Stewart²

¹Southwest Florida Water Management District, 2379 Broad St., Brooksville, Florida 34604

²University of South Florida, SCA 533 4202 E. Fowler, Tampa, Florida 33620

Abstract

The MODFLOW-2005 Conduit Flow Process (CFP) was used to simulate discharge and matrix-conduit water levels in a dual-permeability karst aquifer in the vicinity of Weeki Wachee, west-central Florida. The performance of MODFLOW-2005 with an equivalent continuum model, which simulates only laminar flow, relative to MODFLOW-2005 CFP Mode 1, which simulates both laminar and turbulent flow, as well as fluid exchange between the matrix and conduit networks in a dual-conductivity model, was evaluated. Simulated water levels in the matrix and conduit networks were evaluated by comparing these levels to observed values from monitoring wells penetrating the matrix and conduit networks. Additionally, observed discharge hydrographs following convective and tropical storms, as well as drought conditions, were compared to simulated discharges from transient simulations using MODFLOW-2005 and MODFLOW-2005 CFP Mode 1. Results indicate that the application of MODFLOW-2005 CFP Mode 1, with the dual-conductivity model, improves the overall match between simulated and observed discharges by 12 to 40%. We conclude that the dual-conductivity model, using MODFLOW-2005 CFP Mode 1 is a better tool for simulating discharge from the dual-permeability Upper Floridan aquifer, particularly during periods of low net recharge, than the equivalent continuum model using MODFLOW-2005.

INTRODUCTION

Karst aquifers differ from other porous media aquifers because of the secondary porosity that develops in them as a result of dissolution (Palmer, 1999). Karst aquifers consist of triple porosity that includes: (1) intergranular, (2) fracture, and (3) conduit (or cave) porosities (Palmer, 1999; Worthington et al., 2000; Martin and Sreaton, 2001; White, 2002). Intergranular porosity comprises the matrix network, whereas the conduit porosity comprises the conduit network (Palmer, 1999; Worthington et al., 2000; Martin and Sreaton, 2001). Fracture porosity can be lumped with either the matrix or conduit network depending on aperture widths (White, 1988; Worthington et al., 2000; Martin and Sreaton, 2001). Dual-permeability arises from both the matrix and conduit networks (White, 1999). Groundwater flow in dual-permeability karst aquifers can exhibit both Darcian (laminar) and non-Darcian (turbulent) flow, with Darcian flow generally dominating in the matrix network and non-Darcian flow occurring in the conduit network (Martin and Sreaton, 2001). Complicating the

understanding of flow in karst aquifers is the head-dependent fluid exchange between the matrix and conduit networks, which is site specific (Bauer et al., 2003; Martin and Sreaton, 2001; Martin et al., 2006; Hill, 2008; Hill et al., 2008). Moreover, conduit wall conductance between the matrix and conduit networks is an important parameter for improving the match between observed and simulated discharge in transient simulations during periods of low net recharge (Hill, 2008; Hill et al., 2008).

In this study, we compare the relative performance between a transient, laminar/turbulent, dual-conductivity site-scale model using MODFLOW-2005 CFP Mode 1 (Shoemaker et al., 2008) and a comparable transient, laminar equivalent continuum model using MODFLOW-2005 (Harbaugh, 2005) for the dual-permeability Upper Floridan aquifer in the vicinity of Weeki Wachee, west-central Florida, fig. 1. The purpose of this article is to present the results of the model performances.

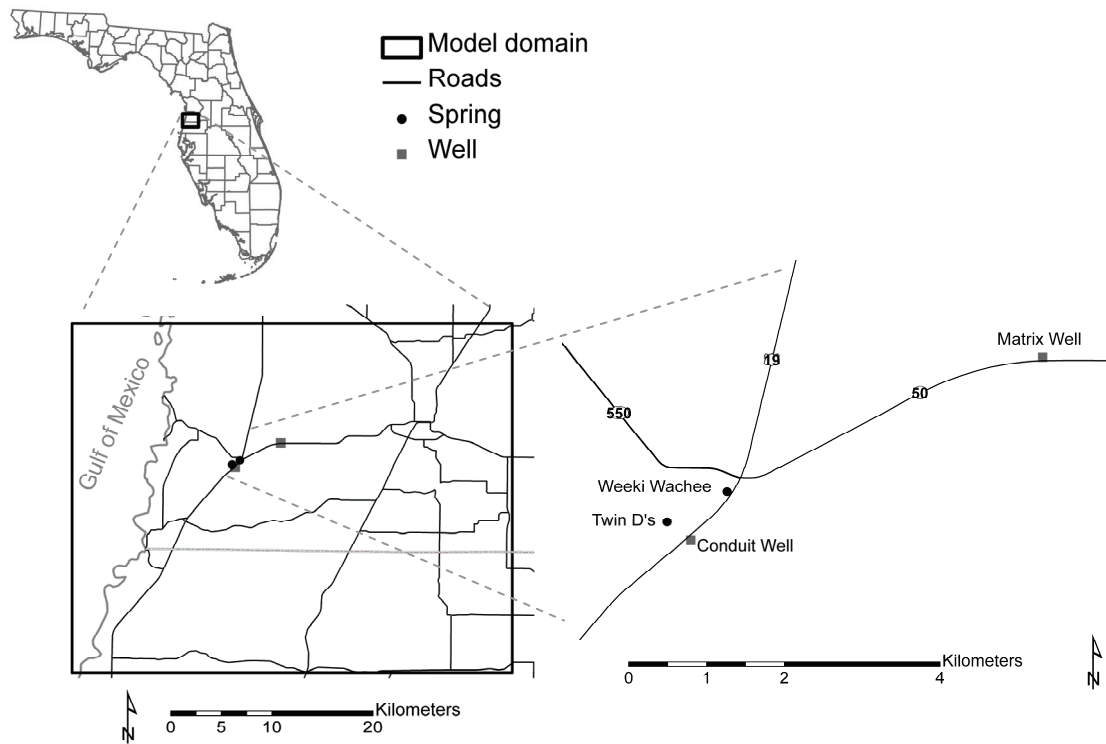


Figure 1. Site and location map with springs and monitoring wells.

STUDY AREA

The dual-permeability Upper Floridan aquifer underlies the study area. The Upper Floridan aquifer is composed of soluble Oligocene and Eocene carbonates and varies from unconfined to semi-confined conditions. The Upper Floridan aquifer comprises the Suwannee Limestone, Ocala Limestone, and Avon Park Formation, in descending order (Miller, 1986). Throughout the study area, a thin mantle varying from less than a meter to 61 m in thickness blankets the Upper Floridan aquifer (Hill, 2008). Springs, sinkholes, and underwater caves are present throughout the study area. Multiple episodes of karstification resulted during the Cenozoic Era in response to sea level fluctuations (Florea et al., 2007). Sea level fluctuations coupled with possible former mixing zones (Reeder and Brinkmann, 1998) produced large, horizontal elliptically shaped conduits sub-parallel to depositional layers, circular chambers, and vertical elliptically

shaped conduits normal to depositional layers. Passage widths can exceed 15 m at Weeki Wachee Spring and at the outermost mapped portions of Twin D's Spring (Southwest Florida Water Management District, 2001; Karst Underwater Research, Inc., written communication, 2008).

STUDY APPROACH

A site-scale laminar equivalent continuum model using MODFLOW-2005 and a comparable laminar/turbulent, dual-conductivity model using MODFLOW-2005 CFP Mode 1 were developed for the study area. The models consist of uniform grids with 285 columns and 236 rows. Cell widths are 152 m. The transient models consist of 24 stress periods spanning from June 2004 through May 2006. Observed discharges and water levels in monitoring wells penetrating the matrix and conduit networks during the 2-year period span extreme hydrologic conditions including 2 wet and dry

seasons (Jordan, 1984) passage of Tropical Storms Frances and Jeanne (fig. 2) in September 2004 and a cessation of flow at Twin D's Spring in May 2006 (Hill, 2008; Hill et al., 2008; Reimann and Hill, 2008).

Conduits were explicitly incorporated into the dual-conductivity model using cave-survey data provided by Karst Underwater Research, Inc., written communication, 2008. Parameters were kept constant between the transient equivalent continuum and dual-conductivity models with the exception of hydraulic conductivity, the conduit wall conductance that permits fluid exchange between the matrix and conduit networks, and the upper and lower Reynolds numbers (Reimann and Hill, 2008). Conduit wall conductance was constrained using observed data (Hill, 2008; Hill et al., 2008). Conduit wall diameters were constrained using descriptions provided by cave divers (Southwest Florida Water Management District, 2001; Karst Underwater Research, Inc., written communication, 2008).

Model performance was evaluated in terms of the match between observed and simulated discharges and water levels for monitoring wells penetrating the matrix and conduit networks, fig. 1. Discharge from two springs, Weeki Wachee, a first magnitude (≥ 3 m³/s) spring Meinzer 1927; Scott et al. 2004, and Twin D's, locally referred to as Little Spring, or Twin Dees, Scott et al. (2004), a spring that under average flow conditions from, June 2004 through May 2006, was a third magnitude (≤ 0.3 m³/s) spring (Meinzer, 1927; Hill, 2008; Hill et al., 2008). During that period, flow occasionally exceeded 0.3 m³/s at Twin D's Spring (second magnitude) (Meinzer, 1927; Hill, 2008; Hill et al., 2008) during high recharge events. Both springs discharge fresh water (Southwest Florida Water Management District, 2001).

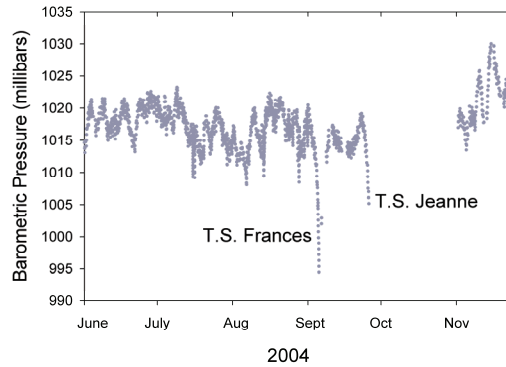


Figure 2. Hourly barometric pressure data from a National Oceanographic and Atmospheric Association (NOAA) station located 12 km from Weeki Wachee. Note the decrease in barometric pressure with passage of Tropical Storms (T.S.) Frances and Jeanne. Gaps represent missing data.

PERFORMANCE OF MODFLOW-2005 CFP MODE 1 RELATIVE TO MODFLOW-2005

The dual-conductivity model using MODFLOW-2005 CFP Mode 1 matched observed and simulated discharges more closely, particularly during low net recharge periods, compared to the equivalent continuum model using MODFLOW-2005 (fig. 3). Simulated discharges for Weeki Wachee Spring using the dual-conductivity model were on average 89% of observed values as compared to 77% using the equivalent continuum model. Simulated discharges for Twin D's Spring using the dual-conductivity model were, on average, 85% of observed values as compared to 45% using the equivalent continuum model. Application of MODFLOW-2005 CFP Mode 1 with the dual-conductivity model resulted in an overall improvement of 12 to 40% in the match between observed and simulated discharges. Although a percentage of the increase in simulated discharges was attributed to decreases in bulk hydraulic conductivities, some of the improvement was attributed to fluid exchange between the matrix and conduit networks (Hill, 2008; Hill et al., 2008; Reimann and Hill, 2008). Simulated water levels in the conduit and matrix wells did not differ significantly from each other in the equivalent continuum and dual-conductivity models as seen in figure 3 (Hill, 2008; Hill et al., 2008; Reimann and Hill, 2008).

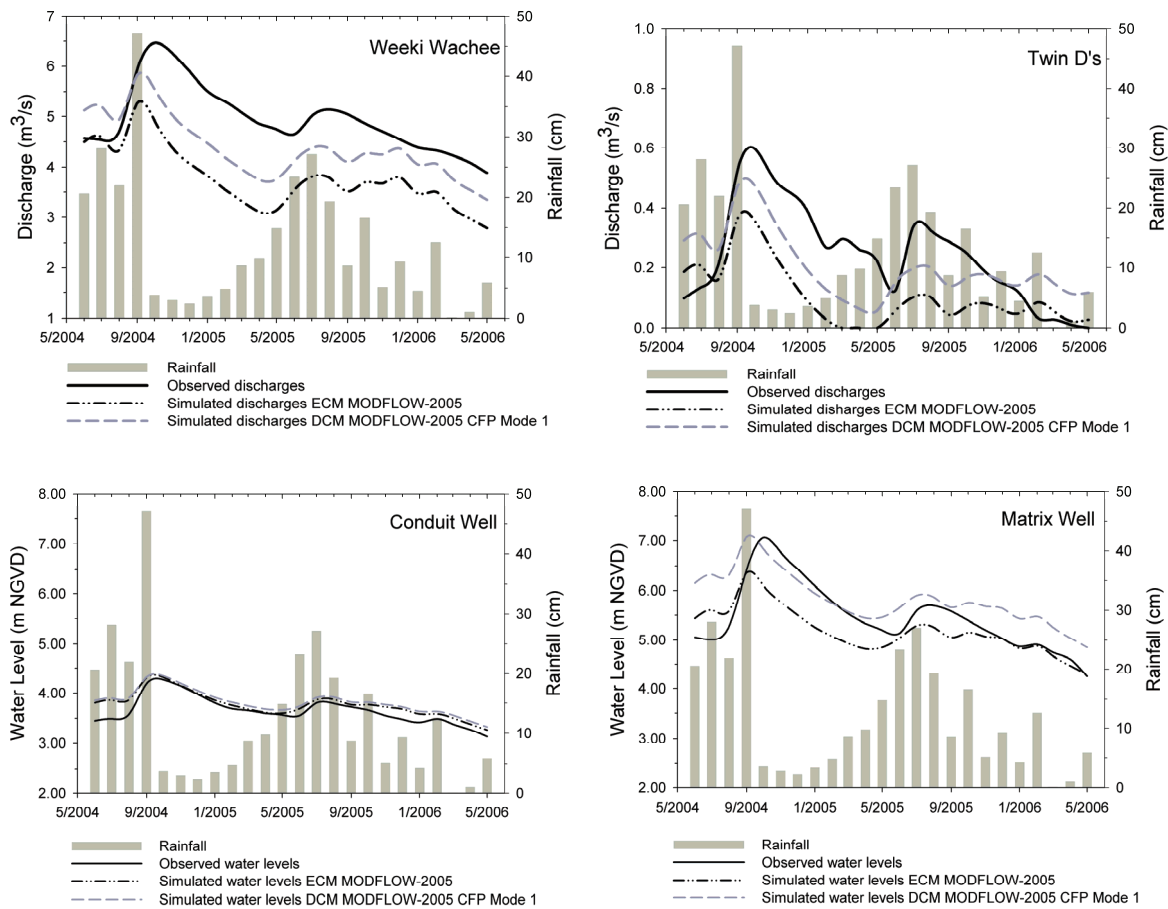


Figure 3. Plots of observed and simulated discharges at Weeki Wachee and Twin D's Springs for the laminar equivalent continuum model (ECM) using MODFLOW-2005 and the laminar/turbulent dual-conductivity model (DCM) using MODFLOW-2005 CFP Mode 1. Average monthly rainfall quantities are for a 132 km² area. Rainfall estimates provided by OneRain, Inc. and consist of Doppler radar distributions coupled with rainfall quantities calibrated using rainfall gauges (Hoblit and Curtis, 2005). Note the increase in discharge and water levels during September 2004 with passage of Tropical Storms Frances and Jeanne and the cessation of discharge in May 2006 at Twin D's Spring. Caliper or video logs were used to determine if wells monitor the matrix or conduit networks. The conduit well intercepts an underwater cave with a height of approximately 8 m (Hill, 2008; Hill et al., 2008).

SUMMARY AND CONCLUSION

The performance between a transient dual-conductivity model using MODFLOW-2005 CFP Mode 1 and a comparable transient equivalent continuum model using MODFLOW-2005 was evaluated in the vicinity of Weeki Wachee, west-central Florida. The study area is underlain by the dual-permeability Upper Floridan aquifer. The models spanned extreme hydrologic conditions that included high recharge events associated with tropical storms and a drought that included a cessation of flow at Twin D's Spring.

Results obtained during these simulations indicate that the dual-conductivity model using MODFLOW-2005 CFP Mode 1 performed better than the equivalent continuum model using MODFLOW-2005. A better match between observed and simulated discharges during extreme hydrologic conditions was obtained with MODFLOW-2005 CFP Mode 1. These results indicate that the dual-conductivity model using MODFLOW-2005 CFP Mode 1 is a better tool for simulating discharge in the dual-permeability Upper Floridan aquifer during periods of low net recharge, relative to the equivalent continuum model that considers the bulk properties of the matrix and conduit

networks. This conclusion particularly applies near areas of focused discharge where fluid exchange is present between the matrix and conduit networks.

ACKNOWLEDGEMENTS

The authors gratefully thank W. Barclay Shoemaker of the USGS for providing the MODFLOW-2005 Conduit Flow Process. We also thank Karst Underwater Research, Inc. for providing the cave survey data. This study was partly funded by the Southwest Florida Water Management District.

REFERENCES

- Bauer, S., Liedl, R., and Sauter, M., 2003, Modeling of karst aquifer genesis: influence of exchange flow, *Water Resources Research* 39, 1285, doi:10.1029/2003WR002218.
- Florea, L.J., Vacher, H.L., Donahue, B., and Naar, D., 2007, Quaternary cave levels in peninsular Florida, *Quaternary Science Reviews*, v. 26, p. 1334-1361.
- Harbaugh, A.W., 2005, MODFLOW-2005, The U.S. Geological Survey modular ground-water Model -- the Ground-Water Flow Process: U.S. Geological Survey Techniques and Methods 6-A16, variously p.
- Hill, M.E., 2008, Conduit conceptualizations and model performance, Ph.D. diss., Department of Geology, University of South Florida, Tampa, variously p.
- Hill, M.E., Stewart, M.T., and Martin, A., 2008, Characterizing dual-permeability karst aquifers: constraining new parameters, Submitted to *Ground Water*.
- Hoblit, B.C. and Curtis, D.C., 2005, Radar estimates + gauge data a perfect union. *Southwest Hydrology* 4, no. 3, SAHRA, University of Arizona, Tucson, variously p.
- Jordan, C.L., 1984, Florida's weather and climate: Implications for water, in E.A. Fernald and D.J. Patton (eds.), *Water Resources Atlas of Florida*, Tallahassee: Institute of Science and Public Affairs, Florida State University, p. 18-35.
- Martin, J.M., Sreaton, E.J., and Martin, J.B., 2006, Monitoring well responses to karst conduit head fluctuations: implications for fluid exchange and matrix transmissivity in the Floridan aquifer, in R.S. Harmon and C. Wicks (eds.), *Perspectives on karst geomorphology, hydrology, and geochemistry-A tribute volume to Derek C. Ford and William B. White*, Boulder, Colorado: Geological Society of America, p. 209-217.
- Martin, J.B. and Sreaton, E.J., 2001, Exchange of matrix and conduit water with examples from the Floridan aquifer, in E.L. Kuniansky (ed.), *U.S. Geological Survey Karst Interest Group Proceedings, Water-Resources Investigations Report 01-4011*, p.38-44.
- Meinzer, O.E., 1927, Large springs in the United States. U.S. Geological Survey Water-Supply Paper 557, 94 p.
- Miller, J.A., 1986, Hydrogeologic framework of the Floridan aquifer system in Florida and in parts of Georgia, Alabama, and South Carolina: U.S. Geological Survey Professional Paper 1403-B, variously p.
- Palmer, A.N., 1999, Introduction, in A.N. Palmer, M.V. Palmer, and I.D. Sasowsky (eds.), *Karst Modeling: Charles Town, West Virginia, Karst Waters Institute Special Publication 5*, p 1-9.
- Reeder, P. and Brinkmann, R., 1998, Palaeoenvironmental reconstruction of an Oligocene-aged island remnant in Florida, USA, *Cave and Karst Science* v. 25, p. 7-13.
- Reimann, T. and Hill, M.E., 2008, Performance review of the MODFLOW-2005 Conduit Flow Process, Software Spotlight, Submitted to *Ground Water*.
- Scott, T.M., Means, G.H., Meegan, R.P., Means, R.C., Upchurch, S.B., Copeland, R.E., Jones, J., Roberts, T., and Willet, A., 2004, Springs of Florida, *Florida Geological Survey Bulletin No. 66*, Tallahassee: Florida Geological Survey, 377 p.
- Shoemaker, W.B., Kuniansky, E.L., Birk, S., Bauer, S., and Swain, E.D., 2008, Documentation of a Conduit Flow Process (CFP) for MODFLOW-2005: U.S. Geological Survey Techniques and Methods, Book 6, Chapter A24, 50 p.

Southwest Florida Water Management District, 2001, The hydrology and water quality of springs in west-central Florida: Tampa, Report on file, 149 p.

White, W.B., 2002, Ground water flow in karst: matrix flow and conduit flow with implications for the Floridan aquifer, in J.B. Martin, C.M. Wicks, and I.D. Sasowsky (eds.), Hydrogeology and biology of post-Paleozoic carbonate aquifers: Charles Town, West Virginia, Karst Waters Institute Special Publication 7, p. 9-13.

White, W.B., 1999, Conceptual models for karstic aquifers, in A.N. Palmer, M.V. Palmer, and I.D. Sasowsky (eds.), Karst Modeling: Charles Town, West Virginia, Karst Waters Institute Special Publication 5, p. 11-16.

White, W.B., 1988, Geomorphology and hydrology of karst terrains, New York: Oxford University Press, 464 p.

Worthington, S.R.H., Ford, D.C., and Beddows, P.A., 2000, Porosity and permeability enhancement in unconfined carbonate aquifers as a result of dissolution, in A.B. Klimchouk, D.C. Ford, A.N. Palmer, and W. Dreybrodt (eds.), Speleogenesis Evolution of Karst Aquifers: Huntsville, Alabama, National Speleological Society, Inc., p. 463-472. Geological Survey Department of Cyprus, 1995, Geological map of Cyprus: 1:250,000 scale, 1 sheet.

Machette, M.N., 1985, Calcic soils of the southwestern United States: Geological Society of America Special Paper 203, p. 1-21.

Makris, J. Stacker, J., and Kramvis, S., 2000, Microseismic studies and tectonic implications of Cyprus; in Panayides, I., Xenophontos, C., and Malpas, J., eds., Proceeding of the Third International Conference on the Geology of the Eastern Mediterranean, p. 137-145.

MISCELLANEOUS TOPICS IN MODELING AND GEOPHYSICS

The Value of Single-Well Tracer Studies for Characterizing Karst Sites

By Tarra M. Beach^{1,2*}, Michael W. Bradley², Roger Painter¹, and Thomas D. Byl^{2,1}

¹College of Engineering, Technology and Computer Science, Tennessee State University, 3500 John A. Merritt Blvd., Nashville, TN 37209

²U.S. Geological Survey, 640 Grassmere Park, Suite 100, Nashville, TN 37211

*currently at Environmental Science and Engineering, Vanderbilt University, Nashville, TN

Abstract

Water movement, contaminant migration and energy transfer in heterogeneous karst aquifers is challenging to describe quantitatively. Karst ground-water aquifers may be characterized by high velocity, turbulent flow within solution-enhanced fractures, conduits, or stratiform passageways. In other parts of the same aquifer, ground-water flow may be stagnant or very slow. Once a contaminant has entered a karst aquifer, it is often difficult to determine its precise flow-path or residence time in the bedrock. Attempts to characterize a karst site with traditional tracer tests may yield limited information, especially if the tracer cannot be detected at down-gradient monitoring sites. This project applied an integrated approach using local geology, data from fracture mapping, borehole geophysics, and hydraulic testing, as well as geochemical and single-well tracer tests to characterize aquifer hydraulic properties at several karst sites in Middle Tennessee. Two types of wells; existing wells with the characteristics of typical domestic-water wells, and wells constructed to meet project specifications were also evaluated. Single-well tracer studies were conducted by injecting a conservative salt tracer of known concentrations into several wells at known depths and measuring the decrease in tracer concentration with time. Changes in tracer concentration were then analyzed to provide information about aquifer advection and dispersion properties in the immediate proximity of the wells. Unfortunately, some of the wells used in this study were drilled approximately 25 years ago and proved to be less than ideal for single-well injection studies. The most difficult problem encountered involved wells characterized by long vertical sections with no bedrock openings for the tracer to enter the aquifer freely. These wells yielded very little useful information. For example, the mean residence time in the water column of bedrock wells with few openings was 65 hours or greater. Conversely, tracer injections in wells with good hydraulic communication with the bedrock aquifer provided useful data with mean residence times ranging from 14 to 45 hours. Single-well tracer studies conducted in properly designed wells provided valuable hydrologic information on the residence-time distribution and dispersion of the tracer in the vicinity of the injection wells. The information collected from single-well injection tests when combined with water chemistry and water level data can be useful for the design of remediation strategies at contaminated karst sites.

GIS and Spatial Statistical Methods for Determining Sinkhole Potential in Frederick Valley, Maryland

By Katarina Z. Doctor

George Mason University, katarina@doctor.com

Abstract

Urban development is rapidly occurring in the karstic terrain of the Frederick Valley, Maryland, USA. Sinkholes are an inherent feature of the landscape; they present hazards and engineering challenges to the development of residential, commercial and industrial infrastructure. Here, a new approach is presented for assessing susceptibility of sinkhole occurrence. A sinkhole dataset and geologic map was obtained from the Maryland Geological Survey (Brezinski, 2004). Clustering and kernel density analyses were performed on the sinkhole location data to assess interdependence of sinkhole locations. External factors relating to sinkhole development were examined separately using Geographically Weighted Regression (GWR) and ordinary linear regression. These factors included geologic structure (folds axes and faults), rock type, proximity to impervious surfaces and surface drainage patterns. In order to determine the relative likelihood of sinkhole formation, the results of the cluster analysis, density analysis, and regression analyses resulted in map layers that could be weighted and overlain to create a sinkhole susceptibility map.

Cluster analysis is important for analyzing sinkhole development for two reasons: 1) human activities tend to fill an empty space by creating a more uniform pattern than random, 2) the eye tends to “see clusters where none exist” as the result of the mind’s desire to organize spatial information (Rogerson, 2001). Nearest neighbor analysis (NNA) is the most common method of cluster analysis; however, this method will not capture a pattern that is non-homogeneous over a study area (Wong, 2005). The statistical method that is able to identify clustering in different scales is the K-function analysis, which compares the observed distribution of sinkholes to the same number of randomly distributed points. This method also considers the shape of the study region. In the Frederick Valley case study this was an important issue because of the elongated shape of the valley.

Sinkhole density is an important factor for determining the area most prone to sinkhole development. Where a closed depression has collapsed into a sinkhole we know that the underlying subsurface contains unstable voids, and possibly a cave system. In areas where active sinkholes have developed there is a greater possibility that a new sinkhole will form (Brezinski, 2004; Zhou, 2003). Two methods were used to determine sinkhole density. The first method is the Kernel Density Estimation (KDE) for which bandwidths were calculated with the previously described K-function analysis. The second method takes into account a radial buffer area around each sinkhole and is expressed as the number of sinkholes inside each buffer zone. As a result each sinkhole receives an attribute that is the density of sinkholes within its surrounding radial buffer zone. This result is used later for further calculations for estimating sinkhole susceptibility.

Several geologic and anthropogenic factors were identified in Frederick Valley that influence sinkhole development. These factors include proximity of sinkholes to quarries, water-bodies, fault lines, anticline and syncline fold axes, streams, roads and ground-water table depth (Zhou, 2003; Brezinski, 2004; Magdalene, 1995; Ordorff, 2000; Hack, 1965). The locations of these features are known from detailed geologic maps (Brezinski, 2004). Geographically Weighted Regression (GWR) analysis was used to express the significance of these factors in relation to sinkhole density. GWR is a multivariate regression which assumes that the relationship of weights of each influencing factor vary across space. From the GWR results, a map surface was produced for predicting highest sinkhole density using the Inverse Distance Weights method (Fig. 1).

These results may be a guide for future development activities in this region and others like it.

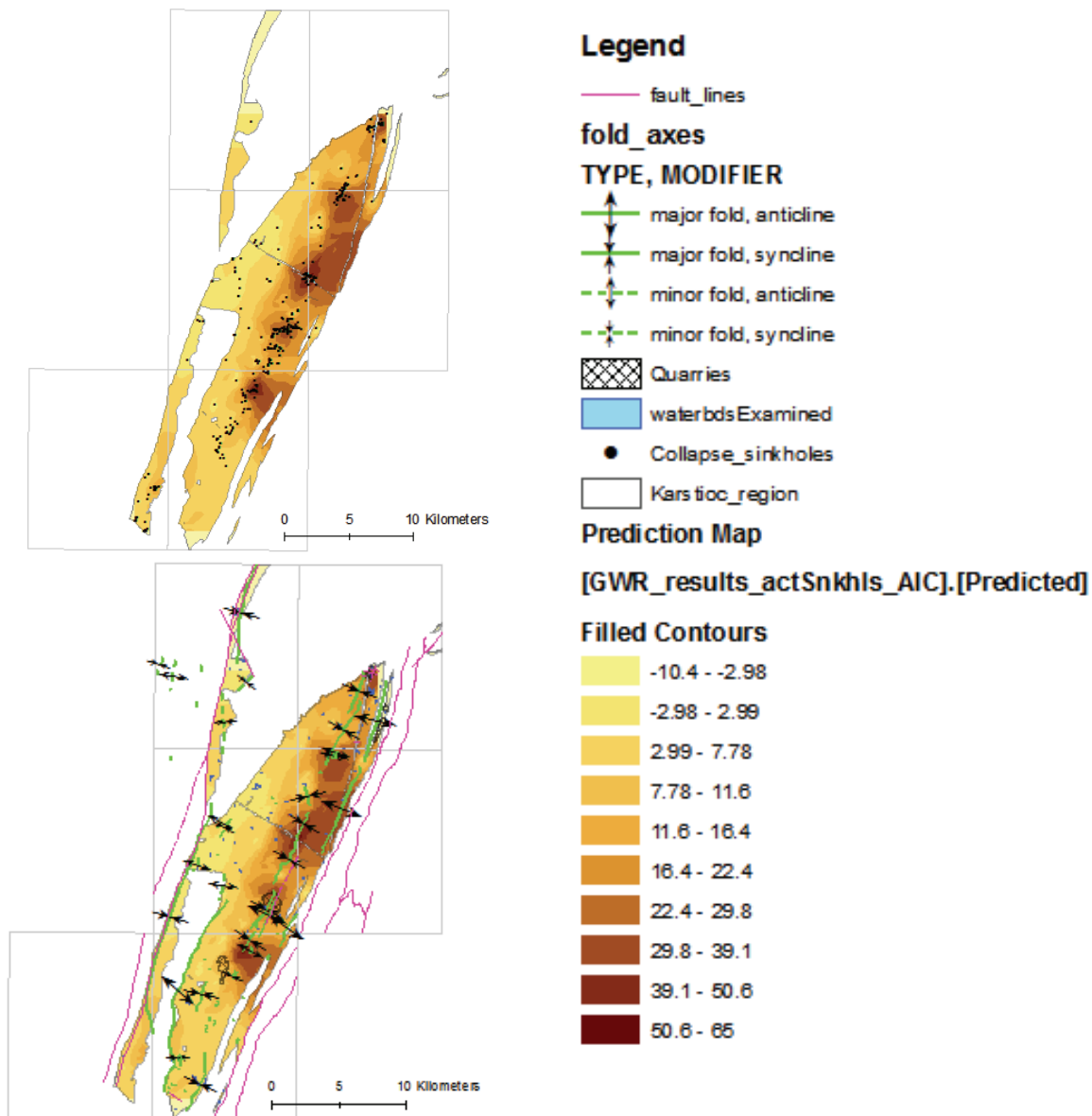


Figure 1. The top panel shows predicted sinkhole density and the actual sinkhole point locations. The bottom panel shows the predicted sinkhole density and some factors that influence sinkhole collapse.

REFERENCES

- Brezinski, D.K., 2004, Stratigraphy of the Frederick Valley and its Relationship to Karst, Rep. No. 75., Annapolis: Maryland Department of Natural Resources.
- Hack, J.T., 1965, Gomorphology of the Shenandoah Valley, Virginia and West Virginia, and origin of the residual ore deposits: U.S. Geological Survey Professional Paper, 484 p.
- Magdalene, S. and Alexander, E.C.Jr., 1995, Sinkhole Distribution in Winona County, Minnesota Revised. Proceedings of the Fifth Multidisciplinary Conference on Sinkholes and the Engineering and Environmental Impacts of Karst. Gatlinburg, Tennessee.

Ordorff, R.C. and Weary, D.J. and Lagueux, K.M., 2000, Geographic Information Systems analysis of Goloegic controls on the Distribution of Dolines in the Ozarks of South-Central Missouri, USA. *Acta Carsologica*, Vol. 29- No. 2, 11.

Rogerson, P.A., 2001, *Statistical Methods for Geography*, London, Sage Publications, 232 p.

Wong, D.W.S., and Lee, J., 2005, *Statistical Analysis of Geographic Information with ArcView GIS and ArcGIS*, Hoboken, New Jersey, John Wiley & Sons, Inc.

Zhou, W., Beck, B.F., and Adams, A.L., 2003, Application of Matrix Analysis in Delineating Sinkhole Risk Areas along Highway (I-70 near Fredrick, Maryland), *Environmental Geology*, No. 44, pg. 834-842.

Geophysical Analysis of the Salmon Peak Formation near Amistad Reservoir Dam, Val Verde County, Texas, and Coahuila, Mexico, March 2006, to Aid in Piezometer Placement

By Gregory P. Stanton¹, Wade H. Kress², Andrew P. Teeple², Michael L. Greenslate¹, and Allan K. Clark³

¹U.S. Geological Survey, 8027 Exchange Drive, Austin, Texas 78754

²U.S. Geological Survey, 944 Arroyo Drive, San Angelo, Texas 76903

³U.S. Geological Survey, 5563 De Zavala Road, Suite 290, San Antonio, Texas 78249

Abstract

Since 1992, numerous sinkholes have developed northwest of the Amistad Reservoir dam on the Rio Grande. Increases in the discharge of springs south of the dam, on the western side of the Rio Grande, in Coahuila, Mexico, have been documented. In 1995 the Mexico Section of the International Boundary and Water Commission (IBWC) completed a study of the western embankment (Coahuila, Mexico) of the dam that included surface geophysics, borehole geophysics, and installation of piezometers to learn more about subsurface conditions. As part of a 5-year safety inspection in 2005, technical advisors recommended that one line of similarly constructed piezometers be installed on the eastern embankment (Val Verde County, Texas) of the dam for comparison of water levels (potentiometric head) on both the western and eastern embankments of Amistad Reservoir dam. To provide technical assistance for the horizontal and vertical placement of piezometers on the eastern embankment of Amistad Reservoir dam, the U.S. Geological Survey, in cooperation with the U.S. Section of the IBWC, conducted a study along both the western and eastern embankments of Amistad Reservoir dam. The study involved an integrated approach using surface and borehole geophysical methods. In the western embankment investigation, geological and geophysical characteristics that indicate relatively large water-yielding properties of the Salmon Peak Formation were identified. The direct-current (DC) resistivity method was selected as the surface geophysical reconnaissance technique to correlate relatively large water-yielding properties of the Salmon Peak Formation, identified from analysis of borehole geophysical logs, with variations in subsurface resistivity. The dipole-dipole array and the reciprocal Schlumberger array were selected as the most applicable DC resistivity arrays. Two resistivity units were identified in both the dipole-dipole array data and the reciprocal Schlumberger array data along DC resistivity profiles on both embankments. Resistivity unit 1 generally is of relatively low resistivity, ranging from 45 to 150 ohm-meters compared with resistivity unit 2, which ranges from 120 to 345 ohm-meters (depending on the DC array type). The presence of mapped sinkholes in the reservoir north of the western embankment study area and the zone of increased water content (as indicated by zones of low neutron log count rates in nearby piezometers) leads to the conclusion that resistivity unit 1 is a preferential flow path where surface water from Amistad Reservoir is forced into the ground-water system (because of increased head from the reservoir). In the eastern embankment investigation, trends in the spatial distribution of sinkholes and the occurrence of weathered zones were identified from geologic descriptions of cores. The correlation of surface geophysical DC resistivity, historical lithologic data, and general trend of documented sinkholes along the eastern end of the eastern embankment profile were used to justify further exploration (drilling of piezometers) in the eastern expression of resistivity unit 1. The spatial location of the piezometers and the screened intervals were selected to best match the locations of the screened intervals of the western embankment piezometers. Six piezometers were installed on the eastern embankment and logged using borehole geophysical techniques. Surface DC resistivity sections superimposed on the resistivity logs for two piezometers indicate three discernible resistivity units that correlate with resistivity units 2, 1, and 2, respectively, identified in the western embankment study area. Resistivity units 1 and 2 in the DC resistivity profiles generally correspond with low and high resistivity zones, respectively, on the normal and lateral resistivity logs collected in the nearby piezometers at the time of installation (Stanton and others, 2007, Stanton and others, 2008).

REFERENCES

- Stanton, G.P., Kress, W.H., Teeple, A.P., Greenslate, M.L., and Clark, A.K., 2007, Geophysical analysis of the Salmon Peak Formation near Amistad Reservoir dam, Val Verde County, Texas, and Coahuila, Mexico, March 2006, to aid in piezometer placement: U.S. Geological Survey Scientific Investigations Report 2007-5143, 70 p. <http://pubs.usgs.gov/sir/2007/5143/>.
- Stanton, G.P., Kress, W.H., Teeple, A.P., and Clark, A.K., 2008, Geophysical analysis of the Salmon Peak Formation near Amistad Reservoir dam, Val Verde County, Texas, and Coahuila, Mexico, March 2006, to aid in piezometer placement *in* 21st Symposium on the Application of Geophysics to Engineering and Environmental Problems (SAGEEP), Philadelphia, Pennsylvania, April 6-10, 2008, Proceedings: 18 p.

Construction and Use of a Fractured-Rock Simulator to Test Horizontal Borehole Flow-Measuring Technologies

By E. Randall Bayless

U.S. Geological Survey, 5957 Lakeside Boulevard, Indianapolis, IN 46278

Abstract

Measurements of horizontal flow directions and velocities of ground water in bedrock aquifers that have significant secondary porosity can be invaluable to many hydrologic investigations. Calibration studies to evaluate performance of several horizontal flow-measuring technologies have been done in a simulated unlithified aquifer but have not been done in a fractured-rock simulator. This study describes the construction and initial use of a fractured-rock simulator to calibrate horizontal flow-measuring technologies.

During 2007, a fractured-rock simulator was built at the U.S. Geological Survey Hydrologic Instrumentation Facility. The fracture was simulated by two parallel, horizontal plates of 0.875-inch-thick plexiglass, sealed along the long dimension by a flexible gasket. The plates were 42 inches wide by 60 inches long. Screw adjustments allowed the fracture aperture to be uniformly opened. One 4- and one 6-inch well casing intersected the upper and lower plates. Both wells were completely open to the fracture. The hydraulic gradient across the fracture length was controlled precisely by adjusting water levels in reservoirs connected to the up-gradient and down-gradient ends of the fracture plates. A dye manifold was installed near the water inlet to the fracture to permit visual observation of flow lines.

Horizontal ground-water velocity magnitude and direction were measured in the 4- and 6-inch wells with five horizontal flow-measuring technologies. The technologies consisted of an acoustic Doppler velocimeter, a heat-pulse flowmeter, a colloidal borescope flowmeter, a scanning colloidal borescope flowmeter, and a hydrophysical logging system. Each horizontal flow-measuring technology was used to measure the water velocity magnitude and direction in both wells, except the hydrophysical logging system, which measures velocity magnitude only.

Various flow simulations were established by managing the hydraulic gradient and the fracture aperture. The tested range of hydraulic heads ranged from 0.0006 ft/ft to 0.0028 ft/ft. Measurements were made at fracture apertures of 0.039, 0.118 and 0.394 in. The linear velocity of water through the fracture was computed from tank discharges at the down-gradient end of the fracture and ranged from 605 to 6,120 ft/day.

Results indicated that the horizontal flow-measuring technologies were capable of measuring ground-water vectors at velocities less than 3,800 ft/d. Evaluation of the performance of individual technologies, however, was not possible because the simulator was determined to have some unforeseen inadequacies. Water leaked from the fracture gasket at two locations, possibly affecting the flow measurements. Ferrous metal weights, used to counteract the buoyancy of the upper fracture plate, may have interfered with magnetometer-based measurements of the flowmeter and flow orientation. Future plans call for repairs and adjustments to the fractured-rock simulator to address these issues, followed by retesting of the horizontal flow-measuring technologies in 2008 over a similar range of hydraulic conditions.

Collection of Bathymetric Data Along Two Reaches of the Lost River Within Bluespring Cavern Near Bedford, Lawrence County, Indiana, July 2007

By David C. Lampe and Scott E. Morlock

U.S. Geological Survey Indiana Water Science Center, 5957 Lakeside Blvd, Indianapolis, IN 46278

Abstract

The U.S. Geological Survey (USGS), in cooperation with the Indianapolis Museum of Art (IMA), Ohio River Valley Water Sanitation Commission (ORSANCO), and Bluespring Caverns collected bathymetric data along two reaches of the Lost River within the Bluespring Cavern near Bedford, Indiana. The two reaches, designated as "upstream reach", and "downstream reach", had lengths of approximately 200 feet and 300 feet, respectively. These data were collected in support of an artwork commissioned by the IMA.

The USGS used an acoustic Doppler current profiler (ADCP) to collect the bathymetric data. ADCPs are acoustic instruments commonly used by the USGS to measure streamflow. To compute streamflow, ADCPs also measure water velocities, boat velocities, and water depths. Water-velocity measurements are made by transmitting sound at a known frequency into the water and measuring the Doppler shift, or change in sound frequency, from signals reflected off particles in the water (Oberg, Morlock, and Caldwell, 2005). Measurement of the Doppler shift of signals reflected from the river bottom determines the boat speed, and the ADCP on-board compass determines the boat direction (Wilson, Morlock, and Baker, 1997). The signals reflected from the bottom also are used to compute the depth of water. Although it has become commonplace for the USGS to use ADCPs for streamflow measurements, the collection of bathymetric data within a cavern for use in three-dimensional data-visualization products is an innovative use of the technology.

All data were collected on July 10, 2007. The ADCP was deployed from a small tethered flotation platform. All ADCP data were collected in real time on a laptop computer as binary files. The USGS quality assured the ADCP binary data files and output the water-velocity and bathymetry data in a text-file format. Computer programs were written to screen the text files for erroneous data and to format the data so they could be imported into three-dimensional data-visualization software. This software was used to create three-dimensional plots of the river reaches that showed river depths.

REFERENCES

- Oberg, K.A., Morlock, S.E., and Caldwell, W.S., 2005, Quality-assurance plan for discharge measurements using acoustic Doppler current profilers: U.S. Geological Survey Scientific Investigations Report 2005-5183, 35 p.
- Wilson, J.T., Morlock, S.E., and Baker, N.T., 1997, Bathymetric surveys of Morse and Geist Reservoirs in central Indiana made with acoustic Doppler current profiler and global positioning system technology, 1996: U.S. Geological Survey Water Resources Investigations Report 97-4099, 49 p.

A Multi-Tool Geophysical and Hydrogeological Investigation of a Karst Aquifer System, Cibolo Canyon Development Area, Bexar County, Texas

By Sachin D. Shah¹, Bruce D. Smith², Allan K. Clark³, and Wade H. Kress⁴

¹U.S. Geological Survey, 8027 Exchange Drive, Austin, Texas 78754

²U.S. Geological Survey, P.O. Box 25046, MS 973, Denver, Colorado 80225

³U.S. Geological Survey, 5563 De Zavala, Suite 290, San Antonio, Texas 78249

⁴U.S. Geological Survey, 944 Arroyo Drive, San Angelo, Texas 76901

Abstract

The U.S. Geological Survey, in cooperation with San Antonio Water System, conducted a geophysical and geological study of the Cibolo Canyon development area, northeast Bexar County, Texas, to characterize hydrostratigraphic features and to map surface and subsurface hydrogeologic features of the Edwards aquifer. Capacitively-coupled (CC) resistivity and frequency-domain electromagnetic (FDEM) profiling, direct current resistivity depth imaging (2D–DC) profiles, and time-domain electromagnetic (TDEM) soundings were used in conjunction with new geologic mapping, and borehole logging. This study shows that near surface geophysical methods were effective in defining electrical signatures of the various stratigraphic members of the Edwards aquifer. In general the upper hydrostratigraphic units of the Edwards aquifer (Kainer Formation) are less resistive than the lower units (Person Formation). The upper hydrostratigraphic units of the underlying Trinity aquifer have a lower resistivity than the overlying Edwards. The TDEM soundings were able to delineate changes in elevation of the base of the resistive units and define the amount of vertical displacement across the faults. Both CC resistivity and FDEM methods were used to map hydrostratigraphic contacts, fault zones, and possible karst features. The 2D–DC resistivity imaging techniques showed lateral changes in the subsurface lithology that correlate well with the CC and FDEM data. The TDEM and 2D–DC methods had limited application due to site accessibility and project time lines. Results from the study demonstrated that combining multiple geophysical methods and geological mapping significantly improved the hydrogeologic mapping the Cibolo Canyon development area.

INTRODUCTION

The Edwards aquifer is a very productive karst aquifer system located throughout central and western Texas. The dissolution-modified, faulted limestone aquifer is the primary source of public-water for the city of San Antonio and most of central Texas. In Bexar County, residential and commercial development of the Edwards aquifer recharge zone is increasing. The aquifer could become contaminated by spills, leakage of hazardous materials, or runoff from the rapidly developing urban areas that surround, or are built on, the fractured and faulted karstic limestone outcrops that form the recharge zone (Buszka, 1987, p. 2). Currently (2007), a large area northeast of San Antonio, Texas, is being developed in the Cibolo Canyon area (fig. 1). In August 2007, The U.S. Geological Survey (USGS), in cooperation with the San Antonio Water System (SAWS),

conducted a multi-tool geophysical and geologic study to map surface and subsurface hydrostratigraphic features, including karst features, within the Edwards. Data collection and analysis was targeted along one section of the fault where equal comparisons of each method can be made (fig. 1). Methodologies used include TDEM soundings, continuous CC resistivity and FDEM profiles, and 2D–DC resistivity imaging profiles. The goal of the project was to better understand the framework and structure of the Edwards aquifer in the Cibolo Canyon development area.

SITE DESCRIPTION AND GEOLOGIC CHARACTERIZATION

The study area encompasses about 20 square kilometers and is located in northeast Bexar County (fig. 1). Cibolo Creek, located on the northeast side of the development area, forms

the border between Bexar County and Comal County. The Lower Cretaceous rocks that crop out at the Cibolo Canyon area, from oldest to youngest, are the Trinity Group and Edwards Group. The hydrostratigraphic divisions of the Edwards Group correspond with the lithologic divisions based on depositional environments. The Edwards Group in Bexar County is composed of approximately 450 ft of limestone, chert and dolomite (Stein and Ozuna, 1995). According to Rose (1972) the Edwards Group is composed of the Kainer and Person Formations informally referred to as the upper and lower Edwards Group. Rose (1972) further subdivided

the Kainer Formation into four informal stratigraphic units which are the basal nodular member, the dolomitic member, Kirschberg evaporite member, and the grainstone member (table 1). Rose (1972) also subdivided the Person Formation into the regional dense member, the leached member, the collapsed member, the cyclic member and the marine member (table 1).

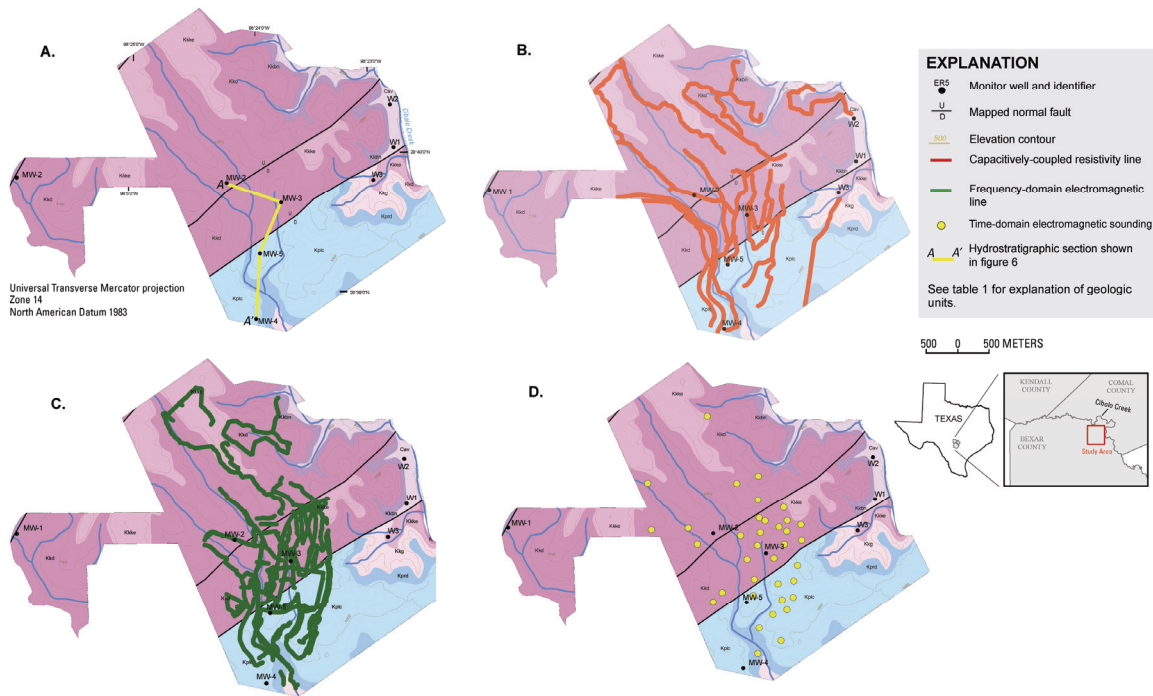


Figure 1. Location of the study with hydrogeology adapted from Stein and Ozuna (1995) and location of geologic transects: (A) hydrostratigraphic section A-A' through existing wells, (B) capacitively-coupled resistivity lines, (C) frequency-domain electromagnetic lines, and (D) time-domain electromagnetic soundings, Cibolo Canyon development area, Bexar County, Texas.

Table 1. Summary of stratigraphic units that crop out on the Cibolo Canyon development area, Bexar County, Texas

| Period, Group, Formation, or member | | Thickness (meters) | Lithology | Aquifer | Zone | Hydrologic function | Porosity permeability type | | |
|-------------------------------------|---------------|---------------------------|--------------------------------------|---------|---|-----------------------|----------------------------|---|---|
| Lower Cretaceous | Edwards Group | Person Formation | Cyclic and marine members (Kpcm) | 24-27 | Mudstone to packstone; <i>miotolid</i> grainstone; chert | Upper Zone | Aquifer | Fabric and not-fabric/ high permeability | |
| | | | Leached and collapsed members (Kpcl) | 21-27 | Crystalline limestone; mudstone to grainstone; chert | | Aquifer | Majority not-fabric/ high permeability | |
| | | | Regional dense member (Kprd) | 6-7.5 | Dense, argillaceous mudstone | | Confining unit | Not-fabric/low permeability; vertical barrier | |
| | | Kainer Formation | Grainstone member (Kkg) | 15-18 | <i>Miotolid</i> grainstone; mudstone to wackestone; chert | Lower Zone | Aquifer | Not-fabric/ generally low permeability except in conduits | |
| | | | Kirschberg Evaporite member (Kkkc) | 15-18 | Highly altered crystalline limestone; chalky mudstone; chert | | Aquifer | Fabric selective porosity, moderate permeability | |
| | | | Dolomitic member (Kkd) | 33-40 | Mudstone to grainstone; crystalline limestone; chert | | Aquifer | Not-fabric selective porosity and high permeability associated with fractures and caves | |
| | Trinity Group | Upper Glen Rose Limestone | Basal nodular member (Kkbn) | 15-18 | Shalely, nodular limestone; mudstone and <i>miotolid</i> grainstone | Upper Trinity Aquifer | Upper zone | Aquifer | Not-fabric selective; conduit, generally low permeability except in conduits |
| | | | Cavernous member (Kgru) | 37 | Alternating & inter-fingering medium-bedded mudstone, wackestone, & packstone with local solution zones | | | Aquifer; associated with fractures, caves | Fabric selective in banded mudstones; Not-fabric selective fracture and cavern porosity; very permeable near contact with Edwards Group |

Lithology, stratigraphy, diagenesis, and karstification account for the high effective porosity and permeability in the Edwards aquifer. Karst features that can greatly enhance the effective porosity and permeability in the outcrop include sinkholes and caves. The primary controlling factor on cave development appears to be fractures (Veni, 1988). Also, extensions perpendicular to primary fault trends appears to have acted as the catalyst for cave formation and location of caves (Clark and Journey, 2006). Faulting may have an effect on ground-water flow paths at the Cibolo Canyon development area. An important fault at the site is Bat Cave fault trending southwest to northeast within the study area. The amount of displacement along this particular fault tends to vary, and thus the effectiveness of the fault as a barrier to flow

probably changes along the fault plane. Because fault zones can serve as fracture conduits for ground-water flow, characterizing and mapping hydrostratigraphic features in the study area is vital for understanding lateral and vertical ground-water flow for future water-quality studies.

HYDROGEOLOGIC MAPPING AND GEOPHYSICAL METHODS

First, a reconnaissance-level surface geologic mapping was done to refine the existing regional geologic map of the area (Stein and Ozuna, 1995) and to prioritize areas for geophysical surveys. Hydrostratigraphic units were identified from outcrops and borehole geophysical logs to revise the original geologic map by Stein and Ozuna (1995). Distinctive marker beds were identified in the field and used to correlate hydrogeologic subdivisions and their respective thicknesses.

In order to estimate the electrical signature (resistivity range) for particular geophysical hydrostratigraphic units, ground geophysical data were acquired in areas where new reconnaissance geologic mapping identified exposed units. Forty-four TDEM soundings, 16.8 km of continuous CC resistivity profiles, approximately 30 km of continuous FDEM survey lines, and two 480-m long 2D-DC resistivity imaging profiles were collected along intersecting lines (fig. 1). Near-surface profiles were collected using both continuous CC resistivity and FDEM methods. 2D-DC resistivity and TDEM were used to delineate electrical changes in the deeper subsurface; specifically to identify any offsetting caused by faulting, as well as to define the hydrostratigraphy. Using these methods, a range of resistivities were acquired that corresponded to a particular hydrostratigraphic unit or geologic member in the Cibolo Canyon development area (table 1).

Capacitively-Coupled Resistivity

The Geometrics¹ OhmMapper (Geometrics Inc., 2007) TR-5 was used to measure the resistivity of the near surface along profiles in the study site. The OhmMapper TR-5 is a capacitively-coupled, towed-array resistivity

¹ Any use of brand or trade names does not imply endorsement by the USGS

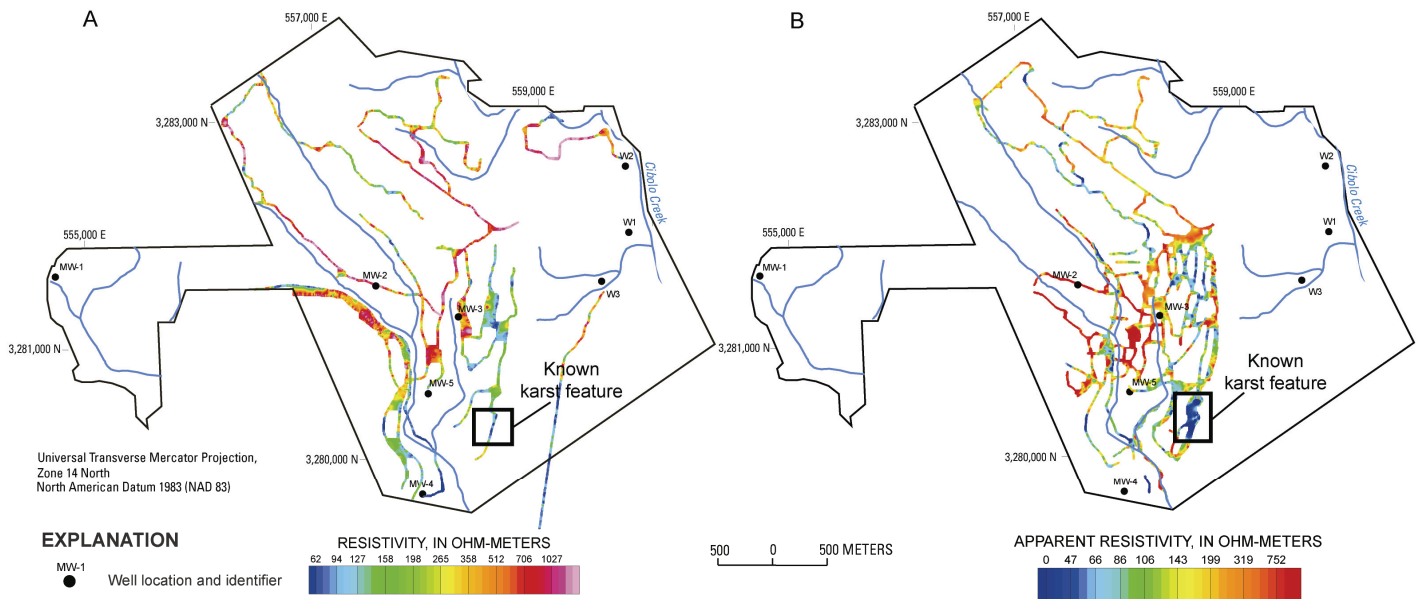


Figure 2. Map of near-surface profiles geophysical of (A) gridded resistivity along capacitively-coupled survey lines and (B) gridded apparent resistivity along frequency-domain electromagnetic survey lines, Cibolo Canyon development area, Bexar County, Texas.

system consisting of one transmitter and a combination of one to five receivers (Geometrics Inc., 2007). A dipole-dipole array with a dipole length of 10 m and a dipole separation of 5 m produced the best results for this investigation and was used to collect all of the CC resistivity data for each profile (fig. 2).

The data are directly compared to the results of the FDEM survey (described below). The inversion results show that the area has a highly resistive surface of up to 1,500 ohm-m across most of the site (fig. 2). Figure 3 shows an example of a two-dimensional CC-resistivity profile that was collected on a north-south transect through the site across Bat Cave fault. The geology shown at the top of the profile is the original from Stein and Ozuna (1995). Geology shown at the bottom of the profiles (figs. 2 and 3) is the revised geology based on the geophysics and new geologic mapping. The CC profiles (figs. 2 and 3) and resistivity depth sections demonstrate that the geophysical survey data suggests a more complex hydrostratigraphy than originally mapped. The data also provides a more accurate location for the Bat Cave fault.

Frequency-Domain Electromagnetic Survey

FDEM data were collected in the same areas as the OhmMapper and was also used to fill in data gaps in areas where the OhmMapper could

not be used due to limited access (figs. 1 and 2) due to dense vegetation. FDEM data were compared to CC resistivity data. The FDEM surveys were performed with the GEM-2, a broadband, multi-frequency, fixed-coil EM induction instrument (Geophex, Ltd., 2007). The GEM-2 was operated in vertical-dipole mode (horizontal, coplanar coils) having a fixed 1.67 m spacing between coils. Five frequencies were measured: 6,270, 12,030, 24,450, 31,470, and 43,530 Hz (hertz).

Once the data were corrected for instrument drift using the calibration station data (Abraham and others, 2006), CC resistivity data were used to calculate a parts-per-million response and was then used to calibrate the GEM-2 data. FDEM was effective in detecting lateral electrical changes and anomalies that could be interpreted as karst features throughout the area. The FDEM data correlate well with the CC resistivity data and serve as a quality assurance/quality control method for both continuous profiling methods (fig. 2).

Direct-Current Resistivity

The IRIS Instruments Syscal Pro system was used to collect two 2D-DC resistivity profiles of apparent resistivity data using the dipole-dipole and Wenner-Schlumberger arrays (Iris Instruments, 2006). IRIS software was used for the

data interpretation. The raw field data (current and voltage measurements) were also used to review uncertainty by evaluating the minimum and maximum current (transmitter) and voltage (receiver) values as well as the standard deviation of the computed apparent resistivity data using Prosys II version 2.15 (Iris Instruments, 2006).

The 2D–DC resistivity data model resolves lateral and vertical changes in electrical resistivity across Bat Cave fault. The data map resistive limestone units in the geologic section. An integrated interpretation of the 2D–DC resistivity data is given in a following section.

Time-Domain Electromagnetic Soundings

Forty-four TDEM soundings were collected to provide a uniform distribution of data to define the vertical electrical stratigraphy near Bat Cave fault (fig. 1D). The Alpha Geophysics terraTEM system, and the Geonics Protem 47 and 57, were evaluated for data quality at the site.

Approximately eight soundings were collected using the Protem system, whereas, the terraTEM was used to collect approximately 36 40-m² TDEM soundings. After each sounding was inverted, a layered-earth model was generated and compared with other soundings along the same profile. Inversion results depicted a distinct electrical contrast between the Edwards aquifer and the more conductive hydrostratigraphic units of the underlying Trinity aquifer.

Generally, all of the TDEM soundings show a highly resistive first layer about 25-75 m thick with an underlies conductive layer (fig. 4). The resistive first layer consistently correlates with the lower Edwards aquifer (dolomitic member) that overlay the more conductive units of the upper Trinity aquifer. The elevation of this contact compares well with interpretation of elevations of hydrostratigraphic units picked from nearby borehole geophysical logs. Equivalence models show that the depth at which the contact is interpreted in the TDEM soundings could vary by approximately 10-15 m.

INTEGRATION OF GEOPHYSICAL AND HYDROGEOLOGIC DATA

The data from surveys using four geophysical methods, new surface geological mapping, and

borehole geologic data were used to define the electrical properties of hydrostratigraphic units and map them in the surface and subsurface. As part of the study, possible new karst features and structures were mapped in the Cibolo Canyon development area. The integrated interpretations are divided into the two main objectives of the study: hydrostratigraphic electrical properties, and near-surface and subsurface mapping of hydrogeology.

Hydrostratigraphic Electrical Properties

The geologic features that are important in controlling the distribution and flow of ground water constitute the hydrogeology. In this study area, the important elements of the hydrogeology are the lithology, structure, and karst features. Each element has particular, but not unique, electrical signatures in the ground surveys that have been used to revise the hydrogeologic map of Stein and Ozuna (1995).

In general the different hydrogeologic units of the aquifers have a predictable difference in electrical resistivity based on their mineralogy, rock type, and water content (Smith and others, 2003 and 2007). The upper zone of the Edwards Group (Person Formation in the study area) has greater amounts of mudstones and wackestone than the lower zone (Kainer Formation) and thus has a lower resistivity. The highest resistivities are associated with the massive limestone units in the Leached and Collapsed Member of the upper zone and the Dolomitic and Kirschberg evaporite member of the lower zone. The high resistive units are shown in the 2D-DC resistivity profiles in figure 4 where the upper and lower zones of the Edwards Group are in fault contact and well mapped in the two profiles. It should be noted in figure 4 that the very near surface to a depth of one to two meters has highly variable resistivity which can be due to weathering and construction activities (mostly bulldozing) which created the open areas in the study area. There is not a significant weathered zone, regolith, or epikarst layer in the study area. Table 2 gives a qualitative assessment of the resistivities of the units of the Edwards aquifer in the study area.

The upper Trinity Group (not shown in table 2) has moderate to low resistivities. The relatively lower resistivity in comparison to the lower zone

Table 2. Generalized ranges in resistivity for units of the Edwards aquifer, in ohm-meters, Cibolo Canyon development area, Bexar County, Texas

| Edwards aquifer unit | Hydrologic characterization | Generalized resistivity range |
|-----------------------|---|-------------------------------|
| Cyclic and marine | high permeability, local low permeability mudstone | Moderate 100-300 |
| Leached and collapsed | high permeability | High 300-500 |
| Regional dense | low permeability, barrier to vertical flow | Low Below 100 |
| Grainstone | generally low permeability, local high permeability in conduits and fractures | Moderate 100-300 |
| Kirschberg evaporite | moderate permeability | High 300-500 |
| Dolomitic | high permeability associated with fractures and caves | Very high Above 500 |
| Basal nodular | generally low permeability, local high permeability in conduits and fractures | Low Below 100 |

of the Edwards Group (Kkd and Kkke) is shown best by the deeper TDEM soundings in figure 4 (also shown in the borehole logs).

Karst features can have an electrical signature ranging from resistive to conductive. Sinkholes and dolines may be associated with near surface clay-filled fissures possibly associated with deeper voids. Thus, in resistive terrains, these features may be anomalous low resistivity areas. In contrast, large near surface air-filled voids (caves and caverns) may be very high resistivity areas. Some of the anomalously low resistive areas in the

CC profile shown in figure 3 within the resistive Dolomitic member could be karst features.

Structures can be either barriers to or channels for ground-water flow. One mechanism by which they can become barriers is through development of a clay “seal” along the fault plane. Maclay and Small (1976) developed a model by which normal faulting could juxtapose impermeable (mudstone) and permeable (limestone) units thus forming a barrier to ground-water flow in the limestone. They demonstrated that this type of model could produce the unusual ground-water flow paths of the Edwards aquifer that are nearly perpendicular to the topographic gradient. Thus, knowing fault offset and local hydrostratigraphy is critical to understanding possible ground-water flow. Figure 5 shows that the Bat Cave fault is associated with a local, nearly vertical low resistivity zone (blue) that can be interpreted as a clay filling along the fault which could influence local ground-water flow. The resistivity depth section in figure 5 also suggests that the permeable leached and collapsed members of the upper Edwards aquifer are at the same elevation as the Dolomitic member of the lower Edwards aquifer. Thus there could be a flow path across the fault if there is not a “seal.”

Figure 4 makes use of the deeper penetrating TDEM sounding data interpretation and the data from boreholes to show structures and elevation changes of hydrostratigraphic units. As noted above, the shallow mapping profile data as well as the borehole data show that the upper and lower zones of the Edwards Group are in fault contact but still constitute a possible shallow flow path. Small faults on the south end of the profile (distance 1,950 m in fig. 4) have been mapped by geologic reconnaissance and geophysical profiling discussed above, which may also influence ground-water flow. There is a fracture zone interpreted north of Bat Cave fault in the hydrogeologic section (fig. 4) between distance 325 and 650 m. This fracture zone is in the same general location as a fault shown in the Stein and Ozuna (1995) hydrogeologic map (fig. 1). The TDEM soundings at sites 1 and 7 show an interpreted resistivity which is much lower than predicted from the general electrical signature of the Dolomitic unit (table 2). In addition, TDEM sounding at sites 13 and 14 have suggest resistivities for the Dolomitic unit more in agreement with the range in table 2. One reason

for the low resistivity at site 1 and 7 may be the intense fracturing observed at outcrops in the area. These may be clay and water filled fractured areas of lower resistivity that could provide conduits for ground-water flow.

Hydrogeologic Mapping

The integration of surface geophysics with hydrogeologic mapping was conducted to focus on critical areas defined by each member of the Edwards aquifer. In general, the geophysical data show a sharp electrical contrast across Bat Cave fault (figs. 2-5). Preliminary CC resistivity data more accurately located Bat Cave fault than the previous geologic mapping (figs. 2 and 3). In the profile shown in figure 3, approximately 100 m from the southern end of the line, there is a sharp change from low resistivity (20-80 ohm-m) to a moderate resistivity (200-600 ohm-m). This sharp break in resistivity did not correspond to any previously mapped contacts or faults. During reconnaissance field mapping, a new cross fault was found that exposed the Regional dense member (Kprd) not mapped previously. Another abrupt resistivity change is observed in the profile (fig. 3) approximately 50 m north of the original mapped location of Bat Cave fault. A moderately resistive (200-600 ohm-m) zone characteristic of the Leached and collapsed member is juxtaposed upon a highly resistive (900-1,000 ohm-m) zone, and is interpreted to be the Dolomitic member (Kkd) of the Edwards aquifer. Multiple continuous CC resistivity profile lines were collected (fig. 1) that crossed the suspected fault location and the same distinct resistivity change to very high resistivity was found. This resistivity expression of Bat Cave fault decreases in the eastern-most CC resistivity transects, which appear to remain moderately conductive north of the fault (figs. 2 and 3). Geologic mapping from new exposures in this area suggests previously unknown cross faulting (figs. 5 and 6). Surface geologic mapping revealed a previously unmapped exposure of the Cyclic and marine member south of Bat Cave fault as well as another unmapped Grainstone member exposure immediately to the north of Bat Cave fault. The Grainstone member appears to have approximately the same electrical signature as the other moderately conductive layers south of the fault.

Figure 2 (boxed area) shows a relatively large

conductive area (blues) on the west side of the site. These areas are interpreted as possible karst or intensely fractured areas (figs. 2 and 6) that have been filled with clays and conductive soils. The highly conductive areas observed in the Leached and collapsed member southeast of Bat Cave fault correspond to a sinkhole discovered at the site. These same two features are also evident in the FDEM data (fig. 2). Geophysical data collected around the area provided an accurate electrical signature of the karst feature. The sinkhole, at the time of data collection, was retaining water. This observation suggests that some karst areas in the study area may be filled with clay or other soils that may help in retaining water. The FDEM gridded apparent resistivity in the same area (fig. 2) shows a similar conductive area. Other potential karst areas are noticeable throughout the site both from the geophysical profile data (anomalous resistivity values) and the reconnaissance mapping (fig. 6).

CONCLUSIONS AND APPLICABILITY OF THE INTEGRATED STUDY

Each of the geophysical techniques used contributed to enhancing the understanding of the electrical properties of the members of the Edwards aquifer in the Cibolo Canyon development area and to refining the location of fault zones, such as the Bat Cave fault located on the southern half of the site. The CC resistivity and FDEM methods complemented each other in providing information on the lateral variations of the near surface resistivity relating to the contacts of the various members of the Edwards and Trinity aquifers. Two adjacent 2D-DC resistivity profiles show a vertical conductive feature associated with Bat Cave fault (fig. 5). The highly conductive features along the southwest portions of the 2D-DC resistivity profiles could possibly be clay filled fractures saturated from heavy rains that occurred during much of the data collection effort. TDEM results helped locate the elevation of the base of the Edwards aquifer at depths beyond the shallow penetrating methods used in profiling. TDEM interpretations suggest the amount of displacement associated with Bat Cave fault (fig. 4). Incorporating previous knowledge of faulting in the area with TDEM soundings and hydrostratigraphic characterization of the subsurface structure can help conceptualize the

hydrologic system at the Cibolo Canyon development area.

A revised geologic map of the Cibolo Canyon development area (fig. 6) was constructed by utilizing preliminary surface geologic mapping and surface geophysical data collected during the investigation. Previously unknown hydrostratigraphic features such as sinkholes and zones of intense fracturing were mapped using integrated interpretation of all data. Locations of the geologic contacts of the members of the Edwards aquifer (as well as Bat Cave fault) were improved and could alter previous concepts of ground-water flow on the northeast side of the fault.

The results of this geophysical investigation could help water managers to better understand the hydrogeology, ground water flow paths and areas of recharge at the Cibolo Canyon development area. This study could also assist planners in characterizing the subsurface by improving knowledge of what can be expected from integrated geophysical and geological investigations in karstic areas and by suggesting where potential areas of interest may be when evaluating possible locations for monitoring wells.

REFERENCES

- Abraham, J.D., Deszcz-Pan, M., Fitterman, D.V., and Burton, B.L., 2006, Use of a handheld broadband EM induction system for deriving resistivity depth images: Proceedings 19th Annual Symposium on the Applications for Environmental and Engineering Hazard, Environmental Engineering and Geophysical Society, 10p.
- Advanced Geosciences Inc., 2007, EarthImager resistivity inversion software: accessed October 30, 2007 at <http://www.agiusa.com/earthimager3d.shtml>.
- Buszka, P.M., 1987, Relation of water chemistry of the Edwards aquifer to hydrogeology and land use, San Antonio region, Texas: U.S. Geological Survey Water-Resources Investigations Report 87-4116, 100
- Clark, A.K., and Journey, C.A., 2006, Flow paths in the Edwards aquifer, northern Medina and northeastern Uvalde Counties, Texas, based on hydrologic identification and geochemical characterization and simulation, U.S. Geological Survey Scientific Investigations Report 2006-5200.
- Geometrics, 2007, OhmMapper capacitively coupled resistivity system: accessed October 30, 2007, at <http://www.geometrics.com/OhmMapper/ohmmap.html>
- Geophex, Ltd., 2007, GEM-2 broadband EMI sensor: accessed October 30, 2007, at <http://www.geophex.com/GEM-2/GEM-2%20home.htm>.
- Geosoft Inc., 2007, Mapping and processing system help topics: Oasis Montaj MAPS version 6.4.
- Iris Instruments, 2006, Principles of geophysical methods for groundwater investigations: accessed August 30, 2006, at <http://www.iris-instruments.com>
- Maclay, R.W., and Small, T.A., 1976, Progress report on geology of the Edwards aquifer, San Antonio area, Texas, and preliminary interpretation of borehole geophysical and laboratory data on carbonate rocks: U.S. Geological Survey Open-File Report 76-627, p 65.
- Rose, P.R., 1972, Edwards group, surface and subsurface, central Texas: Austin, University of Texas, Bureau of Economic Geology Report of Investigations 74, 198 p.
- Smith, B.D., Irvine, R., Blome, C.D., Clark, A.K., and Smith, D.V., 2003, Preliminary results, helicopter electromagnetic and magnetic survey of the Seco Creek area, Medina and Uvalde Counties, Texas: Proceedings for the Symposium on the Application of Geophysics to Environmental and Engineering Problems, San Antonio, Texas, 13p.
- Smith, B. D., Blome, C.D., Clark, A. C., Kress, W., Smith, D.V., 2007, Using geophysics to define hydrostratigraphic units in the Edwards and Trinity aquifers, Texas: Proceedings American Geophysical Union Spring Meeting 2007, 1p.
- Stein, W.G., and Ozuna, G.B., 1995, Geologic Framework and Hydrogeologic Characteristics of the Edwards Aquifer Recharge Zone, Bexar County, Texas, United States Geological Survey, Water-Resources Investigations Report 95-4030.
- Veni, George, 1988, The caves of Bexar County, 2d ed.: Austin, Tex., University of Texas, Texas Memorial Museum Speleological Society Bulletin, v. 10, p. 199-213.

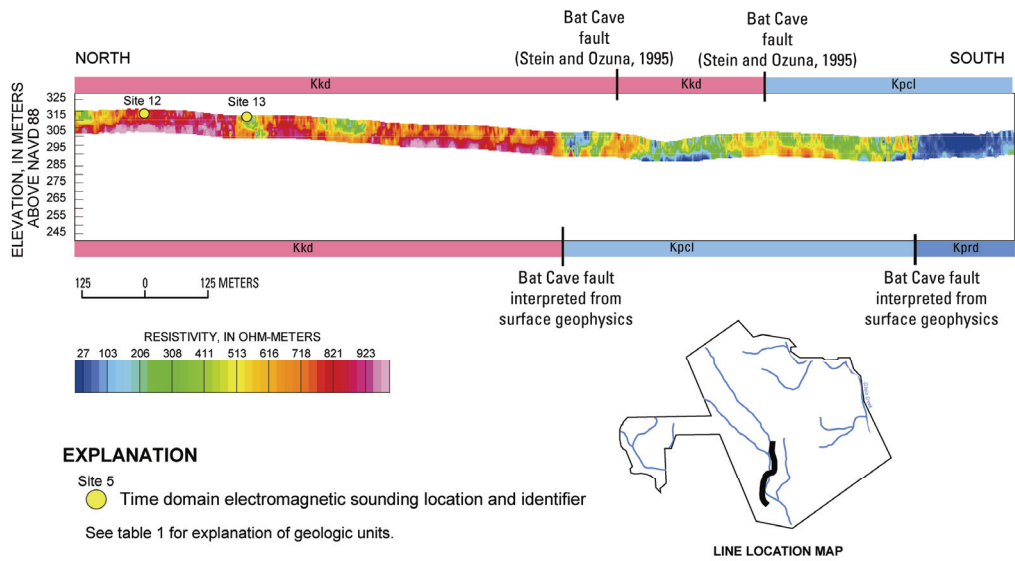


Figure 3. Resistivity depth section for one capacitively-coupled survey line crossing Bat Cave fault, Cibolo Canyon development area, Bexar County, Texas. Geologic units and location of Bat Cave fault adapted from Stein and Ozuna (1995) are shown along the top of the panel. Note that the survey line crossed Bat Cave fault twice as positioned in the older hydrogeologic map. Shown along the bottom of the profile are the location of geologic units and structure as interpreted from the geophysical data and geological reconnaissance from this study.

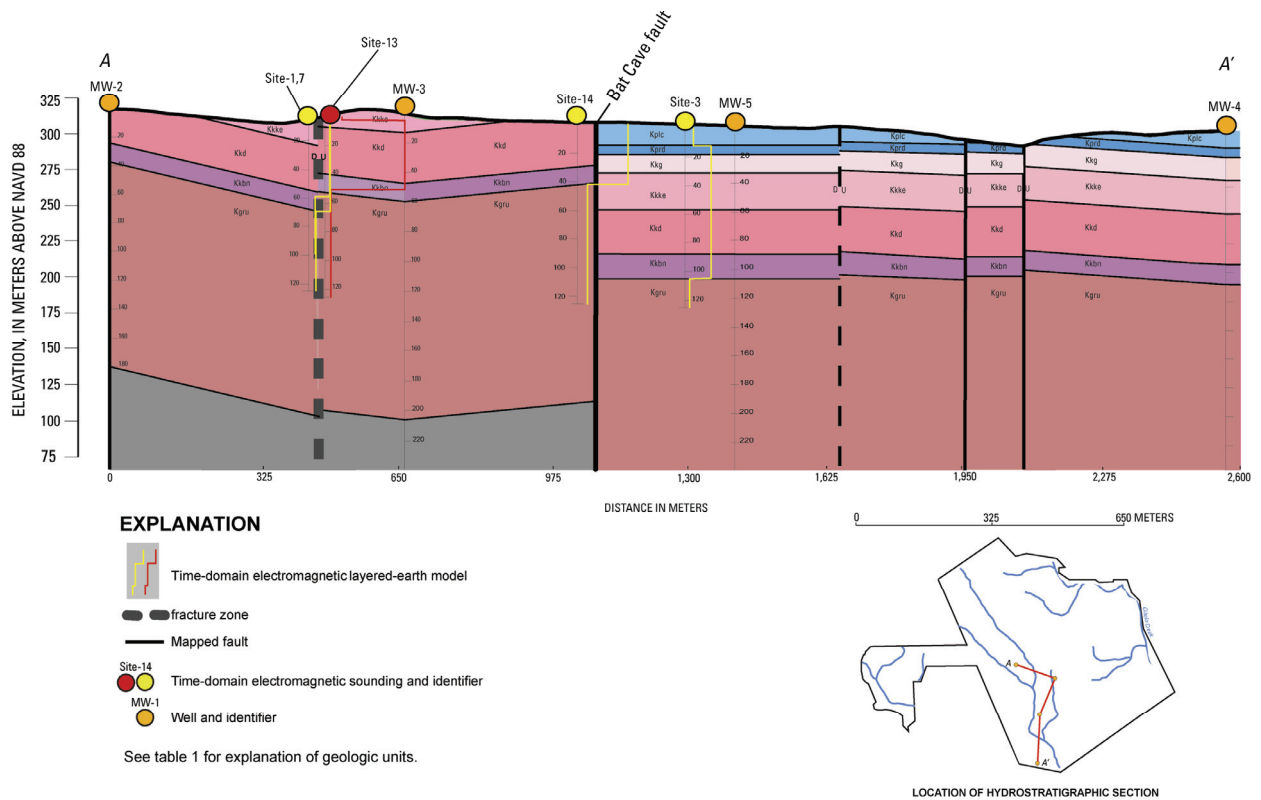


Figure 4. Conceptual hydrostratigraphic section A-A' across Cibolo Canyon development area, Bexar County, Texas. Interpreted resistivity-with-depth profiles for time domain electromagnetic soundings near the section are shown. Note that soundings 1 and 7 are located near each other and yield similar results (lighter lines).

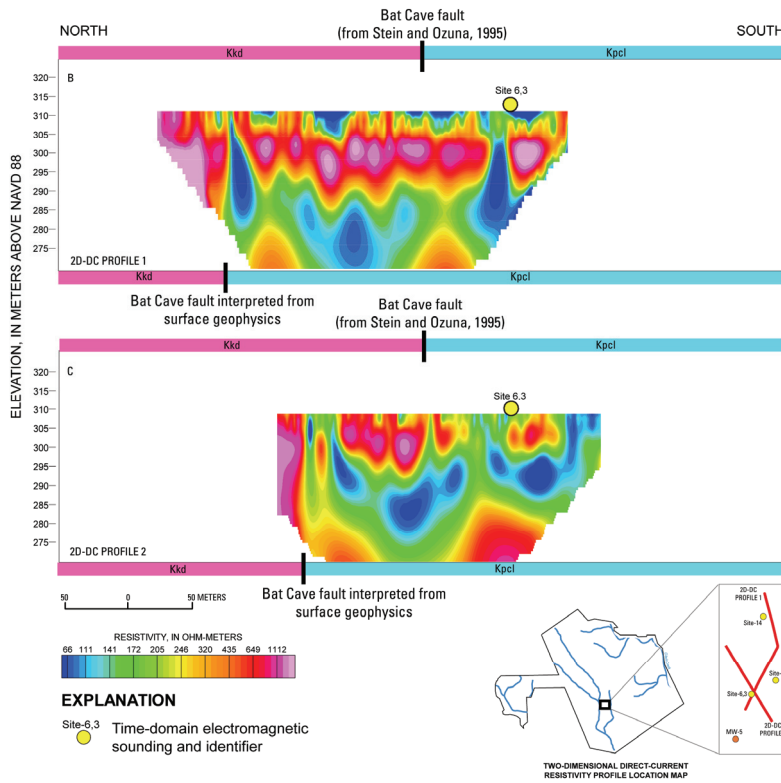


Figure 5. Resistivity depth sections for two-dimensional direct-current (2D-DC) resistivity profiles 1 and 2 with time-domain electromagnetic sounding location, Cibolo Canyon development area, Bexar County, Texas.

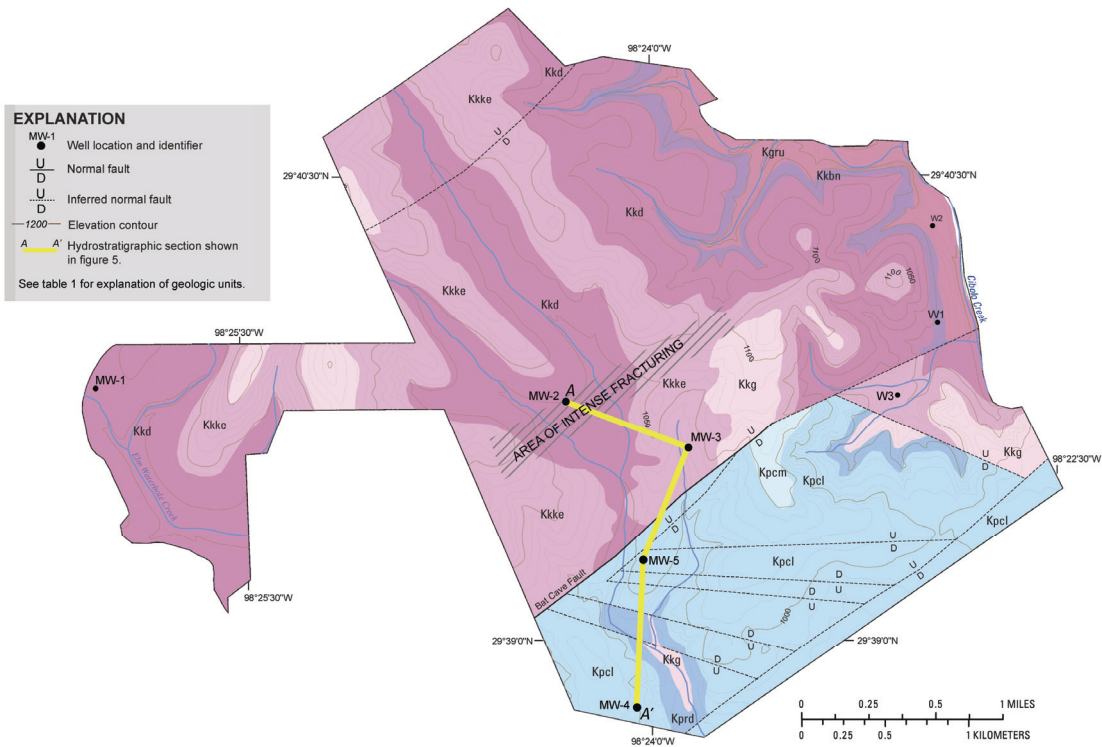


Figure 6. Revised surface geologic map incorporating geologic reconnaissance, well data, and geophysical data of the Cibolo Canyon development area, Bexar County, Texas.

FIELD TRIP GUIDES

Mammoth Cave National Park Tour, Tuesday Evening May 27, 2008

Field Trip Led By Rickard S. Toomey, III¹ and Rick Olson²

¹Mammoth Cave International Center for Science and Learning, 1906 College Heights Blvd #31066, Bowling Green, KY 42101-1066

²Mammoth Cave National Park, P.O. Box 7, Mammoth Cave, KY 42259

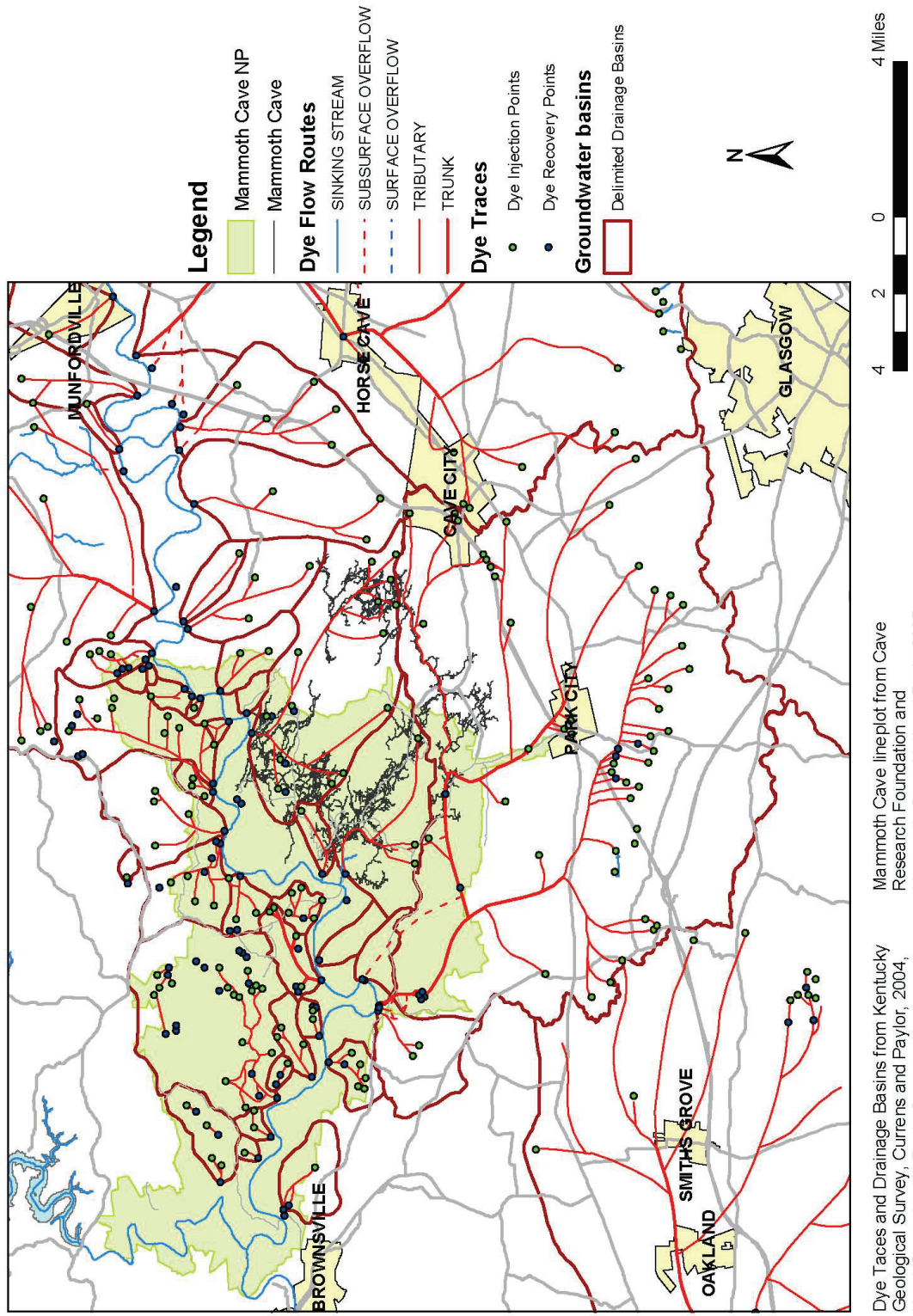
Abstract

The materials provided for this field guide come from brochures and briefing papers that are used as handouts at Mammoth Cave National Park. Sections are authored by different individuals or organizations. Numerous tracer tests have been conducted in and around the park to help determine the underground drainage basins and a map is provided by the Cave Research Foundation. Arthur N. Palmer developed a brochure on the Geology of the Mammoth Cave Area and Guide to the Historic Route of Mammoth Cave. Rick Olson, the Park Ecologist, developed a briefing paper on Biospeleology of Mammoth Cave. All material reprinted in this proceedings obtained by permission from the authors and from the U. S. Department of the Interior, National Park Service, Mammoth Cave National Park.



Beneath the surface of south-central Kentucky lays a world characterized by miles of dark, seemingly endless passageways. The geological processes which formed this world referred to as Mammoth Cave began hundreds of millions of years ago and continue today. (Photo and caption from U.S. Department of the Interior, National Park Service Mammoth Cave National Park, Karst Geology Brochure).

Karst Underground Drainage In and Around Mammoth Cave National Park



Dye Traces and Drainage Basins from Kentucky Geological Survey, Currins and Paylor, 2004, Karst Groundwater Basin Coverages

Mammoth Cave lineplot from Cave Research Foundation and Mammoth Cave National Park, 2005

GEOLOGY OF THE MAMMOTH CAVE AREA

By Arthur N. Palmer

Reprinted with permission of the author and Mammoth Cave National Park

Mammoth Cave is the longest known cave in the world, with about 350 miles of interconnected passages known today. Exploration and mapping continue, and there is no end in sight. The cave consists of several large sections explored separately through various entrances and connected by later discoveries (Figure 1). It is located mainly within Mammoth Cave National Park, established in 1941 and administered by the National Park Service. The Park was designated a World Heritage Site in 1981 on the basis of its geological, archaeological, and biological significance, and it was designated an International Biosphere Reserve in 1990. About 9 miles of trails in the cave are open to the public on a variety of guided tours.

A landscape that is dominated by solutional features such as sinkholes, sinking streams, caves, and large springs is known as *karst*. This

name comes from a plateau in western Slovenia (south of Austria) where some of the earliest studies of these features were made. Figure 2 shows the extent of karst regions and volcanic caves in the USA.

The cave is located in a low plateau of limestone, a rock that dissolves readily in most natural water. The great majority of caves are formed by the dissolving action of underground water as it seeps through the cracks in limestone. This particular limestone was originally deposited on the floor of a shallow sea that covered this part of the continent about 330-340 million years ago. At Mammoth Cave the limestone is capped by insoluble rocks, mainly sandstone, which form a resistant cap over the cavernous rocks below. This cap-rock helps to protect the upper-level passages in the cave from being eroded away. The rock layers are tilted an average of about 0.3 degrees toward the northwest (Figure 3).

The sandstone-capped region is called the Chester Upland (Figure 4). It rises to about 800 ft above sea level. Stream erosion has carved valleys into the caprock in many places, leaving irregular flat-topped ridges between them. To the

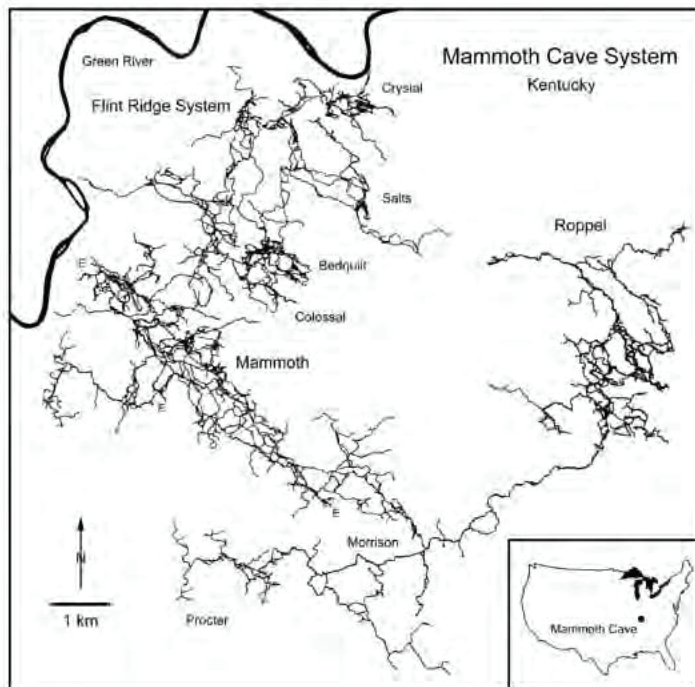


Figure 1: Map of Mammoth Cave, showing the various sections of the cave that were explored independently and connected by later discoveries. From map by Cave Research Foundation and Central Kentucky Karst Coalition.

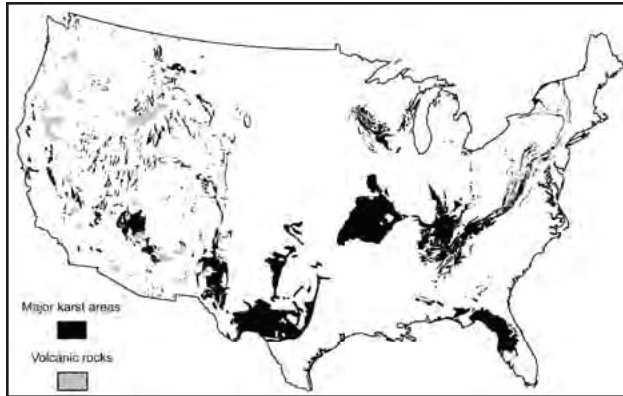


Figure 2: Map of “Lower 48” States showing areas of karst (including solution caves) and also caves in volcanic rock.

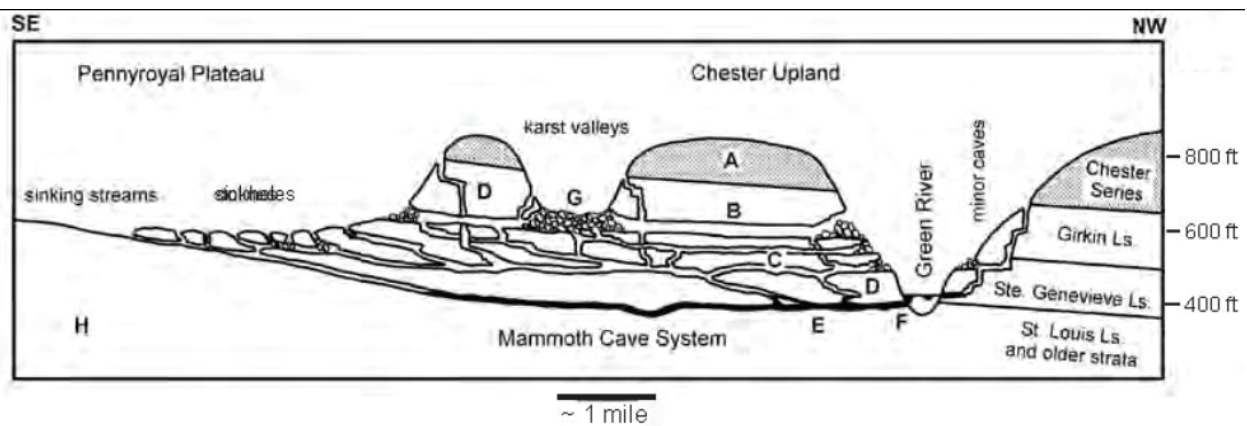


Figure 3: Simplified profile through Mammoth Cave, showing passage relationships, elevations, landscape types, and relation to rock layers. A=sandstone caprock; B=upper levels, partly sediment-filled; C, D = lower levels; E= presently active stream passages; F=springs; G=stream valley cut into Chester Upland, now drained through sinkholes in its bottom; H = poorly soluble limestones that support surface streams.



Figure 4: Scene in the Chester Upland, where a dry karst valley has dissected the sandstone-capped ridges.

south and east, where the caprock has been completely eroded away, the limestone is exposed in a broad and nearly flat plateau, called the Pennyroyal Plateau (Figure 5), which lies about 150-200 ft below the ridge crests of the

Chester Upland. It too is underlain by many caves, and its surface is dimpled with thousands of sinkholes. Sinkholes are depressions formed by solution of the limestone by descending water and collapse of the limestone into underlying caves. All explored passages of the Mammoth Cave System lie in the Chester Upland, but dye-tracing of underground water shows that many of the cave streams in the cave are fed by sinking streams and sinkholes in the Pennyroyal Plateau.

Water in Mammoth Cave drains through springs into the Green River, which is one of the few permanent surface rivers in the region. During its travels through the limestone, the water is able to form long passageways that join and branch in a very complex array. In most rocks, groundwater flows in a diffuse manner through tiny pores and cracks. Even in



Figure 5: Scene in the Pennyroyal Plateau. Note the many sinkholes, some of which contain ponded water.

limestone, this is the case at first. But with time, the groundwater paths with the greatest amount of flow enlarge the cracks into large tunnels, such as those in Mammoth Cave. The flow of a cave stream can be as fast as any surface stream. The water surrounding the caves is still slow-moving and diffuse. Most of the limestone actually contains this kind of water, and this is the water that feeds most water wells. If a well encounters an active cave stream, there is usually plenty of water, but the water quality may be limited. The rapid flow of water, and the lack of filtering, allow contaminants to travel easily through cave passages. For that reason, most springs in cave regions are not reliable water sources.

Passages in the cave have formed not only by water from sinkholes in the Pennyroyal Plateau, but also from stream valleys in the Chester Upland (Figure 3). Much of the water in these valleys enters along the eroded edge of the sandstone cap to form small tributary passages. Most passages in Mammoth Cave have been abandoned by their streams. As the Green River valley deepens by erosion, older passages lose their water to lower routes, which form new passages, while the older ones are left high and dry.

The cave extends through several major lime-in Mammoth Cave have been abandoned by their stone units: the Girkin Formation, Ste. Genevieve streams. As the Green River valley deepens by Limestone, and St. Louis Limestone (Figures 3, erosion, older passages lose their water to lower 6, 7). Limestone consists of calcium carbonate, which includes small fragments of fossils that have been broken apart

by wave action and cemented together by additional calcium carbonate. Each limestone has slightly different characteristics. The Girkin Formation contains thick lime-stone beds interspersed with thin, soft, shaly beds that recess inward in cave walls. The Ste. Genevieve contains a broad variety of mainly thin-bedded limestones and dolomites (a magnesium rich variant of limestone). The St. Louis contains many beds of chert (flint), which project from the cave walls. All three limestone units can be subdivided into many thinner beds (Figure 7), and by recognizing these in the cave, it is possible to tell one's position relative to the bottom of the caprock.

Mammoth Cave contains several types of passages. Above the water table (the level below which water fills all openings in the rock), the typical passages are narrow and canyon-like (Figure 8). They are higher than they are wide, with curving, sinuous paths. These passages form where the water drains along the bedding (layering) of the rock, generally in the direction of local dip (tilt) of the beds. Their sinuosity is caused by irregularities in the local direction of tilt. Canyons in Mammoth Cave range up to 10-30 feet wide and up to 80-100 feet high, but most are much narrower and not so high. Where water is able to descend more or less vertically along fractures, vertical shafts are formed (Figure 9). Shafts are generally round or oval in horizontal cross section and nearly all have developed in stages by periodic downward dissolution from bed to bed. Most shafts show a sequence of drains at various elevations in their walls. Water descending a shaft today of course exits by the lowest drain, which is located at the shaft floor. The largest shafts in Mammoth Cave range up to 150 feet deep and several tens of feet in diameter. Above the water table, water descends along the steepest available paths through the limestone. Most of the resulting passages are canyons interrupted in places along their length by shafts, to form descending stair-step profiles.

Below the water table, water follows the most efficient paths to the nearest surface outlet (such as the Green River). The caves transmit water so easily that the water table in them is almost equivalent to the Green River level. Most passages that form below the water table have

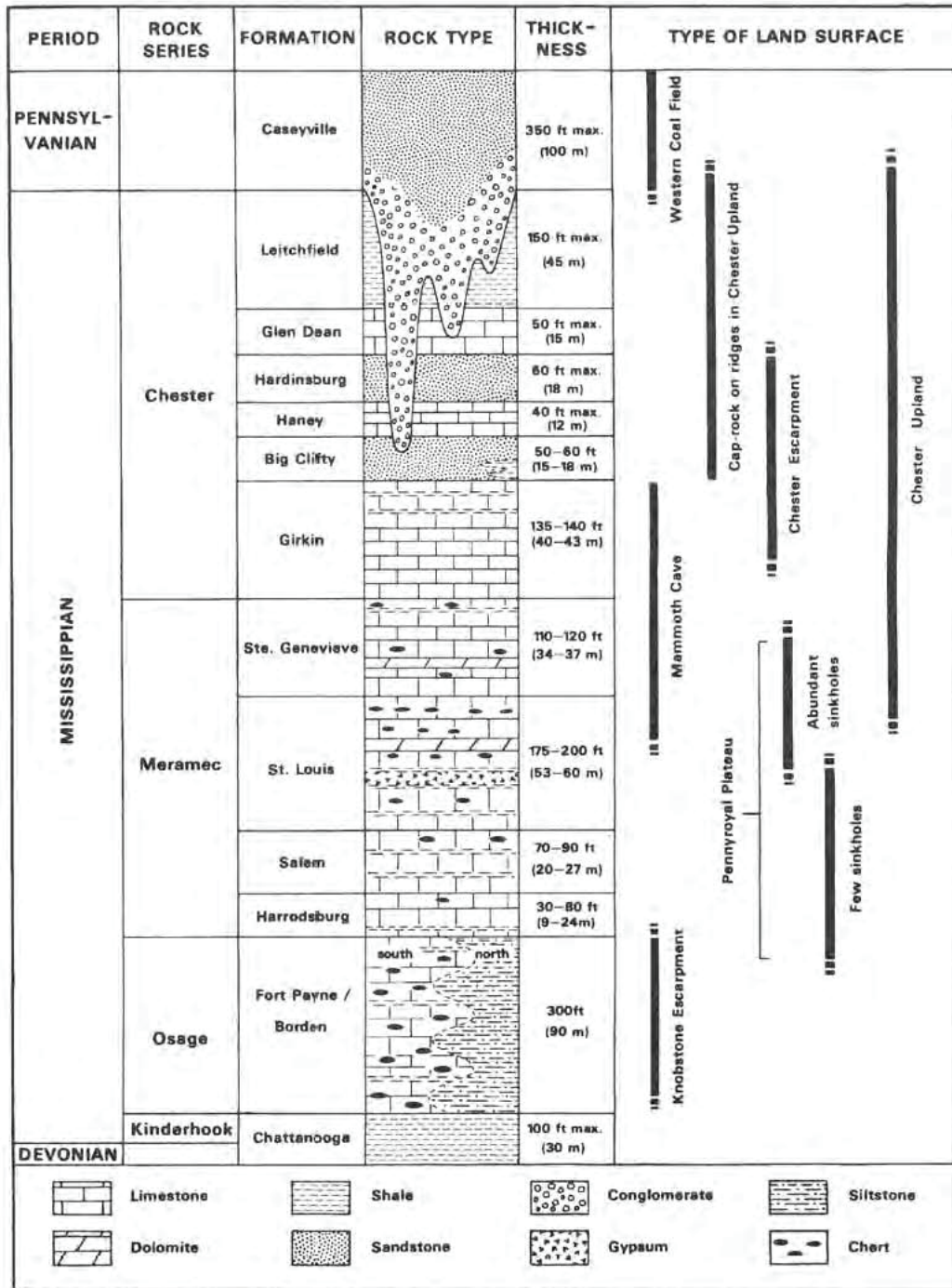


Figure 6: Rock layers in the Mammoth Cave region, and their relation to landscape types.

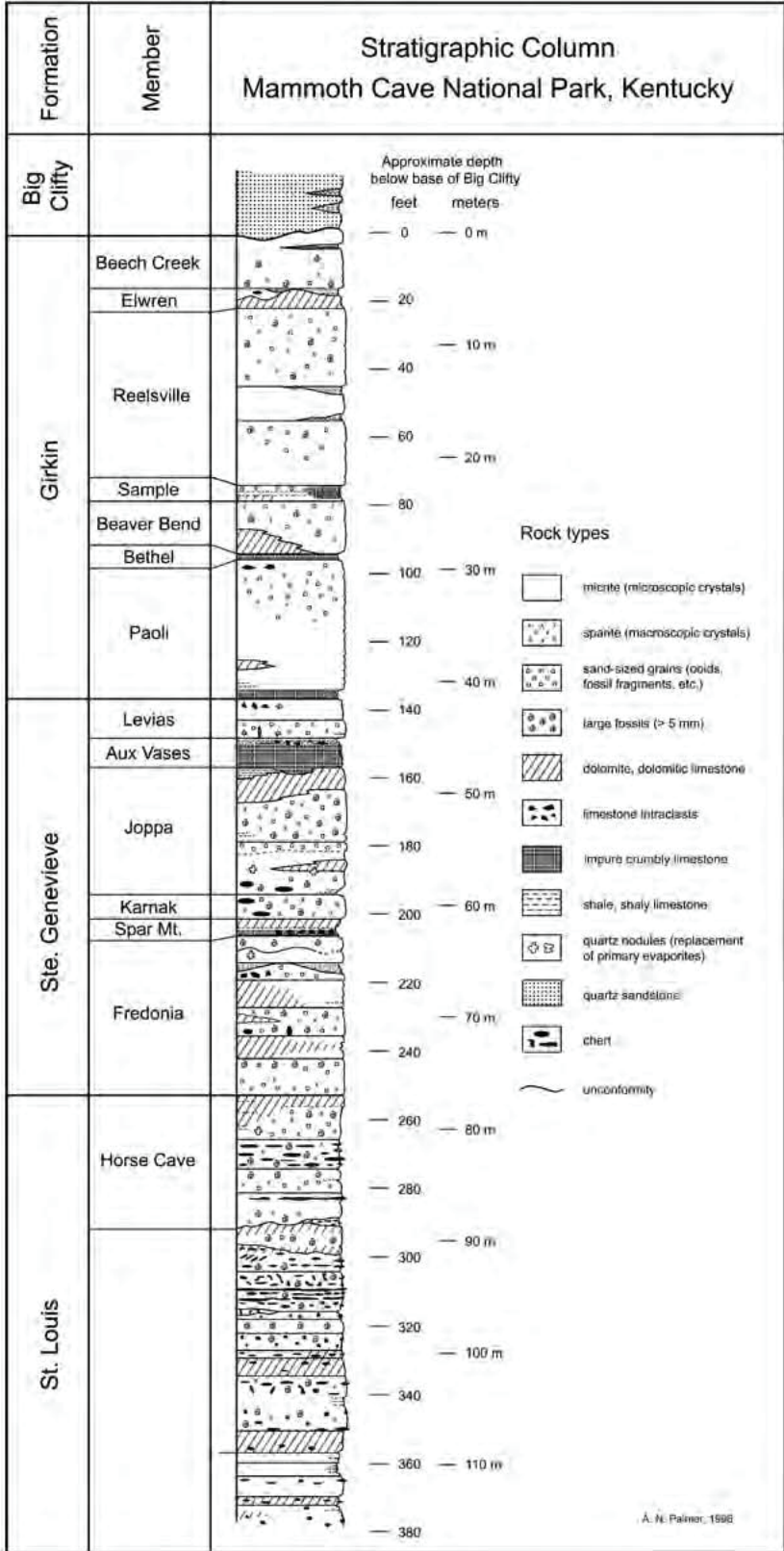


Figure 7: Details of the rock sequence exposed in Mammoth Cave.



Figure 8: A typical canyon passage in Mammoth Cave (Pass of El Ghor, near the Grand Avenue Tour in Mammoth Cave).



Figure 9: A typical shaft formed by descending water (Edna's Dome, on the Wild Cave Tour).

tubular shapes with rounded cross sections and very gentle slopes (Figure 10). Tubes tend to be sinuous, like canyon passages or surface rivers.

Although most of them form at or just below the water table, some extend well below the water table and rise back up farther downstream.

Also formed below the water table are passages that follow prominent fractures. These are straight, narrow, and fissure-like. Many solution-ally enlarged fractures can be seen in passage ceilings here and there in Mammoth Cave, but there are only a few small passages of this type that can actually be followed.



Figure 10: A typical tubular cave passage formed at or below the water table. This is Pensico Avenue, just off the Historic Route, at the 550-foot level.

Passages in Mammoth Cave occupy a vertical range of about 350 feet. Canyons can form anywhere above the water table, and roughly half of them are still active today. But tubular passages cluster at only a few elevations, which correspond to significant pauses in deepening of the Green River valley. These elevations are most easily recognized by places where canyon passages (formed above the water table) change downstream to tubular passages (formed at or below the water table). Today these points cluster at about 500, 550, 600, and 690 feet above sea level (Figure 3). They provide clues to the drainage history of the major rivers of the region, including the Ohio River and its tributaries, the Green River being one of them.

It is difficult to determine when a cave passage formed. First of all, the passage enlarges over many tens of thousands of years (and probably more), so there is no distinct birth date. Second, what is left to measure? One way of

determining when the latest enlargement took place is to analyze the sand and gravel sediment that is left in most passages by the underground streams. By measuring tiny amounts of radioactive materials in the rocks, it is possible to tell how long ago the sediment was carried underground into the cave. While the sediment is at the surface, radioactive aluminum and beryllium are produced in tiny quantities by cosmic radiation. When the sediment is carried underground, these radioactive materials are no longer produced, and they gradually decay. The aluminum and beryllium decay at different rates, and their ratio indicates how long they have been underground. The technique works well, with a small amount of scatter, for ages up to 5 million years.

The two upper levels (above 550 ft) are wide canyons and tubes filled to various depths with stream-borne quartz silt, sand, and gravel (Figure 11). Some are completely filled. In a few passages at these levels, most of sediment has been removed by stream erosion. The greatest sediment thickness is about 70 ft. Passages at these levels have sediment dates of 2.5-4 million years, and of course the passages are older still. These passages represent slow cave development, alternating with sediment accumulation, when rivers were fairly stable, with very slow erosion interrupted periodically by sediment filling (probably when the climate was relatively dry). The rather flat surface of the Pennyroyal Plateau formed at this time. It is located at the same elevations as the upper-level passages in the cave.

About 2.5 million years ago there was widespread accumulation of sediment with thicknesses as much as 100 ft. It filled all upper-level passages, some partially and others completely, and also covered the Pennyroyal surface. This event took place at about the same time as the first major advances of glaciers in North America.

In the lower cave levels the passages are smaller in cross section (as in Figure 10), partly because groundwater recharge had become fragmented into many sub-basins by that time, and also because pauses in base level were shorter. Prior to this time, karst was probably sparse on the Pennyroyal because of limited

entrenchment. The rapid drop in base level during the past 2 million years has caused nearly all surface drainage on the Pennyroyal to be



Figure 11: Collins Avenue, in the Crystal Cave section of Mammoth Cave, is the highest and oldest passage level in the cave. Typical of all high-level passages, it was nearly filled with sediment about 2.5 million years ago. Most of the sediment has been removed at this point by later erosion by a cave stream, exposing the full 70-foot height of the canyon.

diverted underground, and the extensive sinkhole-pocked surface of today began to form (Figure 5). Cave levels at 550 and 500 ft are well-developed tubes with little sediment fill. Sediments at these levels are respectively about 1.5 and 1.2 million years old. Passages at other elevations are mainly shafts, small canyons, and crawlways, mostly formed above the water table. Many are still active today as water drains from the overlying land surface (Figure 12). Some large tubes have formed below the 500 ft level, but their elevations are not consistent. They include local tube segments fed by many small tributaries, as well as passages perched on relatively insoluble beds.

The sudden abandonment of the large upper-level passages and development of many small passages at lower levels apparently resulted

from major changes in the patterns of surface drainage. Until the beginning of glacial



Figure 12: A waterfall in the Flint Ridge section of Mammoth Cave is fed by an overlying canyon. Here it intersects an older tube and continues into another canyon at a lower level.

advances, the Ohio River was rather small, not significantly larger than the Green River. Most of the drainage from the east followed more northerly routes, which first drained northward, toward where the St. Lawrence River is today. Later it diverted into the Mississippi River through northern Indiana and Illinois (the so-called “Teays River”). The first major glacial advances into the region blocked these older routes and diverted their flow into the Ohio. Suddenly the Ohio became the largest river in the eastern US. It began to deepen its valley rapidly, and the Green River, a tributary of the Ohio, did the same. Diversion of water to form the Teays River took place about 1.5 million years ago, accounting for the rapid entrenchment below the upper two cave levels. Diversion of

the Teays to form the present Ohio River took place about a million years ago. These are the most recent sediment dates for the passages at 550 and 500 feet and represent the times just before the passages were abandoned.

Mineral deposits in Mammoth Cave are highly varied. Stalactites, stalagmites, and flowstone (made of the mineral calcite, the same as the limestone bedrock) are somewhat rare because the rather impermeable caprock limits the amount of water seepage into the cave. But

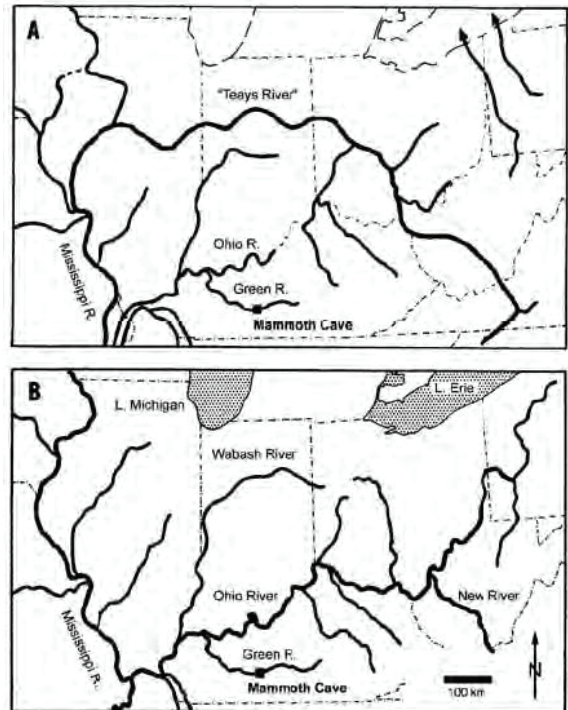


Figure 13: Development of the Ohio River drainage over the past 2 million years. Originally the drainage from the northeastern U.S. went northward (1), then diverted to the Mississippi as the “Teays River” (2). Eventually it was diverted by glacial ice into the Ohio River, which was formerly fairly small. The uppermost passages in Mammoth Cave formed during stage 1, and the lower levels formed during stages 2 and 3.

minerals that form by evaporation, such as gypsum (a calcium sulfate mineral) are abundant in dry passages (Figure 14).

The astonishing length of Mammoth Cave is the result of from several factors: Its drainage basin is large, about 100 square miles. Prominent layering in the rock allows water to

divert along many successively lower routes. The resistant caprock has protected many of the uppermost passages from erosional destruction. Finally, the many small but discrete changes in base level have allowed the development of many rather independent cave levels.

Mammoth Cave is also of great archeological, biological, and historical interest. As early as 4000 years ago native humans ranged through many miles of the cave on a quest for minerals or adventure, using only reed torches for light. Artifacts and several mummified bodies have been discovered in the cave. Cave biota include the rare Kentucky cave shrimp and eyeless fish. Sediment in the main passage of Mammoth Cave was mined for nitrates to make gunpowder during the War of 1812. Since then the cave has been more or less continually open to the public, first by a series of private owners, and later by the National Park Service.



Figure 14: A gypsum “flower” in Mammoth Cave, formed by evaporation of water from the cave ceiling, which allowed hydrated calcium sulfate (gypsum) to precipitate from the moisture.

REFERENCES

- Granger, D.E., Fabel, D. & Palmer, A.N. 2001. Pliocene-Pleistocene incision of the Green River, Kentucky, determined from radioactive decay of ^{26}Al and ^{10}Be in Mammoth Cave sediments. *Geological Society of America Bulletin*, 113(7): 825-836.
- Palmer, A.N. 1981. *A Geological Guide to Mammoth Cave National Park*. Teaneck, N.J.: Zephyrus Press.
- Palmer, A.N. 1989. Geomorphic history of the Mammoth Cave System. In: *Karst Hydrology: Concepts from the Mammoth Cave Area*, edited by W.B. White & E.L. White, New York: Van Nostrand Reinhold.
- Pohl, E.R. 1970. Upper Mississippian deposits of south-central Kentucky. *Kentucky Academy of Science Transactions*, 31: 1-15.
- White, W.B. & White, E.L. (editors) 1989. *Karst Hydrology – Concepts from the Mammoth Cave Area*. New York: Van Nostrand Reinhold.
- White, W.B., Watson, R.A., Pohl, E.R. & Brucker, R.W. 1970. The central Kentucky karst. *Geographical Review*, 60: 88-115.

GUIDE TO THE HISTORIC ROUTE OF MAMMOTH CAVE

By Arthur N. Palmer

Reprinted with permission of the author and Mammoth Cave National Park

Of all the tours in Mammoth Cave, this one gives the best view of the various rock layers and passage levels. It also emphasizes the historical aspects of the cave, particularly its exploration, saltpeter mining, and archeology. Remnants of a saltpeter mining operation of the early 1800s are still preserved in the cave. These include wooden vats for leaching saltpeter from the cave sediment, and an impressive system of hollow wooden pipes for conveying water to and from the leaching vats. There are several exhibits of prehistoric Indian artifacts that have been found in the cave.

A map of the passages on the Historic Tour is shown in Figure 15. The tour begins at the Historic Entrance, the only natural opening to Mammoth Cave. This entrance was formed when a tributary valley of the Green River cut

into one of the main cave passages. The entrance descends steeply through the Beaver Bend Member of the Girkin Formation and leads to the main level of the cave (level B on Figure 3) at an altitude of 600 feet (180 m). A short passage in the Paoli Member (Houchins' Narrows, labeled #1 on the map) leads to an impressive junction called the Rotunda (#2). The 19th century saltpeter leaching vats and water pipes are located in this part of the cave. Three passages branch from the Rotunda (Houchins' Narrows, Broadway, and Audubon Avenue), all at the same level. [Note: In this area, beds in the upper half of the column are locally about half as thick as shown in Figure 7, and most of those below are about twice as thick.] In what direction did the water flow when they were being formed? Most of the clues to flow directions are absent. These large passages are only the upper third of canyons that were once as much as 80 feet (25 m) deep and that were partially filled by sediment and modified by breakdown. From the passage directions, it looks as though both Audubon Avenue and Houchin's

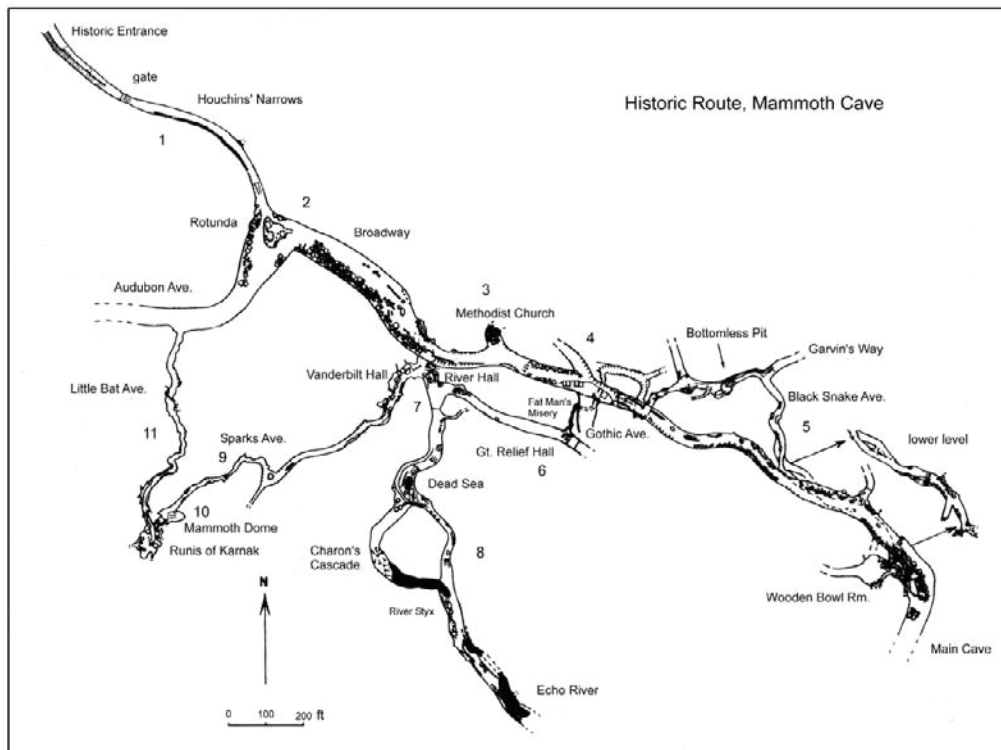


Figure 15: Map of the Historic Route of Mammoth Cave. The numbers refer to various features of interest described in this trail guide.

Narrows were probably fed by Broadway and drained out of the Rotunda to the Green River. Audubon Avenue leads to the right for approximately 1000 feet (300 m) and ends in breakdown at the edge of the Green River valley. It is unlikely that both Houchins' Narrows and Audubon Avenue formed at the same time by branching of the main cave stream. Probably Houchins' Narrows, the smallest of the three passages, formed later than Audubon Avenue as a diversion route for the underground water.

Here is a good chance to look at how the different kinds of limestone affect the cave. The medium-bedded Paoli Member occupies nearly the entire height of the Rotunda. It consists of 21 feet (6.4 m) of finely crystalline dolomitic limestone. Near the ceiling is an irregular, recessed ledge formed by the Bethel Member, a shaly and relatively weak limestone only a few feet thick. The base of the Paoli (unit P1), a granular, silty limestone, is even less resistant and forms a sharply recessed niche of crumbly, dark-gray rock a few feet above the floor of the passages in this area.

The tour proceeds through Broadway in what was originally the upstream direction for the underground water (Figure 16). Here the sediment has been partly removed through lower-level passages by stream action, so the floor descends into the Ste. Genevieve Limestone as far as the Joppa Member, while the ceiling remains at the same level as in the Rotunda. Some sediment has also been moved around by saltpeter miners.



Figure 16: Part of the Main Cave beyond the Historic Route (see Figure 15). This is the upstream end of Broadway (more specifically, the lower half of Broadway).

At point #3, at the “Methodist Church,” about 1000 feet (300 m) beyond the Rotunda, the passage branches into two separate levels, each only half as high as Broadway. The upper level disappears into a pile of breakdown (collapse material), and the lower one continues straight ahead as the “Main Cave.”

What is the relationship between the two levels? Continuing on to point #4, we see the upper level come in again, cross over the Main Cave, and disappear in the former upstream direction as Gothic Avenue, a tube about 15-20 feet (4.66 m) high. The great ceiling height of Broadway represents the combined height of the two branches.

The trail continues through the Main Cave for a short distance to the Giant's Coffin, an enormous breakdown block. It then exits to the right through a narrow canyon (Dante's Gateway), which once drained water from the Main Cave to the lower levels. The canyon descends through the light-gray Joppa and Karnak Members to the Wooden Bowl Room. Named for one of the prehistoric Indian artifacts found here, the Wooden Bowl Room is located at level C, (550 feet = 168 m; see Figure 3) where several passages intersect one another. The thick-bedded Karnak Member forms the flat ceiling of this wide, low room.

A steep descent through the upper Fredonia Member leads to the tour's first tubular passage, a lower loop of level C called Black Snake Avenue (location #5 on the map; see Figure 17). This passage is located in the thick, crystalline F3 unit. In this part of the cave the F3 unit contains a yellow dolomite bed, which forms the smooth passage floor.

At one point there are fissures extending into the ceiling. Many geologists consider such features to have formed when water descending through the fissure mixed with water in Black Snake Avenue. Groundwater is able to dissolve more limestone if it has a high level of carbon dioxide. Most carbon dioxide is contributed by the soil as the water seeps through it. The mixture of two saturated solutions having different carbon dioxide contents can produce an undersaturated solution capable of dissolving more limestone.



Figure 17: Black Snake Avenue, a tube at level C. This is the upstream end of Pensico Avenue, shown in Figure 10. Here it occupies two closely spaced tiers.

Is this a feasible explanation for the ceiling fissures? What are a few flaws in this argument? It is more likely that the fissures were formed by periodic flooding, back when the passage was at or near the water table. Each flood would deliver water rapidly from the surface, water that was highly capable of dissolving limestone. Filling of the passage under hydraulic pressure would force this aggressive water into all cracks in the surrounding cave walls and ceilings, enlarging the cracks into fissures. The water would then drain out as the flood subsided.

Just beyond the fissures, the contacts between several limestone beds have been dissolved inward into the passage walls to form a tiny maze of tubes. Below these tubes the walls are deeply grooved by water that apparently flowed out of the tubes. Do these features clarify the origin of the fissures in the ceiling?

Note the excellent solutional hollows (scallops) in the nearby floors of the passage. The direction of flow is shown by their asymmetry (as in sand dunes). The steep side of each hollow is on the former upstream side. Our tour is moving in the direction of former flow. Also, the average length of the scallops can be used to estimate the former flow velocity. Measure the average length of the well-developed scallops in centimeters and divide that number into 275 to get the former flow velocity in centimeters per second. For example, scallops 5 cm in length would indicate a local flow velocity of about 55 cm/sec. Obviously this

is approximate, because the flow velocities vary with time. These probably represent the high-flow velocities that last enlarged the passage.

Black Snake Avenue passes beneath the Main Cave and extends along the northeastern edge of Mammoth Cave Ridge, where a great deal of water enters from the nearby limestone-floored valley. This water forms many impressive vertical shafts that intersect the otherwise dry passages in this part of the cave. While the tubes at this level were forming, they lay close to the level of the Green river, but they are now located far above the river. Water drains from the surface through narrow canyons into the tops of vertical shafts and flows out through the shaft drains to the lowest and still active passages near the level of the Green River.

A typical shaft is Bottomless Pit, which yawns to a depth of about 100 feet (30 m) below the level of the trail and rises 60 feet (18 m) above. A bridge now spans the chasm, but before this addition, in order to pass this point, early explorers were treated to the unforgettable experience of crawling around the pit on a narrow ledge.

The tube continues as Pensico Avenue, but the tour follows a branch to the left and descends a short flight of stairs through an opening called Scotchman's Trap. This opening leads to several low, wide passages in the dolomitic limestone of unit F2, at level D (500 feet = 152 m). The trail branches into a narrow canyon called Fat Man's Misery. This passage is shaped like a keyhole, wide at the top but quickly narrowing to little more than a foot toward the floor. It is too low to walk through without stooping. Although it is not tight by explorers' standards, this is as close a view of the limestone as most visitors wish.

Just as Fat Man's Misery looks as though it is going to pinch down to an impasse, it opens into a spacious tubular passage called Great Relief Hall (location #6 on map). This originally received its name from the relief that visitors presumably felt when emerging from the narrow canyon. Its name took on a new meaning when restrooms were installed in the Hall.

Great Relief Hall is also at level D (Figure 17). The ceiling is formed by the base of the

thick-bedded, coarse-grained unit F3. Here the rock contains many joints enlarged upward by solution, as well as irregular chert nodules that protrude downward from the ceiling because they are so resistant to solution. The lower walls of this passage have a moth-eaten appearance caused by solution pockets in a dolomite bed in unit F2. This distinctive rock unit is seen at two other places on this tour. Can you spot them?



Figure 17: Great Relief Hall, at an elevation of 500 feet, is a typical tube at level D. In the ceiling, note the solutionally enlarged fissures and the “dikes” of resistant chert (flint) protruding from the limestone. Near the floor is a bed of dolomite that has a distinctive pock-marked texture.

The tubular passage descends about 20-30 feet into River Hall (location #7). This descent was originally part of a loop that the passage took below the water table. It is still level D, and drained to a former spring at the 500-foot elevation; but here its elevation is about 470 feet (143 m). The contact between the Ste. Genevieve Limestone and the underlying St. Louis Limestone is not very distinct in the Mammoth Cave area. It appears as a prominent contact between beds at the level of several old bowl-shaped electric lights. The upper St. Louis does not contain the bedded chert that is so typical lower down in the formation.

The opening at the lower end of River Hall leads to River Styx and Echo River, which are parts of one of the largest stream passages in the

cave. These river passages are located at the same level as the present-day Green River (about 425 ft = 130 m above sea level).

Large scallops in the ceiling of River Hall indicate that the original water flow came from River Styx, joined the water from Great Relief Hall, and continued straight ahead in a passage now blocked with breakdown.

The passages at river level therefore developed at the same time as River Hall, which is the same age as Great Relief Hall. Together, these passages span a vertical range of 75 feet (23 m), and yet they all formed when the Green River was at 500 feet. River Hall, River Styx, and Echo River formed below the water table simply because those particular routes were most efficient at transmitting water.

Our tour descends into River Styx. This is the largest passage we have seen since leaving the Main Cave. No wonder it is large --it is still actively enlarging today, and has continued to do so since level D began to form more than a million years ago.

Those who think this explanation is too idealistic should follow the River Styx passage upstream to Echo River and beyond (Figure 18). The passage begins to climb in the upstream direction, still as a tube, but then as it passes above an elevation of 500 feet it changes to a canyon passage. Part of the canyon is shown in Figure 8. This was the former water table when the river passages first started to form.



Figure 18: The upstream end of Echo River is at exactly the same elevation as the present Green River and is nearly filled with water and sediment.

We return to River Hall and exit through an upper-level passage. On the way out, note the

brass markers that indicate levels of recent floods. This entire part of the cave fills with water every couple of decades.

Soon the walls and ceiling draw near and the tour enters Sparks Avenue, a wide, low tube along the Ste. Genevieve/St. Louis contact (location #9 on map). The walls are obscured nearly everywhere by banks of sand and gravel deposited by the stream that once flowed through this passage. The gravel consists of white quartz pebbles weathered out of the Caseyville Formation that once capped Mammoth Cave Ridge (see Figure 6). These pebbles have been instrumental in helping to date the ages of the various cave levels (see page 6).

Large, fissure-like solution pockets occur here and there in the ceiling along joints in the thick-bedded F1 unit. At Leopard's Arch the passage rises abruptly into the F1 unit along a joint, a rare occurrence in Mammoth Cave. Sand on the floor contains cross beds that indicate water movement in the direction we are traveling. So the water that deposited the sand must have flowed upward at the point where the passage jogs into the F1 unit (Figure 19). Wall scallops also show this direction of flow, although their directions are complicated by the many back-eddies that occurred at the sharp bends in the passage.

Sparks Avenue opens into the impressive Mammoth Dome (location #10). This is one of the largest vertical shafts in the cave. It is about 190 feet (58 m) high and extends from the Beaver bend Member of the Girkin Formation through the entire Ste. Genevieve Limestone, and 29 feet (8.8 m) into the St. Louis. Water descends from the top of the shaft as a spray and filters into rocks that choke the bottom of the shaft. This water probably comes from a sinkhole located almost directly above. Several canyons open from the south wall of Mammoth Dome, and it is possible to see, by peering straight up through a haze of descending water drops, a narrow, wiggly canyon at the very top of the dome. The contact between the Ste. Genevieve and the St. Louis can be clearly seen 7 feet (2.1 m) below the floor of the lowest balcony in Mammoth Dome.

A metal staircase leads almost to the top of the dome, giving a spectacular view of almost the entire Ste. Genevieve Limestone. Here the F3 is essentially a single massive bed of crystalline gray limestone. Looming to the left are the Ruins of Karnak, which are monolithic pillars of the Fredonia Member sculpted by descending water.

The flat ceiling above is the base of the thick-bedded Karnak Member. (Early explorers were fond of drawing from antiquity and mythology for their names of cave features. The Ruins of Karnak are named for the ancient ruins near the village of Karnak on the banks of the Nile River. However, except in name, the Ruins of Karnak have no direct connection with the Karnak Member, which was named for the little town of Karnak in southern Illinois.)

The tour climbs to a final overlook of Mammoth Dome, then doubles back into Little Bat Avenue. This is a tube at level B, which at one time drained water from Audubon Avenue. Little Bat Avenue is located along the contact between the Aux Vases and Joppa Members. The tube suddenly opens into the enormous void of Audubon Avenue, which leads a short distance to the Rotunda. Having completed a long, intricate loop, the tour exits through the Historic Entrance.



Figure 19: Leopard's Arch is a fissure in Sparks Avenue that rises in the downstream direction. Like a hose, water filled it and rose under pressure. The direction of flow is indicated by scallops and by cross-beds in nearby floor sediment (like those in sand dunes).

BIOSPELEOLOGY OF MAMMOTH CAVE: A BRIEFING PAPER

By Rick Olson

Park Ecologist, Mammoth Cave National Park
2003, all photos by author reprinted by
permission.

INTRODUCTION

In order to understand the biospeleology of Mammoth Cave, it must be viewed in context of the South-Central Kentucky Karst where there are two historical and four functioning ecosystems. In pre-settlement times, prairie and savanna maintained by fire were prevalent. These ecosystems were converted to agriculture over the past two centuries, but forest, river, and cave ecosystems are relatively intact. Mammoth Cave biota are among the most diverse in the world (Culver et al. 1999), with approximately 130 regularly occurring species roughly divided between troglobites, trolophiles, and troglonexes (Barr, 1967 Poulson 1992, 1993). Troglobites are fully cave adapted, and cannot survive in surface habitats. Aquatic troglobites are also referred to as stygobites. Troglrophiles are species that can complete their life cycle in both cave and surface habitats, and troglonexes use caves for refuge or may come in to prey upon other species.

INTERCONNECTIONS AND HABITATS

Functionally, since sinking streams and cave streams are tributaries of base-level rivers by way of springs, they are all part of the river continuum, with the important distinction that the middle section is underground. These distinct but connected aquatic ecosystems are energetically supported by in-washed organic debris from the forest and former prairie/savanna ecosystems. Food transport is usually down gradient, but natural back flooding from the river into cave streams is also important.

Cave aquatic habitats can be roughly divided on the basis of water quantity. Ephemeral pools occur in rimstone dams, near terminal breakdowns, in passages rarely flooded, and shafts. These may feed nearby shallow streams

tributary to master shaft drains grading into base level streams, which feed springs on the Green River. As the river lowers its channel, cave streams follow and leave dry upper levels.

These upper levels are habitat for the terrestrial cave ecosystem, also dependent upon forest and agricultural land for food. The import of food is mostly accomplished by cave crickets and to a lesser degree woodrats and bats, which feed in the forest, and use caves for refuge where guano accumulates. Crickets also lay eggs in caves, which support a separate community. Raccoons, entering caves to feed on bats and cave crickets, may leave significant quantities of scat. Habitats here are determined by proximity to entrances with variable temperature and humidity, which in turn determines the species leaving guano. Leaf litter falling into entrances, and flood debris deposited on passage surfaces are also locally important to the terrestrial cave ecosystem.

THE BIOTA AND THEIR INTERACTIONS

One prevalent aspect of aquatic life in the Mammoth Cave System is habitat partitioning by similar species within a taxonomic group. Two troglobitic species each of planaria (*Sphalloplana percocea* and *S. buchmanii*), amphipods (*Stygobromus vitreus* and *S. excilis*), isopods (*Caecidotea stygia* and *C. bicrenata*), and fish (*Typhlichthys subterraneus* and *Amblyopsis spelaea*) occupy upstream and downstream habitats respectively. Troglobites found only in base level streams include a snail (*Antroselates spiralis*), and the endangered Kentucky Cave Shrimp (*Palaemonias ganteri*).

The more adaptable cave crayfish *Orconectes pellucidus* occupies habitats ranging from base level to tiny streams, and can travel out of water if necessary. The troglphilic amphipod *Crangonyx packardi*, crayfish *Cambarus tenebrosus*, the sculpin *Cottus carolinae*, and the springfish *Chologaster agassizi* often occur in organically rich situations. With the exception of sculpin, fish and crayfish are predators and the remaining species are primarily grazers.

Common organisms living within the sediments of Mammoth Cave streams (Whitman



Figure 1. The Southern Cavefish at left and the Kentucky Cave Shrimp at right are good examples of fully troglitic aquatic cave life, otherwise known as stygobites.



Figure 2. Note how slender the white eyeless cave adapted (troglitic) crayfish at left is compared with the robust surface (trogliphilic) crayfish at right. This cave crayfish has eggs, which are shown in the middle photo.

1989) are nematodes (undescribed), copepods (*Maraenobiotus*, *Moraria*, *Nitocra*, and *Parastenocaris*), tardigrades (*Macrobiotus*), and oligochaete worms (*Aeolosoma*). Worm castings and tracks are also visible on mud banks of cave streams, and these organisms are preyed upon by the troglitic beetles *Pseudanophthalmus striatus*, *P. menetriesi*, and *Neaphaenops tellkampfi* (Kane and Ryan, 1983). This zone is an ecotone between aquatic and terrestrial cave ecosystems. As part of the community dependent upon flood-deposited organic films, the springtails *Folsomia candida* and *Pseudosinella* are preyed upon by the troglitic harvestman *Phalangodes armata*. Another major ecotone exists at cave entrances where litter from surface vegetation accumulates via gravity and woodrats. Here are found the collembolans *Tomocerus*, *Hypogastrura*, *Sinella*, and *Arrhopalites*. Predators include the beetle *Pseudanophthalmus*, and a rhabdigid mite (Poulson, 1992).

The cave cricket *Hadenoeus subterraneus* buries its eggs in sandy passages with moderate moisture in the constant temperature zone

(Hubbell and Norton, 1978), and the blind beetle *Neaphaenops* is especially skilled at finding those eggs. After cave crickets, this beetle has the highest density of any species in Mammoth Cave, and a small community subsists on beetle feces (Poulson 1992, 1993). The springtail *Arrhopalites* and the dipluran *Litocampa* are consumers, which are preyed upon by the mite *Arctoseius*, the spider *Anthrobia*, and the pseudoscorpion *Kleptochthonius*. These latter two are in turn preyed upon by *Neaphaenops* cave beetles.

In addition to eggs, *Hadenoeus* guano is also important. Crickets feed in surface habitats at night, and return to the cave to roost. Here their guano supports the millipedes *Scoterpes* and *Antriadesmus*, the springtails *Hypogastrura*, *Arrhopalites*, *Pseudosinella*, *Tomocerus*, and *Lepidocyrtus*, plus the bristletail *Litocampa*, the beetles *Ptomophagus hirtus* and *Batrisodes henroti*, the snail *Carychium stygius*, and the mites *Ceratozetes* and *Belba*.



Figure 3. Tiny springtails such as these shown at left are prey for several predators including the troglotic harvestman or daddy longlegs shown at right.

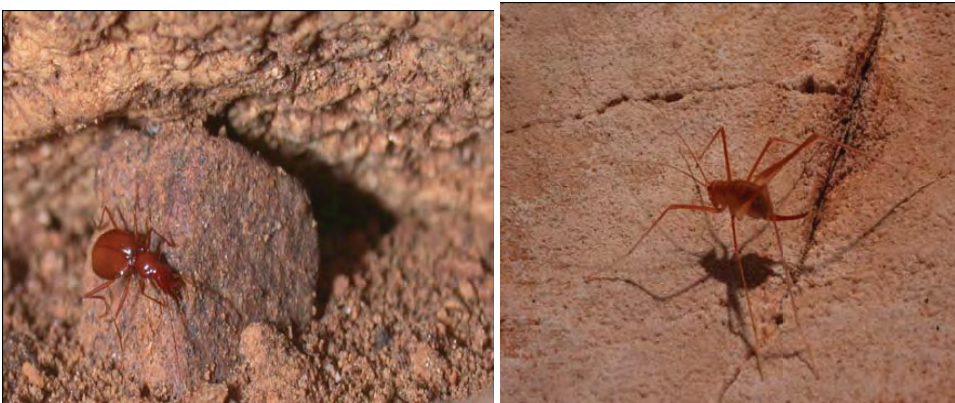


Figure 4. The blind cave beetle at left is especially adept at finding the buried eggs of the cave cricket seen in the right photo.



Figure 5. The troglitic millipede, snails, and troglitic springtail, (left to right) are all consumers of cricket guano.



Figure 6. Gray bats (left) were once abundant and are now listed as endangered, Rafinesque's Big Eared bat (center) populations were never large, but are today a matter of concern. The Eastern Pipistrelle bat shown at right is an example of a very adaptable and tolerant species.



Figure 7. Populations of Indiana bats once numbered in the millions within park caves, but today are counted in the low thousands and are considered critically endangered. These individuals were photographed in Long Cave in 2003.

These in turn are preyed upon by the pseudoscorpion *Kleptochthonius*, the beetle *Pseudanophthalmus menetriesi*, the larval dipteran *Macrocera nobilis*, and the spider *Phanetta*. As well, the spider *Meta americana*, and the cave salamander *Eurycea lucifuga* are present to prey upon crickets.

Woodrats and raccoons were formerly abundant in Mammoth Cave, and though today reduced, their feces support specialized

communities. Latrines of the Eastern Woodrat *Neotoma floridana* sustain larva of the fly *Psychoda* and fungus gnat *Bradysia*, and the beetle *Ptomaphagus hirtus*, which are preyed upon by the rove beetle *Quedius* (Richards, 1989, 1990). Raccoon feces support a similar community with the exception that cave crickets may preempt fly larvae, most notably *Spelobia*, and *Amoebelaria*.

Due to low populations, bat guano in Mammoth Cave is today negligible as an energy source (Barr and Kuehne, 1967), but would have been highly significant during pre-settlement times since Mammoth Cave was formerly one of the largest bat hibernacula in the world. Indiana Bats (*Myotis sodalis*) and to a lesser extent Gray Bats (*M. grisescens*) were prominent species in Mammoth Cave only 150 years ago, but are today listed as endangered. Little Brown Bats (*M. lucifugus*) were also abundant with the Big Brown Bat (*Eptesicus fuscus*), and Eastern Pipistrelle (*Pipistrellus subflavus*) being less common (Toomey et al., 1998). All together, these and more rare bat species such as *M. leibii* and *M. septentrionalis* had estimated populations of 9-12 million just in the Historic Section (Tuttle, 1997). Ecological restoration of this portion of Mammoth Cave, and facilitating the return of bats is an ongoing effort (Olson, 1996).

MAJOR CONSERVATION ISSUES

In addition to correcting ecological distortions to the Historic Section of Mammoth Cave, lampflora such as algae and mosses are a problem as in all show caves, and elimination via wavelength selection has been achieved on a small scale (Olson 2001). On a karst landscape scale, contamination of groundwater recharge is a major issue, especially from Interstate Highway 65 (Olson and Schaefer 2002). However, nothing is known about likely contaminants entering park waters from the CSX Railroad. Finally, a problem exists downstream on Green River in the form of Lock and Dam #6, which ponds water up into Mammoth Cave and degrades habitat for the endangered Kentucky Cave Shrimp (Olson and Leibfreid 1999).

REFERENCES CITED

- Barr, T., 1985, Cave Life of Kentucky. In *Caves and Karst of Kentucky*, edited by P.H. Dougherty, Kentucky Geological Survey, Series XI, Special Publication 12, Lexington, Kentucky, p. 146-167.
- Barr, T., 1967, Ecological Studies in the Mammoth Cave System of Kentucky, I. The Biota. *International Journal of Speleology*, 3:147-203.
- Culver, D., Master, L., Christman, M., and H. Hobbs, 1999, Obligate Cave Fauna of the 48 Contiguous United States. *Conservation Biology* 14:386-401.
- Hubbell, T. and R. Norton, 1978, The Systematics and Biology of the cave crickets of the North American Tribe Hadenocini (Orthoptera Saltatoria: Ensifera: Raphidophoriinae: Dolichopodinae). *Miscellaneous Publication of the Museum of Zoology, University of Michigan*, 156:1-80. Kane, T. and T. Ryan. 1983. Population Ecology of Carabid Cave Beetles. *Oecologia*, 60:46-55.
- Olson, R., 1996, This Old Cave: The Ecological Restoration of the Historic Entrance Ecotone of Mammoth Cave, and Mitigation of Visitor Impact. *Proceedings of the Fifth Annual Mammoth Cave National Park Science Conference*. Mammoth Cave National Park, KY: National Park Service, p. 87-95.
- Olson, R., 2001, Control of Lamp Flora in Mammoth Cave National Park. International Conference on Cave Lighting Proceedings, edited by Tamas Hazslinszky, Hungarian Speleological Society, Budapest, Hungary, p. 131.
- Olson, R., and T. Leibfreid, 1999, The Importance of Inventory and Monitoring Data sets in Resolving Ecosystem Management Problems at Mammoth Cave National Park. In: *On the Frontiers of Conservation, Proceedings of the 10th Conference on Research and Resources Management in Parks and on Public Lands*, edited by Dave Harmon, p.149-155.
- Olson, R. and J. Schaefer, 2002, Planned Spill Retention and Runoff Filtration Structures on Interstate 65 in the South-Central Kentucky Karst. 15th National Cave and Karst Management Symposium Proceedings, USDA Forest Service, Tucson, AZ, p 203.
- Poulson, T., 1992, The Mammoth Cave Ecosystem. In *The Natural History of Biospeleology*, edited by A. I. Camancho, Monographs of the National Museum of Natural Sciences, Madrid, Spain, p. 564-611.
- Poulson, T., 1993, Cave Animals of Mammoth Cave National Park. Unpublished guide on file at Mammoth Cave National Park. 35 p.
- Richards, P., 1989, Predation in the Cave Rat Fecal Latrine. *Cave Research Foundation Annual Report*, p. 45-47.

Richards, P., 1990, The Effects of Predation on Invertebrate Community Structure in the Cave Rat Fecal latrine. Cave Research Foundation Annual Report, p. 58-61.

Toomey, R., Colburn, M., Schubert, B., and R. Olson, 1998, Vertebrate Paleontological Projects at Mammoth Cave National Park. Proceedings of Mammoth Cave National Park's Seventh Science Conference. Mammoth Cave National Park, KY: National Park Service, p. 9-14.

Tuttle, M, 1997, A Mammoth Discovery. Bats. Bat Conservation International, 15:4, p. 3.

Whitman, R., 1989, Sand Dwelling Animals of Mammoth Cave. Unpublished report on meiofauna in Mammoth Cave on file at Mammoth Cave National Park. 75 p.

Field Trip Road Log: Karst Features of the Mammoth Cave Kentucky Area, Thursday, May 29, 2008

By Chris Groves¹ and Rick Toomey²

¹Hoffman Environmental Research Institute, Department of Geography and Geology, Western Kentucky University, Bowling Green, KY 42101

²Mammoth Cave International Center for Science and Learning, 1906 College Heights Blvd #31066, Bowling Green, KY 42101-1066

This field trip is in collaboration with the Fourth US Geological Survey Karst Interest Group Conference, Western Kentucky University.

The trip log begins at the Hampton Inn Hotel, 233 Three Springs Road, Bowling Green, KY 42104

| <i>interval</i> | <i>total</i> | |
|-----------------|--------------|--|
| 0 | 0 | Leave parking lot of Hampton Inn (see Figure 1) |
| 0.1 | 0.1 | Turn left onto Three Springs Road |
| 0.4 | 0.4 | Turn right on Scottsville Road (Rt. 231) |
| 0.6 | 0.6 | Take exit for I65 north |
| 4.5 | 4.5 | I65 crosses over the Barren River, which is the main base level stream draining the Pennyroyal karst plain in Warren County. It drains westward to the Green River, the base level stream for the Mammoth Cave System and other large caves of Hart, Barren, and Edmonson Counties in and around Mammoth Cave National Park (for background see Palmer, 1981; White and White, 1989). |
| 6 | 6 | Take exit 28 |
| 6.7 | 6.7 | Turn north on Rt. 31-W |
| 9.5 | 9.5 | Light at Rt. 526 |
| 10.8 | 10.8 | Pass Kentucky Trimodal Transpark (KTT) on right. The proposed KTT entails siting a 4,000-acre air-, rail-, and truck-terminal facility and associated industrial park on the karst plain, 8 miles from Mammoth Cave National Park near Bowling Green. A large automotive parts plant is in operation at the site, and more heavy industry is being encouraged to locate there. The siting of such a large facility in this setting on a sinkhole plain has been controversial because of the interactions between political considerations and the environmental concerns that had been detailed by a list of credible hydrogeologists and biologists. A measure of the level of controversy that ultimately developed within the local community was expressed one night in May 2004, when armed police were stationed at a County Planning and Zoning Commission rezoning hearing. |
| 16.9 | 16.9 | Buttram's Cave on left. The entrance to Buttram's Cave is in a sinkhole that has formed from the actual collapse of the ceiling of a cave passage. In contrast, most of the other sinks in the area are formed by focused dissolution at and thus lowering of the soil/bedrock interface underneath the soil. The cave is about one km long and is subject to dramatic flooding, even though nearly nine km from the Green River. |
| 18.9 | 18.9 | Cross into Edmonson County |
| 18.7 | 18.7 | Dripping Springs Community and Liberty Hill Church. We are at the physiographic boundary between the Pennyroyal Plateau limestone sinkhole plain to our right and the overlying sandstone capped Mammoth Cave Plateau to the left. The boundary between the two is called the Dripping Springs Escarpment, which gets its name from the small community here that goes back at least into the 1830s. |

Both of these plateau surfaces fall within the larger Interior Low Plateaus physiographic province. The Mammoth Cave System and other mapped caves with a combined length of more than 800 kilometers are formed in and around the dissected Mammoth Cave Plateau, ultimately draining to springs along the Green River to the north. We are not far from the divide between the karst groundwater drainage system that sends water north to the Green River in the Turnhole Bend Groundwater Basin, and south to the Barren River in the Graham Springs Basin.

All rocks that we will see up close on this trip are of Mississippian age.

- | | | |
|------|------|---|
| 19.3 | 19.3 | Turn right on Upper Smiths Grove Rd. (Rt. 422) |
| 21.3 | 21.3 | STOP ONE: SMITHS GROVE UVALA. We are passing a large uvala (elongated, compound sinkhole) that extends for almost a kilometer. The large main passage of Crump's Cave, our next stop, is truncated along the far wall of the depression. Here we will take a longitudinal or "down-valley" view of this feature. The uvala has a maximum topographic relief of more than 30 meters on its east end. Also note the general flatness of the topography farther to the east. This is caused by a semi-confining layer of chert within the upper part of the St. Louis Limestone, concordant with the ground surface here and which that to some degree protects the underlying karst features in this locale. This uvala may have formed where the chert layer was breached, ultimately resulting in collapse of the cave ceiling. |
| 22.1 | 22.1 | STOP TWO: CAVE SPRING CAVERNS. Turn into parking area of Cave Springs Caverns. Long known as Crump's Cave, this is a site of geologic, archeological, and historic interest. Research investigating epikarst hydrogeology and its influence on the fate and transport of agricultural contaminants is underway at the site (Groves and Bolster, 2005), funded by the USDA Agricultural Research Service. |
| 0 | 22.1 | After finishing at Cave Springs Caverns, go back (right) |
| 0.7 | 22.8 | Turn right at uvala |
| 4.1 | 26.2 | Turn left on Rt. 259 at Rocky Hill |
| 5.7 | 27.8 | Cross 31-W |
| 9 | 31.1 | Pig Community and Porky Pig Diner |
| 9 | 31.1 | After finishing at Pig go back (left) on 259 |
| 10.2 | 32.3 | Turn left on Chaumont Rd. at Cedar Spring Community |
| 11.2 | 33.3 | The entrance to Whigpistle Cave, at the bottom of the karst valley to the right, was discovered in 1976 and explored over the next seven years by summer field crews of cavers working for Jim Quinlan. Quinlan was for years the geologist for Mammoth Cave National Park and a pioneer in delineating karst groundwater basins and their boundaries. By 1984 the cave had grown to had grown to about 35 km. Subsequent exploration in the 1990s of several nearby caves resulted in connection of Whigpistle Cave to both Jackpot and Martin Ridge Caves, with the system subsequently exceeding 50 km in length. Exploration continues. For more information see < http://www.uweb.ucsb.edu/~glennon/martin/ >. |
| 12.7 | 34.8 | Bear right on Chaumont Rd. |
| 14.4 | 36.5 | Turn right on 31-W |
| 16.7 | 38.8 | Turn left on Park Mammoth Rd. |
| 17.3 | 39.4 | Just past Slave Cave Rd. go straight, up the hill |
| 17.5 | 39.6 | STOP THREE: PARK MAMMOTH OVERLOOK. Park to right of the gate, not blocking it, and walk to the overlook by walking straight ahead along the small gauge railroad. Bear to the left where the tracks reach an intersection. At the overlook, on the property of the Park Mammoth resort, we are on the Big Clifty Sandstone. The Girkin Limestone below is exposed in the face of the steep |

escarpment that falls away below us. Dipping gently towards the north, the rocks of the Ste. Genevieve and St. Louis limestones floor the vast sinkhole plain below.

| | | |
|------|------|--|
| 0 | 39.6 | After returning to bus, go back to 31-W |
| 0.8 | 40.4 | Turn left on 31-W |
| 1.9 | 41.5 | Turn left on Route 255 at Parkland Motel (note gorilla in parking lot) |
| 2.3 | 41.9 | Enter Mammoth Cave National Park |
| 3.5 | 43.1 | Pass Diamond Caverns on right. This is a very well decorated show cave with many different styles of travertine speleothems, or cave formations, in contrast to the more typical scenes of bare or muddy rock walls seen in much of the Mammoth Cave System and other nearby caves. In those areas passages are overlain with clastic rocks that inhibit infiltration of waters above the cave. |
| 4.5 | 44.1 | Turn left on Rt. 70 |
| 7.1 | 46.7 | Turn left on Rt. 70 |
| 10.9 | 50.5 | STOP FOUR: GREEN RIVER. Pull off at Turnhole Bend Trail parking area. This short walk goes across the sandstone Caprock past some large steep sinks, to an overlook of the Green River gorge. Turnhole Spring, the largest of the Green River springs draining the Mammoth Cave area, emerges here (see White and White, Glennon, 2002; Glennon and Groves, 2002). The river has cut downward through here in the last several million years, with a number of the details having been worked out by Granger <i>et al.</i> (2001) using the cosmogenic isotopes ²⁶ Al and ¹⁰ Be. They have tied absolute dating of major abandoned cave stream levels to the down cutting evolution of the Green, and thus the Ohio, Rivers. |
| 0 | 50.5 | When done at Turnhole go back east on Rt. 70 |
| 0.4 | 50.9 | Turn right on Cedar Sink Road (Rt. 422) |
| 0.9 | 51.4 | Rock fall on left hand side |
| 1 | 51.5 | Go past Cedar Sink Trail parking area |
| 2.8 | 53.3 | Go straight on Rt. 422 across Rt. 259 at Pig |
| 5.7 | 56.2 | Turn right on Rt. 31-W |
| 18.2 | 68.7 | Take exit for I65, onto access road |
| 18.9 | 69.4 | Go right on I65 south |
| 24.3 | 74.8 | Take Bowling Green exit 22 |
| 24.5 | 75 | Turn right on Scottsville Rd. (Rt. 231), get into left lane asap |
| 24.8 | 75.3 | Turn left on Three Springs Road |
| 24.9 | 75.4 | Turn right into Hampton Inn parking area, end of field trip |

REFERENCES

- Glennon, J.A., 2002, Application of Morphometric Relationships to Active Flow Networks within the Mammoth Cave Watershed: Unpublished M.S. Thesis, Department of Geography and Geology, Western Kentucky University.
- Glennon, J.A. and C. Groves, 2002, An examination of perennial stream drainage patterns within the Mammoth Cave watershed: *Journal of Cave and Karst Studies*, vol. 64, pp. 82-91.
- Granger, D., D. Fabel, and A.N. Palmer, 2001, Pliocene–Pleistocene incision of the Green River, Kentucky, determined from radioactive decay of cosmogenic ²⁶Al and ¹⁰Be in Mammoth Cave sediments. *Geological Society of American Bulletin*, v. 113, pp. 825-836.
- Groves, C., C. Bolster, and J. Meiman, 2005, Spatial and Temporal Variations in Epikarst Storage and Flow in South Central Kentucky’s Pennyroyal Plateau Sinkhole Plain. *US Geological Scientific Investigations Report 2005-5160*, pp. 64-73.

Palmer, A.N., 1981, *A Geological Guide to Mammoth Cave National Park*. Teaneck, N.J.: Zephyrus Press.

White, W.B., and White, E.L, 1989, *Karst hydrology: Concepts from the Mammoth Cave Area*. New York: Van Nostrand Reinhold.

KIG2008 Meeting -- Karst Features of the Mammoth Cave, KY Area Field Trip

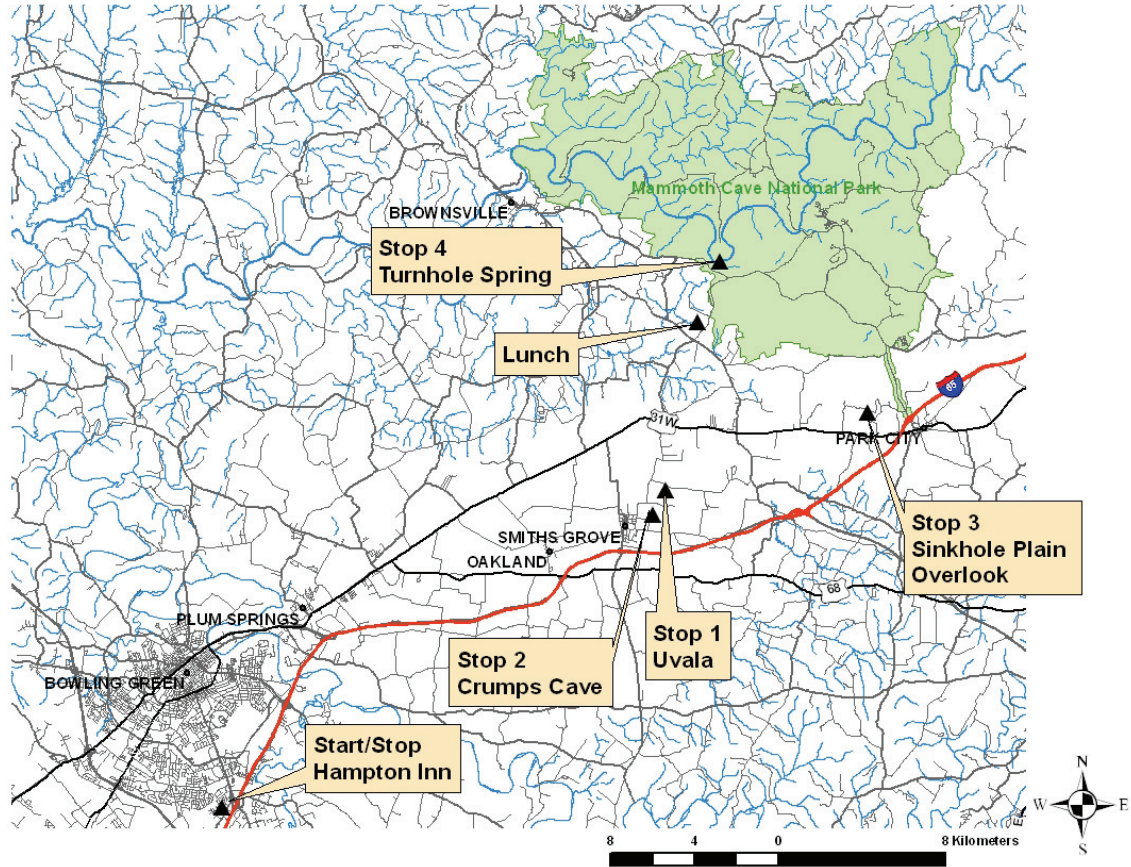


Figure 13. Map of field trip area, showing principal stops.